

This electronic thesis or dissertation has been downloaded from the King's Research Portal at <https://kclpure.kcl.ac.uk/portal/>



## Relaxed Stability Analysis for Fuzzy-Model-Based Observer-Control Systems

Liu, Chuang

*Awarding institution:*  
King's College London

The copyright of this thesis rests with the author and no quotation from it or information derived from it may be published without proper acknowledgement.

### END USER LICENCE AGREEMENT



**Unless another licence is stated on the immediately following page** this work is licensed

under a Creative Commons Attribution-NonCommercial-NoDerivatives 4.0 International

licence. <https://creativecommons.org/licenses/by-nc-nd/4.0/>

You are free to copy, distribute and transmit the work

Under the following conditions:

- Attribution: You must attribute the work in the manner specified by the author (but not in any way that suggests that they endorse you or your use of the work).
- Non Commercial: You may not use this work for commercial purposes.
- No Derivative Works - You may not alter, transform, or build upon this work.

Any of these conditions can be waived if you receive permission from the author. Your fair dealings and other rights are in no way affected by the above.

### Take down policy

If you believe that this document breaches copyright please contact [librarypure@kcl.ac.uk](mailto:librarypure@kcl.ac.uk) providing details, and we will remove access to the work immediately and investigate your claim.

*A thesis submitted for the degree of  
Doctor of Philosophy*

# **Relaxed Stability Analysis for Fuzzy-Model-Based Observer-Control Systems**

Author : Chuang Liu

Student Number : 1125826

First Supervisor : Dr. Hak-Keung Lam

Second Supervisor : Prof. Kaspar Althoefer

31/05/2016

Ph.D. in Robotics

Department of Informatics

Faculty of Natural & Mathematical Sciences

King's College London

# Acknowledgment

My sincerest gratitude is given to my supervisor Dr. Hak-Keung Lam, of the Department of Informatics, King's College London. I appreciate his patience, inspiration and professional guidance. Without his leading, I cannot get involved in this research area.

I would also like to thank the Kings-China Scholarship Council PhD Scholarship Program, my parents and my friends for the financial support.

Special thanks are given to my friends in London. They are all the motivation I need in pursuing this degree.

# Abstract

Fuzzy-model-based (FMB) control scheme is an efficient approach to conduct stability analysis for nonlinear systems. Both Takagi-Sugeno (T-S) FMB and polynomial fuzzy-model-based (PFMB) control systems have been widely investigated. In this thesis, the stability analysis of FMB control systems is conducted via Lyapunov stability theory. The main contribution of the thesis is improving the applicability of T-S FMB and PFMB control strategies by relaxing stability conditions and designing fuzzy observer-controller, which is presented in the following three parts:

- 1) The stability conditions of FMB control systems are relaxed such that the FMB control strategy can be applied to a wider range of nonlinear systems. For T-S FMB control systems, higher order derivatives of Lyapunov function (HODLF) are employed, which generalizes the commonly used first order derivative. For PFMB control systems, Taylor series membership functions (TSMF) are brought into stability conditions such that the relation between membership grades and system states is expressed.
- 2) Two types of T-S fuzzy observer-controller are designed such that the T-S FMB control strategy can be applied to systems with unmeasurable states. For the first type, the T-S fuzzy observer with unmeasurable premise variables is designed to estimate the system states and then the estimated states are employed for state-feedback control of nonlinear systems. Convex stability conditions are obtained through matrix decoupling technique. For the second type, the T-S fuzzy functional observer is designed to directly estimate the control input instead of the system states, which can reduce the order of the observer. A new form of fuzzy functional observer is proposed to facilitate the stability analysis such that the observer gains can be numerically obtained and the stability can be guaranteed simultaneously.
- 3) The polynomial fuzzy observer-controller with unmeasurable premise variables is designed for systems with unmeasurable states. Although the consideration of the polynomial fuzzy model and unmeasurable premise variables enhances the applicability of the FMB control strategy, it leads to non-convex stability conditions. Therefore, two methods are applied to derive convex stability conditions: refined completing square approach and matrix decoupling technique.

Additionally, the designed polynomial fuzzy observer-controller is extended for systems where only sampled-output measurements are available. Furthermore, the membership functions of the designed polynomial observer-controller are optimized by the improved gradient descent method.

Simulation examples are provided to demonstrate and verify the theoretical analysis.

# Contents

<b>Acknowledgment</b>	<b>2</b>
<b>Abstract</b>	<b>3</b>
<b>Contents</b>	<b>5</b>
<b>List of Publication</b>	<b>8</b>
<b>List of Figures</b>	<b>10</b>
<b>List of Tables</b>	<b>13</b>
<b>Acronyms</b>	<b>14</b>
<b>1 Overview</b>	<b>15</b>
1.1 Introduction . . . . .	15
1.2 Literature Review . . . . .	16
1.2.1 FMB Control System . . . . .	16
1.2.2 Relaxation of Stability Conditions . . . . .	17
1.2.3 Extensions of FMB Control Strategy . . . . .	19
1.2.4 Optimization of Membership Functions . . . . .	22
1.3 Objectives and Organization . . . . .	22
<b>2 Preliminary</b>	<b>24</b>
2.1 Notations . . . . .	24
2.2 Sector Nonlinearity Technique . . . . .	24
2.3 T-S FMB Control System . . . . .	26
2.3.1 T-S Fuzzy Model . . . . .	27
2.3.2 T-S Fuzzy Controller . . . . .	27
2.3.3 T-S FMB Control System . . . . .	28
2.4 PFMB Control System . . . . .	28
2.4.1 Polynomial Fuzzy Model . . . . .	28
2.4.2 Polynomial Fuzzy Controller . . . . .	29
2.4.3 PFMB Control System . . . . .	29
2.5 Lyapunov Stability Theory . . . . .	30

2.6	LMI/SOS Stability Conditions . . . . .	31
2.7	Useful Lemmas . . . . .	31
<b>3</b>	<b>Relaxation of Stability Conditions</b>	<b>34</b>
3.1	Higher Order Derivatives of Lyapunov Function for T-S FMB Control Systems . . . . .	34
3.1.1	Introduction . . . . .	34
3.1.2	Stability Analysis . . . . .	35
3.1.3	Simulation Examples . . . . .	40
3.1.4	Conclusion . . . . .	42
3.2	Taylor Series Membership Functions for PFMB Control Systems . . .	43
3.2.1	Introduction . . . . .	43
3.2.2	Preliminary . . . . .	44
3.2.3	Stability Analysis . . . . .	44
3.2.4	Simulation Examples . . . . .	52
3.2.5	Conclusion . . . . .	55
<b>4</b>	<b>Design of T-S Fuzzy Observer-Controller</b>	<b>58</b>
4.1	Design of Relaxed T-S Fuzzy Observer-Controller with Unmeasurable Premise Variables . . . . .	58
4.1.1	Introduction . . . . .	58
4.1.2	Preliminary . . . . .	59
4.1.3	Stability Analysis . . . . .	60
4.1.4	Simulation Examples . . . . .	65
4.1.5	Conclusion . . . . .	70
4.2	Design of T-S Fuzzy Functional Observer . . . . .	70
4.2.1	Introduction . . . . .	70
4.2.2	Stability Analysis . . . . .	70
4.2.3	Simulation Examples . . . . .	76
4.2.4	Conclusion . . . . .	79
<b>5</b>	<b>Design of Polynomial Fuzzy Observer-Controller</b>	<b>81</b>
5.1	Design of Polynomial Fuzzy Observer-Controller Using Matrix Decoupling Technique . . . . .	81
5.1.1	Preliminary . . . . .	82
5.1.2	Stability Analysis . . . . .	83
5.1.3	Simulation Examples . . . . .	88
5.1.4	Conclusion . . . . .	95
5.2	Design of Polynomial Fuzzy Observer-Controller Using Completing Square Approach . . . . .	96
5.2.1	Introduction . . . . .	96
5.2.2	Preliminary . . . . .	96

5.2.3	Stability Analysis . . . . .	97
5.2.4	Conclusion . . . . .	104
5.3	Combination with Sampled-Output Measurement . . . . .	104
5.3.1	Introduction . . . . .	104
5.3.2	Stability Analysis . . . . .	104
5.3.3	Simulation Examples . . . . .	113
5.3.4	Conclusion . . . . .	117
5.4	Optimization of Membership Functions . . . . .	117
5.4.1	Introduction . . . . .	117
5.4.2	Algorithm Design . . . . .	118
5.4.3	Simulation Examples . . . . .	123
5.4.4	Conclusion . . . . .	139
<b>6</b>	<b>Conclusion and Future Work</b>	<b>140</b>
6.1	Conclusion . . . . .	140
6.2	Future Work . . . . .	143
<b>A</b>	<b>Proof of (4.58)</b>	<b>146</b>
<b>B</b>	<b>Boundary Information for Examples in Subsection 4.1.4</b>	<b>147</b>
<b>C</b>	<b>MATLAB Code Example</b>	<b>148</b>
	<b>References</b>	<b>149</b>



# List of Publication

## Journal Papers

- [1] Hugo Araujo, Bo Xiao, **Chuang Liu**, Yanbin Zhao and H.K. Lam, “Design of type-1 and interval type-2 fuzzy PID control for anesthesia using genetic algorithms,” *Journal of Intelligent Learning Systems and Applications*, vol. 6, no. 2, pp. 70-93, May 2014.
- [2] **Chuang Liu** and H.K. Lam, “Design of polynomial fuzzy observer-controller with sampled-output measurements for nonlinear systems considering unmeasurable premise variables,” *IEEE Transactions on Fuzzy Systems*, vol. 23, no. 6, pp. 2067-2079, Dec. 2015.
- [3] H.K. Lam, **Chuang Liu**, Ligang Wu and Xudong Zhao, “Polynomial fuzzy-model-based control systems: stability analysis via approximated membership functions considering sector nonlinearity of control input,” *IEEE Transactions on Fuzzy Systems*, vol. 23, no. 6, pp. 2202-2214, Dec. 2015.
- [4] **Chuang Liu**, H.K. Lam, Xiaojun Ban and Xudong Zhao, “Design of polynomial fuzzy observer-controller with optimized membership functions considering unmeasurable premise variables for nonlinear systems,” *Information Sciences*, vol. 355-356, pp. 186-207, Aug. 2016.
- [5] **Chuang Liu**, H.K. Lam, Tyrone Fernando and H.H.C. Iu, “Design of fuzzy functional observer-controller via higher order derivatives of Lyapunov function for nonlinear systems,” *IEEE Transactions on Cybernetics*, 2016 (DOI: 10.1109/TCYB.2016.2554141).
- [6] Peng Qi, **Chuang Liu**, Ahmad Ataka, H.K. Lam, and Kaspar Althoefer, “Kinematic control of continuum manipulators using a fuzzy-model-based approach,” *IEEE Transactions on Industrial Electronics*, vol. 63, no. 8, pp. 5022-5035, Aug. 2016.

## Conference Papers

- [7] **Chuang Liu**, H.K. Lam, Xian Zhang, Hongyi Li and Sai Ho Ling, “Relaxed stability conditions based on Taylor series membership functions for polynomial fuzzy-model-based control systems,” in *2014 IEEE International Conference on Fuzzy Systems (FUZZ-IEEE)*, 6-11 July, 2014, Beijing, China, pp.2111-2118.
- [8] Yanbin Zhao, Bo Xiao, **Chuang Liu**, Hongyi Li and H.K. Lam, “Relaxed LMI-based stability conditions for fuzzy-model-based control systems under imperfect premise matching: approximated membership function approach,” in *11th World Congress on Intelligent Control and Automation (WCICA 2014)*, 29 June - 4 July, 2014, Shenyang, China.
- [9] Xiaomiao Li, **Chuang Liu**, H.K. Lam, Fucai Liu and Xudong Zhao, “Stability analysis of fuzzy polynomial positive systems with time delay,” in *2014 International Conference on Fuzzy Theory and Its Applications (iFuzzy2014)*, November 26-28, 2014, Kaohsiung, Taiwan, pp. 53-57. (received “Best Paper in Theory Award”)
- [10] Peng Qi, **Chuang Liu**, Linan Zhang, Shuxin Wang, H.K. Lam and Kaspar Althoefer, “Fuzzy logic control of a continuum manipulator for surgical applications,” in *2014 IEEE International Conference on Robotics and Biomimetics (ROBIO 2014)*, December 5-10, 2014, Bali, Indonesia, pp. 413-418.
- [11] **Chuang Liu**, H.K. Lam, Shun-Hung Tsai and Chin-Sheng Chen, “Control of nonlinear systems by fuzzy observer-controller with unmeasurable premise variables,” in *2015 International Conference on Advanced Robotics and Intelligent System (ARIS 2015)*, 29-31 May, 2015, Taipei, Taiwan, pp.1-6.

# List of Figures

1.1	Intelligent control methods. . . . .	16
1.2	Procedure of FMB control design extended from [1]. . . . .	17
1.3	Sources of conservativeness. . . . .	18
1.4	Techniques for T-S fuzzy observer. . . . .	20
1.5	Relation of main chapters. . . . .	23
2.1	Procedure of sector nonlinearity technique. . . . .	25
2.2	A block diagram of FMB control systems. . . . .	26
2.3	A simplified block diagram of FMB control systems. . . . .	27
2.4	Geometric meaning of Lyapunov functions. . . . .	30
3.1	Procedure of proof for Theorem 1. . . . .	37
3.2	Stabilization regions obtained from Theorem 1 (“○” and “+”), Theorem 6 in [2] (“×”) and Theorem 7 in [2] (“□”). . . . .	41
3.3	Phase plot of $x_1(t)$ and $x_2(t)$ for $a = 5$ and $b = -40$ in “○” in Fig. 3.2 where the initial conditions are indicated by “o”. . . . .	42
3.4	Phase plot of $x_1(t)$ and $x_2(t)$ for $a = 1$ and $b = -42$ in “+” in Fig. 3.2 where the initial conditions are indicated by “o”. . . . .	43
3.5	Procedure of proof for Theorem 2. . . . .	47
3.6	Stabilization regions obtained from Theorem 2 with only $\mathbf{Y}_{ij}(x_1)$ , indicated by “×” for Case 1, “+” for Case 2, “□” for Case 3 and “o” for Case 4. . . . .	54
3.7	Stabilization regions obtained from Theorem 2 with only $\mathbf{Y}_{ij}(x_1)$ , $\underline{\mathbf{W}}_{ij}(x_1)$ and $\overline{\mathbf{W}}_{ij}(x_1)$ , indicated by “×” for Case 1, “+” for Case 2, “□” for Case 3 and “o” for Case 4. . . . .	55
3.8	Stabilization regions obtained from Theorem 2 with only $\mathbf{Y}_{ij}(x_1)$ , $\underline{\mathbf{W}}_{ij}(x_1)$ , $\overline{\mathbf{W}}_{ij}(x_1)$ and $\mathbf{L}(x_1)$ , indicated by “×” for Case 1, “+” for Case 2, “□” for Case 3 and “o” for Case 4. . . . .	56
3.9	Stabilization regions obtained from Theorem 2 with all slack matrices ( $\mathbf{Y}_{ij}(x_1)$ , $\underline{\mathbf{W}}_{ij}(x_1)$ , $\overline{\mathbf{W}}_{ij}(x_1)$ , $\mathbf{L}(x_1)$ and $\mathbf{K}(x_1)$ ), indicated by “×” for Case 1, “+” for Case 2, “□” for Case 3 and “o” for Case 4. . . . .	56
3.10	Phase plot of $x_1(t)$ and $x_2(t)$ for $a = 10$ and $b = 220$ in Case 4. . . . .	57

3.11	Transient response of $\mathbf{x}(t)$ and control input $u(t)$ for $a = 10$ and $b = 220$ in Case 4. . . . .	57
4.1	A block diagram of FMB observer-control systems. . . . .	61
4.2	Procedure of the proof for Theorem 3. . . . .	63
4.3	Time responses of system states $x_1(t)$ and $x_2(t)$ and estimated states $\check{x}_1(t)$ and $\check{x}_2(t)$ . . . . .	67
4.4	Time responses of system states $x_1(t)$ and $x_2(t)$ and estimated states $\check{x}_1(t)$ and $\check{x}_2(t)$ . . . . .	69
4.5	A block diagram of FMB functional observer-control systems. . . . .	72
4.6	Procedure of proof for Theorem 4. . . . .	74
4.7	The inverted pendulum on a cart. . . . .	77
4.8	Time response of system state $x_1(t)$ with $\mathbf{z}_1(0) = \mathbf{z}_2(0) = 0$ . . . . .	78
4.9	Time response of system state $x_2(t)$ with $\mathbf{z}_1(0) = \mathbf{z}_2(0) = 0$ . . . . .	79
4.10	Time response of objective control input $\mathbf{u}(t)$ and estimated control input $\check{\mathbf{u}}(t)$ with $\mathbf{x}(0) = [\frac{80\pi}{180} \ 0]^T$ and $\mathbf{z}_1(0) = \mathbf{z}_2(0) = 0$ . . . . .	80
5.1	Procedure of the proof for Theorem 5. . . . .	86
5.2	Time response of system states of the inverted pendulum with 4 different initial conditions. . . . .	90
5.3	Time response of system states and estimated states for $\mathbf{x}(0) = [\frac{70\pi}{180} \ 0]^T$ . . . . .	91
5.4	Time response of control input $u(t)$ for $\mathbf{x}(0) = [\frac{70\pi}{180} \ 0]^T$ . . . . .	92
5.5	The nonlinear mass-spring-damper system. . . . .	93
5.6	Time response of system states of the mass-spring-damper system with 4 different initial conditions. . . . .	94
5.7	Time response of system states and estimated states for $\mathbf{x}(0) = [1 \ 0]^T$ . . . . .	95
5.8	Procedure of the proof for Theorem 6. . . . .	100
5.9	A block diagram of PFMB observer-control systems with sampled-output measurement. . . . .	106
5.10	Procedure of the proof for Theorem 7. . . . .	109
5.11	Time response of system states of the inverted pendulum with 4 different initial conditions. . . . .	114
5.12	Time response of system states and estimated states for $\mathbf{x}(0) = [\frac{70\pi}{180} \ 0]^T$ . . . . .	115
5.13	Time response of sampled output, estimated sampled output and control input for $\mathbf{x}(0) = [\frac{70\pi}{180} \ 0]^T$ . . . . .	116
5.14	Procedure of proof for Theorem 8. . . . .	120
5.15	The descent of the gradient $\nabla J(\alpha)$ , where the arrow indicates the direction of the gradient descent and the contour indicates the value of the cost $J(\alpha)$ . . . . .	124

5.16	Membership functions. . . . .	126
5.17	Time response of system state $x_1$ , its estimation $\check{x}_1$ and its counterpart by PDC approach. . . . .	127
5.18	Time response of system state $x_2$ , its estimation $\check{x}_2$ and its counterpart by PDC approach. . . . .	128
5.19	Time response of the control input $u$ and its counterpart by PDC approach. . . . .	129
5.20	The descent of the gradient $\nabla J(\alpha)$ , where the arrow indicates the direction of the gradient descent and the contour indicates the value of the cost $J(\alpha)$ . . . . .	130
5.21	Membership functions. . . . .	131
5.22	Time response of system state $x_1$ , its estimation $\check{x}_1$ and its counterpart by PDC approach. . . . .	132
5.23	Time response of system state $x_2$ , its estimation $\check{x}_2$ and its counterpart by PDC approach. . . . .	133
5.24	Time response of the control input $u$ and its counterpart by PDC approach. . . . .	134
5.25	The ball-and-beam system . . . . .	135
5.26	Time response of system state $x_1$ , its estimation $\check{x}_1$ and its counterpart by PDC approach. . . . .	136
5.27	Time response of system state $x_2$ , its estimation $\check{x}_2$ and its counterpart by PDC approach. . . . .	137
5.28	The unicycle model. . . . .	138
5.29	The trajectory of the mobile robot where “ $\times$ ” indicates the initial position and “ $\square$ ” indicates the obstacle position. . . . .	139

# List of Tables

3.1	Comparison of different orders of TSMFs and intervals of expansion points. . . . .	53
5.1	Numerical complexity of Theorem 6. . . . .	136
5.2	Numerical complexity of Theorem 8. . . . .	137
5.3	Comparison of optimization algorithms. . . . .	138
6.1	Comparison between the proposed HODLF and existing methods. . .	141
6.2	Comparison between the proposed TSMF and existing methods. . .	141
6.3	Comparison between the proposed relaxed T-S fuzzy observer and existing methods. . . . .	142
6.4	Comparison between the proposed T-S fuzzy functional observer and existing methods. . . . .	142
6.5	Comparison between the proposed polynomial fuzzy observer and existing methods. . . . .	143
6.6	Comparison between the proposed polynomial fuzzy observer using matrix decoupling technique and competing square approach. . . .	143
6.7	Comparison between the proposed polynomial fuzzy observer under sampled-output measurement and existing methods. . . . .	144
6.8	Comparison between the proposed optimization algorithm and existing methods. . . . .	144
B.1	The upper bounds of membership functions for Example 4.1.4.1. . .	147
B.2	The upper bounds of membership functions for Example 4.1.4.2. . .	147

# Acronyms

T-S	Takagi-Sugeno
FMB	Fuzzy-model-based
LMI	Linear matrix inequality
SOS	Sum of squares
PDC	Parallel distributed compensation
HODLF	Higher order derivatives of Lyapunov function
PFMB	Polynomial fuzzy-model-based
TSMF	Taylor series membership functions
N/A	Not applicable

# Chapter 1

## Overview

### 1.1 Introduction

Stability analysis is a mathematical and systematic process proving the feasibility of designed controllers for stabilizing dynamic systems. For nonlinear systems, the stability analysis is very challenging even though mathematical models of systems are known beforehand. On one hand, some nonlinear control methods can only be applicable to specific systems. On the other hand, some practical control strategies lack of rigorous stability analysis. Consequently, when traditional nonlinear control methods fail in some cases, a more general control methodology with rigorous stability analysis is necessarily investigated.

Fuzzy control approach, being one of the intelligent control methods as shown in Fig. 1.1, has been widely applied for nonlinear systems. Fuzzy control has become one of the strong candidates for nonlinear control. The advantage of fuzzy control is that the linear control techniques can be employed for nonlinear systems. The fuzzy control was initially proposed as a model-free approach. Although it is easy to be implemented since the model of the system is not required, this approach lacks of rigorous stability analysis. As a result, the model-based fuzzy control has been developed. With the help of modern control theory and convex optimization technique, the rigorous stability analysis can be achieved for general nonlinear systems and controller can be numerically designed. Apart from fuzzy control approach, other intelligent control methods in Fig. 1.1 can also be employed for complex systems. Evolutionary computation allows adaptation without human intervention and can be applied for automatic learning of nonlinear mappings and multi-objective optimization problems. Neural networks takes advantage of human brain capabilities and can be trained to perform complex mappings. Hybrid methods can take advantage of the merits of the above intelligent control methods and eliminate their drawbacks.

In this thesis, the model-based fuzzy control approach is applied for stabilizing general nonlinear systems. The main effort is put into the mathematical stabil-



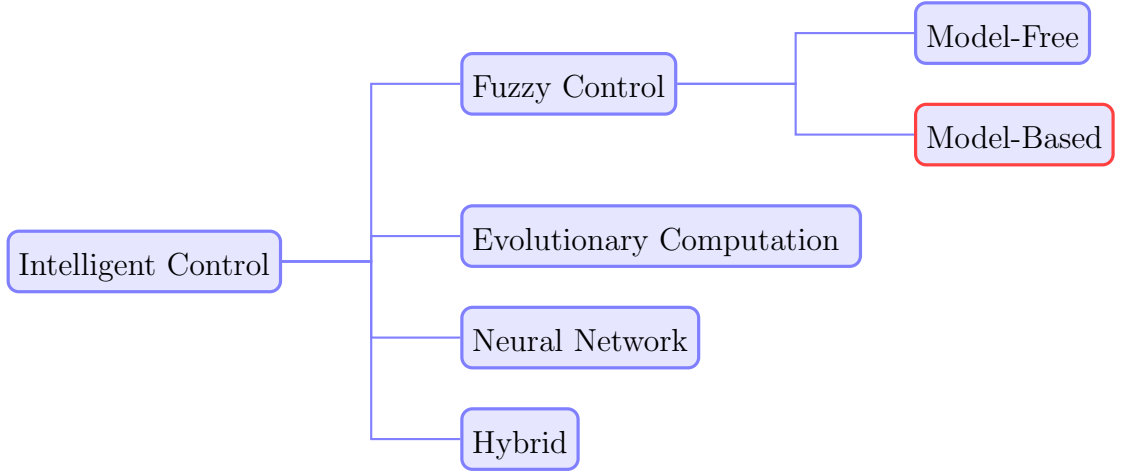


Figure 1.1: Intelligent control methods.

ity analysis. The main contribution of the thesis is improving the applicability of this control strategy by relaxing stability conditions and designing fuzzy observer-controller. Convex stability conditions will be derived for each case. Users can easily apply the derived stability conditions to design their controllers for stabilizing nonlinear systems and do not need to continually derive the stability conditions. Simulation examples will be provided to demonstrate the design procedure.

## 1.2 Literature Review

### 1.2.1 FMB Control System

Stability analysis and control synthesis for nonlinear systems are difficult to be systematically conducted. Polynomial fuzzy model [3,4] is one of the effective tools to model and analyze nonlinear systems, which is a generalization of Takagi-Sugeno (T-S) fuzzy model [5,6] in terms of modeling capability. The nonlinear systems can be divided to several linear subsystems which are smoothly combined by membership functions. In this way, linear control techniques such as state-feedback control can be applied and extended to fuzzy state-feedback controller for nonlinear systems.

Both of T-S and polynomial fuzzy models are employed in fuzzy-model-based (FMB) control strategies, which means that the stability analysis and control synthesis are carried out based on the fuzzy model instead of the nonlinear system [7]. Several techniques are widely employed under the FMB control scheme. First, the sector nonlinearity technique [8,9] (or other modeling methods such as fuzzy identification method [10]) is employed to represent fuzzy model of a nonlinear system. Second, Lyapunov stability theory [1] is applied to provide sufficient stability conditions. Third, linear matrix inequality (LMI) [8,11] and sum of squares (SOS) approaches [12] are used to describe the stability conditions for a T-S fuzzy model and a polynomial fuzzy model, respectively, which can be solved by convex programming

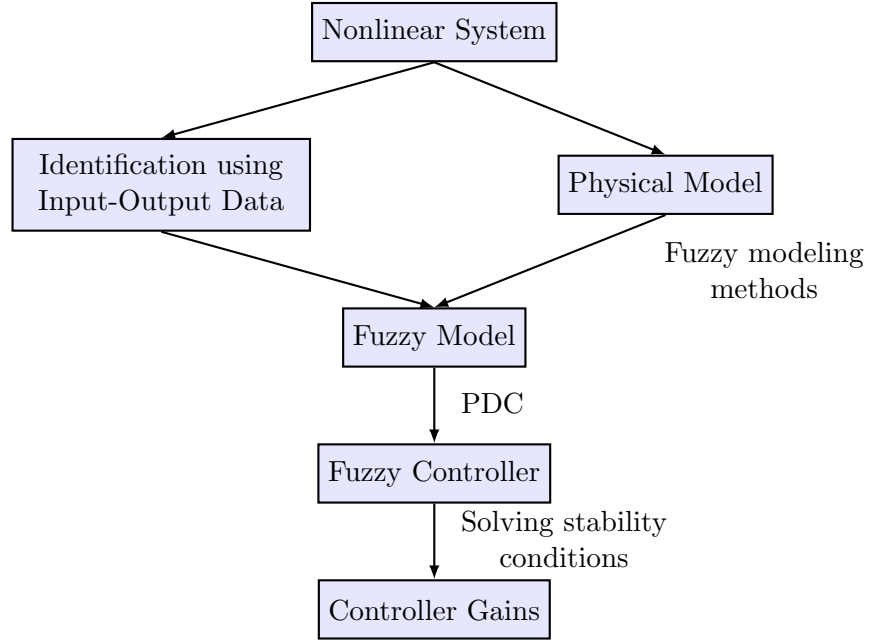


Figure 1.2: Procedure of FMB control design extended from [1].

techniques. The SOS conditions can be converted into semidefinite programming problem by SOSTOOLS [13] and then solved by SeDuMi [14]. Furthermore, the parallel distributed compensation (PDC) [1] is implemented for the control synthesis. The feasibility of applying FMB control scheme, especially the polynomial fuzzy model and SOS approach, has been demonstrated by existing literature [15–17].

Once the stability conditions are available, users may follow the procedure of FMB control design as shown in Fig. 1.2. Given a nonlinear system, one can obtain a mathematical model either by physical modeling or input-output data. Next, the fuzzy modeling methods such as sector nonlinearity technique [8,9] is employed to establish a fuzzy model. Then by PDC approach, the form of the fuzzy controller is settled. Subsequently, by numerically solving the LMI/SOS stability conditions via convex programming techniques, if a feasible solution exists, the feedback gains in the fuzzy controller will be obtained and the stability of the closed-loop nonlinear system will be guaranteed simultaneously. Finally, users can apply the designed fuzzy controller to stabilize the nonlinear systems.

### 1.2.2 Relaxation of Stability Conditions

In the development of FMB control scheme, the conservativeness of stability conditions is a critical problem which attracts researchers' attention [18, 19]. When solving stability conditions, even though system is controllable, the conservativeness results in infeasible solutions, which means feedback gains cannot be obtained. It restricts the applicability of FMB control scheme. There are several sources of conservativeness as listed in Fig. 1.3, which will be discussed in the following paragraphs. To relax the stability conditions (that is to reduce the conservativeness),

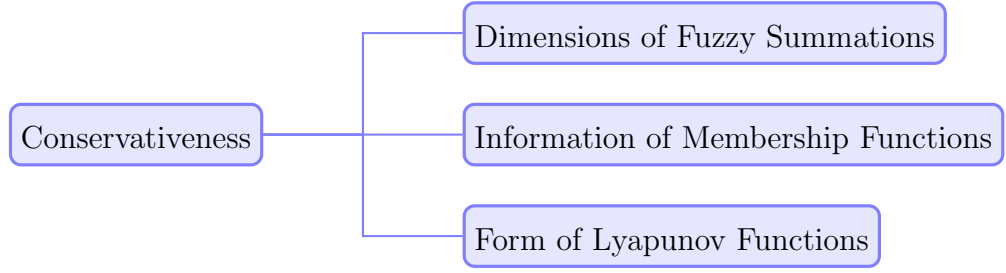


Figure 1.3: Sources of conservativeness.

slack matrices (or Positivstellensatz multipliers) are added to stability conditions through S-procedure [20], which brings more freedom for satisfying the conditions. In other words, the free variables in the slack matrices will be chosen such that feasible solutions to stability conditions are obtained.

#### 1.2.2.1 Dimensions of Fuzzy Summations

The first source of conservativeness is the fuzzy summations. Since the FMB control system is in the form of fuzzy summations, the way of grouping the subsystems that have the same membership grades affects the conservativeness of stability conditions. To relax the stability conditions, the fuzzy summations were investigated in [21, 22] and further generalized by Pólya's theory in [23, 24]. Pólya's theory was applied to investigate higher dimensions of fuzzy summations, which offers progressively necessary and sufficient conditions.

#### 1.2.2.2 Information of Membership Functions

Another source is the information of membership functions. Due to the abandon of membership functions during the analysis, the stability conditions are membership-function-independent, which means that the stability conditions do not depend on the membership functions under consideration. Therefore, the membership-function-dependent approach is exploited to make the stability conditions consider the specific membership functions, which can reduce the conservativeness. With regard to the information of membership functions, symbolic variables were employed to represent membership functions [9, 25, 26] such that they can remain in SOS-based conditions. Moreover, approximated membership functions were exploited to directly bring the information into stability analysis [27, 28] such that the relation between membership grades and system states is expressed rather than the information independent of system states. In [27], polynomial membership functions were proposed to approximate the original membership functions in each operating sub-domain. Whereas, there was no systematic way to determine approximated membership functions. In [28], a piecewise linear membership function was proposed to achieve the approximation of membership functions in stability analysis. Nonetheless, the approximation errors need to be improved due to the limited ex-

pression capability of the linear functions. Consequently, a systematic method of approximating membership functions is required for reducing the conservativeness of stability conditions. Other types of information of membership functions have also been investigated [29–32].

### 1.2.2.3 Form of Lyapunov Functions

Apart from the above two sources, the form of Lyapunov function affects the conservativeness meanwhile. The quadratic Lyapunov function and its first order derivative are commonly investigated in the stability analysis [1]. To relax the stability conditions, more general types of Lyapunov function candidates have been employed such as piecewise linear Lyapunov function [33, 34], switching Lyapunov function [35], fuzzy Lyapunov function [2, 36, 37] and polynomial Lyapunov function [35]. Furthermore, instead of using the first order derivative, higher order derivatives of Lyapunov function (HODLF) have been considered to relax the stability conditions. The HODLF was proposed in [38], and later generalized by [39]. One of the advantages in [39] is that the stability conditions are convex which can be numerically solved by convex programming techniques. However, only specific types of nonlinear systems were studied such as polynomial systems. Due to the universal approximation capability of fuzzy models [8], the HODLF should be combined with FMB control scheme such that general nonlinear systems can be dealt with. In discrete-time FMB control system, the non-monotonic Lyapunov function [40–42] and the multi-step Lyapunov function were investigated [43–46]. Similar to HODLF, they involve the difference of Lyapunov function in more steps instead of only one step. To the best of the author’s knowledge, the HODLF has not been applied to continuous-time FMB control system. In continuous-time FMB control system, the HODLF is difficult to be exploited to relax the stability conditions due to the existence of the derivative of membership functions. The combination of HODLF and continuous-time FMB control system is important since it improves the applicability of both HODLF and FMB control scheme, which is a worth investigation.

## 1.2.3 Extensions of FMB Control Strategy

With relaxed stability conditions being extensively investigated, FMB control strategy is applied to various control problems, for instance, output feedback [47], uncertainty [48] and sampled-data system [49, 50].

### 1.2.3.1 T-S Fuzzy Observer

As one of the output feedback control schemes, fuzzy observer was proposed to estimate system states according to the system outputs [11]. If measurable premise variables are used in membership functions, separation principle [51] can be employed

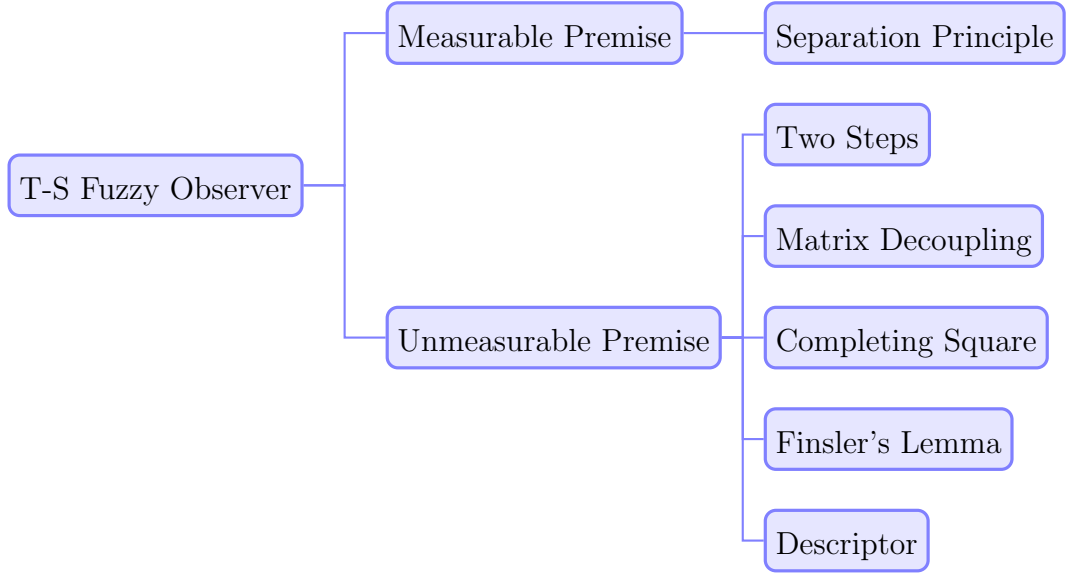


Figure 1.4: Techniques for T-S fuzzy observer.

to independently design the fuzzy controller and the fuzzy observer. However, the assumption of measurable premise variables is only valid for a limited class of non-linear systems. To increase the applicability of the fuzzy observer, membership functions depending on unmeasurable states were considered in [52], where a two-step procedure was required due to the non-convex stability conditions [52]. Therefore, several techniques were proposed to transform the non-convex stability conditions to convex ones, for example, completing square [53], matrix decoupling [54], Finsler's lemma [55] and descriptor representation [56]. These techniques are summarized in Fig. 1.4. In [54], the convex conditions are achieved by successfully applying the matrix decoupling technique. However, there are a number of scalars to be predefined by users or other numerical methods such as genetic algorithm due to complex control problems considered in [54]. Furthermore, the conditions are conservative resulting from approximations of non-convex terms. If only the observer is considered and other complex control problems in [54] are not considered, the analysis can be adjusted to achieve less number of predefined scalars and less conservative conditions.

### 1.2.3.2 T-S Fuzzy Functional Observer

While the fuzzy observer is widely studied, the fuzzy functional observer receives relatively less attention. Since the ultimate goal of estimating the system states is for state-feedback control, it is more straightforward to estimate the control input instead of the system states. Moreover, the order of the functional observer is lower than the traditional observer, which reduces the complexity of the observer. In [57], the fuzzy functional observer was proposed. Although the separation principle can be exploited to separately design the fuzzy controller and fuzzy observer, a number of observer gains have to be manually designed. To ease the design pro-

cedure, the technique for linear functional observer [58] was employed to design the fuzzy functional observer in [59]. Nevertheless, the stability of the FMB functional observer-control system has to be checked after designing the feedback gains due to the non-convex stability conditions. To the best of the author's knowledge, the one-step design, which means the stability can be guaranteed while the feedback gains are acquired, has not been developed.

### 1.2.3.3 Polynomial Fuzzy Observer

While the T-S fuzzy observer is widely studied, the polynomial fuzzy observer receives relatively less attention. The polynomial fuzzy observer was proposed in [60] which generalizes the T-S fuzzy observer. The polynomial system matrices and polynomial input matrices are allowed to exist in the polynomial fuzzy observer, and the observer gains can also be polynomial. Nonetheless, the polynomial fuzzy observer-controller is designed by two steps. The polynomial controller gains have to be obtained first by assuming all system states are measurable. The polynomial observer gains can be subsequently determined. Moreover, only measurable premise variables and constant output matrices are considered, which narrow the applicability. To the best of the author's knowledge, the polynomial fuzzy observer-controller with one-step design, unmeasurable premise variables and polynomial output matrices has not been investigated.

### 1.2.3.4 Sampled-Data Control

Sampled-data control system is a control system whose states are measured only at the sampling instants. The zero-order-hold unit keeps the control signal constant between sampling instants, which complicates the system dynamics and makes the stability analysis much more difficult. Various methods were proposed to investigate the stability of sampled-data control system such as lifting technique [61], hybrid discrete/continuous approach [62], input-delay approach [63] and exact discrete-time design approach [64]. Among these approaches, input-delay approach represents the discrete-time input measurements into time-delayed input measurements, and makes continuous-time stability analysis applicable to sampled-data control systems. Combined with FMB control, fruitful results were obtained [65–69] for full-state feedback case. Sampled-data fuzzy observer-controller receives much less attention because of its complexities on stability analysis. Fuzzy observer [70–72] or dynamic output feedback [73, 74] using sampled-output measurements can be found in the literature for nonlinear systems represented by T-S fuzzy models. To the best of the author's knowledge, polynomial fuzzy observer has not been applied to systems with sampled-output measurements.

### 1.2.4 Optimization of Membership Functions

Under the FMB control strategy, while the PDC approach is mainly employed to design the membership functions for the fuzzy controller, few works have been carried out to optimize the membership functions. Given a performance index (cost function) to evaluate the time response of the system, the membership functions from PDC approach may not be the optimal membership functions to offer the best time response. In [75], the optimal membership functions were designed under the frequency domain such that a desired closed-loop behavior is guaranteed throughout the entire operating domain. However, in some cases, only approximate optimal membership functions can be obtained. In [76–78], a systematic method for designing optimal membership functions was proposed in a general setting. The variational method is employed to acquire the gradient of the cost function with respect to design parameters in the membership functions, and the gradient descent approach is used to obtain the stationary point of the cost function. Nevertheless, the cost function does not take the control input into account, and the summation-one property of the membership functions is not considered resulting in imprecise calculation of the dynamics of the closed-loop system and the gradients. To the best of the author’s knowledge, the optimization of membership functions has only been investigated for fuzzy controllers and it has not been investigated for fuzzy observer-controllers.

## 1.3 Objectives and Organization

The main objective of the thesis is improving the applicability of FMB control strategy by relaxing stability conditions and designing fuzzy observer-controller, which is detailed as follows:

- 1) Relax stability conditions by HODLF for T-S FMB control systems and by Taylor series membership functions (TSMFs) for polynomial fuzzy-model-based (PFMB) control systems.
- 2) Design relaxed T-S fuzzy observer-controller with unmeasurable premise variables and T-S fuzzy functional observer.
- 3) Design polynomial fuzzy observer-controller with unmeasurable premise variables, combine it with sampled-output measurement and optimize its membership functions.

According to these objectives, this thesis is separated to three main chapters as shown in Fig. 1.5. The relaxation of stability conditions is discussed in a single chapter. The fuzzy observer is separated into two chapters. One is for T-S fuzzy observer, and the other is for polynomial fuzzy observer which generalizes the T-S one. The rest of the thesis is organized as follows:

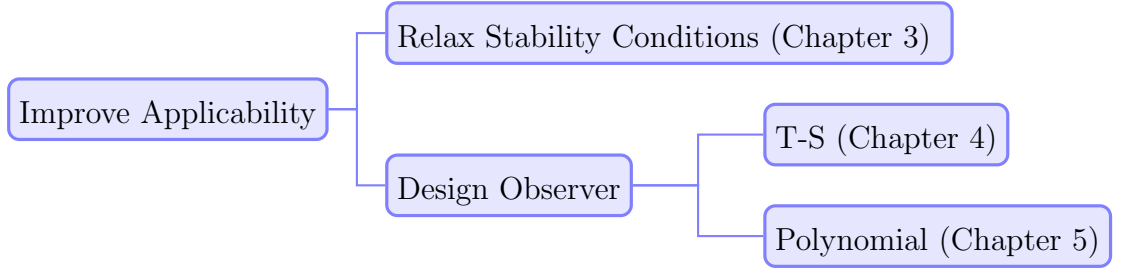


Figure 1.5: Relation of main chapters.

- In Chapter 2, the method for fuzzy modeling is given first. Next, the basic formulation of T-S FMB control systems and PFMB control systems are provided. The Lyapunov stability theory and LMI/SOS stability conditions are introduced. Moreover, some useful lemmas are presented. These contents are the background knowledge of the subsequent chapters.
- In Chapter 3, the relaxation of stability conditions of FMB control systems are proposed. The HODLF is employed for T-S FMB control systems, and TSMFs are applied for PFMB control systems.
- In Chapter 4, the T-S fuzzy observer is considered and two types of T-S fuzzy observer-controller are designed. One is relaxed T-S fuzzy observer-controller with unmeasurable premise variables. Another is T-S fuzzy functional observer, which estimates the control input directly.
- In Chapter 5, the polynomial fuzzy observer-controller with unmeasurable premise variables is designed, which is a generalization of T-S fuzzy observer-controller. Two methods are applied to derive convex stability conditions: matrix decoupling technique and refined completing square approach. Additionally, the designed polynomial fuzzy observer-controller is extended for systems where only sampled-output measurements are available. The membership functions of the designed polynomial observer-controller are optimized by the improved gradient descent method for better performance.
- In Chapter 6, the conclusion of this thesis is drawn and the some potential research problems are proposed for future work. The comparisons between the proposed methods and existing methods are summarized.



# Chapter 2

## Preliminary

### 2.1 Notations

The following notation is employed throughout this thesis [12]. The expressions of  $\mathbf{M} > 0$ ,  $\mathbf{M} \geq 0$ ,  $\mathbf{M} < 0$  and  $\mathbf{M} \leq 0$  denote the positive, semi-positive, negative and semi-negative definite matrices  $\mathbf{M}$ , respectively. The symbol “\*” in a matrix represents the transposed element in the corresponding position. The symbol “diag{...}” stands for a block-diagonal matrix. The superscript “ $-T$ ” represents the inverse of the transpose. The superscript “ $+$ ” stands for the Moore-Penrose generalized inverse.

A monomial in  $\mathbf{x}(t) = [x_1(t), x_2(t), \dots, x_n(t)]^T$  is a function of the form  $x_1^{d_1}(t)x_2^{d_2}(t)\cdots x_n^{d_n}(t)$ , where  $d_i \geq 0, i = 1, 2, \dots, n$ , are integers. The degree of a monomial is  $d = \sum_{i=1}^n d_i$ . A polynomial  $\mathbf{p}(\mathbf{x}(t))$  is a finite linear combination of monomials with real coefficients. A polynomial  $\mathbf{p}(\mathbf{x}(t))$  is an SOS if it can be written as  $\mathbf{p}(\mathbf{x}(t)) = \sum_{j=1}^m \mathbf{q}_j(\mathbf{x}(t))^2$ , where  $\mathbf{q}_j(\mathbf{x}(t))$  is a polynomial and  $m$  is a nonnegative integer. It can be concluded that if  $\mathbf{p}(\mathbf{x}(t))$  is an SOS, then  $\mathbf{p}(\mathbf{x}(t)) \geq 0$ .

Other mathematical fonts are in standard format: scalars are in italic fonts; vectors are in bold fonts; and matrices are in bold and capital fonts.

In some figures, readers may wish to look at the changes at the beginning of time more closely. To save space, we will put such “zoom-in” figures at the empty space within the original figures.

### 2.2 Sector Nonlinearity Technique

The general nonlinear system investigated in this thesis is the autonomous (not explicitly depend on time  $t$ ) input-affine system in the following state-space form:

$$\dot{\mathbf{x}}(t) = \mathbf{A}(\mathbf{x}(t))\mathbf{x}(t) + \mathbf{B}(\mathbf{x}(t))\mathbf{u}(t), \quad (2.1)$$

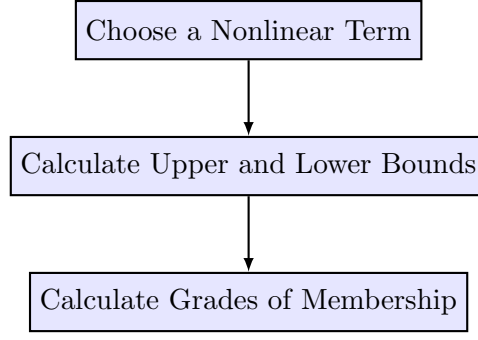


Figure 2.1: Procedure of sector nonlinearity technique.

where  $t$  is the continuous time in seconds;  $\mathbf{x}(t)$  is the system state vector;  $\mathbf{A}(\mathbf{x}(t))$  is the system matrix;  $\mathbf{B}(\mathbf{x}(t))$  is the input matrix; and  $\mathbf{u}(t)$  is control input.

The fuzzy modeling process in this thesis is achieved by sector nonlinearity technique [1, 8]. The sector nonlinearity technique is employed to represent each nonlinear term in  $\mathbf{A}(\mathbf{x}(t))$  and  $\mathbf{B}(\mathbf{x}(t))$ . The procedure is shown in Fig. 2.1.

For example (time  $t$  is omitted in this example), if the nonlinear term is chosen to be  $f_1(\mathbf{x})$ , we have the upper and lower bounds  $f_{1_{max}}, f_{1_{min}}$ . Conceptually, we use following fuzzy rules to interpret the modeling process:

$$\begin{aligned}
 \text{Rule 1 : IF } f_1(\mathbf{x}) \text{ is around } f_{1_{min}}, \\
 \text{THEN } f_1(\mathbf{x}) &= f_{1_{min}}, \\
 \text{Rule 2 : IF } f_1(\mathbf{x}) \text{ is around } f_{1_{max}}, \\
 \text{THEN } f_1(\mathbf{x}) &= f_{1_{max}}.
 \end{aligned}$$

The membership functions are employed to combine the fuzzy rules. To calculate the grades of membership, we employ the following relations:

$$\begin{aligned}
 f_1(\mathbf{x}) &= \mu_{M_1^1}(\mathbf{x})f_{1_{min}} + \mu_{M_1^2}(\mathbf{x})f_{1_{max}}, \\
 \mu_{M_1^1}(\mathbf{x}) + \mu_{M_1^2}(\mathbf{x}) &= 1,
 \end{aligned}$$

where  $\mu_{M_1^1}(\mathbf{x})$  and  $\mu_{M_1^2}(\mathbf{x})$  are the grades of membership corresponding to the fuzzy terms  $M_1^1$  and  $M_1^2$ , respectively. In this case, the fuzzy terms  $M_1^1$  and  $M_1^2$  are “around  $f_{1_{min}}$ ” and “around  $f_{1_{max}}$ ”, respectively. Therefore, we can obtain

$$\mu_{M_1^1}(\mathbf{x}) = \frac{f_1(\mathbf{x}) - f_{1_{max}}}{f_{1_{min}} - f_{1_{max}}}, \mu_{M_1^2}(\mathbf{x}) = 1 - \mu_{M_1^1}(\mathbf{x}).$$

By representing each nonlinear term in the nonlinear system, a fuzzy model is eventually established. The overall form of the fuzzy model will be introduced in the following sections.

There are several conditions and properties for this technique:

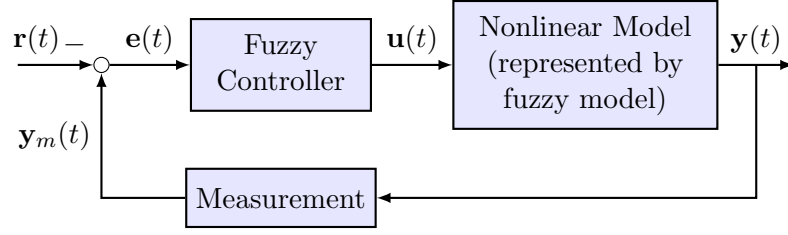


Figure 2.2: A block diagram of FMB control systems.

- 1) The nonlinear terms can be chosen in different ways, and thus the fuzzy model is not unique. For example, treat two single terms “ $\sin(\mathbf{x}) + \cos(\mathbf{x})$ ” as a whole term. Note that a single nonlinear term cannot be separately represented. Taking “ $(\sin(\mathbf{x}))^2$ ” for instance, it is not allowed to represent “ $\sin(\mathbf{x})$ ” twice. The reason is that if separately represented the grade of membership for each nonlinear term cannot be factored out to form the overall membership functions.
- 2) If a nonlinear term is unbounded, the region of interest (that is the domain of system states) has to be assumed such that the nonlinear term can be bounded.
- 3) The grades of membership as well as the over membership functions have non-negative and summation-one properties.

Due to the occurrence of polynomial fuzzy model, the sector nonlinearity technique was extended using Taylor series expansion [9] to establish progressively precise polynomial fuzzy models. Since this more advanced technique is not applied in this thesis, the technical details will be omitted here.

## 2.3 T-S FMB Control System

A general structure of the FMB control system is shown in Fig. 2.2, where  $\mathbf{r}(t)$  is the reference signal,  $\mathbf{e}(t) = \mathbf{y}_m(t) - \mathbf{r}(t)$  is error between the reference signal and the measured output,  $\mathbf{u}(t)$  is the control input,  $\mathbf{y}(t)$  is the system output, and  $\mathbf{y}_m(t)$  is the measured output.

In this thesis, without losing generality, we consider the stabilization of systems at the equilibrium point  $\mathbf{x}(t) = \mathbf{0}$  where  $\mathbf{x}(t)$  is the system state vector. Then the reference signal is  $\mathbf{r}(t) = \mathbf{0} \forall t$ . If the equilibrium point is not zero in some cases, one can apply the coordinate transformation such that the equilibrium point becomes zero at the new coordinates.

Additionally, in this section, we introduce a simplified case, that is the full-state feedback  $\mathbf{y}_m(t) = \mathbf{y}(t) = \mathbf{x}(t) \forall t$ . Note that this assumption will be changed when considering other control problems such as observer and sampled-output measurement in the following chapters. The simplified structure becomes Fig. 2.3.

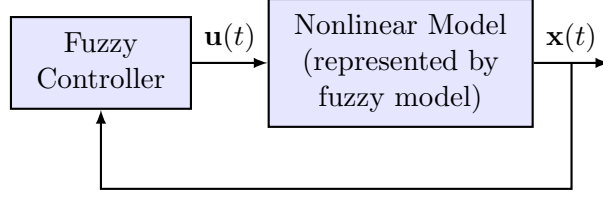


Figure 2.3: A simplified block diagram of FMB control systems.

### 2.3.1 T-S Fuzzy Model

T-S fuzzy model [5,6] has been widely used as a modeling tool for nonlinear systems. It represents nonlinear systems as a combination of local linear subsystems weighted by membership functions. This particular modeling structure allows analysis techniques and control methods used for linear systems to be applied.

The  $i^{th}$  rule of the T-S fuzzy model [5,6] representing a nonlinear plant is given as follows:

$$\begin{aligned} \text{Rule } i : & \text{ IF } f_1(\mathbf{x}(t)) \text{ is } M_1^i \text{ AND } \cdots \text{ AND } f_\Psi(\mathbf{x}(t)) \text{ is } M_\Psi^i, \\ & \text{ THEN } \dot{\mathbf{x}}(t) = \mathbf{A}_i \mathbf{x}(t) + \mathbf{B}_i \mathbf{u}(t), \end{aligned}$$

where  $\mathbf{x}(t) = [x_1(t), x_2(t), \dots, x_n(t)]^T$  is the state vector, and  $n$  is the dimension of the nonlinear system;  $f_\eta(\mathbf{x}(t))$  is the premise variable corresponding to its fuzzy term  $M_\eta^i$  in rule  $i$ ,  $\eta = 1, 2, \dots, \Psi$ , and  $\Psi$  is a positive integer;  $\mathbf{A}_i \in \mathfrak{R}^{n \times n}$  and  $\mathbf{B}_i \in \mathfrak{R}^{n \times m}$  are the known system and input matrices, respectively;  $\mathbf{u}(t) \in \mathfrak{R}^m$  is the control input vector. The dynamics of the nonlinear system is described by the following T-S fuzzy model:

$$\dot{\mathbf{x}}(t) = \sum_{i=1}^p w_i(\mathbf{x}(t)) (\mathbf{A}_i \mathbf{x}(t) + \mathbf{B}_i \mathbf{u}(t)), \quad (2.2)$$

where  $p$  is the number of fuzzy rules;  $w_i(\mathbf{x}(t))$  is the normalized grade of membership,  $w_i(\mathbf{x}(t)) = \frac{\prod_{\eta=1}^{\Psi} \mu_{M_\eta^i}(f_\eta(\mathbf{x}(t)))}{\sum_{k=1}^p \prod_{\eta=1}^{\Psi} \mu_{M_\eta^k}(f_\eta(\mathbf{x}(t)))}$ ,  $w_i(\mathbf{x}(t)) \geq 0, i = 1, 2, \dots, p$ , and  $\sum_{i=1}^p w_i(\mathbf{x}(t)) = 1$ ;  $\mu_{M_\eta^i}(f_\eta(\mathbf{x}(t)))$ ,  $\eta = 1, 2, \dots, \Psi$ , are the grades of membership corresponding to the fuzzy term  $M_\eta^i$ . Note that if the sector nonlinearity technique is used for fuzzy modeling, no normalization is required, that is  $w_i(\mathbf{x}(t)) = \prod_{\eta=1}^{\Psi} \mu_{M_\eta^i}(f_\eta(\mathbf{x}(t)))$ , since  $\sum_{k=1}^p \prod_{\eta=1}^{\Psi} \mu_{M_\eta^k}(f_\eta(\mathbf{x}(t))) = 1$ .

### 2.3.2 T-S Fuzzy Controller

Using the PDC approach [1], the  $j^{th}$  rule of the fuzzy controller is described as follows:

$$\text{Rule } j : \text{ IF } f_1(\mathbf{x}(t)) \text{ is } M_1^j \text{ AND } \cdots \text{ AND } f_\Psi(\mathbf{x}(t)) \text{ is } M_\Psi^j,$$

$$\text{THEN } \mathbf{u}(t) = \mathbf{G}_j \mathbf{x}(t),$$

where  $\mathbf{G}_j \in \mathbb{R}^{m \times n}$  is the controller gain. The fuzzy controller, which is to control the nonlinear system, is given by

$$\mathbf{u}(t) = \sum_{j=1}^p w_j(\mathbf{x}(t)) \mathbf{G}_j \mathbf{x}(t). \quad (2.3)$$

The PDC approach means that the fuzzy controller shares the same membership functions as the fuzzy model. Although the concept is straightforward and the conservativeness is less, the flexibility, the complexity and the performance of the fuzzy controller are not taken into account. In this thesis, the non-PDC approach is also considered for some cases.

### 2.3.3 T-S FMB Control System

The T-S FMB control system consisting of the T-S fuzzy model (2.2) and the T-S fuzzy controller (2.3) is formulated as follows:

$$\dot{\mathbf{x}}(t) = \sum_{i=1}^p \sum_{j=1}^p w_i(\mathbf{x}(t)) w_j(\mathbf{x}(t)) (\mathbf{A}_i + \mathbf{B}_i \mathbf{G}_j) \mathbf{x}(t). \quad (2.4)$$

This system is simply formed by substituting the fuzzy controller (2.3) into the fuzzy model (2.2).

## 2.4 PFMB Control System

Since the PFMB control system was proposed [3, 4] to generalize the T-S FMB control system, the forms of PFMB control systems are similar to the T-S ones. The overall structure is the same as the one in Fig. 2.3.

### 2.4.1 Polynomial Fuzzy Model

With the enhanced modeling capability of the polynomial fuzzy model, the polynomial terms do not need to be modeled by the sector nonlinearity technique. It reduces the number of fuzzy rules and provides global stability instead of local stability in some cases. Moreover, polynomials can be used to approximate the nonlinear terms to establish approximated fuzzy model.

The  $i^{th}$  rule of the polynomial fuzzy model for the nonlinear plant is presented

as follows [3]:

$$\begin{aligned} \text{Rule } i : & \text{IF } f_1(\mathbf{x}(t)) \text{ is } M_1^i \text{ AND } \cdots \text{ AND } f_\Psi(\mathbf{x}(t)) \text{ is } M_\Psi^i \\ \text{THEN } & \dot{\mathbf{x}}(t) = \mathbf{A}_i(\mathbf{x}(t))\hat{\mathbf{x}}(\mathbf{x}(t)) + \mathbf{B}_i(\mathbf{x}(t))\mathbf{u}(t), \end{aligned}$$

where  $\mathbf{x}(t) = [x_1(t), x_2(t), \dots, x_n(t)]^T$  is the state vector, and  $n$  is the dimension of the nonlinear plant;  $f_\alpha(\mathbf{x}(t))$  is the premise variable corresponding to its fuzzy term  $M_\alpha^i$  in rule  $i$ ,  $\alpha = 1, 2, \dots, \Psi$ , and  $\Psi$  is a positive integer;  $\mathbf{A}_i(\mathbf{x}(t)) \in \Re^{n \times n}$  and  $\mathbf{B}_i(\mathbf{x}(t)) \in \Re^{n \times m}$  are the known polynomial system and input matrices, respectively;  $\hat{\mathbf{x}}(t) = [\hat{x}_1(t), \hat{x}_2(t), \dots, \hat{x}_N(t)]^T$  is a vector of monomials in  $\mathbf{x}(t)$ , and it is assumed that  $\hat{\mathbf{x}}(t) = \mathbf{0}$ , iff  $\mathbf{x}(t) = \mathbf{0}$ ;  $\mathbf{u}(t) \in \Re^m$  is the control input vector. Thus, the dynamics of the nonlinear plant is given by

$$\dot{\mathbf{x}}(t) = \sum_{i=1}^p w_i(\mathbf{x}(t)) (\mathbf{A}_i(\mathbf{x}(t))\hat{\mathbf{x}}(\mathbf{x}(t)) + \mathbf{B}_i(\mathbf{x}(t))\mathbf{u}(t)), \quad (2.5)$$

where  $p$  is the number of rules in the polynomial fuzzy model;  $w_i(\mathbf{x}(t))$  is the normalized grade of membership,  $w_i(\mathbf{x}(t)) = \frac{\prod_{l=1}^{\Psi} \mu_{M_l^i}(f_l(\mathbf{x}(t)))}{\sum_{k=1}^p \prod_{l=1}^{\Psi} \mu_{M_l^k}(f_l(\mathbf{x}(t)))}$ ,  $w_i(\mathbf{x}(t)) \geq 0$ ,  $i = 1, 2, \dots, p$ , and  $\sum_{i=1}^p w_i(\mathbf{x}(t)) = 1$ ;  $\mu_{M_\alpha^i}(f_\alpha(\mathbf{x}(t)))$ ,  $\alpha = 1, 2, \dots, \Psi$ , are grades of membership corresponding to the fuzzy term  $M_\alpha^i$ .

## 2.4.2 Polynomial Fuzzy Controller

The  $j^{\text{th}}$  rule of the polynomial fuzzy controller is presented as follows:

$$\begin{aligned} \text{Rule } j : & \text{IF } f_1(\mathbf{x}(t)) \text{ is } M_1^j \text{ AND } \cdots \text{ AND } f_\Psi(\mathbf{x}(t)) \text{ is } M_\Psi^j \\ \text{THEN } & \mathbf{u}(t) = \mathbf{G}_j(\mathbf{x}(t))\hat{\mathbf{x}}(\mathbf{x}(t)), \end{aligned}$$

where  $\mathbf{G}_j(\mathbf{x}(t)) \in \Re^{m \times N}$  is the polynomial feedback gain in rule  $j$ . Thus, the following polynomial fuzzy controller is applied to the nonlinear plant represented by the polynomial fuzzy model (2.5):

$$\mathbf{u}(t) = \sum_{j=1}^p w_j(\mathbf{x}(t)) \mathbf{G}_j(\mathbf{x}(t))\hat{\mathbf{x}}(\mathbf{x}(t)). \quad (2.6)$$

## 2.4.3 PFMB Control System

The PFMB control system formed by the polynomial fuzzy model (2.5) and the polynomial fuzzy controller (2.6) is

$$\dot{\mathbf{x}}(t) = \sum_{i=1}^p \sum_{j=1}^p w_i(\mathbf{x}(t)) w_j(\mathbf{x}(t)) (\mathbf{A}_i(\mathbf{x}(t)) + \mathbf{B}_i(\mathbf{x}(t))\mathbf{G}_j(\mathbf{x}(t)))\hat{\mathbf{x}}(\mathbf{x}(t)). \quad (2.7)$$

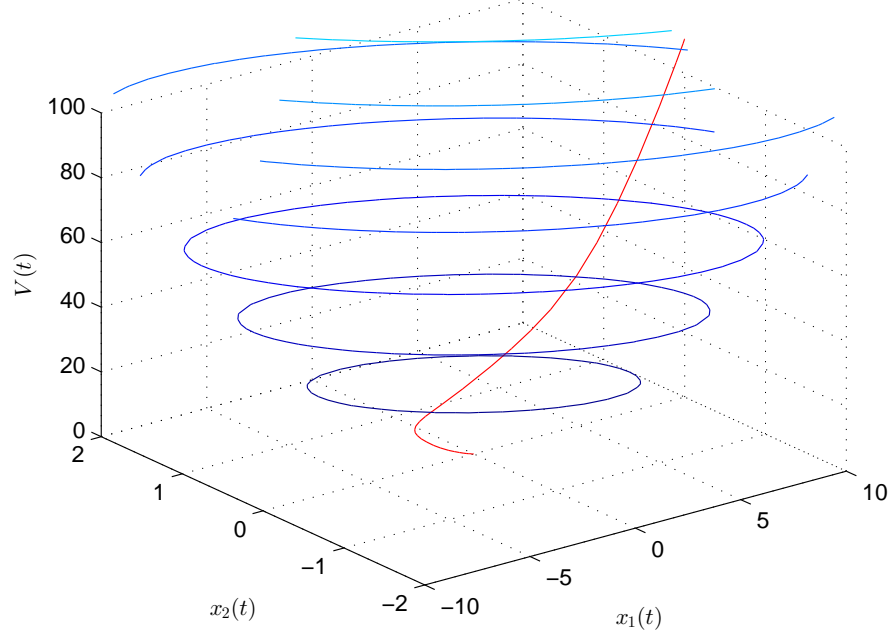


Figure 2.4: Geometric meaning of Lyapunov functions.

This system is simply formed by substituting the polynomial fuzzy controller (2.6) into the polynomial fuzzy model (2.5).

## 2.5 Lyapunov Stability Theory

The Lyapunov stability theory is a useful tool to investigate the stability of dynamic system in time domain. The nonlinear system  $\dot{\mathbf{x}}(t) = f(\mathbf{x}(t))$  ( $f : \mathbb{R}^n \rightarrow \mathbb{R}^n$  has an equilibrium point at the origin) is guaranteed to be asymptotically stable if there exist a Lyapunov function  $V(\mathbf{x}(t))$  such that the following conditions are satisfied [79]:

$$\begin{aligned} V(\mathbf{x}(t) = \mathbf{0}) &= 0, \\ V(\mathbf{x}(t)) &> 0 \quad \forall \mathbf{x}(t) \neq \mathbf{0}, \\ \dot{V}(\mathbf{x}(t)) &< 0 \quad \forall \mathbf{x}(t) \neq \mathbf{0}. \end{aligned}$$

The Lyapunov function  $V(\mathbf{x}(t))$  describes the energy of a dynamic system, which can be chosen as different forms. Fig. 2.4 shows the geometric meaning of Lyapunov functions. The blue lines indicate the energy levels of the Lyapunov function. The red line indicates the trajectory of system states. As time goes by, the system states reach the equilibrium point (the origin) and the energy level of the Lyapunov function decays to zero at the same time. Consequently, to ensure the stability of the system, we only need to ensure the decay of the Lyapunov function.

## 2.6 LMI/SOS Stability Conditions

The Lyapunov stability theory results in the development of LMI problem in history since the stability conditions become a set of LMIs [20]. For example, the linear system  $\dot{\mathbf{x}}(t) = \mathbf{A}\mathbf{x}(t)$  is stable if and only if there exists a matrix  $\mathbf{P}$  with appropriate dimensions such that

$$\begin{aligned}\mathbf{P} &> 0, \\ \mathbf{A}^T\mathbf{P} + \mathbf{P}\mathbf{A} &< 0,\end{aligned}$$

In these LMIs, the variables are matrices and the inequalities represent the positive or negative definite matrices. More importantly, the inequalities are linear (convex) in matrix variable  $\mathbf{P}$ , which can be solved via MATLAB LMI toolbox. However, for FMB control systems, the inequalities are often nonlinear (non-convex) in matrix variables. Due to the limitation of current convex programming technique, only LMIs and some related problems can be numerically solved with tractable results from both theoretical and practical viewpoints [20]. Therefore, how to transform non-convex stability conditions into convex ones is a critical problem for FMB control strategy. In addition, how to introduce less conservativeness during the transformation is also a crucial problem. Consequently, in this thesis, the main effort is put into the derivation of convex stability conditions and the relaxation of stability conditions.

The SOS approach is a generalization of LMI approach. Not only can it deal with constant matrices, it can also tackle polynomial matrices. For this reason, it is widely applied to polynomial systems and polynomial fuzzy systems. To prove a symmetric polynomial matrix  $\mathbf{P}(\mathbf{x}(t))$  to be positive semidefinite, the following relation is employed to establish SOS stability conditions [12]:

$$\begin{aligned}\nu(t)^T\mathbf{P}(\mathbf{x}(t))\nu(t) &\text{ is an SOS} \\ \implies \mathbf{P}(\mathbf{x}(t)) &\geq 0 \ \forall \ \mathbf{x}(t)\end{aligned}$$

where  $\nu$  is an arbitrary vector independent of  $\mathbf{x}$ . The SOS conditions can be converted into semidefinite programming problem by SOSTOOLS [13] and then solved by SeDuMi [14]. Both of them are third party MATLAB toolboxes. For some complex SOS conditions, the numerical solutions are not absolutely reliable due to the numerical error. The time response of the system or eigenvalues of the local linearized system need to be checked after obtaining the solutions.

## 2.7 Useful Lemmas

The following lemmas are employed in the chapters to follow.



**Lemma 1 (Schur complement)** *With matrices  $\mathbf{A}$ ,  $\mathbf{B}$  and  $\mathbf{C}$  of appropriate dimensions and  $\mathbf{A} = \mathbf{A}^T, \mathbf{C} = \mathbf{C}^T$ , the following relation holds [20]:*

$$\begin{bmatrix} \mathbf{A} & \mathbf{B} \\ \mathbf{B}^T & \mathbf{C} \end{bmatrix} > 0 \iff \mathbf{C} > 0, \mathbf{A} - \mathbf{B}\mathbf{C}^{-1}\mathbf{B}^T > 0$$

**Lemma 2 (S-procedure)** *With symmetric matrices  $\mathbf{T}_0, \dots, \mathbf{T}_p$  and vector  $\mathbf{v}$  of appropriate dimensions, the following relation holds [20]:*

$$\begin{aligned} & \text{there exists } \tau_1 \geq 0, \dots, \tau_p \geq 0 \text{ such that } \mathbf{T}_0 - \sum_{i=1}^p \tau_i \mathbf{T}_i > 0 \\ \implies & \mathbf{v}^T \mathbf{T}_0 \mathbf{v} > 0 \text{ holds for all } \mathbf{v} \neq \mathbf{0} \text{ that satisfy } \mathbf{v}^T \mathbf{T}_i \mathbf{v} > 0, i = 1, 2, \dots, p. \end{aligned}$$

**Lemma 3 (HODLF)** *The nonlinear system  $\dot{\mathbf{x}}(t) = f(\mathbf{x}(t))$  ( $f : \mathbb{R}^n \rightarrow \mathbb{R}^n$  has an equilibrium point at the origin) is guaranteed to be asymptotically stable if there exist Lyapunov functions  $V_1(\mathbf{x}(t))$  and  $V_2(\mathbf{x}(t))$  such that the following conditions are satisfied [39]:*

$$W(\mathbf{0}) = \dot{V}_2(\mathbf{0}) + V_1(\mathbf{0}) = 0, \quad (2.8)$$

$$W(\mathbf{x}(t)) = \dot{V}_2(\mathbf{x}(t)) + V_1(\mathbf{x}(t)) > 0 \quad \forall \mathbf{x}(t) \neq \mathbf{0}, \quad (2.9)$$

$$\dot{W}(\mathbf{x}(t)) = \ddot{V}_2(\mathbf{x}(t)) + \dot{V}_1(\mathbf{x}(t)) < 0 \quad \forall \mathbf{x}(t) \neq \mathbf{0}. \quad (2.10)$$

**Lemma 4 (completing square)** *With matrices  $\mathbf{X}$  and  $\mathbf{Y}$  of appropriate dimensions and scalar  $\beta > 0$ , the following inequality holds [80]:*

$$\mathbf{X}^T \mathbf{Y} + \mathbf{Y}^T \mathbf{X} \leq \beta \mathbf{X}^T \mathbf{X} + \frac{1}{\beta} \mathbf{Y}^T \mathbf{Y}.$$

**Lemma 5 (completing square)** *With  $\mathbf{P}, \mathbf{Q}$  of appropriate dimension,  $\mathbf{Q} > 0$  and a scalar  $\gamma$ , the following inequality holds [80]:*

$$-\mathbf{P}^T \mathbf{Q}^{-1} \mathbf{P} \leq \gamma^2 \mathbf{Q} - \gamma(\mathbf{P}^T + \mathbf{P}).$$

**Lemma 6 (Jensen's inequality)** *With  $\mathbf{x}(t), \mathbf{Q}$  of appropriate dimension,  $\mathbf{Q} > 0$  and  $h > 0$ , the following inequality holds [81]:*

$$\begin{aligned} & -h \int_{t-h}^t \dot{\mathbf{x}}(\varphi)^T \mathbf{Q} \dot{\mathbf{x}}(\varphi) d\varphi \\ & \leq -(\mathbf{x}(t) - \mathbf{x}(t-h))^T \mathbf{Q} (\mathbf{x}(t) - \mathbf{x}(t-h)). \end{aligned}$$

**Lemma 7** *For any invertible polynomial matrix  $\mathbf{X}(\mathbf{y})$  where  $\mathbf{y} = [y_1, y_2, \dots, y_n]^T$ ,*

the following equation is true [3, 12].

$$\frac{\partial \mathbf{X}(\mathbf{y})^{-1}}{\partial y_j} = -\mathbf{X}(\mathbf{y})^{-1} \frac{\partial \mathbf{X}(\mathbf{y})}{\partial y_j} \mathbf{X}(\mathbf{y})^{-1} \quad \forall j$$

# Chapter 3

## Relaxation of Stability Conditions

When solving the stability conditions, even though the system is controllable, the conservativeness leads to infeasible solutions, which means the feedback gains cannot be obtained. It restricts the applicability of FMB control scheme. To improve the applicability of FMB control strategy, the conservativeness of stability conditions needs to be reduced. In this chapter, the relaxation of stability conditions of FMB control systems is proposed. The HODLF is employed for T-S FMB control systems, and TSMFs are applied for PFMB control systems.

### 3.1 Higher Order Derivatives of Lyapunov Function for T-S FMB Control Systems

#### 3.1.1 Introduction

In this section, we aim to enhance the applicability of T-S FMB control scheme by relaxing the stability conditions. The HODLF in [39] is exploited to achieve the relaxation of stability analysis when designing the fuzzy controller. To tackle the difficulty of the derivative of membership functions and obtaining convex stability conditions, the technique used in [2] is employed and improved in this section. First, more properties of membership functions and the dynamics of FMB control system are utilized to derive convex conditions due to the occurrence of higher order terms. Second, the lower bound of the derivative of membership functions is allowed to be different from the upper bound, which leads to more relaxed conditions. Compared with existing work in discrete time [40–46], this is the first attempt to consider HODLF in continuous-time FMB control systems. Also, it can be demonstrated from the simulation that the proposed stability conditions from HODLF are more relaxed than those from the fuzzy Lyapunov function in [2] by comparing the stabilization region. Note that the boundary requirement of the derivative of membership functions may not be met in some cases [37]. More advanced techniques such as [36, 37] may be applied in the future to meet the boundary requirement or

to provide more relaxed conditions.

This section is organized as follows. Stability analysis of FMB control system is conducted via HODLF in Subsection 3.1.2. Simulation examples are given in Subsection 3.1.3 to demonstrate the proposed design procedure. Finally, a conclusion is drawn in Subsection 3.1.4.

### 3.1.2 Stability Analysis

In this section, we conduct the stability analysis for T-S FMB control systems. The stability conditions are derived via HODLF.

For brevity, time  $t$  is dropped without ambiguity and the membership function  $w_i(\mathbf{x})$  is denoted as  $w_i$ . The FMB control system consisting of the T-S fuzzy model (2.2) and the T-S fuzzy controller (2.3) is formulated as follows:

$$\dot{\mathbf{x}} = \sum_{i=1}^p \sum_{j=1}^p h_{ij}(\mathbf{A}_i + \mathbf{B}_i \mathbf{G}_j) \mathbf{x}, \quad (3.1)$$

where  $h_{ij} \equiv w_i w_j$ .

The control objective is to make the T-S FMB control system (3.1) asymptotically stable, i.e.,  $\mathbf{x} \rightarrow 0$  as time  $t \rightarrow \infty$ , by determining the feedback gain  $\mathbf{G}_j$ .

**Theorem 1** *The FMB control system (3.1) with differentiable membership functions is guaranteed to be asymptotically stable if there exist an invertible matrix  $\mathbf{X} \in \mathbb{R}^{n \times n}$ , matrices  $\tilde{\mathbf{P}}_{1i} = \tilde{\mathbf{P}}_{1i}^T \in \mathbb{R}^{n \times n}$ ,  $\tilde{\mathbf{P}}_2 = \tilde{\mathbf{P}}_2^T \in \mathbb{R}^{n \times n}$ ,  $\tilde{\mathbf{Y}}_1 = \tilde{\mathbf{Y}}_1^T \in \mathbb{R}^{n \times n}$ ,  $\tilde{\mathbf{Y}}_2 \in \mathbb{R}^{n \times n}$ ,  $\tilde{\mathbf{S}}_i = \tilde{\mathbf{S}}_i^T \in \mathbb{R}^{n \times n}$ ,  $\mathbf{N}_j \in \mathbb{R}^{m \times n}$ , and predefined scalars  $\beta_{ij} > 0, \mu_1, \mu_2, \dots, \mu_6, i, j = 1, 2, \dots, p$  such that the following LMI-based conditions are satisfied:*

$$\tilde{\Theta}_{ij} + \tilde{\Theta}_{ji} > 0 \quad \forall i \leq j, \quad (3.2)$$

$$\tilde{\mathbf{P}}_{1i} - \tilde{\mathbf{Y}}_1 \leq \tilde{\mathbf{S}}_i \quad \forall i, \quad (3.3)$$

$$\tilde{\mathbf{S}}_i \geq 0 \quad \forall i, \quad (3.4)$$

$$\Psi_{ij} + \Psi_{ji} < 0 \quad \forall i \leq j, \quad (3.5)$$

where

$$\begin{aligned} \tilde{\Theta}_{ij} &= \begin{bmatrix} \tilde{\Theta}_{ij}^{(11)} & * \\ \tilde{\Theta}_{ij}^{(21)} & \tilde{\Theta}^{(22)} \end{bmatrix}, \\ \tilde{\Theta}_{ij}^{(11)} &= \tilde{\mathbf{P}}_{1i} + \mu_1(\mathbf{A}_i \mathbf{X}^T + \mathbf{B}_i \mathbf{N}_j) + \mu_1(\mathbf{A}_i \mathbf{X}^T + \mathbf{B}_i \mathbf{N}_j)^T, \\ \tilde{\Theta}_{ij}^{(21)} &= \tilde{\mathbf{P}}_2 - \mu_1 \mathbf{X} + \mu_2(\mathbf{A}_i \mathbf{X}^T + \mathbf{B}_i \mathbf{N}_j), \\ \tilde{\Theta}^{(22)} &= -\mu_2(\mathbf{X} + \mathbf{X}^T), \end{aligned}$$

$$\begin{aligned}
\Psi_{ij} &= \begin{bmatrix} \tilde{\Xi}_{ij} & * & * & * & \cdots & * \\ \tilde{\Upsilon} & \Psi^{(22)} & * & * & \cdots & * \\ \tilde{\Omega}_{11} & \mathbf{0} & -\beta_{11}\mathbf{I} & * & \cdots & * \\ \tilde{\Omega}_{12} & \mathbf{0} & \mathbf{0} & -\beta_{12}\mathbf{I} & \cdots & * \\ \vdots & \vdots & \vdots & \vdots & \ddots & \vdots \\ \tilde{\Omega}_{pp} & \mathbf{0} & \mathbf{0} & \mathbf{0} & \cdots & -\beta_{pp}\mathbf{I} \end{bmatrix}, \\
\Psi^{(22)} &= -\frac{1}{\sum_{r=1}^p \sum_{s=1}^p \beta_{rs}} \mathbf{I}, \\
\tilde{\Xi}_{ij} &= \begin{bmatrix} \tilde{\Xi}_{ij}^{(11)} & * & * \\ \tilde{\Xi}_{ij}^{(21)} & \tilde{\Xi}_{ij}^{(22)} & * \\ \tilde{\Xi}_{ij}^{(31)} & \tilde{\Xi}_{ij}^{(32)} & \tilde{\Xi}_{ij}^{(33)} \end{bmatrix}, \\
\tilde{\Xi}_{ij}^{(11)} &= \sum_{r=1}^p (\bar{\phi}_r - \underline{\phi}_r) \tilde{\mathbf{S}}_r + \sum_{r=1}^p \underline{\phi}_r (\tilde{\mathbf{P}}_{1r} - \tilde{\mathbf{Y}}_1) \\
&\quad + (\mathbf{A}_i \mathbf{X}^T + \mathbf{B}_i \mathbf{N}_j) + (\mathbf{A}_i \mathbf{X}^T + \mathbf{B}_i \mathbf{N}_j)^T, \\
\tilde{\Xi}_{ij}^{(21)} &= \tilde{\mathbf{P}}_{1i} - \mathbf{X} + \mu_3 (\mathbf{A}_i \mathbf{X}^T + \mathbf{B}_i \mathbf{N}_j) \\
&\quad + \mu_4 (\mathbf{A}_i \mathbf{X}^T + \mathbf{B}_i \mathbf{N}_j)^T, \\
\tilde{\Xi}_{ij}^{(22)} &= 2\tilde{\mathbf{P}}_2 - \mu_3 (\mathbf{X} + \mathbf{X}^T) + \mu_5 (\mathbf{A}_i \mathbf{X}^T + \mathbf{B}_i \mathbf{N}_j) \\
&\quad + \mu_5 (\mathbf{A}_i \mathbf{X}^T + \mathbf{B}_i \mathbf{N}_j)^T, \\
\tilde{\Xi}_{ij}^{(31)} &= \tilde{\mathbf{P}}_2 - \mu_4 \mathbf{X}, \\
\tilde{\Xi}_{ij}^{(32)} &= \mu_6 (\mathbf{A}_i \mathbf{X}^T + \mathbf{B}_i \mathbf{N}_j) - \mu_5 \mathbf{X}, \\
\tilde{\Xi}_{ij}^{(33)} &= -\mu_6 (\mathbf{X} + \mathbf{X}^T), \\
\tilde{\Upsilon} &= \begin{bmatrix} \mu_4 \mathbf{I} & \mu_5 \mathbf{I} & \mu_6 \mathbf{I} \end{bmatrix}, \\
\tilde{\Omega}_{ij} &= \begin{bmatrix} \rho_{ij} (\mathbf{A}_i \mathbf{X}^T + \mathbf{B}_i \mathbf{N}_j - \tilde{\mathbf{Y}}_2) & \mathbf{0} & \mathbf{0} \end{bmatrix};
\end{aligned}$$

$\underline{\phi}_i$  and  $\bar{\phi}_i$  are the lower and upper bounds of  $w_i$ , respectively;  $\rho_{ij}$  is the upper bound of  $|\dot{h}_{ij}|$ ; and the controller gains are obtained by  $\mathbf{G}_j = \mathbf{N}_j \mathbf{X}^{-T} \forall j$ .

**Proof** To ensure the stability of (3.1), we employ the HODLF (Lemma 3). Choosing a fuzzy Lyapunov function candidate  $V_1(\mathbf{x}) = \mathbf{x}^T (\sum_{i=1}^p w_i \mathbf{P}_{1i}) \mathbf{x}$  and a quadratic Lyapunov function candidate  $V_2(\mathbf{x}) = \mathbf{x}^T \mathbf{P}_2 \mathbf{x}$  where  $\mathbf{P}_{1i} \in \Re^{n \times n} \forall i$  and  $\mathbf{P}_2 \in \Re^{n \times n}$  are symmetric matrices, condition (2.8) in Lemma 3 is satisfied.

**Remark 1** In general, the Lyapunov functions  $V_1(\mathbf{x})$  and  $V_2(\mathbf{x})$  can be chosen as any candidates by users. In this section, we aim to compare the HODLF with existing fuzzy Lyapunov function. Consequently, we choose  $V_1(\mathbf{x})$  as a fuzzy Lyapunov function candidate. It can be seen that the additional matrix  $\mathbf{P}_2$  may lead  $W(\mathbf{x})$  to provide more relaxed stability conditions than only employing fuzzy Lyapunov function  $V_1(\mathbf{x})$ . Note that the HODLF is not strictly relaxed than the compared one due to the introduction of conservativeness in the analysis.

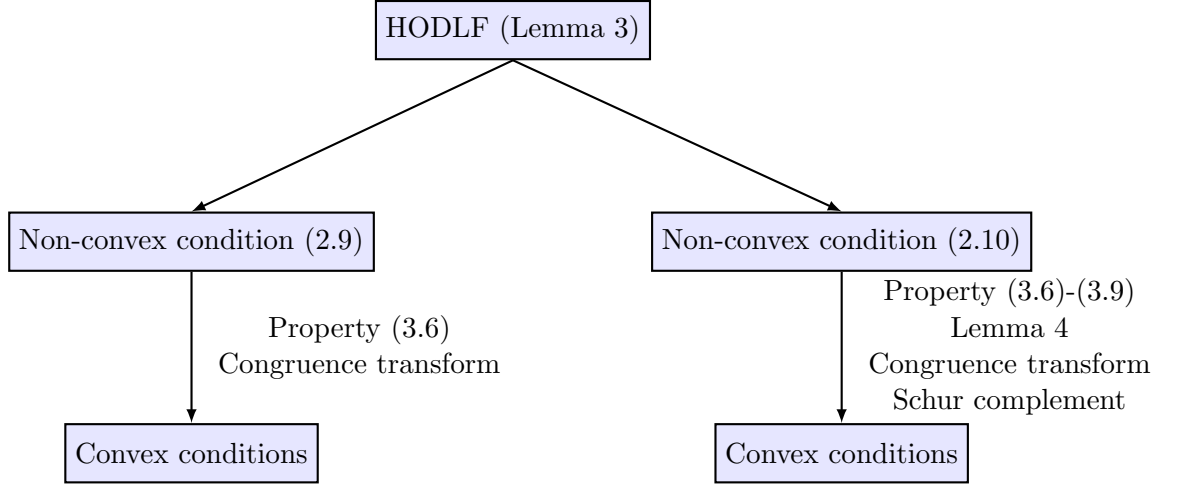


Figure 3.1: Procedure of proof for Theorem 1.

To satisfy conditions (2.9) and (2.10) and facilitate stability analysis, the following properties are exploited [2]:

$$\begin{aligned} \Gamma_1 = & 2(\mathbf{x}^T \mu_{k_1} \mathbf{M} + \dot{\mathbf{x}}^T \mu_{k_2} \mathbf{M}) \\ & \times \left( \sum_{i=1}^p \sum_{j=1}^p h_{ij} (\mathbf{A}_i + \mathbf{B}_i \mathbf{G}_j) \mathbf{x} - \dot{\mathbf{x}} \right) = 0, \end{aligned} \quad (3.6)$$

$$\begin{aligned} \Gamma_2 = & 2(\mathbf{x}^T \mu_{k_3} \mathbf{M} + \dot{\mathbf{x}}^T \mu_{k_4} \mathbf{M} + \ddot{\mathbf{x}}^T \mu_{k_5} \mathbf{M}) \\ & \times \left( \sum_{r=1}^p \sum_{s=1}^p \dot{h}_{rs} (\mathbf{A}_r + \mathbf{B}_r \mathbf{G}_s) \mathbf{x} \right. \\ & \left. + \sum_{i=1}^p \sum_{j=1}^p h_{ij} (\mathbf{A}_i + \mathbf{B}_i \mathbf{G}_j) \dot{\mathbf{x}} - \ddot{\mathbf{x}} \right) = 0, \end{aligned} \quad (3.7)$$

$$\Gamma_3 = \sum_{r=1}^p \dot{w}_r \mathbf{Y}_1 = \mathbf{0}, \quad (3.8)$$

$$\Gamma_4 = \sum_{r=1}^p \sum_{s=1}^p \dot{h}_{rs} \mathbf{Y}_2 = \mathbf{0}, \quad (3.9)$$

where  $\mathbf{M} \in \Re^{n \times n}$  is an invertible matrix;  $\mu_{k_l} \forall k_l$  are arbitrary scalars;  $\mathbf{Y}_1 \in \Re^{n \times n}$  is a symmetric matrix; and  $\mathbf{Y}_2 \in \Re^{n \times n}$  is an arbitrary matrix.

**Remark 2** In [2], only properties (3.6) and (3.8) are used in the analysis. In this section, however, the terms  $\ddot{\mathbf{x}}$  and  $\dot{h}_{rs}$  appear in the analysis resulted from applying HODLF. Therefore, properties (3.7) and (3.9) are added to handle this more complex situation.

To make the proof more readable, we present the procedure in Fig. 3.1 first. As can be seen, the proof is separated into two parts and convex conditions will be obtained in both parts.

Defining the augmented vector  $\mathbf{z}_1 = [\mathbf{x}^T \quad \dot{\mathbf{x}}^T]^T$  and using property (3.6) with  $k_1 = 1$  and  $k_2 = 2$ , we have

$$\begin{aligned} W(\mathbf{x}) &= 2\dot{\mathbf{x}}^T \mathbf{P}_2 \mathbf{x} + \mathbf{x}^T \sum_{i=1}^p w_i \mathbf{P}_{1i} \mathbf{x} + \Gamma_1 \\ &= \sum_{i=1}^p \sum_{j=1}^p h_{ij} \mathbf{z}_1^T \boldsymbol{\Theta}_{ij} \mathbf{z}_1, \end{aligned} \quad (3.10)$$

where

$$\begin{aligned} \boldsymbol{\Theta}_{ij} &= \begin{bmatrix} \boldsymbol{\Theta}_{ij}^{(11)} & * \\ \boldsymbol{\Theta}_{ij}^{(21)} & \boldsymbol{\Theta}_{ij}^{(22)} \end{bmatrix}, \\ \boldsymbol{\Theta}_{ij}^{(11)} &= \mathbf{P}_{1i} + \mu_1 \mathbf{M}(\mathbf{A}_i + \mathbf{B}_i \mathbf{G}_j) + \mu_1 (\mathbf{A}_i + \mathbf{B}_i \mathbf{G}_j)^T \mathbf{M}^T, \\ \boldsymbol{\Theta}_{ij}^{(21)} &= \mathbf{P}_2 - \mu_1 \mathbf{M}^T + \mu_2 \mathbf{M}(\mathbf{A}_i + \mathbf{B}_i \mathbf{G}_j), \\ \boldsymbol{\Theta}_{ij}^{(22)} &= -\mu_2 (\mathbf{M} + \mathbf{M}^T), \end{aligned}$$

and  $\mu_1$  and  $\mu_2$  are arbitrary scalars.

Therefore, condition (2.9) holds if  $\sum_{i=1}^p \sum_{j=1}^p h_{ij} \boldsymbol{\Theta}_{ij} > 0$ . By congruence transform with pre-multiplying  $\text{diag}\{\mathbf{X}, \mathbf{X}\}$  and post-multiplying  $\text{diag}\{\mathbf{X}^T, \mathbf{X}^T\}$  where  $\mathbf{X} = \mathbf{M}^{-1}$ , denoting  $\mathbf{N}_j = \mathbf{G}_j \mathbf{X}^T$ ,  $\tilde{\mathbf{P}}_{1i} = \mathbf{X} \mathbf{P}_{1i} \mathbf{X}^T$ ,  $\tilde{\mathbf{P}}_2 = \mathbf{X} \mathbf{P}_2 \mathbf{X}^T$ , and grouping the terms with the same membership functions, we obtain the stability condition (3.2).

To eliminate the term  $\dot{w}_i$  in the following analysis, using property (3.8) and assuming  $\underline{\phi}_i \leq \dot{w}_i \leq \bar{\phi}_i$ ,  $\mathbf{P}_{1i} - \mathbf{Y}_1 \leq \mathbf{S}_i \forall i$  where  $\mathbf{S}_i \geq 0$ , the time derivative of  $W(\mathbf{x})$  is

$$\begin{aligned} \dot{W}(\mathbf{x}) &= \Lambda + \mathbf{x}^T \left( \sum_{r=1}^p \dot{w}_r \mathbf{P}_{1r} - \Gamma_3 \right) \mathbf{x} \\ &= \Lambda + \mathbf{x}^T \left( \sum_{r=1}^p (\dot{w}_r - \underline{\phi}_r) (\mathbf{P}_{1r} - \mathbf{Y}_1) \right. \\ &\quad \left. + \sum_{i=1}^p \underline{\phi}_r (\mathbf{P}_{1r} - \mathbf{Y}_1) \right) \mathbf{x} \\ &\leq \Lambda + \mathbf{x}^T \left( \sum_{r=1}^p (\bar{\phi}_r - \underline{\phi}_r) \mathbf{S}_r \right. \\ &\quad \left. + \sum_{r=1}^p \underline{\phi}_r (\mathbf{P}_{1r} - \mathbf{Y}_1) \right) \mathbf{x}. \end{aligned} \quad (3.11)$$

where  $\Lambda = 2\dot{\mathbf{x}}^T \mathbf{P}_2 \mathbf{x} + 2\dot{\mathbf{x}}^T \mathbf{P}_2 \dot{\mathbf{x}} + 2\dot{\mathbf{x}}^T \sum_{i=1}^p w_i \mathbf{P}_{1i} \mathbf{x}$ .

**Remark 3** In [2], it is required that  $-\bar{\phi}_i \leq \dot{w}_i \leq \bar{\phi}_i \forall i$ . However, it is not necessary to require the lower bound of  $\dot{w}_i$  to be  $\underline{\phi}_i = -\bar{\phi}_i$ . Therefore, in this section, we consider a more general case that  $\underline{\phi}_i \leq \dot{w}_i \leq \bar{\phi}_i$ . By introducing the information of the lower bound  $\underline{\phi}_i$  and corresponding slack matrix  $\mathbf{S}_i$  in (3.11), more relaxed

stability conditions can be obtained.

Defining the augmented vector  $\mathbf{z}_2 = [\mathbf{x}^T \quad \dot{\mathbf{x}}^T \quad \ddot{\mathbf{x}}^T]^T$  and using properties (3.6), (3.7) and (3.9) on (3.11) with  $k_2 = 3$ ,  $k_3 = 4$ ,  $k_4 = 5$ ,  $k_5 = 6$  and  $\mu_{k_1} = 1$  (same as [2], it is redundant to keep all  $\mu_{k_l}$  as variables due to the existence of matrix variable  $\mathbf{M}$ ), we have

$$\begin{aligned} \dot{W}(\mathbf{x}) \leq & \sum_{i=1}^p \sum_{j=1}^p h_{ij} \mathbf{z}_2^T (\Xi_{ij} \\ & + \sum_{r=1}^p \sum_{s=1}^p (\Upsilon^T \Omega_{rs} + \Omega_{rs}^T \Upsilon)) \mathbf{z}_2 \end{aligned} \quad (3.12)$$

where

$$\begin{aligned} \Xi_{ij} &= \begin{bmatrix} \Xi_{ij}^{(11)} & * & * \\ \Xi_{ij}^{(21)} & \Xi_{ij}^{(22)} & * \\ \Xi_{ij}^{(31)} & \Xi_{ij}^{(32)} & \Xi_{ij}^{(33)} \end{bmatrix}, \\ \Xi_{ij}^{(11)} &= \sum_{r=1}^p (\bar{\phi}_r - \underline{\phi}_r) \mathbf{S}_r + \sum_{r=1}^p \underline{\phi}_r (\mathbf{P}_{1r} - \mathbf{Y}_1) \\ &\quad + \mathbf{M}(\mathbf{A}_i + \mathbf{B}_i \mathbf{G}_j) + (\mathbf{A}_i + \mathbf{B}_i \mathbf{G}_j)^T \mathbf{M}^T, \\ \Xi_{ij}^{(21)} &= \mathbf{P}_{1i} - \mathbf{M}^T + \mu_3 \mathbf{M}(\mathbf{A}_i + \mathbf{B}_i \mathbf{G}_j) \\ &\quad + \mu_4 (\mathbf{A}_i + \mathbf{B}_i \mathbf{G}_j)^T \mathbf{M}^T \\ \Xi_{ij}^{(22)} &= 2\mathbf{P}_2 - \mu_3 (\mathbf{M} + \mathbf{M}^T) + \mu_5 \mathbf{M}(\mathbf{A}_i + \mathbf{B}_i \mathbf{G}_j) \\ &\quad + \mu_5 (\mathbf{A}_i + \mathbf{B}_i \mathbf{G}_j)^T \mathbf{M}^T \\ \Xi_{ij}^{(31)} &= \mathbf{P}_2 - \mu_4 \mathbf{M}^T \\ \Xi_{ij}^{(32)} &= \mu_6 \mathbf{M}(\mathbf{A}_i + \mathbf{B}_i \mathbf{G}_j) - \mu_5 \mathbf{M}^T \\ \Xi_{ij}^{(33)} &= -\mu_6 (\mathbf{M} + \mathbf{M}^T) \\ \Upsilon &= \begin{bmatrix} \mu_4 \mathbf{M}^T & \mu_5 \mathbf{M}^T & \mu_6 \mathbf{M}^T \end{bmatrix}, \\ \Omega_{ij} &= \begin{bmatrix} \dot{h}_{ij}(\mathbf{A}_i + \mathbf{B}_i \mathbf{G}_j - \mathbf{Y}_2) & \mathbf{0} & \mathbf{0} \end{bmatrix}, \end{aligned}$$

and  $\mu_3, \mu_4, \mu_5, \mu_6$  are arbitrary scalars.

To eliminate the term  $\dot{h}_{ij}$  in  $\Omega_{ij}$ , assuming  $|\dot{h}_{ij}| \leq \rho_{ij}$  and using Lemma 4 and the property that  $(\mathbf{A}_i + \mathbf{B}_i \mathbf{G}_j - \mathbf{Y}_2)^T (\mathbf{A}_i + \mathbf{B}_i \mathbf{G}_j - \mathbf{Y}_2) \geq 0 \forall i, j$ , condition (2.10) holds if

$$\begin{aligned} & \sum_{i=1}^p \sum_{j=1}^p h_{ij} (\Xi_{ij} + \sum_{r=1}^p \sum_{s=1}^p (\Upsilon^T \Omega_{rs} + \Omega_{rs}^T \Upsilon)) \\ & \leq \sum_{i=1}^p \sum_{j=1}^p h_{ij} (\Xi_{ij} + \sum_{r=1}^p \sum_{s=1}^p (\beta_{rs} \Upsilon^T \Upsilon + \frac{1}{\beta_{rs}} \Omega_{rs}^T \Omega_{rs})) \end{aligned}$$



$$\begin{aligned}
&\leq \sum_{i=1}^p \sum_{j=1}^p h_{ij}(\Xi_{ij} + \sum_{r=1}^p \sum_{s=1}^p (\beta_{rs} \Upsilon^T \Upsilon + \frac{1}{\beta_{rs}} \hat{\Omega}_{rs}^T \hat{\Omega}_{rs})) \\
&< 0,
\end{aligned} \tag{3.13}$$

where

$$\hat{\Omega}_{ij} = \begin{bmatrix} \rho_{ij}(\mathbf{A}_i + \mathbf{B}_i \mathbf{G}_j - \mathbf{Y}_2) & \mathbf{0} & \mathbf{0} \end{bmatrix},$$

and  $\beta_{ij} > 0 \forall i, j$ .

**Remark 4** We have the relation that  $|\dot{h}_{ij}| = |\dot{w}_i w_j + w_i \dot{w}_j| \leq |\dot{w}_i w_j| + |w_i \dot{w}_j| \leq |\dot{w}_i| + |\dot{w}_j|$ . The upper bound of  $|\dot{h}_{ij}|$  can be approximated by the bounds of  $\dot{w}_i$ . However, it is very conservative to apply this relation to choose  $\rho_{ij}$ . More relaxed stability conditions can be obtained by choosing smaller  $\rho_{ij}$ . The assumption  $|\dot{h}_{ij}| \leq \rho_{ij}$  as well as  $\underline{\phi}_i \leq \dot{w}_i \leq \bar{\phi}_i$  can be verified after the stability analysis.

By congruence transform with pre-multiplying  $\text{diag}\{\mathbf{X}, \mathbf{X}, \mathbf{X}\}$  and post-multiplying  $\text{diag}\{\mathbf{X}^T, \mathbf{X}^T, \mathbf{X}^T\}$  to (3.13), denoting  $\tilde{\mathbf{Y}}_1 = \mathbf{X} \mathbf{Y}_1 \mathbf{X}^T$ ,  $\tilde{\mathbf{Y}}_2 = \mathbf{Y}_2 \mathbf{X}^T$ ,  $\tilde{\mathbf{S}}_i = \mathbf{X} \mathbf{S}_i \mathbf{X}^T$ , using Schur complement and grouping the terms with the same membership functions, we obtain stability condition (3.5).

This completes the proof.

### 3.1.3 Simulation Examples

A numerical model is presented for comparison of the conservativeness. Consider the following 2-rule T-S fuzzy model [2]:

$$\begin{aligned}
\mathbf{A}_1 &= \begin{bmatrix} 3.6 & -1.6 \\ 6.2 & -4.3 \end{bmatrix}, \mathbf{A}_2 = \begin{bmatrix} -a & -1.6 \\ 6.2 & -4.3 \end{bmatrix}, \\
\mathbf{B}_1 &= [-0.45 \quad -3]^T, \mathbf{B}_2 = [-b \quad -3]^T,
\end{aligned}$$

where  $a$  and  $b$  are constant parameters to be determined. The region of stabilization will be revealed with  $a$  and  $b$  being chosen in the range of  $0 \leq a \leq 10$  and  $-44 \leq b \leq -24$  at the interval of 1 and 2, respectively.

The region of interest is defined as  $x_1 \in [-0.2, 0.2]$  and  $x_2 \in [-0.5, 0.5]$  where  $\mathbf{x} = [x_1 \quad x_2]^T$  are the system states. The membership functions are chosen as  $w_1(x_1) = e^{-\frac{x_1^2}{18}}$  and  $w_2(x_1) = 1 - w_1(x_1)$ .

Theorem 1 is employed to design the fuzzy controller to stabilize the system. We choose  $\beta_{ij} = 1$ ,  $\mu_1 = -10^{-2}$ ,  $\mu_2 = -10^{-4}$ ,  $\mu_3 = 0.04$ ,  $\mu_4 = -10^{-2}$ ,  $\mu_5 = 10^{-4}$ ,  $\mu_6 = 10^{-6}$ ,  $\underline{\phi}_i = -1$ ,  $\bar{\phi}_i = 1$ ,  $\rho_{11} = \rho_{22} = 1$ ,  $\rho_{12} = \rho_{21} = 0.1$ ,  $i, j = 1, 2$ . Finding the solution using MATLAB LMI toolbox, the stabilization region is indicated by “○” in Fig. 3.2.

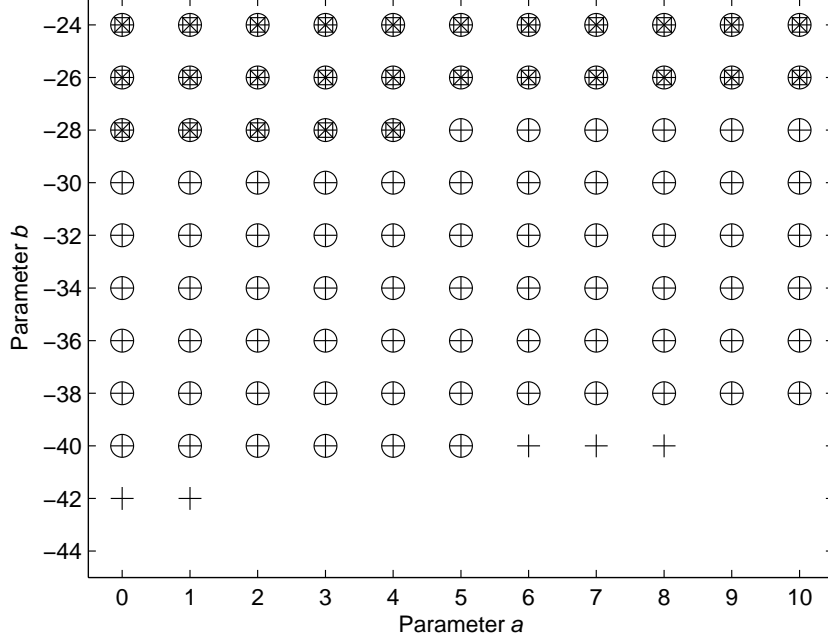


Figure 3.2: Stabilization regions obtained from Theorem 1 (“ $\times$ ” and “+”), Theorem 6 in [2] (“ $\circ$ ”) and Theorem 7 in [2] (“ $\square$ ”).

**Remark 5** *To our experience, the predefined parameters  $\beta_{ij} > 0$ ,  $\mu_1, \mu_2, \dots, \mu_6$ ,  $i, j = 1, 2, \dots, p$  in Theorem 1 can be determined in the following way in order to obtain more relaxed results. According the conditions in Theorem 1, the sign of  $\mu_2$  should be opposite to those of  $\mu_3$  and  $\mu_6$ . Users can start choosing the magnitudes of  $\mu_1, \mu_2, \dots, \mu_6$  very small such as  $10^{-6}$ , and then gradually increase the magnitudes. For  $\beta_{ij}$ , start from large values and gradually reduce them. The reason is that by starting with these settings, the conditions are similar to those in [2] using fuzzy Lyapunov function. Then the adjustment enlarges the effect of HODLF.*

To show the influence of adding the information of the lower bound  $\underline{\phi}_i$  and corresponding slack matrix  $\mathbf{S}_i$  in the proposed analysis, we consider another case where  $\underline{\phi}_i \neq -\bar{\phi}_i$ . We choose  $\underline{\phi}_1 = -0.4$ ,  $\bar{\phi}_2 = 0.4$  and keep other parameters the same, the corresponding stabilization region is obtained as “+” in Fig. 3.2. It can be seen that the slack matrix leads to more relaxed results.

**Remark 6** *To compare the proposed stability conditions with those derived from the fuzzy Lyapunov function [2], we consider two set of conditions: time-derivative dependent conditions (Theorem 6) and time-derivative independent conditions (Theorem 7). We apply Theorem 6 in [2] by choosing  $\mu = 0.04$  and  $\phi_{1,2} = 1$ . Also, Theorem 7 in [2] is employed by choosing  $\mu = 0.04$  and all possible substructures of decision matrices. Finding the solution using MATLAB LMI toolbox, the stabilization region is obtained and indicated by “ $\times$ ” and “ $\square$ ” in Fig. 3.2. It is shown that the HODLF in this section provides more relaxed stability conditions than fuzzy Lyapunov function [2].*

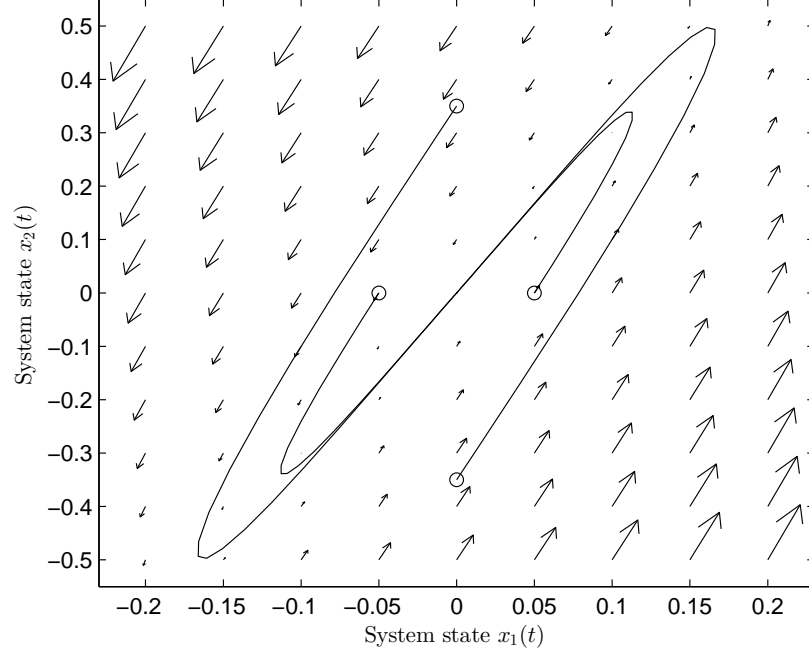


Figure 3.3: Phase plot of  $x_1(t)$  and  $x_2(t)$  for  $a = 5$  and  $b = -40$  in “○” in Fig. 3.2 where the initial conditions are indicated by “o”.

To verify the stabilization results, we consider two cases by choosing  $a = 5$  and  $b = -40$  in “○” and  $a = 1$  and  $b = -42$  in “+”. The controller feedback gains are obtained as  $\mathbf{G}_1 = [-1.0335 \times 10 \quad 2.6297]$ ,  $\mathbf{G}_2 = [8.0449 \times 10^{-2} \quad 3.2949 \times 10^{-2}]$  and  $\mathbf{G}_1 = [-1.1608 \times 10 \quad 2.9394]$ ,  $\mathbf{G}_2 = [-1.9578 \times 10^{-1} \quad 7.6306 \times 10^{-2}]$ , respectively, for both cases. With the initial conditions indicated by “o”, the phase plots of  $x_1(t)$  and  $x_2(t)$  are shown in Fig. 3.3 and Fig. 3.4. It can be seen that all the trajectories asymptotically reach the equilibrium point  $\mathbf{x} = \mathbf{0}$ . Furthermore, we check that the constraints  $\underline{\phi}_i \leq \dot{w}_i \leq \bar{\phi}_i$  and  $|\dot{h}_{ij}| \leq \rho_{ij}$  are satisfied for these two cases. For  $a = 5$  and  $b = -40$  in “○”, we have  $-6.0569 \times 10^{-2} \leq \dot{w}_1 \leq 6.4402 \times 10^{-3}$ ,  $-6.4402 \times 10^{-3} \leq \dot{w}_2 \leq 6.0569 \times 10^{-2}$ ,  $|\dot{h}_{11}| \leq 1.2087 \times 10^{-1}$ ,  $|\dot{h}_{12}|$ ,  $|\dot{h}_{21}| \leq 6.0300 \times 10^{-2}$  and  $|\dot{h}_{22}| \leq 2.6890 \times 10^{-4}$ . Similarly for  $a = 1$  and  $b = -42$  in “+”, we have  $-6.3499 \times 10^{-2} \leq \dot{w}_1 \leq 6.6410 \times 10^{-3}$ ,  $-6.6410 \times 10^{-3} \leq \dot{w}_2 \leq 6.3499 \times 10^{-2}$ ,  $|\dot{h}_{11}| \leq 1.2672 \times 10^{-1}$ ,  $|\dot{h}_{12}|$ ,  $|\dot{h}_{21}| \leq 6.3217 \times 10^{-2}$  and  $|\dot{h}_{22}| \leq 2.8191 \times 10^{-4}$ . Therefore, the constraints are all satisfied for these two cases.

### 3.1.4 Conclusion

In this section, the applicability of T-S FMB control scheme has been improved by relaxing stability conditions. First, the HODLF is employed to obtain relaxed stability conditions. To derive convex conditions, the properties of membership functions and the dynamics of the FMB control system have been exploited. Next, more information of the derivative of membership functions has been utilized to

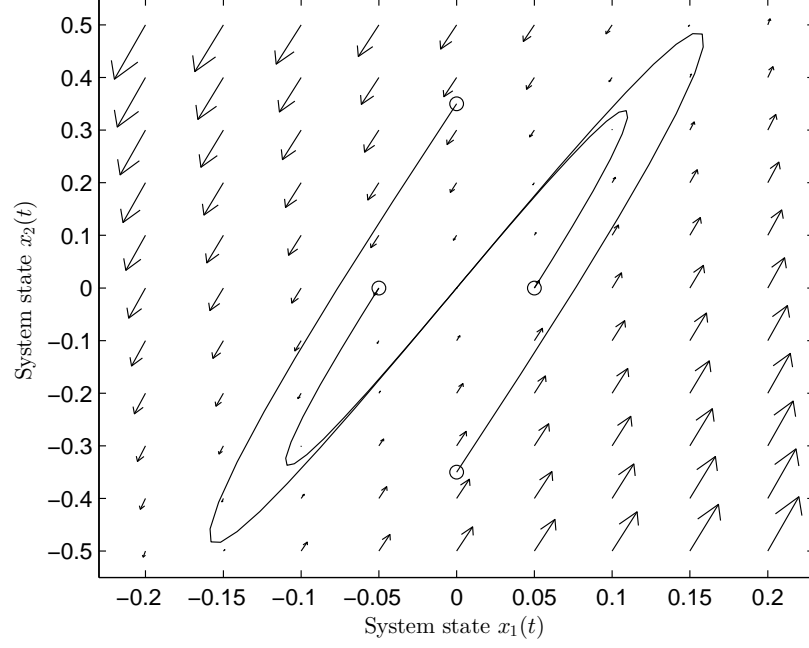


Figure 3.4: Phase plot of  $x_1(t)$  and  $x_2(t)$  for  $a = 1$  and  $b = -42$  in “+” in Fig. 3.2 where the initial conditions are indicated by “o”.

further relax the stability conditions. A simulation example has been presented to verify the relaxation. In the future, more advanced techniques may be applied to meet the boundary requirement of the derivative of membership functions or to provide more relaxed conditions.

## 3.2 Taylor Series Membership Functions for PFMB Control Systems

### 3.2.1 Introduction

In this section, we aim to relax stability conditions for PFMB control systems by considering the information of membership functions. Inspired by [28], we extend the piecewise linear membership functions to more systematic approximated membership functions with the consideration of approximation error. As an example, Taylor series expansion is chosen to implement the approximation. The advantage of Taylor series is that it yields polynomials which can be handled in SOS-based conditions and it provides the truncation order and expansion points to be determined by users. Based on TSMFs, stability conditions can be progressively relaxed as the truncation order increases and the interval of expansion points decreases. Meanwhile, we consider the following information: the boundary of membership functions, the property of membership functions, and the boundary of operating domain, which can further relax the SOS conditions.

This section is organized as follows. In Subsection 3.2.2, the formulation of non-PDC polynomial fuzzy controller is presented. In Subsection 3.2.3, TSMFs and relaxed SOS-based conditions are proposed. In Subsection 3.2.4, simulation examples are offered to show the improvement of designed controllers. In Subsection 3.2.5, a conclusion is drawn.

### 3.2.2 Preliminary

#### 3.2.2.1 Polynomial Fuzzy Controller

The polynomial fuzzy model and controller in this section do not share the same membership functions, meaning non-PDC design is employed which improves the design flexibility and reduces the complexity of the controller [82].

The  $j^{th}$  rule of the polynomial fuzzy controller is presented as follows:

$$\begin{aligned} \text{Rule } j : & \text{IF } g_1(\mathbf{x}(t)) \text{ is } N_1^j \text{ AND } \cdots \text{ AND } g_\Omega(\mathbf{x}(t)) \text{ is } N_\Omega^j \\ & \text{THEN } \mathbf{u}(t) = \mathbf{G}_j(\mathbf{x}(t))\hat{\mathbf{x}}(\mathbf{x}(t)), \end{aligned} \quad (3.14)$$

where  $g_\beta(\mathbf{x}(t))$  is the premise variable corresponding to its fuzzy term  $N_\beta^j$  in rule  $j$ ,  $\beta = 1, 2, \dots, \Omega$ , and  $\Omega$  is a positive integer;  $\mathbf{G}_j(\mathbf{x}(t)) \in \Re^{m \times N}$  is the polynomial feedback gain in rule  $j$ . Thus, the following polynomial fuzzy controller is applied to the nonlinear plant represented by the polynomial fuzzy model (2.5):

$$\mathbf{u}(t) = \sum_{j=1}^c m_j(\mathbf{x}(t)) \mathbf{G}_j(\mathbf{x}(t)) \hat{\mathbf{x}}(\mathbf{x}(t)), \quad (3.15)$$

where  $c$  is the number of rules in the polynomial fuzzy controller;  $m_j(\mathbf{x}(t))$  is the normalized grade of membership,  $m_j(\mathbf{x}(t)) = \frac{\prod_{l=1}^{\Omega} \mu_{N_l^j}(g_l(\mathbf{x}(t)))}{\sum_{k=1}^c \prod_{l=1}^{\Omega} \mu_{N_l^k}(g_l(\mathbf{x}(t)))}$ ,  $m_j(\mathbf{x}(t)) \geq 0$ ,  $j = 1, 2, \dots, c$ , and  $\sum_{j=1}^c m_j(\mathbf{x}(t)) = 1$ ;  $\mu_{N_\beta^j}(g_\beta(\mathbf{x}(t)))$ ,  $\beta = 1, 2, \dots, \Omega$ , are grades of membership corresponding to the fuzzy term  $N_\beta^j$ .

### 3.2.3 Stability Analysis

#### 3.2.3.1 Taylor Series Membership Function

In this section, TSMFs are introduced to approximate the original membership functions such that they can be brought into stability conditions. In the following analysis, for brevity,  $\mathbf{x}(t)$  and  $\hat{\mathbf{x}}(\mathbf{x}(t))$  are denoted as  $\mathbf{x}$  and  $\hat{\mathbf{x}}$  respectively. Without losing generality, we assume that membership functions depend on all system states  $\mathbf{x}$ .

Since the approximation is carried out in each substate space, the overall state space which is denoted as  $\psi$  is divided into  $s$  connected but non-overlapping substate

spaces (hypercubes) which are denoted as  $\psi_l, l = 1, 2, \dots, s$ . Specifically, in each dimension of  $\mathbf{x} = [x_1, x_2, \dots, x_n]^T$ ,  $x_r, r = 1, 2, \dots, n$ , are divided into  $s_r$  connected but non-overlapping substate spaces. Hence, we have the relation that  $\psi = \bigcup_{l=1}^s \psi_l$  and  $s = \prod_{r=1}^n s_r$ . Note that these substate spaces share the same boundaries but are not overlapped, that is  $\psi_{l_1} \cap \psi_{l_2} = \emptyset$  where  $l_1, l_2 = 1, 2, \dots, s$ .

Sample points are exploited to implement the segmentation of state space. Therefore, in each substate space  $\psi_l$ , we have 2 sample points denoted as  $x_{r1l}$  (lower bound) and  $x_{r2l}$  (upper bound) in each dimension  $x_r$ , and  $2^n$  sample points in all. In what follows, these sample points are exploited as expansion points for Taylor series. The approximation of original membership functions is achieved by fuzzy blending of the membership grades at samples points in each substate space.

Let us define  $h_{ij}(\mathbf{x}) = w_i(\mathbf{x})m_j(\mathbf{x})$ , and denote the approximation of  $h_{ij}(\mathbf{x})$  as  $\bar{h}_{ij}(\mathbf{x})$ . Therefore, the approximated membership function is defined as

$$\bar{h}_{ij}(\mathbf{x}) = \sum_{l=1}^s \sigma_l(\mathbf{x}) \sum_{i_1=1}^2 \cdots \sum_{i_n=1}^2 \prod_{r=1}^n v_{ri_r l}(x_r) \delta_{ij i_1 i_2 \dots i_n l}(\mathbf{x}) \quad \forall i, j, \quad (3.16)$$

where  $\sigma_l(\mathbf{x})$  is a scalar index of substate spaces, satisfying  $\sigma_l(\mathbf{x}) = 1, \mathbf{x} \in \psi_l, l = 1, 2, \dots, s$ ; otherwise,  $\sigma_l(\mathbf{x}) = 0$ ;  $\delta_{ij i_1 i_2 \dots i_n l}(\mathbf{x})$  is a predefined scalar polynomial of  $\mathbf{x}$  as grades of membership function  $h_{ij}(\mathbf{x})$  at sample points  $x_r = x_{ri_r l}, r = 1, 2, \dots, n, i_r = 1, 2$ , in substate space  $\psi_l$ ;  $v_{ri_r l}(x_r)$  is the membership function corresponding to fuzzy term  $\delta_{ij i_1 i_2 \dots i_n l}(\mathbf{x})$ , exhibiting the following properties:  $0 \leq v_{ri_r l}(x_r) \leq 1$ ,  $v_{r1l}(x_r) + v_{r2l}(x_r) = 1$  for all  $r, i_r, l, \mathbf{x} \in \psi_l$ , and  $\sum_{l=1}^s \sigma_l(\mathbf{x}) \sum_{i_1=1}^2 \cdots \sum_{i_n=1}^2 \prod_{r=1}^n v_{ri_r l}(x_r) = 1$  (Readers may refer to [28] for further examples of obtaining (3.16), which are some special cases of (3.16)).

**Remark 7** *There are different approaches to define membership grades of sample points  $\delta_{ij i_1 i_2 \dots i_n l}(\mathbf{x})$  in (3.16). In this section, particularly, the method of Taylor series expansion is employed to define  $\delta_{ij i_1 i_2 \dots i_n l}(\mathbf{x})$ . The general form of multi-variable Taylor series expansion [83] is given by*

$$f(\mathbf{x}) = \sum_{k=0}^{\infty} \frac{1}{k!} \left( \sum_{r=1}^n (x_r - x_{r0}) \frac{\partial}{\partial x_r} \right)^k \times f(\mathbf{x})|_{(x_r=x_{r0}, r=1,2,\dots,n)}, \quad (3.17)$$

where  $f(\mathbf{x})$  is an arbitrary function of  $\mathbf{x}$ ;  $x_{r0}, r = 1, 2, \dots, n$ , are expansion points;  $\frac{\partial}{\partial x_r} f(\mathbf{x})|_{(x_r=x_{r0}, r=1,2,\dots,n)}$  is a constant calculated by taking the partial derivative of  $f(\mathbf{x})$  and then substituting  $\mathbf{x}$  by  $x_r = x_{r0}$ . From the Taylor series expansion (3.17), we substitute expansion points and  $f(\mathbf{x})$  by sample points and  $h_{ij}(\mathbf{x})$  such that

$\delta_{ij i_1 i_2 \dots i_n l}(\mathbf{x})$  is obtained:

$$\begin{aligned} \delta_{ij i_1 i_2 \dots i_n l}(\mathbf{x}) &= \sum_{k=0}^{\lambda-1} \frac{1}{k!} \left( \sum_{r=1}^n (x_r - x_{r i_r l}) \frac{\partial}{\partial x_r} \right)^k \\ &\quad \times h_{ij}(\mathbf{x}) \Big|_{(x_r = x_{r i_r l}, r=1,2,\dots,n)} \\ &\quad \forall i, j, i_1, i_2, \dots, i_n, l, \mathbf{x} \in \psi_l, \end{aligned} \quad (3.18)$$

where  $\lambda$  is the predefined truncation order, which means the polynomial with the order  $\lambda - 1$  is applied for approximation. The TSMF is obtained by substituting (3.18) into (3.16). It is noted that the membership function  $h_{ij}(\mathbf{x})$  is required to be differentiable if TSMFs are employed.

### 3.2.3.2 PFMB Control Systems

In this section, the stability of the PFMB control system is analyzed. Without any ambiguity,  $w_i(\mathbf{x}(t))$ ,  $m_j(\mathbf{x}(t))$ ,  $h_{ij}(\mathbf{x})$  and  $\bar{h}_{ij}(\mathbf{x})$  are denoted as  $w_i$ ,  $m_j$ ,  $h_{ij}$  and  $\bar{h}_{ij}$ , respectively. The PFMB control system formed by the polynomial fuzzy model (2.5) and the polynomial fuzzy controller (3.15) is

$$\dot{\mathbf{x}} = \sum_{i=1}^p \sum_{j=1}^c h_{ij}(\mathbf{x}) (\mathbf{A}_i(\mathbf{x}) + \mathbf{B}_i(\mathbf{x}) \mathbf{G}_j(\mathbf{x})) \hat{\mathbf{x}}. \quad (3.19)$$

The control objective is to make the PFMB control system (3.19) asymptotically stable i.e.,  $\mathbf{x}(t) \rightarrow 0$  as time  $t \rightarrow \infty$ , by determining the polynomial feedback gains  $\mathbf{G}_j(\mathbf{x}(t))$ .

To proceed with the stability analysis, from (3.19), we have

$$\begin{aligned} \dot{\mathbf{x}} &= \frac{\partial \hat{\mathbf{x}}}{\partial \mathbf{x}} \frac{d\mathbf{x}}{dt} = \mathbf{T}(\mathbf{x}) \dot{\mathbf{x}} \\ &= \sum_{i=1}^p \sum_{j=1}^c h_{ij}(\mathbf{x}) (\tilde{\mathbf{A}}_i(\mathbf{x}) + \tilde{\mathbf{B}}_i(\mathbf{x}) \mathbf{G}_j(\mathbf{x})) \hat{\mathbf{x}}, \end{aligned} \quad (3.20)$$

where  $\tilde{\mathbf{A}}_i(\mathbf{x}) = \mathbf{T}(\mathbf{x}) \mathbf{A}_i(\mathbf{x})$ ,  $\tilde{\mathbf{B}}_i(\mathbf{x}) = \mathbf{T}(\mathbf{x}) \mathbf{B}_i(\mathbf{x})$ ,  $\mathbf{T}(\mathbf{x}) \in \mathbb{R}^{N \times n}$  with its  $(i, j)^{th}$  element defined as  $T_{ij}(\mathbf{x}) = \partial \hat{x}_i(\mathbf{x}) / \partial x_j$ . Due to the assumption that  $\hat{\mathbf{x}}(t) = \mathbf{0}$ , iff  $\mathbf{x}(t) = \mathbf{0}$ , the stability of control system (3.20) implies that of (3.19).

The structure of the following analysis is shown in Fig. 3.5 first. As can be seen, relaxed conditions will be obtained by bringing in the approximated membership function and the information of membership function. The theorem will be given immediately after the analysis.

We investigate the stability of (3.20) by employing the following polynomial Lyapunov function candidate:

$$V(\mathbf{x}) = \hat{\mathbf{x}}^T \mathbf{X}(\tilde{\mathbf{x}})^{-1} \hat{\mathbf{x}}, \quad (3.21)$$

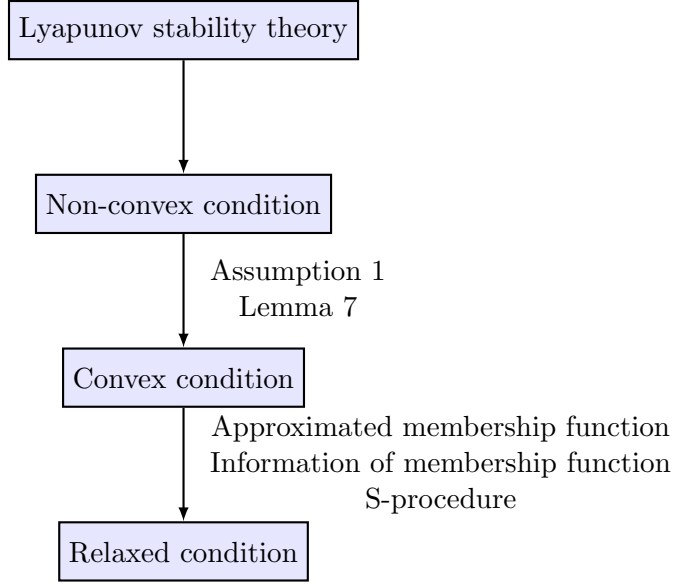


Figure 3.5: Procedure of proof for Theorem 2.

where  $0 < \mathbf{X}(\tilde{\mathbf{x}}) = \mathbf{X}(\tilde{\mathbf{x}})^T \in \Re^{N \times N}$ ;  $\tilde{\mathbf{x}}$  is defined in Assumption 1 in the following. From (3.20) and (3.21), we have

$$\begin{aligned}
 \dot{V}(\mathbf{x}) &= \dot{\hat{\mathbf{x}}}^T \mathbf{X}(\tilde{\mathbf{x}})^{-1} \hat{\mathbf{x}} + \hat{\mathbf{x}}^T \mathbf{X}(\tilde{\mathbf{x}})^{-1} \dot{\hat{\mathbf{x}}} + \hat{\mathbf{x}}^T \frac{d\mathbf{X}(\tilde{\mathbf{x}})^{-1}}{dt} \hat{\mathbf{x}} \\
 &= \sum_{i=1}^p \sum_{j=1}^c h_{ij} \hat{\mathbf{x}}^T \left( (\tilde{\mathbf{A}}_i(\mathbf{x}) + \tilde{\mathbf{B}}_i(\mathbf{x}) \mathbf{G}_j(\mathbf{x}))^T \mathbf{X}(\tilde{\mathbf{x}})^{-1} \right. \\
 &\quad \left. + \mathbf{X}(\tilde{\mathbf{x}})^{-1} (\tilde{\mathbf{A}}_i(\mathbf{x}) + \tilde{\mathbf{B}}_i(\mathbf{x}) \mathbf{G}_j(\mathbf{x})) \right) \hat{\mathbf{x}} \\
 &\quad + \hat{\mathbf{x}}^T \frac{d\mathbf{X}(\tilde{\mathbf{x}})^{-1}}{dt} \hat{\mathbf{x}}.
 \end{aligned} \tag{3.22}$$

**Assumption 1** ([3, 12]) *To deal with the term  $\frac{d\mathbf{X}(\tilde{\mathbf{x}})^{-1}}{dt}$  in (3.22), we define  $\mathbf{K} = \{\zeta_1, \zeta_2, \dots, \zeta_s\}$  as the set of row numbers that entries of the entire row of  $\mathbf{B}_i(\mathbf{x})$  are all zeros for all  $i$ , and  $\tilde{\mathbf{x}} = [x_{\zeta_1}, x_{\zeta_2}, \dots, x_{\zeta_s}]^T$ . Hence, we have  $\frac{d\mathbf{X}(\tilde{\mathbf{x}})^{-1}}{dt} = \sum_{\zeta \in \mathbf{K}} \frac{\partial \mathbf{X}(\tilde{\mathbf{x}})^{-1}}{\partial x_\zeta} \sum_{i=1}^p w_i \mathbf{A}_i^\zeta(\mathbf{x}) \hat{\mathbf{x}}$ , where  $\mathbf{A}_i^\zeta(\mathbf{x}) \in \Re^N$  is the  $\zeta^{\text{th}}$  row of  $\mathbf{A}_i(\mathbf{x})$ . Although this assumption is widely employed, it restricts the capability of polynomial Lyapunov function and further development can be achieved by removing this assumption [84].*

From Assumption 1 and Lemma 7, we have

$$\frac{d\mathbf{X}(\tilde{\mathbf{x}})^{-1}}{dt} = -\mathbf{X}(\tilde{\mathbf{x}})^{-1} \left( \sum_{i=1}^p \sum_{\zeta \in \mathbf{K}} w_i \frac{\partial \mathbf{X}(\tilde{\mathbf{x}})}{\partial x_\zeta} \mathbf{A}_i^\zeta(\mathbf{x}) \hat{\mathbf{x}} \right) \mathbf{X}(\tilde{\mathbf{x}})^{-1}. \tag{3.23}$$

Let us denote  $\mathbf{z} = \mathbf{X}(\tilde{\mathbf{x}})^{-1} \hat{\mathbf{x}}$  and  $\mathbf{G}_j(\mathbf{x}) = \mathbf{N}_j(\mathbf{x}) \mathbf{X}(\tilde{\mathbf{x}})^{-1}$ , where  $\mathbf{N}_j(\mathbf{x}) \in \Re^{m \times N}$ ,  $j =$



$1, 2, \dots, c$ , are arbitrary polynomial matrices. From (3.22) and (3.23), we have

$$\dot{V}(\mathbf{x}) = \sum_{i=1}^p \sum_{j=1}^c h_{ij} \mathbf{z}^T \mathbf{Q}_{ij}(\mathbf{x}) \mathbf{z}, \quad (3.24)$$

where  $\mathbf{Q}_{ij}(\mathbf{x}) = \tilde{\mathbf{A}}_i(\mathbf{x})\mathbf{X}(\tilde{\mathbf{x}}) + \mathbf{X}(\tilde{\mathbf{x}})\tilde{\mathbf{A}}_i(\mathbf{x})^T + \tilde{\mathbf{B}}_i(\mathbf{x})\mathbf{N}_j(\mathbf{x}) + \mathbf{N}_j(\mathbf{x})^T\tilde{\mathbf{B}}_i(\mathbf{x})^T - \sum_{\zeta \in \mathbf{K}} \frac{\partial \mathbf{X}(\tilde{\mathbf{x}})}{\partial x_\zeta} \mathbf{A}_i^\zeta(\mathbf{x}) \hat{\mathbf{x}}$  for  $i = 1, 2, \dots, p, j = 1, 2, \dots, c$ .

**Remark 8** From the Lyapunov stability theory, the asymptotic stability of (3.20) is guaranteed by  $V(\mathbf{x}) > 0$  and  $\dot{V}(\mathbf{x}) < 0$  (excluding  $\mathbf{x} = \mathbf{0}$ ), which can be implied by  $\mathbf{Q}_{ij}(\mathbf{x}) < 0$  for all  $i, j$ . However, the information of membership functions  $w_i$  and  $m_j$  are not considered leading to very conservative stability conditions.

### 3.2.3.3 Relaxed SOS-based Stability Conditions

In the following, we firstly present a general approach for relaxing the non-PDC SOS-based stability conditions with approximated membership functions. Then detailed information to implement this approach is provided. For brevity,  $\sigma_l(\mathbf{x})$  is denoted as  $\sigma_l$ .

In order to relax the stability conditions, we bring the approximated membership functions (3.16) into stability conditions by considering the boundary information of approximation error  $\Delta h_{ijl} = h_{ij} - \bar{h}_{ij}$  for all  $i, j, l, \mathbf{x} \in \psi_l$ . The local lower and upper bounds of  $\Delta h_{ijl}$  are denoted as  $\underline{\gamma}_{ijl}$  and  $\bar{\gamma}_{ijl}$ , respectively, which means  $\underline{\gamma}_{ijl} \leq \Delta h_{ijl} \leq \bar{\gamma}_{ijl}$  for all  $i, j, l, \mathbf{x} \in \psi_l$ . Meanwhile, slack polynomial matrices  $0 < \mathbf{Y}_{ijl}(\mathbf{x}) = \mathbf{Y}_{ijl}(\mathbf{x})^T \in \mathbb{R}^{N \times N}$  for  $\mathbf{x} \in \psi_l$  are introduced, which can be formulated by  $\sum_{l=1}^s \sigma_l \mathbf{Y}_{ijl}(\mathbf{x}) > 0$ . Moreover, it is required that  $\sum_{l=1}^s \sigma_l \mathbf{Y}_{ijl}(\mathbf{x}) \geq \mathbf{Q}_{ij}(\mathbf{x})$  for all  $i, j$ . Recalling that  $\sigma_l(\mathbf{x}) = 1$  for  $\mathbf{x} \in \psi_l$  (otherwise  $\sigma_l(\mathbf{x}) = 0$ ), the above inequalities can be implied by  $\mathbf{Y}_{ijl}(\mathbf{x}) > 0$  and  $\mathbf{Y}_{ijl}(\mathbf{x}) - \mathbf{Q}_{ij}(\mathbf{x}) \geq 0$  for all  $i, j, l$ . Based on the property that  $(\sum_{l=1}^s \sigma_l \mathbf{M}_{1l}(\mathbf{x}))(\sum_{k=1}^s \sigma_k \mathbf{M}_{2k}(\mathbf{x})) = \sum_{l=1}^s \sigma_l \mathbf{M}_{1l}(\mathbf{x}) \mathbf{M}_{2l}(\mathbf{x})$ , (3.24) can be written as follows:

$$\begin{aligned} \dot{V}(\mathbf{x}) &= \sum_{i=1}^p \sum_{j=1}^c h_{ij} \mathbf{z}^T \mathbf{Q}_{ij}(\mathbf{x}) \mathbf{z} \\ &= \mathbf{z}^T \sum_{i=1}^p \sum_{j=1}^c (\bar{h}_{ij} \mathbf{Q}_{ij}(\mathbf{x}) + (h_{ij} - \bar{h}_{ij}) \mathbf{Q}_{ij}(\mathbf{x})) \mathbf{z} \\ &= \mathbf{z}^T \sum_{i=1}^p \sum_{j=1}^c (\bar{h}_{ij} \mathbf{Q}_{ij}(\mathbf{x}) \\ &\quad + \sum_{l=1}^s \sigma_l (\Delta h_{ijl} - \underline{\gamma}_{ijl} + \underline{\gamma}_{ijl}) \mathbf{Q}_{ij}(\mathbf{x})) \mathbf{z} \\ &\leq \mathbf{z}^T \sum_{i=1}^p \sum_{j=1}^c ((\bar{h}_{ij} + \sum_{l=1}^s \sigma_l \underline{\gamma}_{ijl}) \mathbf{Q}_{ij}(\mathbf{x})) \end{aligned}$$

$$\begin{aligned}
& + \sum_{l=1}^s \sigma_l (\Delta h_{ijl} - \underline{\gamma}_{ijl}) \sum_{k=1}^s \sigma_k \mathbf{Y}_{ijk}(\mathbf{x}) \mathbf{z} \\
& \leq \mathbf{z}^T \sum_{l=1}^s \sigma_l \sum_{i=1}^p \sum_{j=1}^c ((\bar{h}_{ij} + \underline{\gamma}_{ijl}) \mathbf{Q}_{ij}(\mathbf{x}) \\
& \quad + (\bar{\gamma}_{ijl} - \underline{\gamma}_{ijl}) \mathbf{Y}_{ijl}(\mathbf{x})) \mathbf{z}.
\end{aligned} \tag{3.25}$$

To further relax stability conditions, we exploit the following information [26]: the boundary information of membership grades (with corresponding slack matrix  $\mathbf{R}_{1\rho_1}(\mathbf{x})$ ) and the property of membership functions ( $\mathbf{R}_{2\rho_2}(\mathbf{x})$ ). Additionally, aiming at the information of substate spaces, we propose another type of information, namely the boundary of operating domain ( $\mathbf{R}_{3\rho_3}(\mathbf{x})$ ). From (3.25), by S-procedure, we have

$$\begin{aligned}
\dot{V}(\mathbf{x}) & \leq \mathbf{z}^T \sum_{l=1}^s \sigma_l \sum_{i=1}^p \sum_{j=1}^c ((\bar{h}_{ij} + \underline{\gamma}_{ijl}) \mathbf{Q}_{ij}(\mathbf{x}) \\
& \quad + (\bar{\gamma}_{ijl} - \underline{\gamma}_{ijl}) \mathbf{Y}_{ijl}(\mathbf{x})) \mathbf{z} \\
& \quad + \mathbf{z}^T \left( \sum_{k=1}^3 \sum_{\rho_k=1}^{P_k} \phi_{k\rho_k}(\mathbf{x}) \mathbf{R}_{k\rho_k}(\mathbf{x}) \right) \mathbf{z},
\end{aligned} \tag{3.26}$$

where  $\phi_{1\rho_1}(\mathbf{x}) \geq 0$ ,  $\phi_{2\rho_2}(\mathbf{x}) = 0$  and  $\phi_{3\rho_3}(\mathbf{x}) \geq 0$ ,  $\rho_k = 1, 2, \dots, P_k$ ,  $k = 1, 2, \dots, 3$ , are predefined scalar polynomial functions;  $\mathbf{R}_{2\rho_2}(\mathbf{x}) = \mathbf{R}_{2\rho_2}(\mathbf{x})^T \in \Re^{N \times N}$  is an arbitrary polynomial matrix;  $0 < \mathbf{R}_{1\rho_1}(\mathbf{x}) = \mathbf{R}_{1\rho_1}(\mathbf{x})^T \in \Re^{N \times N}$  and  $0 < \mathbf{R}_{3\rho_3}(\mathbf{x}) = \mathbf{R}_{3\rho_3}(\mathbf{x})^T \in \Re^{N \times N}$  are polynomial matrices.

In what follows, the details concerning the three pieces of information are discussed. Since the membership functions  $v_{ri,l}(x_r)$  in (3.16) can be either linear or nonlinear, and nonlinear functions cannot be solved in SOS-based stability conditions, we consider  $v_{ri,l}(x_r)$  not exist in final stability conditions for this section.

**Remark 9** *If  $v_{ri,l}(x_r)$  is predefined as linear functions for  $\mathbf{x} \in (-\infty, \infty)$ , it can remain in SOS-based stability conditions. For this linear case, bringing  $v_{ri,l}(x_r)$  into stability conditions has potential to further relax the conditions. Future work can be done following this idea as a comparison with this section.*

**Boundary Information of Membership Grades** Since the approximated membership functions  $\bar{h}_{ij}$  have been brought into stability conditions, we can directly exploit their boundary information. We have  $\underline{\eta}_{ijl} \leq \bar{h}_{ij} \leq \bar{\eta}_{ijl}$  for all  $i, j$ ,  $\mathbf{x} \in \psi_l$ , where  $\underline{\eta}_{ijl}$  and  $\bar{\eta}_{ijl}$  are lower and upper bounds of approximated membership membership grades  $\bar{h}_{ij}$  in substate space  $\psi_l$ , respectively. Then we have

$$\sum_{l=1}^s \sigma_l (\bar{h}_{ij} - \underline{\eta}_{ijl}) \mathbf{W}_{ijl}(\mathbf{x}) \geq 0 \quad \forall i, j, \tag{3.27}$$

$$\sum_{l=1}^s \sigma_l (\bar{\eta}_{ijl} - \bar{h}_{ij}) \bar{\mathbf{W}}_{ijl}(\mathbf{x}) \geq 0 \quad \forall i, j, \quad (3.28)$$

where  $0 < \underline{\mathbf{W}}_{ijl}(\mathbf{x}) = \underline{\mathbf{W}}_{ijl}(\mathbf{x})^T \in \Re^{N \times N}$  and  $0 < \bar{\mathbf{W}}_{ijl}(\mathbf{x}) = \bar{\mathbf{W}}_{ijl}(\mathbf{x})^T \in \Re^{N \times N}$  for  $\mathbf{x} \in \psi_l$  are polynomial matrices.

**Property of Membership Functions** The membership function  $v_{ri_r l}(x_r)$  owns the property that  $\sum_{l=1}^s \sigma_l \sum_{i_1=1}^2 \cdots \sum_{i_n=1}^2 \prod_{r=1}^n v_{ri_r l}(x_r) = 1$ . Since we consider  $v_{ri_r l}(x_r)$  not exist in final stability conditions, this information is lost. Therefore, we aim to bring such information into stability conditions. However, it is difficult to provide general equalities or inequalities representing such information due to different selection of function  $v_{ri_r l}(x_r)$ . In this section, we provide an example by defining  $v_{r1l}(x_r) = (x_{r2l} - x_r) / (x_{r2l} - x_{r1l})$  and  $v_{r2l}(x_r) = 1 - v_{r1l}(x_r)$  for all  $r, l, \mathbf{x} \in \psi_l$ , where  $x_{r1l}$  and  $x_{r2l}$  are lower and upper bounds of  $x_r$  in substate space  $\psi_l$ .

In this case, we have the following equality constraint [28]:

$$\sum_{l=1}^s \sigma_l \sum_{i_1=1}^2 \cdots \sum_{i_n=1}^2 \prod_{r=1}^n v_{ri_r l}(x_r) (\chi(\mathbf{x}) - \bar{\chi}_{i_1 i_2 \cdots i_n l}) \mathbf{K}_l(\mathbf{x}) = 0, \quad (3.29)$$

where we have the property that  $\sum_{l=1}^s \sigma_l \sum_{i_1=1}^2 \cdots \sum_{i_n=1}^2 \prod_{r=1}^n v_{ri_r l}(x_r) (\chi(\mathbf{x}) - \bar{\chi}_{i_1 i_2 \cdots i_n l}) = 0$ ;  $\chi(\mathbf{x})$  is a monomials linear in  $x_r, r = 1, 2, \dots, n$ ;  $\bar{\chi}_{i_1 i_2 \cdots i_n l} = \chi(\mathbf{x})|_{x_r = x_{ri_r l}}$  is the value of  $\chi(\mathbf{x})$  at sample points  $x_r = x_{ri_r l}$  in substate space  $\psi_l$ ;  $\mathbf{K}_l(\mathbf{x}) = \mathbf{K}_l(\mathbf{x})^T \in \Re^{N \times N}$  is an arbitrary polynomial matrix. It is noted that  $\chi(\mathbf{x})$  is not necessarily a monomial in all system states  $x_r$ .

**Boundary Information of Operating Domain** Once SOS-based stability conditions are satisfied, they hold for all  $\mathbf{x} \in (-\infty, \infty)$ . In practice, however, we usually only need to guarantee the satisfaction for a certain domain of  $\mathbf{x}$ , that is  $x_k \in [x_{k1}, x_{k2}], k = 1, 2, \dots, n$ . In this section, we only need to satisfy the local operating domain  $x_k \in [x_{k1l}, x_{k2l}]$  for each substate space  $\psi_l$ . For this reason, we have the following constraint:

$$\sum_{l=1}^s \sigma_l \sum_{k=1}^n (x_k - x_{k1l})(x_{k2l} - x_k) \mathbf{L}_{kl}(\mathbf{x}) \geq 0, \quad (3.30)$$

where  $0 < \mathbf{L}_{kl}(\mathbf{x}) = \mathbf{L}_{kl}(\mathbf{x})^T \in \Re^{N \times N}$  for  $\mathbf{x} \in \psi_l$  is a polynomial matrix.

Now we substitute the approximated membership function  $\bar{h}_{ij}$  in (3.26) by (3.16), and substitute general form of constraints by (3.27), (3.28) and (3.30). For the reason that  $\sum_{l=1}^s \sigma_l \sum_{i_1=1}^2 \cdots \sum_{i_n=1}^2 \prod_{r=1}^n v_{ri_r l}(x_r) = 1$  and  $v_{ri_r l}(x_r)$  is independent of rule

$i, j$ , we have

$$\begin{aligned}
\dot{V}(\mathbf{x}) \leq & \mathbf{z}^T \sum_{l=1}^s \sigma_l \sum_{i_1=1}^2 \cdots \sum_{i_n=1}^2 \prod_{r=1}^n v_{ri_r l}(x_r) \sum_{i=1}^p \sum_{j=1}^c \\
& \times \left( (\delta_{ij i_1 i_2 \dots i_n l}(\mathbf{x}) + \underline{\gamma}_{ijl}) \mathbf{Q}_{ij}(\mathbf{x}) \right. \\
& + (\bar{\gamma}_{ijl} - \underline{\gamma}_{ijl}) \mathbf{Y}_{ijl}(\mathbf{x}) \\
& + (\delta_{ij i_1 i_2 \dots i_n l}(\mathbf{x}) - \underline{\eta}_{ijl}) \underline{\mathbf{W}}_{ijl}(\mathbf{x}) \\
& + (\bar{\eta}_{ijl} - \delta_{ij i_1 i_2 \dots i_n l}(\mathbf{x})) \bar{\mathbf{W}}_{ijl}(\mathbf{x}) \\
& \left. + \sum_{k=1}^n (x_k - x_{k1l})(x_{k2l} - x_k) \mathbf{L}_{kl}(\mathbf{x}) \right) \mathbf{z}. \tag{3.31}
\end{aligned}$$

The satisfaction of  $\dot{V}(\mathbf{x}) < 0$  can be guaranteed by  $\sum_{i=1}^p \sum_{j=1}^c \left( (\delta_{ij i_1 i_2 \dots i_n l}(\mathbf{x}) + \underline{\gamma}_{ijl}) \mathbf{Q}_{ij}(\mathbf{x}) + (\bar{\gamma}_{ijl} - \underline{\gamma}_{ijl}) \mathbf{Y}_{ijl}(\mathbf{x}) + (\delta_{ij i_1 i_2 \dots i_n l}(\mathbf{x}) - \underline{\eta}_{ijl}) \underline{\mathbf{W}}_{ijl}(\mathbf{x}) + (\bar{\eta}_{ijl} - \delta_{ij i_1 i_2 \dots i_n l}(\mathbf{x})) \bar{\mathbf{W}}_{ijl}(\mathbf{x}) + \sum_{k=1}^n (x_k - x_{k1l})(x_{k2l} - x_k) \mathbf{L}_{kl}(\mathbf{x}) \right) < 0$  for all  $i_1, i_2, \dots, i_n, l$ . The above stability analysis result is summarized in the following theorem.

**Theorem 2** *The PFMB system (3.19), which is formed by the polynomial fuzzy model (2.5) and the polynomial fuzzy controller (3.15) connected in a closed loop, is guaranteed to be asymptotically stable if there exist polynomial matrices  $\mathbf{Y}_{ijl}(\mathbf{x}) = \mathbf{Y}_{ijl}(\mathbf{x})^T \in \mathbb{R}^{N \times N}$ ,  $\underline{\mathbf{W}}_{ijl}(\mathbf{x}) = \underline{\mathbf{W}}_{ijl}(\mathbf{x})^T \in \mathbb{R}^{N \times N}$ ,  $\bar{\mathbf{W}}_{ijl}(\mathbf{x}) = \bar{\mathbf{W}}_{ijl}(\mathbf{x})^T \in \mathbb{R}^{N \times N}$ ,  $\mathbf{L}_{kl}(\mathbf{x}) = \mathbf{L}_{kl}(\mathbf{x})^T \in \mathbb{R}^{N \times N}$ ,  $\mathbf{N}_j(\mathbf{x}) \in \mathbb{R}^{m \times N}$ ,  $i = 1, 2, \dots, p, j = 1, 2, \dots, c, k = 1, 2, \dots, n, l = 1, 2, \dots, s$ , and  $\mathbf{X}(\tilde{\mathbf{x}}) = \mathbf{X}(\tilde{\mathbf{x}})^T \in \mathbb{R}^{N \times N}$  such that the following SOS-based conditions are satisfied:*

$$\begin{aligned}
& \nu^T(\mathbf{X}(\tilde{\mathbf{x}}) - \varepsilon_1(\tilde{\mathbf{x}})\mathbf{I})\nu \text{ is SOS;} \\
& \nu^T(\mathbf{Y}_{ijl}(\mathbf{x}) - \varepsilon_2(\mathbf{x})\mathbf{I})\nu \text{ is SOS} \quad \forall i, j, l; \\
& \nu^T(\mathbf{Y}_{ijl}(\mathbf{x}) - \mathbf{Q}_{ij}(\mathbf{x}) - \varepsilon_3(\mathbf{x})\mathbf{I})\nu \text{ is SOS} \quad \forall i, j, l; \\
& \nu^T(\underline{\mathbf{W}}_{ijl}(\mathbf{x}) - \varepsilon_4(\mathbf{x})\mathbf{I})\nu \text{ is SOS} \quad \forall i, j, l; \\
& \nu^T(\bar{\mathbf{W}}_{ijl}(\mathbf{x}) - \varepsilon_5(\mathbf{x})\mathbf{I})\nu \text{ is SOS} \quad \forall i, j, l; \\
& \nu^T(\mathbf{L}_{kl}(\mathbf{x}) - \varepsilon_6(\mathbf{x})\mathbf{I})\nu \text{ is SOS} \quad \forall k, l; \\
& - \nu^T \left( \sum_{i=1}^p \sum_{j=1}^c \left( (\delta_{ij i_1 i_2 \dots i_n l}(\mathbf{x}) + \underline{\gamma}_{ijl}) \mathbf{Q}_{ij}(\mathbf{x}) \right. \right. \\
& \quad + (\bar{\gamma}_{ijl} - \underline{\gamma}_{ijl}) \mathbf{Y}_{ijl}(\mathbf{x}) \\
& \quad + (\delta_{ij i_1 i_2 \dots i_n l}(\mathbf{x}) - \underline{\eta}_{ijl}) \underline{\mathbf{W}}_{ijl}(\mathbf{x}) \\
& \quad + (\bar{\eta}_{ijl} - \delta_{ij i_1 i_2 \dots i_n l}(\mathbf{x})) \bar{\mathbf{W}}_{ijl}(\mathbf{x}) \\
& \quad \left. + \sum_{k=1}^n (x_k - x_{k1l})(x_{k2l} - x_k) \mathbf{L}_{kl}(\mathbf{x}) \right) \\
& \quad \left. + \varepsilon_7(\mathbf{x})\mathbf{I} \right) \nu \text{ is SOS} \quad \forall i_1, i_2, \dots, i_n, l; \tag{3.32}
\end{aligned}$$

where  $\nu \in \mathbb{R}^N$  is an arbitrary vector independent of  $\mathbf{x}$ ;  $\delta_{ij i_1 i_2 \dots i_n l}(\mathbf{x})$  is a predefined scalar polynomial of  $\mathbf{x}$  in (3.16);  $\underline{\gamma}_{ijl}, \bar{\gamma}_{ijl}, \underline{\eta}_{ijl}, \bar{\eta}_{ijl}, x_{k1l}$ , and  $x_{k2l}$  are predefined constant scalars satisfying  $\Delta h_{ij} = h_{ij} - \bar{h}_{ij}, \underline{\gamma}_{ijl} \leq \Delta h_{ij} \leq \bar{\gamma}_{ijl}, \underline{\eta}_{ijl} \leq \bar{\eta}_{ijl}$ , and  $x_{k1l} \leq x_k \leq x_{k2l}$  for all  $i, j, k, l, \mathbf{x} \in \psi_l$ ;  $\varepsilon_1(\tilde{\mathbf{x}}) > 0, \varepsilon_2(\mathbf{x}) > 0, \dots, \varepsilon_7(\mathbf{x}) > 0$ , are predefined scalar polynomials; the feedback gains are defined as  $\mathbf{G}_j(\mathbf{x}) = \mathbf{N}_j(\mathbf{x})\mathbf{X}(\tilde{\mathbf{x}})^{-1}, j = 1, 2, \dots, c$ .

**Remark 10** Referring to Theorem 2, the number of decision matrix variables is  $1 + c + 3pcs + ns$ , and the number of SOS conditions is  $1 + 4pcs + ns + 2^n s$ . When membership function  $v_{ri,l}(x_r)$  is defined as  $v_{r1l}(x_r) = (x_{r2l} - x_r)/(x_{r2l} - x_{r1l})$  and  $v_{r2l}(x_r) = 1 - v_{r1l}(x_r)$  for all  $r, l, \mathbf{x} \in \psi_l$ , where  $x_{r1l} \leq x_r \leq x_{r2l}$ , the information of the property of  $v_{ri,l}(x_r)$  can be brought into stability conditions. The SOS condition (3.32) in Theorem 2 is replaced by

$$\begin{aligned}
& -\nu^T \left( \sum_{i=1}^p \sum_{j=1}^c ((\delta_{ij i_1 i_2 \dots i_n l}(\mathbf{x}) + \underline{\gamma}_{ijl}) \mathbf{Q}_{ij}(\mathbf{x}) \right. \\
& \quad + (\bar{\gamma}_{ijl} - \underline{\gamma}_{ijl}) \mathbf{Y}_{ijl}(\mathbf{x}) \\
& \quad + (\delta_{ij i_1 i_2 \dots i_n l}(\mathbf{x}) - \underline{\eta}_{ijl}) \mathbf{W}_{ijl}(\mathbf{x}) \\
& \quad + (\bar{\eta}_{ijl} - \delta_{ij i_1 i_2 \dots i_n l}(\mathbf{x})) \bar{\mathbf{W}}_{ijl}(\mathbf{x}) \\
& \quad + (\chi(\mathbf{x}) - \bar{\chi}_{i_1 i_2 \dots i_n l}) \mathbf{K}_l(\mathbf{x}) \\
& \quad + \sum_{k=1}^n (x_k - x_{k1l})(x_{k2l} - x_k) \mathbf{L}_{kl}(\mathbf{x}) \\
& \quad \left. + \varepsilon_7(\mathbf{x}) \mathbf{I} \right) \nu \text{ is SOS} \quad \forall i_1, i_2, \dots, i_n, l; \tag{3.33}
\end{aligned}$$

where  $\chi(\mathbf{x})$  is a monomials linear in  $x_r, r = 1, 2, \dots, n$ ;  $\bar{\chi}_{i_1 i_2 \dots i_n l} = \chi(\mathbf{x})|_{x_r = x_{ri,l}}$ ;  $\mathbf{K}_l(\mathbf{x}) = \mathbf{K}_l(\mathbf{x})^T \in \mathbb{R}^{N \times N}$  is an arbitrary polynomial matrix. In this case, the number of variables are  $1 + c + 3pcs + ns + s$ , and the number of SOS conditions remains the same.

### 3.2.4 Simulation Examples

In the following, a 3-rule polynomial fuzzy model with the form of (2.5) is investigated to implement the designed controller. The system states are  $\hat{\mathbf{x}}(t) = \mathbf{x}(t) = [x_1(t) \ x_2(t)]^T$ , and system matrices and input matrices are

$$\begin{aligned}
\mathbf{A}_1(x_1) &= \begin{bmatrix} 1.59 - 0.12x_1^2 & -7.29 - 0.25x_1 \\ 0.01 & -0.1 \end{bmatrix}, \\
\mathbf{A}_2(x_1) &= \begin{bmatrix} 0.02 - 0.63x_1^2 & -4.64 + 0.92x_1 \\ 0.35 & -0.21 \end{bmatrix},
\end{aligned}$$

Table 3.1: Comparison of different orders of TSMFs and intervals of expansion points.

Case	Order $\lambda$	Interval	Expansion points
1	1	4	$x_1 = \{-10, -6, \dots, 6, 10\}$
2	1	2	$x_1 = \{-10, -8, \dots, 8, 10\}$
3	3	4	$x_1 = \{-10, -6, \dots, 6, 10\}$
4	3	2	$x_1 = \{-10, -8, \dots, 8, 10\}$

$$\mathbf{A}_3(x_1) = \begin{bmatrix} -a + 0.31x_1 - 1.12x_1^2 & -4.33 \\ 0 & 0.05 \end{bmatrix},$$

$$\mathbf{B}_1 = \begin{bmatrix} 1 \\ 0 \end{bmatrix}, \mathbf{B}_2 = \begin{bmatrix} 8 \\ 0 \end{bmatrix}, \mathbf{B}_3 = \begin{bmatrix} -b + 6 \\ -1 \end{bmatrix},$$

where  $a$  and  $b$  are predefined constant parameters in the range of  $0 \leq a \leq 10$  and  $0 \leq b \leq 200$  at the interval of 1 and 20, respectively. The operating domain we consider for this model is  $x_1 \in [-10, 10]$ . The membership functions of this polynomial fuzzy model are selected as  $w_1(x_1) = 1 - 1/(1 + e^{-(x_1+4)})$ ,  $w_2(x_1) = 1 - w_1(x_1) - w_3(x_1)$  and  $w_3(x_1) = 1/(1 + e^{-(x_1-4)})$ . To achieve the stabilization, a 2-rule polynomial fuzzy controller with the form of (3.15) is employed, with membership functions defined as  $m_1(x_1) = e^{-x_1^2/12}$  and  $m_2(x_1) = 1 - m_1(x_1)$ .

Theorem 2 is applied to design the feedback gains of polynomial fuzzy controller. TSMFs (3.16) and (3.18) are exploited as approximated membership functions. In order to demonstrate the influence of different orders of TSMFs and intervals of expansion points, we make the comparison as shown in Table 3.1. Without losing generality, we choose membership function  $v_{r_{il}}(x_r)$  in (3.16) as  $v_{11l}(x_1) = (x_{12l} - x_1)/(x_{12l} - x_{11l})$  and  $v_{12l}(x_1) = 1 - v_{11l}(x_1)$ , for all  $l, x_1 \in \psi_l$ , where  $x_{11l} \leq x_1 \leq x_{12l}$ . It is noted that we remove the terms in Taylor series with the magnitude of coefficients less than  $1 \times 10^{-6}$  such that the computational efficiency is improved. Based on original membership functions and TSMFs, the predefined constant scalars  $\underline{\gamma}_{ijl}$ ,  $\bar{\gamma}_{ijl}$ ,  $\underline{\eta}_{ijl}$ , and  $\bar{\eta}_{ijl}$  are obtained for Cases 1-4.

Due the selection of membership function  $v_{r_{il}}(x_r)$ , the SOS condition (3.32) in Theorem 2 is replaced by (3.33) in Remark 10. To further reduce the computational burden, the number of slack matrices is decreased by  $\mathbf{Y}_{ijl}(x_1) = \mathbf{Y}_{ij}(x_1)$ ,  $\underline{\mathbf{W}}_{ijl}(x_1) = \underline{\mathbf{W}}_{ij}(x_1)$ ,  $\bar{\mathbf{W}}_{ijl}(x_1) = \bar{\mathbf{W}}_{ij}(x_1)$ ,  $\mathbf{K}_l(x_1) = \mathbf{K}(x_1)$ ,  $\mathbf{L}_{kl}(x_1) = \mathbf{L}(x_1)$ . Other parameters are chosen as follows:  $\varepsilon_1 = \varepsilon_2 = \dots = \varepsilon_7 = 1 \times 10^{-3}$ ,  $\mathbf{X}$  of degree 0,  $\mathbf{Y}_{ij}(x_1)$  of degree 8,  $\underline{\mathbf{W}}_{ij}(x_1)$  and  $\bar{\mathbf{W}}_{ij}(x_1)$  of degree 6,  $\mathbf{K}(x_1)$  of degree 7 and  $\mathbf{L}(x_1)$  of degree 6. The SOS-based stability conditions are solved numerically by the third-party MATLAB toolbox SOSTOOLS [13].

To demonstrate the effect of each type of slack matrices, the stabilization region obtained with only  $\mathbf{Y}_{ij}(x_1)$ , with only  $\mathbf{Y}_{ij}(x_1)$ ,  $\underline{\mathbf{W}}_{ij}(x_1)$  and  $\bar{\mathbf{W}}_{ij}(x_1)$ , with only

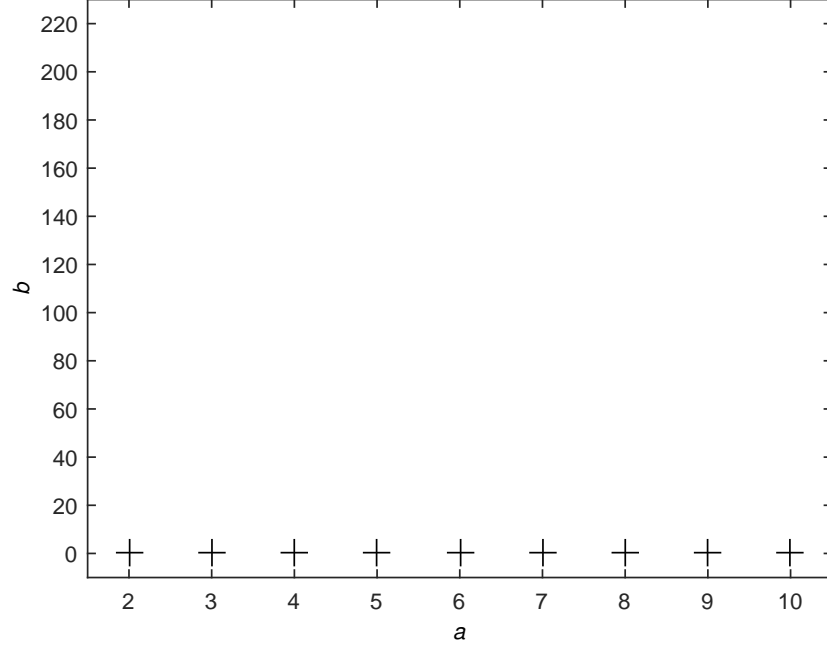


Figure 3.6: Stabilization regions obtained from Theorem 2 with only  $\mathbf{Y}_{ij}(x_1)$ , indicated by “ $\times$ ” for Case 1, “+” for Case 2, “ $\square$ ” for Case 3 and “o” for Case 4.

$\mathbf{Y}_{ij}(x_1)$ ,  $\mathbf{W}_{ij}(x_1)$ ,  $\overline{\mathbf{W}}_{ij}(x_1)$  and  $\mathbf{L}(x_1)$ , and with all slack matrices ( $\mathbf{Y}_{ij}(x_1)$ ,  $\mathbf{W}_{ij}(x_1)$ ,  $\overline{\mathbf{W}}_{ij}(x_1)$ ,  $\mathbf{L}(x_1)$  and  $\mathbf{K}(x_1)$ ) are shown in Fig. 3.6-3.9, respectively. The stabilization region is indicated by “ $\times$ ” for Case 1, “+” for Case 2, “ $\square$ ” for Case 3 and “o” for Case 4.

From Fig. 3.6-3.9, it can be found that the stabilization region grows for all cases with the number of slack matrices increasing. It shows that these information of membership functions and operating domain as well as their corresponding slack matrices are effective for relaxing stability conditions. Moreover, by comparing Case 1 to Case 4, it is indicated that higher order and smaller interval lead to larger stabilization region. Additionally, when the interval is large, both the interval and the order play an important role; when the interval is small, they become less influential. It complies with what we expect because these SOS-based stability conditions are close to sufficient and necessary conditions as the interval is small. However, when higher order TSMFs are employed, corresponding higher order slack matrices are required simultaneously, which leads to unaffordable computational cost and makes sufficient and necessary conditions unattainable.

To verify the stabilization, we provide an example by choosing  $a = 10$  and  $b = 220$  in Case 4. The polynomial feedback gains are obtained that  $\mathbf{G}_1(x_1) = [0.0158x_1^2 + 0.0138x_1 - 0.1312 \quad 0.0720x_1^2 + 0.1453x_1 - 0.4839]$  and  $\mathbf{G}_2(x_1) = [0.0058x_1^2 + 0.0000x_1 - 0.0459 \quad 0.0154x_1^2 - 0.0021x_1 - 0.0158]$ . With initial conditions indicated by “o”, the phase plot of  $x_1(t)$  and  $x_2(t)$  is shown in Fig. 3.10. With initial conditions  $\mathbf{x}(0) = [10 \quad 10]^T$ , the transient response of  $\mathbf{x}(t)$  and control input  $u(t)$  are shown

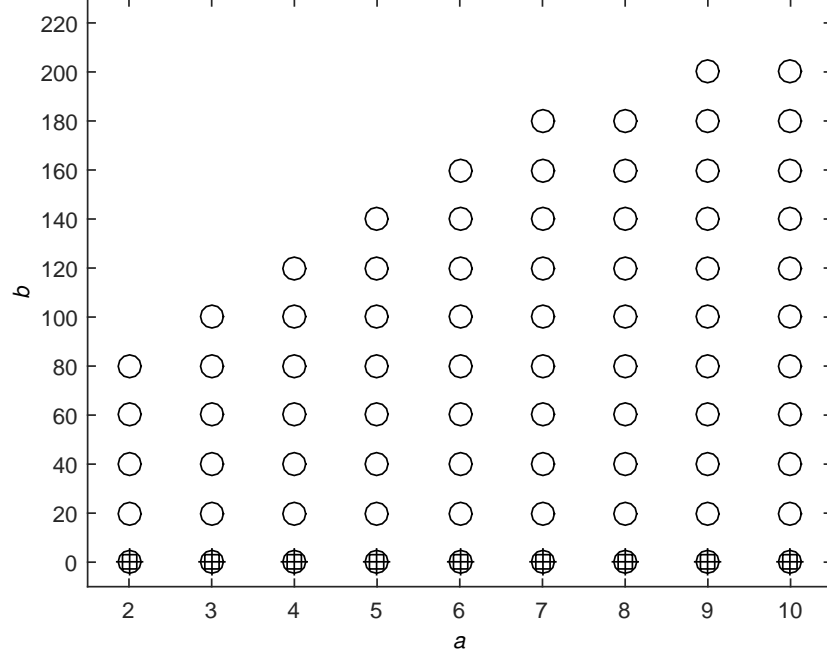


Figure 3.7: Stabilization regions obtained from Theorem 2 with only  $\mathbf{Y}_{ij}(x_1)$ ,  $\mathbf{\underline{W}}_{ij}(x_1)$  and  $\mathbf{\overline{W}}_{ij}(x_1)$ , indicated by “ $\times$ ” for Case 1, “ $+$ ” for Case 2, “ $\square$ ” for Case 3 and “ $o$ ” for Case 4.

in Fig. 3.11. It can be seen that the PFMB control system is guaranteed to be asymptotically stable in the domain  $x_1 \in [-10, 10]$ .

Compared with stability conditions in Remark 8 without any information of membership functions, there is no stabilization region within the same domain of parameters  $a$  and  $b$ . Since the polynomial fuzzy model and controller in this example do not share the same membership functions, PDC SOS-based stability conditions [3, 4, 9] in general cannot be applied. Users have more flexibility to choose the membership functions for fuzzy controllers instead of PDC approach. Accordingly, the relaxation and flexibility of the proposed method are exhibited from the comparison.

### 3.2.5 Conclusion

The stability analysis of PFMB control systems has been carried out. In favor of reducing the conservativeness, TSMFs have been proposed to approximate original membership functions. More information including the boundary of membership functions, the property of membership functions, and the boundary of operating domain, have been brought into stability conditions such that SOS-based conditions can be further relaxed. Future work can be done to bring specific membership function  $v_{r_{i,l}}(x_r)$  into stability conditions, which has potential to further reduce the conservativeness.



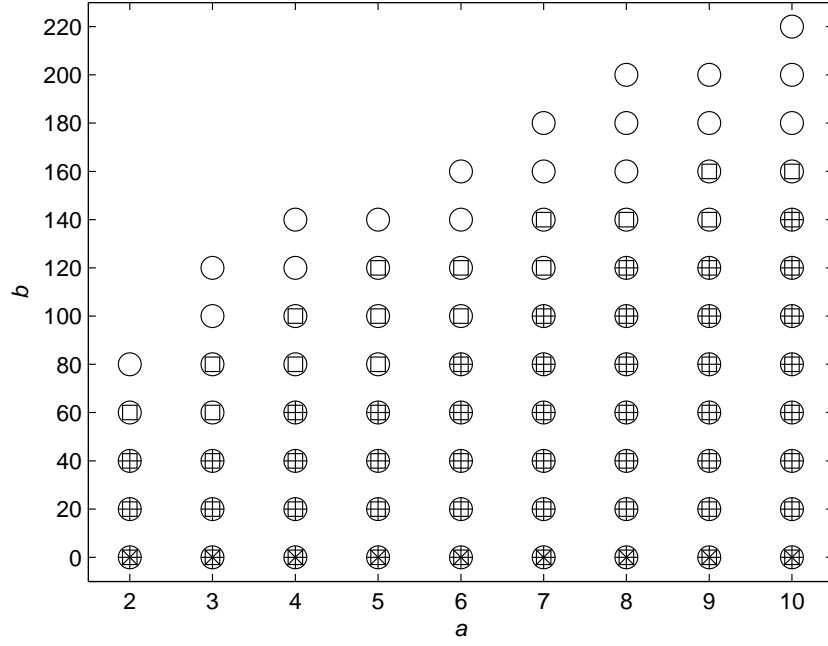


Figure 3.8: Stabilization regions obtained from Theorem 2 with only  $\mathbf{Y}_{ij}(x_1)$ ,  $\underline{\mathbf{W}}_{ij}(x_1)$ ,  $\overline{\mathbf{W}}_{ij}(x_1)$  and  $\mathbf{L}(x_1)$ , indicated by “ $\times$ ” for Case 1, “ $+$ ” for Case 2, “ $\square$ ” for Case 3 and “ $o$ ” for Case 4.

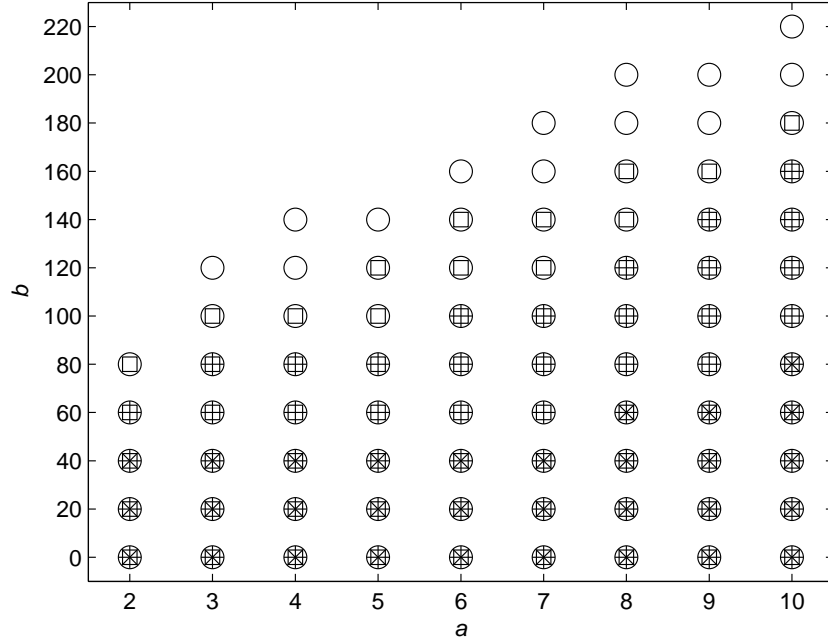


Figure 3.9: Stabilization regions obtained from Theorem 2 with all slack matrices ( $\mathbf{Y}_{ij}(x_1)$ ,  $\underline{\mathbf{W}}_{ij}(x_1)$ ,  $\overline{\mathbf{W}}_{ij}(x_1)$ ,  $\mathbf{L}(x_1)$  and  $\mathbf{K}(x_1)$ ), indicated by “ $\times$ ” for Case 1, “ $+$ ” for Case 2, “ $\square$ ” for Case 3 and “ $o$ ” for Case 4.

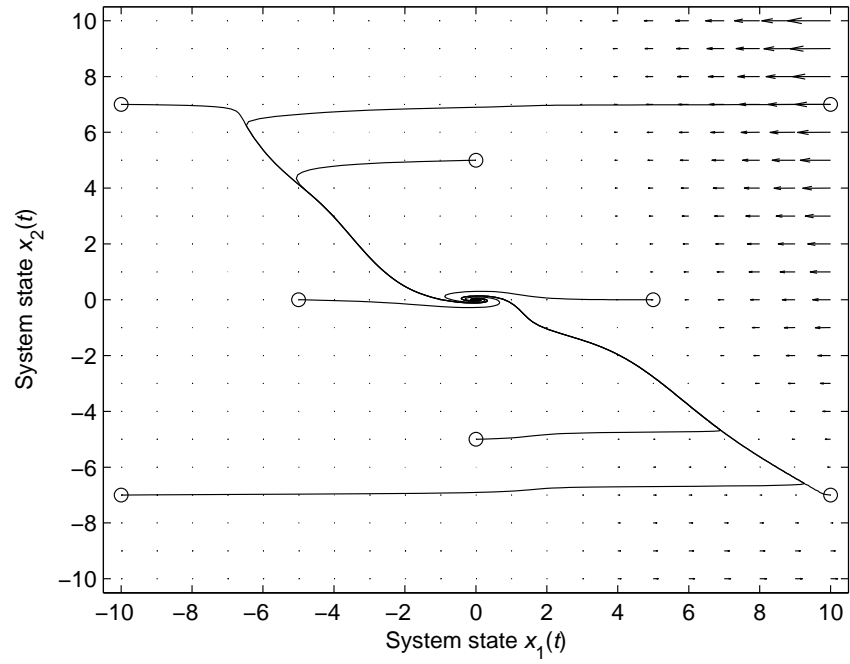


Figure 3.10: Phase plot of  $x_1(t)$  and  $x_2(t)$  for  $a = 10$  and  $b = 220$  in Case 4.

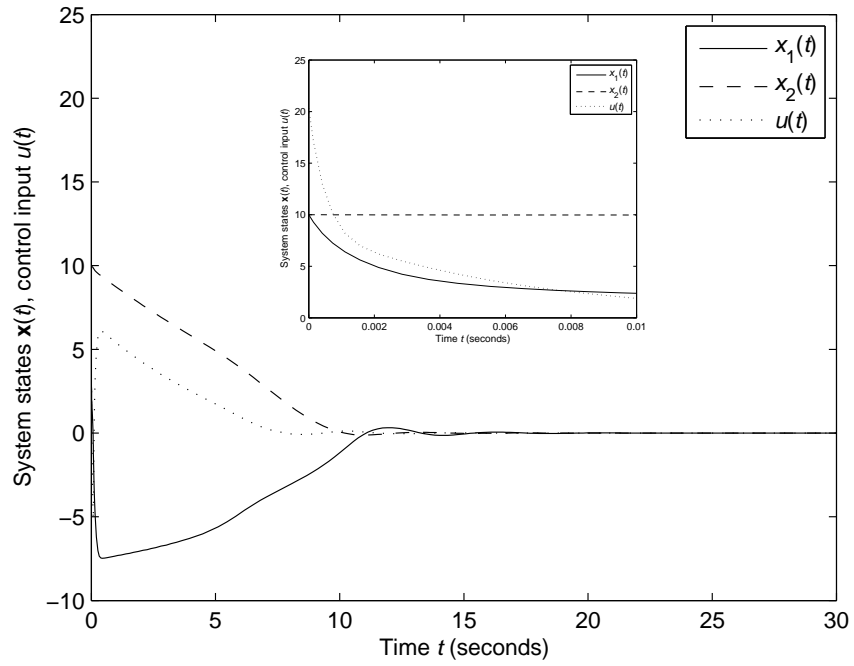


Figure 3.11: Transient response of  $\mathbf{x}(t)$  and control input  $u(t)$  for  $a = 10$  and  $b = 220$  in Case 4.

# Chapter 4

## Design of T-S Fuzzy Observer-Controller

To further improve the applicability of FMB control strategy, not only should conservativeness be considered, other control problems such as observers should also be investigated. When the system states are unmeasurable, the full-state feedback used in FMB control strategy cannot be applied. If an observer is used to estimate the system states, then the FMB observer-control strategy can be applied instead. In this chapter, the T-S fuzzy observer is considered and two types of T-S fuzzy observer-controller are designed. One is relaxed T-S fuzzy observer-controller with unmeasurable premise variables. Another is T-S fuzzy functional observer, which estimates the control input directly.

### 4.1 Design of Relaxed T-S Fuzzy Observer-Controller with Unmeasurable Premise Variables

#### 4.1.1 Introduction

Since both relaxation and membership functions in unmeasurable premise variables are important for widening the applicability of FMB observer-control scheme, it motivates the author to investigate relaxed stability conditions for T-S FMB observer-control systems with unmeasurable premise variables in this section. To achieve convex stability conditions, the matrix decoupling technique [54] is employed. Different from [54], the augmented vector is adequately chosen such that no more approximated transformation (such as completing square) is required before applying the decoupling technique. As a result, the number of predefined scalars can be reduced. However, the stability conditions are still conservative without applying any relaxation techniques. Consequently, membership-function-dependent approach is applied to bring the upper bounds of membership functions into stability conditions through slack matrices. For the proposed fuzzy observer-controller, only two scalars

are required to be predefined by users and the fuzzy observer cannot be replaced by the linear observer.

This section is organized as follows. In Subsection 4.1.2, with the consideration of observer, the new formulation of T-S fuzzy model, T-S fuzzy observer and T-S fuzzy controller are presented. In Subsection 4.1.3, stability analysis is carried out for T-S FMB observer-control system. In Subsection 4.1.4, simulation examples are provided to show the advantages of proposed fuzzy observer-controller. In Subsection 4.1.5, a conclusion is drawn.

## 4.1.2 Preliminary

With the consideration of observer, the new formulation of T-S fuzzy model, T-S fuzzy observer and T-S fuzzy controller are presented first.

### 4.1.2.1 T-S Fuzzy Model

The  $i^{th}$  rule of the T-S fuzzy model is [5]:

$$\begin{aligned} \text{Rule } i : & \text{ IF } f_1(\mathbf{x}(t)) \text{ is } M_1^i \text{ AND } \cdots \text{ AND } f_\Psi(\mathbf{x}(t)) \text{ is } M_\Psi^i, \\ & \text{ THEN } \dot{\mathbf{x}}(t) = \mathbf{A}_i \mathbf{x}(t) + \mathbf{B}_i \mathbf{u}(t), \\ & \mathbf{y}(t) = \mathbf{C} \mathbf{x}(t), \end{aligned}$$

where  $\mathbf{x}(t) = [x_1(t), x_2(t), \dots, x_n(t)]^T$  is the state vector, and  $n$  is the dimension of the nonlinear system;  $f_\eta(\mathbf{x}(t))$  is the premise variable corresponding to its fuzzy term  $M_\eta^i$  in rule  $i$ ,  $\eta = 1, 2, \dots, \Psi$ , and  $\Psi$  is a positive integer;  $\mathbf{A}_i \in \mathbb{R}^{n \times n}$  and  $\mathbf{B}_i \in \mathbb{R}^{n \times m}$  are the known system and input matrices, respectively;  $\mathbf{u}(t) \in \mathbb{R}^m$  is the control input vector;  $\mathbf{y}(t) \in \mathbb{R}^l$  is the output vector;  $\mathbf{C} \in \mathbb{R}^{l \times n}$  is the output matrix. The dynamics of the nonlinear system is given by

$$\begin{aligned} \dot{\mathbf{x}}(t) &= \sum_{i=1}^p w_i(\mathbf{x}(t)) (\mathbf{A}_i \mathbf{x}(t) + \mathbf{B}_i \mathbf{u}(t)), \\ \mathbf{y}(t) &= \mathbf{C} \mathbf{x}(t), \end{aligned} \tag{4.1}$$

where  $p$  is the number of fuzzy rules;  $w_i(\mathbf{x}(t))$  is the normalized grade of membership,  $w_i(\mathbf{x}(t)) = \frac{\prod_{\eta=1}^{\Psi} \mu_{M_\eta^i}(f_\eta(\mathbf{x}(t)))}{\sum_{k=1}^p \prod_{\eta=1}^{\Psi} \mu_{M_\eta^k}(f_\eta(\mathbf{x}(t)))}$ ,  $w_i(\mathbf{x}(t)) \geq 0, i = 1, 2, \dots, p$ , and  $\sum_{i=1}^p w_i(\mathbf{x}(t)) = 1$ ;  $\mu_{M_\eta^i}(f_\eta(\mathbf{x}(t))), \eta = 1, 2, \dots, \Psi$ , are grades of membership corresponding to the fuzzy term  $M_\eta^i$ .

### 4.1.2.2 T-S Fuzzy Observer

For brevity, time  $t$  is dropped for variables from now. Considering the premise variable  $f_\eta(\mathbf{x})$  depending on unmeasurable states, we apply the T-S fuzzy observer

with its  $i^{th}$  rule described as follows:

$$\begin{aligned} \text{Rule } i : & \text{ IF } f_1(\check{\mathbf{x}}) \text{ is } M_1^i \text{ AND } \cdots \text{ AND } f_\Psi(\check{\mathbf{x}}) \text{ is } M_\Psi^i, \\ & \text{ THEN } \dot{\check{\mathbf{x}}} = \mathbf{A}_i\check{\mathbf{x}} + \mathbf{B}_i\mathbf{u} + \mathbf{L}_i(\mathbf{y} - \check{\mathbf{y}}), \\ & \check{\mathbf{y}} = \mathbf{C}\check{\mathbf{x}}, \end{aligned}$$

where  $\check{\mathbf{x}} \in \Re^n$  is the estimated state  $\mathbf{x}$ ;  $\check{\mathbf{y}} \in \Re^l$  is the estimated output  $\mathbf{y}$ ;  $\mathbf{L}_i \in \Re^{n \times l}$  is the observer gain. The T-S fuzzy observer is given by

$$\begin{aligned} \dot{\check{\mathbf{x}}} &= \sum_{i=1}^p w_i(\check{\mathbf{x}}) \left( \mathbf{A}_i\check{\mathbf{x}} + \mathbf{B}_i\mathbf{u} + \mathbf{L}_i(\mathbf{y} - \check{\mathbf{y}}) \right), \\ \check{\mathbf{y}} &= \mathbf{C}\check{\mathbf{x}}. \end{aligned} \quad (4.2)$$

#### 4.1.2.3 T-S Fuzzy Controller

Using the PDC approach [1], the  $i^{th}$  rule of the T-S fuzzy controller is:

$$\begin{aligned} \text{Rule } i : & \text{ IF } f_1(\check{\mathbf{x}}) \text{ is } M_1^i \text{ AND } \cdots \text{ AND } f_\Psi(\check{\mathbf{x}}) \text{ is } M_\Psi^i, \\ & \text{ THEN } \mathbf{u} = \mathbf{G}_i\check{\mathbf{x}}, \end{aligned}$$

where  $\mathbf{G}_i \in \Re^{m \times n}$  is the controller gain. The T-S fuzzy controller is given by

$$\mathbf{u} = \sum_{i=1}^p w_i(\check{\mathbf{x}}) \mathbf{G}_i\check{\mathbf{x}}. \quad (4.3)$$

#### 4.1.3 Stability Analysis

In this section, stability analysis is conducted for T-S FMB observer-control systems. The closed-loop systems are provided first. Then based on the augmented systems and the Lyapunov stability theory, we derive the convex stability conditions by matrix decoupling technique. Finally, the membership-function-dependent approach is applied to relax the stability conditions.

The estimation error is defined as  $\mathbf{e} = \mathbf{x} - \check{\mathbf{x}}$ , and then we have the closed-loop systems (shown in Fig. 4.1):

$$\dot{\mathbf{x}} = \sum_{i=1}^p \sum_{k=1}^p w_i(\mathbf{x}) w_k(\check{\mathbf{x}}) \left( (\mathbf{A}_i + \mathbf{B}_i \mathbf{G}_k) \check{\mathbf{x}} + \mathbf{A}_i \mathbf{e} \right), \quad (4.4)$$

$$\dot{\check{\mathbf{x}}} = \sum_{j=1}^p \sum_{k=1}^p w_j(\check{\mathbf{x}}) w_k(\check{\mathbf{x}}) \left( (\mathbf{A}_j + \mathbf{B}_j \mathbf{G}_k) \check{\mathbf{x}} + \mathbf{L}_j \mathbf{C} \mathbf{e} \right), \quad (4.5)$$

$$\begin{aligned} \dot{\mathbf{e}} &= \sum_{i=1}^p \sum_{j=1}^p \sum_{k=1}^p w_i(\mathbf{x}) w_j(\check{\mathbf{x}}) w_k(\check{\mathbf{x}}) \left( (\mathbf{A}_i - \mathbf{A}_j \right. \\ & \quad \left. + (\mathbf{B}_i - \mathbf{B}_j) \mathbf{G}_k) \check{\mathbf{x}} + (\mathbf{A}_i - \mathbf{L}_j \mathbf{C}) \mathbf{e} \right). \end{aligned} \quad (4.6)$$

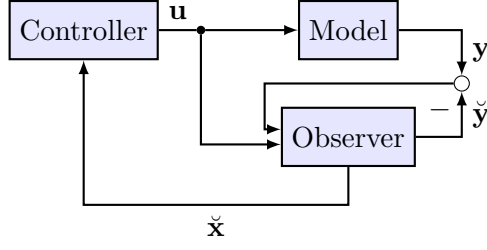


Figure 4.1: A block diagram of FMB observer-control systems.

**Theorem 3** *The augmented T-S FMB observer-control system (formed by (4.5) and (4.6)) is guaranteed to be asymptotically stable if there exist matrices  $\mathbf{X} \in \mathbb{R}^{n \times n}$ ,  $\mathbf{Y} \in \mathbb{R}^{n \times n}$ ,  $\mathbf{N}_k \in \mathbb{R}^{m \times n}$ ,  $\mathbf{M}_j \in \mathbb{R}^{n \times l}$ ,  $\mathbf{R}_{ijk} = \mathbf{R}_{ikj} \in \mathbb{R}^{3n \times 3n}$ ,  $\mathbf{S}_{ij} \in \mathbb{R}^{3n \times 3n}$ ,  $i, j, k = 1, 2, \dots, p$ , and predefined scalars  $\alpha_1 > 0, \alpha_2 > 0$  such that the following LMI-based conditions are satisfied:*

$$\mathbf{X} > 0; \quad (4.7)$$

$$\mathbf{Y} > 0; \quad (4.8)$$

$$\mathbf{R}_{ijk} \geq 0 \quad \forall i \text{ and } j \leq k; \quad (4.9)$$

$$\mathbf{S}_{ij} \geq 0 \quad \forall i, j; \quad (4.10)$$

$$\Phi_{ijk} + \Phi_{ikj} - 2\mathbf{R}_{ijk} + 2 \sum_{l=1}^p \sum_{m=1}^p \sum_{n=1}^p \gamma_{lmn} \mathbf{R}_{lmn} < 0 \quad \forall i \text{ and } j \leq k; \quad (4.11)$$

$$\Theta_{ij} - \mathbf{S}_{ij} + \sum_{l=1}^p \sum_{m=1}^p \gamma_{lm} \mathbf{S}_{lm} < 0 \quad \forall i, j; \quad (4.12)$$

where

$$\Phi_{ijk} = \begin{bmatrix} \hat{\Xi}_{jk}^{(11)} + \hat{\Xi}_{jk}^{(11)T} & \hat{\Xi}_{ijk}^{(21)T} & \mathbf{I} \\ * & -\alpha_2 \mathbf{I} & \mathbf{0} \\ * & * & -\frac{1}{\alpha_1} \mathbf{Y} \end{bmatrix}, \quad (4.13)$$

$$\Theta_{ij} = \begin{bmatrix} -\alpha_1 \mathbf{Y} & \tilde{\Xi}_j^{(12)} & \mathbf{0} \\ * & \tilde{\Xi}_{ij}^{(22)} + \tilde{\Xi}_{ij}^{(22)T} & \mathbf{Y} \\ * & * & -\frac{1}{\alpha_2} \mathbf{I} \end{bmatrix}, \quad (4.14)$$

$$\hat{\Xi}_{jk}^{(11)} = \mathbf{A}_j \mathbf{X} + \mathbf{B}_j \mathbf{N}_k, \quad (4.15)$$

$$\hat{\Xi}_{ijk}^{(21)} = (\mathbf{A}_i - \mathbf{A}_j) \mathbf{X} + (\mathbf{B}_i - \mathbf{B}_j) \mathbf{N}_k, \quad (4.16)$$

$$\tilde{\Xi}_j^{(12)} = \mathbf{M}_j \mathbf{C}, \quad (4.17)$$

$$\tilde{\Xi}_{ij}^{(22)} = \mathbf{Y} \mathbf{A}_i - \mathbf{M}_j \mathbf{C}, \quad (4.18)$$

$\gamma_{ijk}$  and  $\gamma_{ij}$  are the upper bounds of membership functions  $w_i(\mathbf{x})w_j(\check{\mathbf{x}})w_k(\check{\mathbf{x}})$  and  $w_i(\mathbf{x})w_j(\check{\mathbf{x}})$ , respectively; and the controller and observer gains are given by  $\mathbf{G}_k = \mathbf{N}_k \mathbf{X}^{-1}$  and  $\mathbf{L}_j = \mathbf{Y}^{-1} \mathbf{M}_j$ , respectively.

**Proof** Defining the augmented vector  $\mathbf{z} = [\tilde{\mathbf{x}}^T \quad \mathbf{e}^T]^T$  and denote  $w_i(\mathbf{x})w_j(\tilde{\mathbf{x}})w_k(\tilde{\mathbf{x}})$  as  $h_{ijk}$  and  $w_i(\mathbf{x})w_j(\tilde{\mathbf{x}})$  as  $h_{ij}$ , the augmented T-S FMB observer-control system is written as

$$\dot{\mathbf{z}} = \sum_{i=1}^p \sum_{j=1}^p \sum_{k=1}^p h_{ijk} \Xi_{ijk} \mathbf{z}, \quad (4.19)$$

where

$$\Xi_{ijk} = \begin{bmatrix} \Xi_{jk}^{(11)} & \Xi_j^{(12)} \\ \Xi_{ijk}^{(21)} & \Xi_{ij}^{(22)} \end{bmatrix}, \quad (4.20)$$

$$\Xi_{jk}^{(11)} = \mathbf{A}_j + \mathbf{B}_j \mathbf{G}_k, \quad (4.21)$$

$$\Xi_{ijk}^{(21)} = \mathbf{A}_i - \mathbf{A}_j + (\mathbf{B}_i - \mathbf{B}_j) \mathbf{G}_k, \quad (4.22)$$

$$\Xi_j^{(12)} = \mathbf{L}_j \mathbf{C}, \quad (4.23)$$

$$\Xi_{ij}^{(22)} = \mathbf{A}_i - \mathbf{L}_j \mathbf{C}. \quad (4.24)$$

**Remark 11** In this section, we employ the augmented vector  $\mathbf{z} = [\tilde{\mathbf{x}}^T \quad \mathbf{e}^T]^T$  rather than  $\mathbf{z} = [\mathbf{x}^T \quad \mathbf{e}^T]^T$  in [54]. This is in favor of the following derivation by directly separating the controller-related decision matrices from the observer-related decision matrices. In this way, the matrix decoupling technique [54] can be applied without any other approximated transformation. As a result, the number of predefined scalars is reduced.

The procedure of the proof is shown in Fig. 4.2. As can be seen, the matrix decoupling technique will separate the conditions into two parts and convex conditions will be obtained for both parts.

The following Lyapunov function candidate is employed to investigate the stability of the augmented T-S FMB observer-control system (4.19):

$$V(\mathbf{z}) = \mathbf{z}^T \mathbf{P} \mathbf{z}, \quad (4.25)$$

where  $\mathbf{P} = \begin{bmatrix} \mathbf{X}^{-1} & \mathbf{0} \\ \mathbf{0} & \mathbf{Y} \end{bmatrix}$ ,  $\mathbf{X} > 0$ ,  $\mathbf{Y} > 0$ , and thus  $\mathbf{P} > 0$ . The time derivative of the Lyapunov function is given as follows:

$$\dot{V}(\mathbf{z}) = \sum_{i=1}^p \sum_{j=1}^p \sum_{k=1}^p h_{ijk} \mathbf{z}^T (\mathbf{P} \Xi_{ijk} + \Xi_{ijk}^T \mathbf{P}) \mathbf{z}. \quad (4.26)$$

Therefore,  $\dot{V}(\mathbf{z}) < 0$  holds if

$$\sum_{i=1}^p \sum_{j=1}^p \sum_{k=1}^p h_{ijk} (\mathbf{P} \Xi_{ijk} + \Xi_{ijk}^T \mathbf{P}) < 0. \quad (4.27)$$

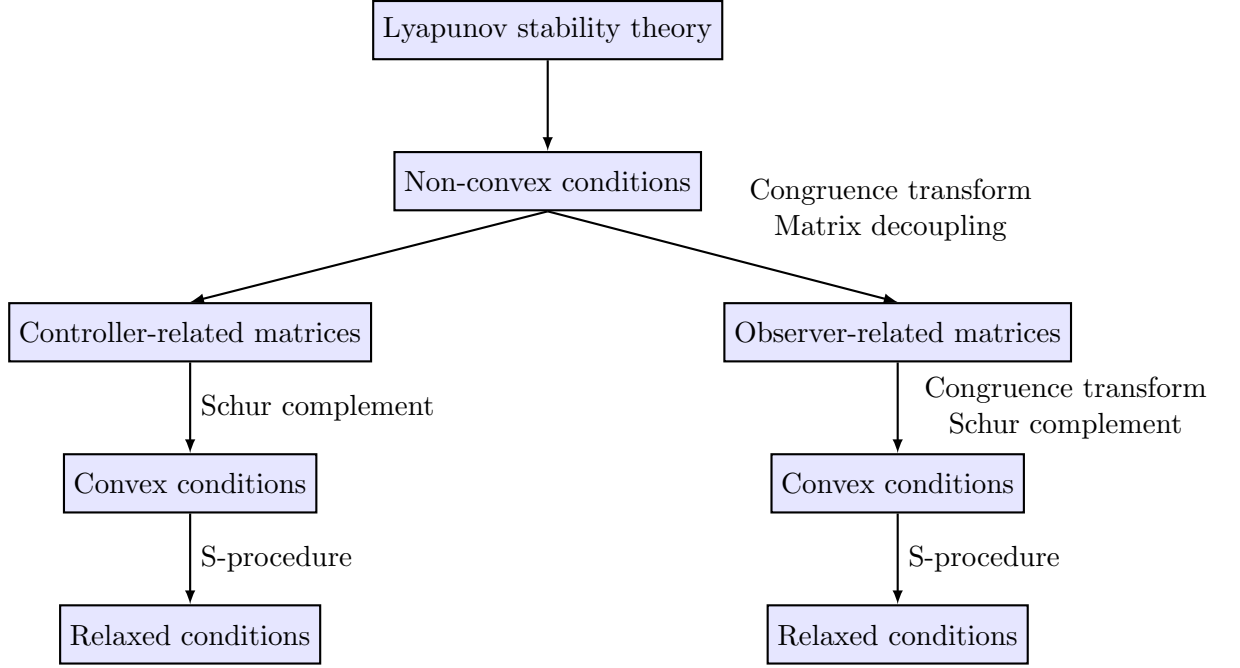


Figure 4.2: Procedure of the proof for Theorem 3.

**Remark 12** *The augmented T-S FMB observer-control system (4.19) is guaranteed to be asymptotically stable if  $V(\mathbf{z}) > 0$  and  $\dot{V}(\mathbf{z}) < 0$  excluding  $\mathbf{z} = \mathbf{0}$ . To ensure  $\dot{V}(\mathbf{z}) < 0$ , in the following, the congruence transformation is employed first, which is in favor of matrix decoupling.*

Performing congruence transformation to (4.27) by pre-multiplying and post-multiplying  $\mathbf{P}^{-1} = \begin{bmatrix} \mathbf{X} & \mathbf{0} \\ \mathbf{0} & \mathbf{Y}^{-1} \end{bmatrix}$  to both sides and denoting  $\mathbf{N}_k = \mathbf{G}_k \mathbf{X}$ , we have

$$\sum_{i=1}^p \sum_{j=1}^p \sum_{k=1}^p h_{ijk} (\hat{\Xi}_{ijk} + \hat{\Xi}_{ijk}^T) < 0, \quad (4.28)$$

where

$$\hat{\Xi}_{ijk} = \begin{bmatrix} \hat{\Xi}_{jk}^{(11)} & \hat{\Xi}_j^{(12)} \\ \hat{\Xi}_{ijk}^{(21)} & \hat{\Xi}_{ij}^{(22)} \end{bmatrix}, \quad (4.29)$$

$$\hat{\Xi}_j^{(12)} = \mathbf{L}_j \mathbf{C} \mathbf{Y}^{-1}, \quad (4.30)$$

$$\hat{\Xi}_{ij}^{(22)} = \mathbf{A}_i \mathbf{Y}^{-1} - \mathbf{L}_j \mathbf{C} \mathbf{Y}^{-1}, \quad (4.31)$$

$\hat{\Xi}_{jk}^{(11)}$  and  $\hat{\Xi}_{ijk}^{(21)}$  are defined in (4.15) and (4.16), respectively.

**Remark 13** *The stability contritions (4.28) are non-convex, which cannot be solved by current convex programming toolboxes. Note that the controller-related decision matrices  $\mathbf{X}$  and  $\mathbf{G}_k$  are separated from the observer-related decision matrices  $\mathbf{Y}$  and  $\mathbf{L}_j$ , and only the observer-related matrices are non-convex. Therefore, the matrix*



decoupling technique [54] is exploited in the following such that more transformation can be enforced on the observer-related matrices without affecting controller-related matrices.

Using matrix decoupling technique [54] to further separate decision variables in order to obtain convex LMI stability conditions, we rewrite  $\hat{\Xi}_{ijk} + \hat{\Xi}_{ijk}^T$  as follows:

$$\hat{\Xi}_{ijk} + \hat{\Xi}_{ijk}^T = \Gamma_{ijk} + \Lambda_{ij}, \quad (4.32)$$

where

$$\Gamma_{ijk} = \begin{bmatrix} \hat{\Xi}_{jk}^{(11)} + \hat{\Xi}_{jk}^{(11)T} + \alpha_1 \mathbf{Y}^{-1} & \hat{\Xi}_{ijk}^{(21)T} \\ * & -\alpha_2 \mathbf{I} \end{bmatrix}, \quad (4.33)$$

$$\Lambda_{ij} = \begin{bmatrix} -\alpha_1 \mathbf{Y}^{-1} & \hat{\Xi}_j^{(12)} \\ * & \hat{\Xi}_{ij}^{(22)} + \hat{\Xi}_{ij}^{(22)T} + \alpha_2 \mathbf{I} \end{bmatrix}. \quad (4.34)$$

Hence,  $\dot{V}(\mathbf{z}) < 0$  holds if

$$\sum_{i=1}^p \sum_{j=1}^p \sum_{k=1}^p h_{ijk} \Gamma_{ijk} < 0, \quad (4.35)$$

$$\sum_{i=1}^p \sum_{j=1}^p h_{ij} \Lambda_{ij} < 0. \quad (4.36)$$

Performing congruence transformation to (4.36) by pre-multiplying and post-multiplying  $\text{diag}\{\mathbf{Y}, \mathbf{Y}\}$  to both sides, denoting  $\mathbf{M}_j = \mathbf{Y}\mathbf{L}_j$ , and then applying Schur complement to both (4.35) and (4.36), we obtain

$$\sum_{i=1}^p \sum_{j=1}^p \sum_{k=1}^p h_{ijk} \Phi_{ijk} < 0, \quad (4.37)$$

$$\sum_{i=1}^p \sum_{j=1}^p h_{ij} \Theta_{ij} < 0, \quad (4.38)$$

where  $\Phi_{ijk}$  and  $\Theta_{ij}$  are defined in (4.13) and (4.14), respectively.

**Remark 14** Although the stability contritions (4.37) and (4.38) are convex now, they are conservative since they are membership-function-independent. Moreover, if there exists  $\mathbf{M}_j \forall j$  such that (4.38) is satisfied, then one can let  $\mathbf{M}_j = \mathbf{M}_1 \forall j$  such that (4.38) is also satisfied. It means that the fuzzy observer can be replaced by a linear observer, and there is no need to use a fuzzy observer. In the following, we try to relax the stability conditions by considering the information of membership functions. In this way, the advantage of fuzzy observer over linear observer is revealed.

Defining the upper bounds of membership functions  $h_{ijk}$  and  $h_{ij}$  as  $\gamma_{ijk}$  and  $\gamma_{ij}$ , respectively, we have  $\gamma_{ijk} - h_{ijk} \geq 0$  and  $\gamma_{ij} - h_{ij} \geq 0$ . Adding these information and slack matrices  $0 \leq \mathbf{R}_{ijk} = \mathbf{R}_{ikj} \in \Re^{3n \times 3n}$  and  $0 \leq \mathbf{S}_{ij} \in \Re^{3n \times 3n}$  by S-procedure, we have

$$\begin{aligned}
& \sum_{i=1}^p \sum_{j=1}^p \sum_{k=1}^p h_{ijk} \Phi_{ijk} \\
& \leq \sum_{i=1}^p \sum_{j=1}^p \sum_{k=1}^p h_{ijk} \Phi_{ijk} + \sum_{i=1}^p \sum_{j=1}^p \sum_{k=1}^p (\gamma_{ijk} - h_{ijk}) \mathbf{R}_{ijk} \\
& = \sum_{i=1}^p \sum_{j=1}^p \sum_{k=1}^p h_{ijk} \left( \Phi_{ijk} - \mathbf{R}_{ijk} + \sum_{l=1}^p \sum_{m=1}^p \sum_{n=1}^p \gamma_{lmn} \mathbf{R}_{lmn} \right) \\
& = \frac{1}{2} \sum_{i=1}^p \sum_{j=1}^p \sum_{k=1}^p h_{ijk} \left( \Phi_{ijk} + \Phi_{ikj} - 2\mathbf{R}_{ijk} \right. \\
& \quad \left. + 2 \sum_{l=1}^p \sum_{m=1}^p \sum_{n=1}^p \gamma_{lmn} \mathbf{R}_{lmn} \right). \tag{4.39}
\end{aligned}$$

Similarly,

$$\begin{aligned}
& \sum_{i=1}^p \sum_{j=1}^p h_{ij} \Theta_{ij} \\
& \leq \sum_{i=1}^p \sum_{j=1}^p h_{ij} \left( \Theta_{ij} - \mathbf{S}_{ij} + \sum_{l=1}^p \sum_{m=1}^p \gamma_{lm} \mathbf{S}_{lm} \right). \tag{4.40}
\end{aligned}$$

Therefore,  $\dot{V}(\mathbf{z}) < 0$  can be achieved by satisfying conditions (4.11) and (4.12). The proof is completed.

#### 4.1.4 Simulation Examples

Two simulation examples are provided to show the advantages of the proposed fuzzy observer-controller. In the first example, we compare the proposed stability conditions with those without slack matrices to demonstrate the merit of relaxation. In the second example, we compare the fuzzy observer with the linear observer to exhibit the improved applicability of the fuzzy observer as well as the effect of slack matrices.

##### 4.1.4.1 Example 1

Consider the following T-S fuzzy model extended from [53]:

$$\mathbf{A}_1 = \begin{bmatrix} 1 & 0 \\ -1 & -1 \end{bmatrix}, \mathbf{A}_2 = \begin{bmatrix} 2.5 & 0 \\ -2.3 & -1 \end{bmatrix},$$

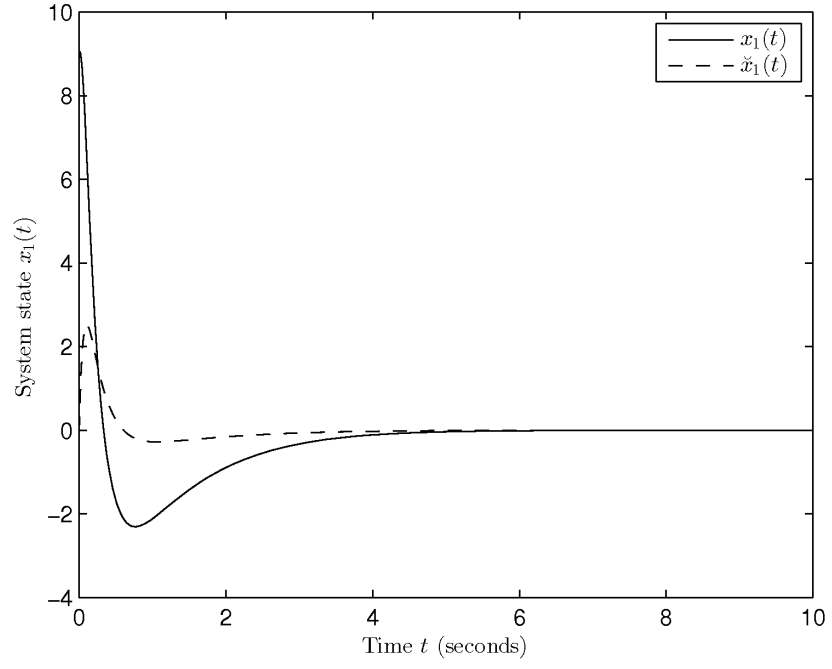
$$\mathbf{A}_3 = \begin{bmatrix} 1.5 & -0.3 \\ 0 & -1 \end{bmatrix}, \mathbf{B}_1 = \mathbf{B}_2 = \begin{bmatrix} 1 \\ 0 \end{bmatrix},$$

$$\mathbf{B}_3 = \begin{bmatrix} 1.3 \\ 0.2 \end{bmatrix}, \mathbf{C} = \begin{bmatrix} 10 & 2 \end{bmatrix},$$

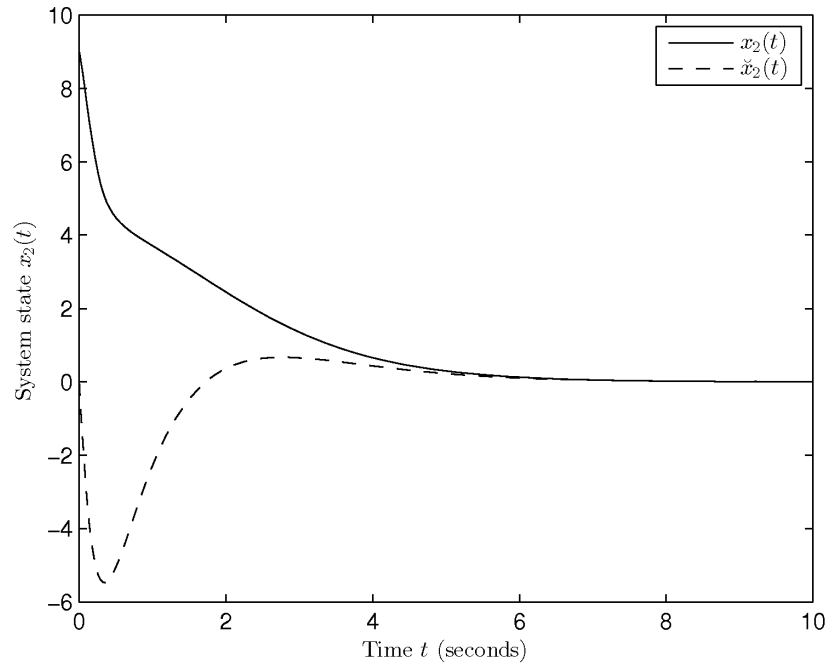
where the membership functions are  $w_1(x_1) = 1 - 1/(1 + e^{-(x_1+0.8)})$ ,  $w_2(x_1) = 1 - w_1(x_1) - w_3(x_1)$  and  $w_3(x_1) = 1/(1 + e^{-(x_1-0.8)})$ . Defining the region of interest as  $x_1 \in [-10, 10]$ , we obtain the upper bounds of membership functions as shown in Table B.1.

This example shows that the proposed stability conditions are more relaxed than [54] which does not include any slack matrices. Choosing  $\alpha_1 = 5.7, \alpha_2 = 1$  and applying Theorem 3, we obtain a feasible solution. The controller gains are  $\mathbf{G}_1 = [-1.3609 \times 10^1 \quad 2.8117 \times 10^{-2}]$ ,  $\mathbf{G}_2 = [-1.5259 \times 10^1 \quad 1.3524 \times 10^{-3}]$  and  $\mathbf{G}_3 = [-1.3798 \times 10^1 \quad -6.4585 \times 10^{-2}]$ , and the observer gains are  $\mathbf{L}_1 = [6.3479 \times 10^{-1} \quad -3.2689 \times 10^{-1}]^T$ ,  $\mathbf{L}_2 = [6.3371 \times 10^{-1} \quad -3.2541 \times 10^{-1}]^T$  and  $\mathbf{L}_3 = [6.3479 \times 10^{-1} \quad -3.2689 \times 10^{-1}]^T$ . Choosing the initial conditions  $\mathbf{x}(0) = [9 \quad 9]^T$  and  $\hat{\mathbf{x}}(0) = [0 \quad 0]^T$ , the responses of system and estimated states are shown in Fig. 4.3.

For comparison purposes, we set  $\mathbf{R}_{ijk} = \mathbf{0}$  and  $\mathbf{S}_{ij} = \mathbf{0} \forall i, j, k$  in Theorem 3 to investigate how the slack matrix variables influence the conservativeness of the stability conditions. While other settings are the same, no feasible solutions can be found. Consequently, the proposed stability conditions are more relaxed due to exploiting the information of membership functions.



(a) System state  $x_1(t)$  and estimated state  $\hat{x}_1(t)$ .



(b) System state  $x_2(t)$  and estimated state  $\hat{x}_2(t)$ .

Figure 4.3: Time responses of system states  $x_1(t)$  and  $x_2(t)$  and estimated states  $\hat{x}_1(t)$  and  $\hat{x}_2(t)$ .

#### 4.1.4.2 Example 2

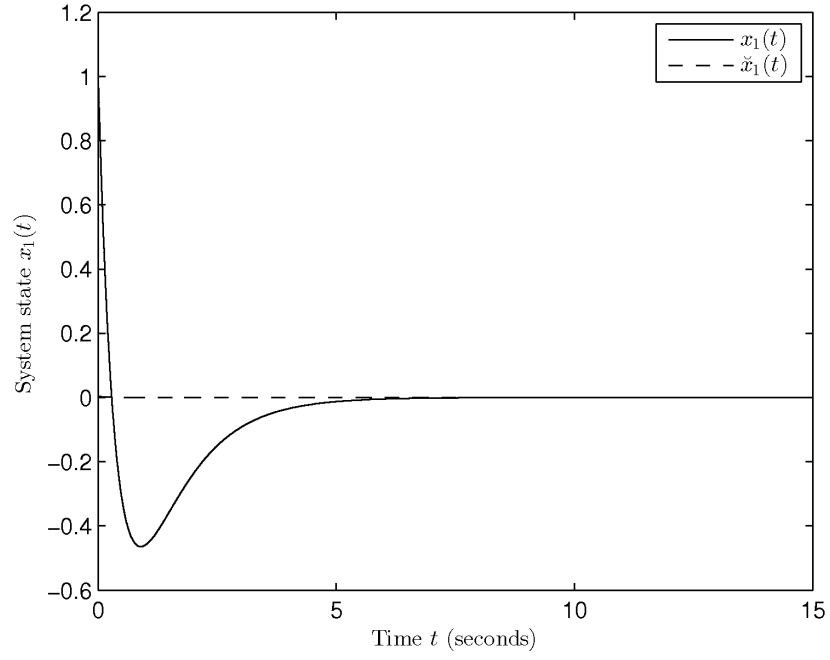
Consider the following T-S fuzzy model:

$$\mathbf{A}_1 = \begin{bmatrix} 2.5 & 0 \\ -2.4 & -1 \end{bmatrix}, \mathbf{A}_2 = \begin{bmatrix} 2.5 & 0 \\ -2.3 & -1 \end{bmatrix},$$

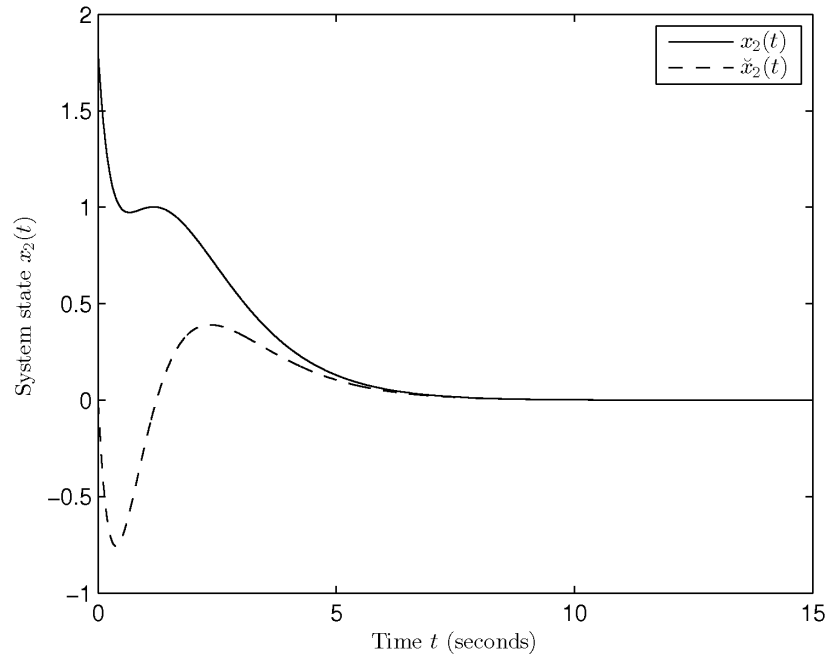
$$\mathbf{B}_1 = \mathbf{B}_2 = \begin{bmatrix} 1 \\ 0 \end{bmatrix}, \mathbf{C} = \begin{bmatrix} 10 & 2 \end{bmatrix},$$

where the membership functions are  $w_1(x_2) = 0.5 + \frac{\arctan(x_2-3.2)}{\pi}$  and  $w_2(x_2) = 1 - w_1(x_2)$ . Defining the region of interest as  $x_2 \in [-1.8, 1.8]$ , we obtain the upper bounds as shown in Table B.2.

In this example, we aim to demonstrate that the proposed fuzzy observer cannot be replaced by the linear observer. Choosing  $\alpha_1 = 5.0001, \alpha_2 = 1$  and applying Theorem 3, we obtain a feasible solution with controller gains as  $\mathbf{G}_1 = [-2.2459 \times 10^3 \quad 3.9537 \times 10^{-3}]$  and  $\mathbf{G}_2 = [-2.3983 \times 10^3 \quad 4.2161 \times 10^{-3}]$  and observer gains as  $\mathbf{L}_1 = [5.7609 \times 10^{-1} \quad -3.8037 \times 10^{-1}]^T$  and  $\mathbf{L}_2 = [5.7610 \times 10^{-1} \quad -3.8044 \times 10^{-1}]^T$ . Choosing the initial conditions  $\mathbf{x}(0) = [1 \quad 1.8]^T$  and  $\check{\mathbf{x}}(0) = [0 \quad 0]^T$ , the corresponding time responses are shown in Fig. 4.4.



(a) System state  $x_1(t)$  and estimated state  $\hat{x}_1(t)$ .



(b) System state  $x_2(t)$  and estimated state  $\hat{x}_2(t)$ .

Figure 4.4: Time responses of system states  $x_1(t)$  and  $x_2(t)$  and estimated states  $\hat{x}_1(t)$  and  $\hat{x}_2(t)$ .

To design the linear observer, we let  $\mathbf{M}_j = \mathbf{M} \forall j$  in Theorem 3 and keep other settings the same. However, no feasible solutions can be found. It indicates that the proposed fuzzy observer is more general than the linear observer, which is attributed to the additional slack matrices.

### 4.1.5 Conclusion

The stability of T-S FMB observer-control system has been investigated. Both the unmeasurable premise variables and membership-function-dependent approach have been considered to widen the applicability of the designed fuzzy observer-controller. Matrix decoupling technique has been employed to obtain convex stability conditions. The number of predefined scalars has been reduced by adequately choosing the augmented vector which is in favor of applying matrix decoupling technique. Simulation examples have been offered to demonstrate the relaxation of proposed observer-controller.

## 4.2 Design of T-S Fuzzy Functional Observer

### 4.2.1 Introduction

Other than the T-S fuzzy observer, we design the fuzzy functional observer to estimate the control input directly, which can reduce the order of the observer. We extend the technique for linear functional observer [58] to design the fuzzy functional observer since similar problems will be handled and observer gains can be obtained with guaranteed stability in [58]. To ease the analysis, we propose a new form of fuzzy functional observer. Based on the proposed form, the separation principle [85] is applied to design the fuzzy functional observer separately from the fuzzy controller. In addition, convex stability conditions are derived. Compared with existing fuzzy functional observers [57, 59], the proposed fuzzy functional observer is designed by numerically solving the stability conditions and the stability of FMB observer-control system is guaranteed simultaneously.

This section is organized as follows. Stability analysis of FMB functional observer-control system is conducted in Subsection 4.2.2. Simulation examples are given in Subsection 4.2.3 to demonstrate the proposed design procedure. Finally, a conclusion is drawn in Subsection 4.2.4.

### 4.2.2 Stability Analysis

In this section, the fuzzy functional observer is proposed to estimate the control input when only system output  $\mathbf{y}$  is measurable instead of system state  $\mathbf{x}$ . A new form of the fuzzy functional observer will be proposed to make the augmented system in triangular form such that the separation principle can be applied. For brevity, time  $t$  is dropped without ambiguity.

The T-S fuzzy model (2.2) is assumed to be in the following form:

$$\dot{\mathbf{x}} = \sum_{i=1}^p w_i(\mathbf{y})(\mathbf{A}_i \mathbf{x} + \mathbf{B}_i \mathbf{\ddot{u}}),$$

$$\mathbf{y} = \mathbf{C}\mathbf{x}, \quad (4.41)$$

where  $\check{\mathbf{u}} \in \mathfrak{R}^m$  is the estimated control input;  $\mathbf{y} \in \mathfrak{R}^l$  is the system output and  $\mathbf{C} \in \mathfrak{R}^{l \times n}$  is the output matrix. Moreover, the fuzzy controller (2.3) is considered to be:

$$\begin{aligned} \mathbf{u} &= \sum_{j=1}^p w_j(\mathbf{y}) \mathbf{u}_j \\ &= \sum_{j=1}^p w_j(\mathbf{y}) \mathbf{G}_j \mathbf{x}, \end{aligned} \quad (4.42)$$

where  $\mathbf{u}_j = \mathbf{G}_j \mathbf{x} \in \mathfrak{R}^m$  is the control input in the  $j^{th}$  rule. Without loss of generality, we assume  $\text{rank}(\mathbf{C}) = l$  and  $\text{rank}(\mathbf{G}_j) = m$  [58], which means  $\mathbf{C}$  and  $\mathbf{G}_j$  are of full row rank.

The following fuzzy functional observer is proposed to estimate the control input  $\mathbf{u}$  in (4.42):

$$\begin{aligned} \dot{\mathbf{z}}_j &= \sum_{i=1}^p w_i(\mathbf{y}) \left( \mathbf{N}_{ij} \mathbf{z}_j + \mathbf{J}_{ij} \mathbf{y} + \mathbf{H}_{ij} \check{\mathbf{u}} \right) \forall j, \\ \check{\mathbf{u}}_j &= \mathbf{z}_j + \mathbf{E}_j \mathbf{y} \forall j, \\ \check{\mathbf{u}} &= \sum_{j=1}^p w_j(\mathbf{y}) \check{\mathbf{u}}_j, \end{aligned} \quad (4.43)$$

where  $\mathbf{z}_j \in \mathfrak{R}^m$  is the observer state;  $\check{\mathbf{u}}_j \in \mathfrak{R}^m$  is the estimated control input in the  $j^{th}$  rule;  $\mathbf{N}_{ij} \in \mathfrak{R}^{m \times m}$ ,  $\mathbf{J}_{ij} \in \mathfrak{R}^{m \times l}$ ,  $\mathbf{H}_{ij} \in \mathfrak{R}^{m \times m}$  and  $\mathbf{E}_j \in \mathfrak{R}^{m \times l}$  are observer gains to be designed.

**Remark 15** *The proposed form of fuzzy functional observer is different from those in [57, 59]. In what follows, the separation principle [85] will be applied to separately design the fuzzy controller and fuzzy functional observer. Furthermore, the technique in [58] and [86] for linear functional observer will be extended to design the fuzzy functional observer. To achieve these two tasks, we choose such form of fuzzy functional observer.*

For brevity, the membership function  $w_i(\mathbf{y})$  is denoted as  $w_i$ . The estimation error is defined as  $\mathbf{e}_j = \mathbf{u}_j - \check{\mathbf{u}}_j = \mathbf{G}_j \mathbf{x} - (\mathbf{z}_j + \mathbf{E}_j \mathbf{y}) = \mathbf{Q}_j \mathbf{x} - \mathbf{z}_j$  where  $\mathbf{Q}_j = \mathbf{G}_j - \mathbf{E}_j \mathbf{C}$ , and then we have the closed-loop system (shown in Fig. 4.5) consisting of the T-S fuzzy model (4.41), the fuzzy controller (4.42) and the fuzzy functional observer (4.43) as follows:

$$\dot{\mathbf{x}} = \sum_{i=1}^p w_i \left( \mathbf{A}_i \mathbf{x} + \mathbf{B}_i \sum_{k=1}^p w_k \check{\mathbf{u}}_k \right)$$



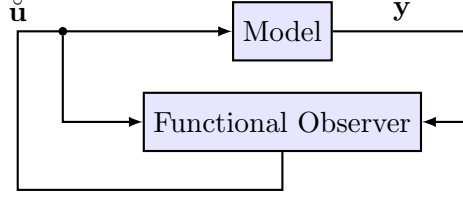


Figure 4.5: A block diagram of FMB functional observer-control systems.

$$\begin{aligned}
&= \sum_{i=1}^p w_i \left( \mathbf{A}_i \mathbf{x} + \mathbf{B}_i \sum_{k=1}^p w_k (\mathbf{u}_k - \mathbf{e}_k) \right) \\
&= \sum_{i=1}^p \sum_{l=1}^p h_{il} \left( \mathbf{A}_i \mathbf{x} + \mathbf{B}_i \mathbf{G}_l \mathbf{x} - \mathbf{B}_i \sum_{k=1}^p w_k \mathbf{e}_k \right), \tag{4.44}
\end{aligned}$$

$$\begin{aligned}
\dot{\mathbf{e}}_j &= \mathbf{Q}_j \dot{\mathbf{x}} - \dot{\mathbf{z}}_j \\
&= \sum_{i=1}^p \sum_{l=1}^p h_{il} \left( \mathbf{Q}_j (\mathbf{A}_i \mathbf{x} + \mathbf{B}_i \mathbf{G}_l \mathbf{x} - \mathbf{B}_i \sum_{k=1}^p w_k \mathbf{e}_k) \right. \\
&\quad \left. - (\mathbf{N}_{ij} (\mathbf{Q}_j \mathbf{x} - \mathbf{e}_j) + \mathbf{J}_{ij} \mathbf{C} \mathbf{x} \right. \\
&\quad \left. + \mathbf{H}_{ij} \sum_{k=1}^p w_k (\mathbf{G}_k \mathbf{x} - \mathbf{e}_k)) \right) \\
&= \sum_{i=1}^p \sum_{l=1}^p h_{il} \left( (\Phi_{ij} + \Lambda_{ij} \mathbf{G}_l) \mathbf{x} + \mathbf{N}_{ij} \mathbf{e}_j \right. \\
&\quad \left. - \Lambda_{ij} \sum_{k=1}^p w_k \mathbf{e}_k \right) \forall j, \tag{4.45}
\end{aligned}$$

where  $h_{il} \equiv w_i w_l$ ,  $\Phi_{ij} = \mathbf{Q}_j \mathbf{A}_i - \mathbf{N}_{ij} \mathbf{Q}_j - \mathbf{J}_{ij} \mathbf{C}$ ,  $\Lambda_{ij} = \mathbf{Q}_j \mathbf{B}_i - \mathbf{H}_{ij}$ .

The control objective is to make the augmented FMB functional observer-control system (formed by (4.44) and (4.45)) asymptotically stable, i.e.,  $\mathbf{x} \rightarrow 0$  and  $\mathbf{e}_j \rightarrow 0 \forall j$  as time  $t \rightarrow \infty$ , by determining the controller gain  $\mathbf{G}_j$  and observer gains  $\mathbf{N}_{ij}$ ,  $\mathbf{J}_{ij}$ ,  $\mathbf{H}_{ij}$ ,  $\mathbf{E}_j$ .

In order to apply the separation principle [85] to design the controller and observer separately, the following constraints can be imposed:

$$\Phi_{ij} = \mathbf{0} \forall i, j, \tag{4.46}$$

$$\Lambda_{ij} = \mathbf{0} \forall i, j. \tag{4.47}$$

Defining the augmented vector  $\mathbf{x}_a = [\mathbf{x}^T \quad \mathbf{e}_1^T \quad \mathbf{e}_2^T \quad \cdots \quad \mathbf{e}_p^T]^T$ , the augmented FMB functional observer-control system is written as

$$\dot{\mathbf{x}}_a = \sum_{i=1}^p \sum_{l=1}^p h_{il} \Gamma_{il} \mathbf{x}_a, \tag{4.48}$$

where

$$\Gamma_{il} = \begin{bmatrix} \mathbf{A}_i + \mathbf{B}_i \mathbf{G}_l & -\mathbf{B}_i w_1 & -\mathbf{B}_i w_2 & \cdots & -\mathbf{B}_i w_p \\ \mathbf{0} & \mathbf{N}_{i1} & \mathbf{0} & \cdots & \mathbf{0} \\ \mathbf{0} & \mathbf{0} & \mathbf{N}_{i2} & \cdots & \mathbf{0} \\ \vdots & \vdots & \vdots & \ddots & \vdots \\ \mathbf{0} & \mathbf{0} & \mathbf{0} & \cdots & \mathbf{N}_{ip} \end{bmatrix}.$$

**Remark 16** *It has been justified in [85] that the separation principle can be applied to the system in triangular form (4.48). In other words, the fuzzy controller and the fuzzy functional observer can be designed separately. The controller gain  $\mathbf{G}_j$  can be obtained by existing methods (for example, Theorem 1 in this thesis). Then the obtained  $\mathbf{G}_j$  is employed to design the fuzzy functional observer.*

To design the fuzzy functional observer, the objective is to find observer gains  $\mathbf{N}_{ij}$ ,  $\mathbf{J}_{ij}$ ,  $\mathbf{H}_{ij}$  and  $\mathbf{E}_j$  such that the error systems

$$\dot{\mathbf{e}}_j = \sum_{i=1}^p w_i \mathbf{N}_{ij} \mathbf{e}_j \quad \forall j \quad (4.49)$$

are asymptotically stable and the constraints (4.46) and (4.47) are satisfied.

In what follows, we first propose the stability conditions ensuring the stability of the error systems (4.49) and facilitating the satisfaction of constraints (4.46) and (4.47). Then a design procedure is presented to obtain all observer gains while satisfying constraints (4.46) and (4.47).

**Theorem 4** *The error systems (4.49) are guaranteed to be asymptotically stable if there exist matrices  $\mathbf{X} = \mathbf{X}^T \in \mathbb{R}^{m \times m}$ ,  $\mathbf{Y}_{ij} \in \mathbb{R}^{m \times 2l}$ ,  $i, j = 1, 2, \dots, p$  such that the following LMI-based conditions are satisfied:*

$$\mathbf{X} > \mathbf{0}; \quad (4.50)$$

$$\mathbf{X} \mathbf{F}_{ij} - \mathbf{Y}_{ij} \mathbf{M}_{ij} + \mathbf{F}_{ij}^T \mathbf{X} - \mathbf{M}_{ij}^T \mathbf{Y}_{ij}^T < \mathbf{0} \quad \forall i, j; \quad (4.51)$$

$$\tilde{\mathbf{E}}_{i_1 j} = \tilde{\mathbf{E}}_{i_2 j} \quad \forall i_1 < i_2, j; \quad (4.52)$$

where

$$\mathbf{F}_{ij} = \mathbf{G}_j \mathbf{A}_i \mathbf{G}_j^+ - \mathbf{G}_j \bar{\mathbf{A}}_{ij} \Sigma_{ij}^+ \begin{bmatrix} \mathbf{C} \mathbf{A}_i \mathbf{G}_j^+ \\ \mathbf{C} \mathbf{G}_j^+ \end{bmatrix}, \quad (4.53)$$

$$\mathbf{M}_{ij} = (\mathbf{I} - \Sigma_{ij} \Sigma_{ij}^+) \begin{bmatrix} \mathbf{C} \mathbf{A}_i \mathbf{G}_j^+ \\ \mathbf{C} \mathbf{G}_j^+ \end{bmatrix}, \quad (4.54)$$

$$\bar{\mathbf{A}}_{ij} = \mathbf{A}_i (\mathbf{I} - \mathbf{G}_j^+ \mathbf{G}_j), \quad (4.55)$$

$$\Sigma_{ij} = \begin{bmatrix} \mathbf{C} \bar{\mathbf{A}}_{ij} \\ \bar{\mathbf{C}}_j \end{bmatrix}, \quad (4.56)$$

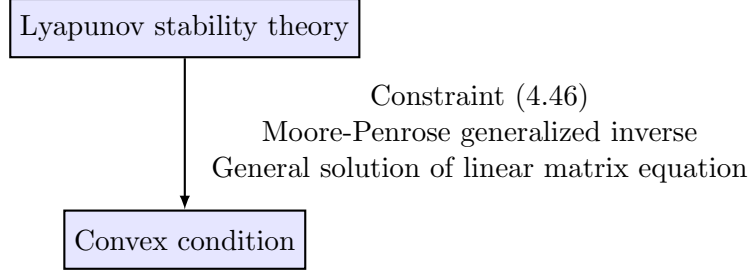


Figure 4.6: Procedure of proof for Theorem 4.

$$\bar{\mathbf{C}}_j = \mathbf{C}(\mathbf{I} - \mathbf{G}_j^+ \mathbf{G}_j); \quad (4.57)$$

the controller gain  $\mathbf{G}_j$  is determined by Theorem 1;  $\tilde{\mathbf{E}}_{ij}$  in (4.52) is obtained by  $[\tilde{\mathbf{E}}_{ij} \quad \tilde{\mathbf{K}}_{ij}] = \mathbf{X}\mathbf{G}_j\bar{\mathbf{A}}_{ij}\Sigma_{ij}^+ + \mathbf{Y}_{ij}(\mathbf{I} - \Sigma_{ij}\Sigma_{ij}^+)$ ; and  $\mathbf{Z}_{ij} = \mathbf{X}^{-1}\mathbf{Y}_{ij}$ .

**Proof** The structure of the following analysis is shown in Fig. 4.6. As can be seen, in order to apply Lyapunov stability theory, the constraint (4.46) will be utilized with some equivalent transformation. With the help of mathematical techniques, convex conditions will be obtained such that the stability and the satisfaction of constraints can be guaranteed simultaneously.

The constraint (4.46) is equivalent to

$$\Phi_{ij}[\mathbf{G}_j^+ \quad \mathbf{I} - \mathbf{G}_j^+ \mathbf{G}_j] = \mathbf{0} \quad \forall i, j, \quad (4.58)$$

where  $\mathbf{G}_j^+$  is the Moore-Penrose generalized inverse of  $\mathbf{G}_j$ . The proof of (4.58) is shown in Appendix A. From (4.58), we get  $\Phi_{ij}\mathbf{G}_j^+ = \mathbf{0}$  and  $\Phi_{ij}(\mathbf{I} - \mathbf{G}_j^+ \mathbf{G}_j) = \mathbf{0}$ . Substituting  $\mathbf{Q}_j = \mathbf{G}_j - \mathbf{E}_j\mathbf{C}$  into  $\Phi_{ij}$ , we have

$$((\mathbf{G}_j - \mathbf{E}_j\mathbf{C})\mathbf{A}_i - \mathbf{N}_{ij}(\mathbf{G}_j - \mathbf{E}_j\mathbf{C}) - \mathbf{J}_{ij}\mathbf{C})\mathbf{G}_j^+ = \mathbf{0} \quad \forall i, j, \quad (4.59)$$

$$\begin{aligned} & ((\mathbf{G}_j - \mathbf{E}_j\mathbf{C})\mathbf{A}_i - \mathbf{N}_{ij}(\mathbf{G}_j - \mathbf{E}_j\mathbf{C}) - \mathbf{J}_{ij}\mathbf{C}) \\ & \times (\mathbf{I} - \mathbf{G}_j^+ \mathbf{G}_j) = \mathbf{0} \quad \forall i, j. \end{aligned} \quad (4.60)$$

Since  $\mathbf{G}_j$  is of full row rank, we have  $\mathbf{G}_j\mathbf{G}_j^+ = \mathbf{I}$ . Using this property, we simplify (4.59) and (4.60) to

$$\mathbf{N}_{ij} = \mathbf{G}_j\mathbf{A}_i\mathbf{G}_j^+ - \mathbf{E}_j\mathbf{C}\mathbf{A}_i\mathbf{G}_j^+ - (\mathbf{J}_{ij} - \mathbf{N}_{ij}\mathbf{E}_j)\mathbf{C}\mathbf{G}_j^+ \quad \forall i, j, \quad (4.61)$$

$$\begin{aligned} & \mathbf{E}_j\mathbf{C}\mathbf{A}_i(\mathbf{I} - \mathbf{G}_j^+ \mathbf{G}_j) + (\mathbf{J}_{ij} - \mathbf{N}_{ij}\mathbf{E}_j)\mathbf{C}(\mathbf{I} - \mathbf{G}_j^+ \mathbf{G}_j) \\ & = \mathbf{G}_j\mathbf{A}_i(\mathbf{I} - \mathbf{G}_j^+ \mathbf{G}_j) \quad \forall i, j. \end{aligned} \quad (4.62)$$

Writing (4.61) and (4.62) into compact forms, we obtain

$$\mathbf{N}_{ij} = \mathbf{G}_j \mathbf{A}_i \mathbf{G}_j^+ - [\mathbf{E}_j \quad \mathbf{K}_{ij}] \begin{bmatrix} \mathbf{C} \mathbf{A}_i \mathbf{G}_j^+ \\ \mathbf{C} \mathbf{G}_j^+ \end{bmatrix} \quad \forall i, j, \quad (4.63)$$

$$[\mathbf{E}_j \quad \mathbf{K}_{ij}] \boldsymbol{\Sigma}_{ij} = \mathbf{G}_j \bar{\mathbf{A}}_{ij} \quad \forall i, j, \quad (4.64)$$

where

$$\mathbf{K}_{ij} = \mathbf{J}_{ij} - \mathbf{N}_{ij} \mathbf{E}_j, \quad (4.65)$$

and  $\bar{\mathbf{A}}_{ij}$  and  $\boldsymbol{\Sigma}_{ij}$  are defined in (4.55) and (4.56), respectively.

According to [87], the general solution of linear matrix equation (4.64) is

$$[\mathbf{E}_j \quad \mathbf{K}_{ij}] = \mathbf{G}_j \bar{\mathbf{A}}_{ij} \boldsymbol{\Sigma}_{ij}^+ + \mathbf{Z}_{ij} (\mathbf{I} - \boldsymbol{\Sigma}_{ij} \boldsymbol{\Sigma}_{ij}^+) \quad \forall i, j, \quad (4.66)$$

where  $\mathbf{Z}_{ij} \in \mathbb{R}^{m \times 2l} \quad \forall i, j$  are arbitrary matrices.

**Remark 17** In [58],  $\mathbf{E}_j$  and  $\mathbf{K}_{ij}$  can be obtained in (4.66) once  $\mathbf{Z}_{ij}$  is determined for linear functional observer. However, in fuzzy functional observer case, since  $\mathbf{Z}_{ij}$  varies with rule  $i$  and  $\mathbf{E}_j$  is obtained from  $\mathbf{Z}_{ij}$ ,  $\mathbf{E}_j$  will also vary with rule  $i$ . That is to say, we will get  $\mathbf{E}_{ij}$  rather than  $\mathbf{E}_j$  as follows:

$$[\mathbf{E}_{ij} \quad \mathbf{K}_{ij}] = \mathbf{G}_j \bar{\mathbf{A}}_{ij} \boldsymbol{\Sigma}_{ij}^+ + \mathbf{Z}_{ij} (\mathbf{I} - \boldsymbol{\Sigma}_{ij} \boldsymbol{\Sigma}_{ij}^+) \quad \forall i, j, \quad (4.67)$$

where  $\mathbf{E}_{ij}$  is obtained by giving  $\mathbf{Z}_{ij}$ . In order to make  $\mathbf{E}_j$  not vary with rule  $i$ , the following constraints need to be imposed:  $\mathbf{E}_{i_1 j} = \mathbf{E}_{i_2 j}, \forall i_1, i_2$ . Defining  $0 < \mathbf{X} = \mathbf{X}^T \in \mathbb{R}^{m \times m}$ , then  $\mathbf{E}_{i_1 j} = \mathbf{E}_{i_2 j}$  is equivalent to stability condition (4.52), where  $\tilde{\mathbf{E}}_{ij} = \mathbf{X} \mathbf{E}_{ij}$ .  $\tilde{\mathbf{E}}_{ij}$  in (4.52) is obtained by  $[\tilde{\mathbf{E}}_{ij} \quad \tilde{\mathbf{K}}_{ij}] = \mathbf{X} \mathbf{G}_j \bar{\mathbf{A}}_{ij} \boldsymbol{\Sigma}_{ij}^+ + \mathbf{Y}_{ij} (\mathbf{I} - \boldsymbol{\Sigma}_{ij} \boldsymbol{\Sigma}_{ij}^+)$ , where  $\mathbf{Y}_{ij} = \mathbf{X} \mathbf{Z}_{ij}$ .

Substituting (4.66) to (4.63), we have

$$\begin{aligned} \mathbf{N}_{ij} &= \mathbf{G}_j \mathbf{A}_i \mathbf{G}_j^+ \\ &\quad - (\mathbf{G}_j \bar{\mathbf{A}}_{ij} \boldsymbol{\Sigma}_{ij}^+ + \mathbf{Z}_{ij} (\mathbf{I} - \boldsymbol{\Sigma}_{ij} \boldsymbol{\Sigma}_{ij}^+)) \begin{bmatrix} \mathbf{C} \mathbf{A}_i \mathbf{G}_j^+ \\ \mathbf{C} \mathbf{G}_j^+ \end{bmatrix} \quad \forall i, j. \end{aligned} \quad (4.68)$$

Writing (4.68) into a compact form, we obtain

$$\mathbf{N}_{ij} = \mathbf{F}_{ij} - \mathbf{Z}_{ij} \mathbf{M}_{ij} \quad \forall i, j, \quad (4.69)$$

where  $\mathbf{F}_{ij}$  and  $\mathbf{M}_{ij}$  are defined in (4.53) and (4.54), respectively. Therefore, the

error system (4.49) becomes

$$\dot{\mathbf{e}}_j = \sum_{i=1}^p w_i \left( \mathbf{F}_{ij} - \mathbf{Z}_{ij} \mathbf{M}_{ij} \right) \mathbf{e}_j \quad \forall j. \quad (4.70)$$

Applying the Lyapunov function  $V(\mathbf{e}_j) = \mathbf{e}_j^T \mathbf{X} \mathbf{e}_j$  to investigate the stability of (4.70) where  $\mathbf{X} \in \Re^{m \times m}$  and  $\mathbf{X} > 0$ , we have the time derivative of  $V(\mathbf{e}_j)$  as follows

$$\dot{V}(\mathbf{e}_j) = \sum_{i=1}^p w_i \mathbf{e}_j^T \left( \mathbf{X} \mathbf{F}_{ij} - \mathbf{Y}_{ij} \mathbf{M}_{ij} + \mathbf{F}_{ij}^T \mathbf{X} - \mathbf{M}_{ij}^T \mathbf{Y}_{ij}^T \right) \mathbf{e}_j,$$

where  $\mathbf{Y}_{ij} = \mathbf{X} \mathbf{Z}_{ij}$ .  $\dot{V}(\mathbf{e}_j) < 0$  holds if the stability condition (4.51) is satisfied.

This completes the proof.

With  $\mathbf{Z}_{ij}$  obtained from Theorem 4, the following procedure [58] is employed to determine the observer gains such that the constraints (4.46) and (4.47) are satisfied:

- 1)  $\mathbf{N}_{ij}$  can be obtained from (4.69);
- 2)  $\mathbf{E}_j$  and the intermediate variable  $\mathbf{K}_{ij}$  are given by (4.66);
- 3)  $\mathbf{J}_{ij}$  can be obtained from (4.65);
- 4)  $\mathbf{H}_{ij}$  is given by (4.47).

**Remark 18** *The stability conditions in Theorem 4 are convex, which can be numerically solved by convex programming techniques. Once  $\mathbf{Z}_{ij}$  is obtained from Theorem 4, all observer gains are determined and the stability of the error system is guaranteed. Compared with [57, 59], in this section, there is no need to manually design any observer gains or check the stability after designing the gains.*

### 4.2.3 Simulation Examples

In this example, we consider an inverted pendulum on a cart as shown in Fig. 4.7 in the following state-space form [1]:

$$\begin{aligned} \dot{x}_1 &= x_2, \\ \dot{x}_2 &= \frac{g \sin(x_1) - a m_p L x_2^2 \sin(x_1) \cos(x_1) - a \cos(x_1) u}{4L/3 - a m_p L \cos^2(x_1)}, \end{aligned} \quad (4.71)$$

where  $\mathbf{x} = [x_1 \ x_2]^T$  are the system states;  $g = 9.8m/s^2$  is the acceleration of gravity;  $m_p = 2kg$  and  $M_c = 8kg$  are the mass of the pendulum and the cart, respectively;  $a = 1/(m_p + M_c)$ ;  $2L = 1m$  is the length of the pendulum;  $u$  is the control input force imposed on the cart.

The region of interest is defined as  $x_1 \in [-\frac{80\pi}{180}, \frac{80\pi}{180}]$ . The dynamics of the inverted pendulum (4.71) is represented by a 2-rule fuzzy model [1] with the following

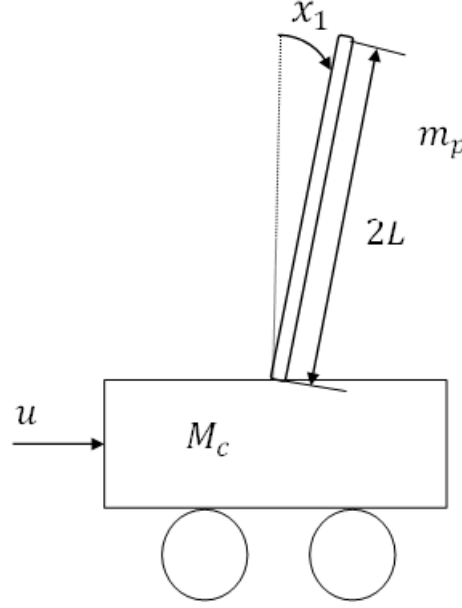


Figure 4.7: The inverted pendulum on a cart.

parameters:

$$\begin{aligned} \mathbf{A}_1 &= \begin{bmatrix} 0 & 1 \\ \frac{g}{\frac{4L}{3} - am_p L} & 0 \end{bmatrix}, \mathbf{A}_2 = \begin{bmatrix} 0 & 1 \\ \frac{2g}{\pi(\frac{4L}{3} - am_p L \beta^2)} & 0 \end{bmatrix}, \\ \mathbf{B}_1 &= [0 \quad -\frac{a}{\frac{4L}{3} - am_p L}]^T, \mathbf{B}_2 = [0 \quad -\frac{a\beta}{\frac{4L}{3} - am_p L \beta^2}]^T, \\ \mathbf{C} &= [1 \quad 0], \end{aligned}$$

where  $\beta = \cos(\frac{80\pi}{180})$ . The membership functions are chosen as  $w_1(x_1) = e^{-\frac{x_1^2}{0.32}}$  and  $w_2(x_1) = 1 - w_1(x_1)$ .

To design the proposed fuzzy functional observer-controller, Theorem 1 is employed to design the fuzzy controller first. We choose  $\beta_{ij} = 1, i, j = 1, 2, \mu_1 = -10^{-2}, \mu_2 = -10^{-4}, \mu_3 = 0.04, \mu_4 = -10^{-3}, \mu_5 = 10^{-4}, \mu_6 = 10^{-6}, \underline{\phi}_1 = -5, \bar{\phi}_1 = 10, \underline{\phi}_2 = -10, \bar{\phi}_2 = 5, \rho_{11} = \rho_{22} = 15$  and  $\rho_{12} = \rho_{21} = 6$ . The controller feedback gains are obtained as  $\mathbf{G}_1 = [3.8334 \times 10^2 \quad 1.1677 \times 10^2]$  and  $\mathbf{G}_2 = [1.2092 \times 10^3 \quad 4.0828 \times 10^2]$  using MATLAB LMI toolbox.

After obtaining the controller feedback gains from Theorem 1, Theorem 4 and the design procedure are employed to design the fuzzy functional observer using MATLAB toolbox SOSTOOLS [12]. The observer gains are obtained as  $\mathbf{N}_{11} = -5.4762, \mathbf{N}_{12} = -2.3765, \mathbf{N}_{21} = -5.4762, \mathbf{N}_{22} = -2.3765, \mathbf{H}_{11} = -2.0606 \times 10, \mathbf{H}_{12} = -7.2049 \times 10, \mathbf{H}_{21} = -3.0554, \mathbf{H}_{22} = -1.0683 \times 10, \mathbf{J}_{11} = -1.4823 \times 10^3, \mathbf{J}_{12} = 4.7550 \times 10^3, \mathbf{J}_{21} = -2.4040 \times 10^3, \mathbf{J}_{22} = 1.5323 \times 10^3, \mathbf{E}_1 = 1.0228 \times 10^3$  and  $\mathbf{E}_2 = 2.1795 \times 10^3$ . In this example, we verify the satisfaction of constraints (4.46) and (4.47). By substituting these gains into constraints (4.46) and (4.47), we have  $\Phi_{ij} \approx \mathbf{0}$  (the magnitude of all values is less than  $10^{-6}$ ) and  $\Lambda_{ij} = 0 \forall i, j$ .

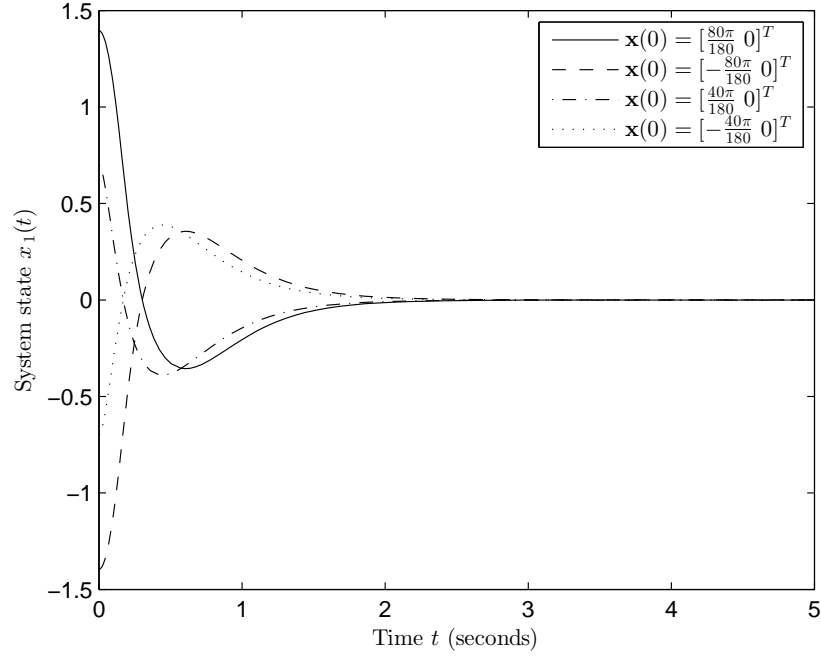


Figure 4.8: Time response of system state  $x_1(t)$  with  $\mathbf{z}_1(0) = \mathbf{z}_2(0) = 0$ .

Accordingly, these constraints are satisfied as proved in the theory.

The designed controller gains and observer gains are applied to the original dynamic system of the inverted pendulum (4.71). Considering 4 different initial conditions, the time response of system states are shown in Fig. 4.8 and Fig. 4.9. The initial conditions for the observer states are chosen as  $\mathbf{z}_1(0) = \mathbf{z}_2(0) = 0$ . It is demonstrated that the inverted pendulum can be successfully stabilized by the proposed fuzzy functional observer-controller.

Choosing initiation conditions  $\mathbf{x}(0) = [\frac{80\pi}{180} \ 0]^T$  for further demonstration, the objective control input  $\mathbf{u}(t)$  and estimated control input  $\hat{\mathbf{u}}(t)$  are shown in Fig. 4.10. Under this case, we also check that the constraints  $\underline{\phi}_i \leq \dot{w}_i \leq \overline{\phi}_i$  and  $|\dot{h}_{ij}| \leq \rho_{ij}$  are satisfied. It can be numerically calculated that  $-1.9179 \leq \dot{w}_1 \leq 8.9285$ ,  $-8.9285 \leq \dot{w}_2 \leq 1.9179$ ,  $|\dot{h}_{11}| \leq 1.1197 \times 10$ ,  $|\dot{h}_{12}|, |\dot{h}_{21}| \leq 3.8055$  and  $|\dot{h}_{22}| \leq 1.0785 \times 10$ . Therefore, the constraints are satisfied according to the previous settings.

**Remark 19** *Instead of estimating the system states, the fuzzy functional observer can estimate the control input directly, which reduces the order of fuzzy observer [11, 53–55] from 2 to 1. Additionally, we compare the proposed fuzzy functional observer with the one in [59]. The closed-loop poles are chosen as  $-2$  and  $-5$  for controller design and  $-3$  for observer design in all rules. The controller gains are obtained as  $\mathbf{K}_1 = [1.5467 \times 10^2 \ 3.9667 \times 10]$  and  $\mathbf{K}_2 = [7.4146 \times 10^2 \ 2.6753 \times 10^2]$ . The observer gains are  $\mathbf{F}_1 = \mathbf{F}_2 = -3$ . Applying Theorem 2 in [59], however, no feasible common matrix  $\mathbf{P}$  is found. Consequently, the stability cannot be guaranteed. This comparison demonstrates the superiority of the proposed method that the stability is guaranteed while the feedback gains are obtained.*

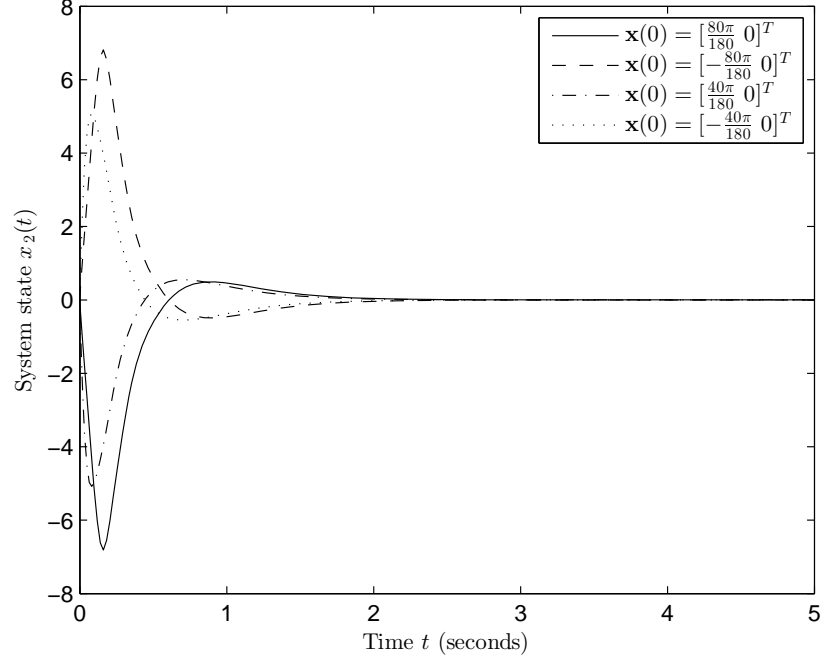


Figure 4.9: Time response of system state  $x_2(t)$  with  $\mathbf{z}_1(0) = \mathbf{z}_2(0) = 0$ .

#### 4.2.4 Conclusion

In this section, the applicability of FMB control scheme has been improved by considering unmeasurable system states. The fuzzy functional observer has been designed to estimate the control input rather than the system states, which can reduce the order of the observer by one in the simulation example. A new form of fuzzy functional observer has been proposed which is in favor of applying the separation principle and deriving convex stability conditions. Based on the proposed fuzzy functional observer, users can easily obtain the observer gains while ensuring the stability. Simulation examples have been presented to verify the validity of designed fuzzy functional observer-controller. In the future, the discrete-time fuzzy functional observer can also be investigated by extending the technique in discrete-time linear functional observer.



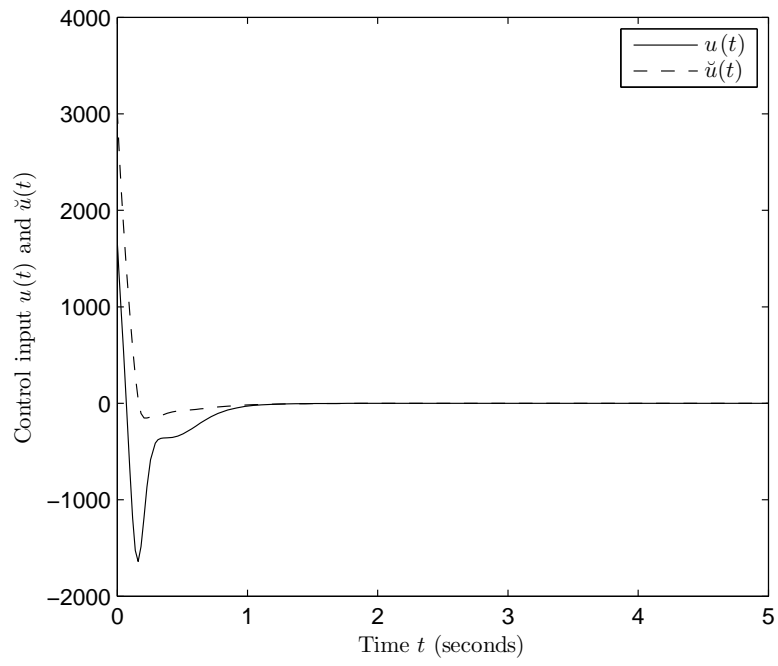


Figure 4.10: Time response of objective control input  $\mathbf{u}(t)$  and estimated control input  $\check{\mathbf{u}}(t)$  with  $\mathbf{x}(0) = [\frac{80\pi}{180} \ 0]^T$  and  $\mathbf{z}_1(0) = \mathbf{z}_2(0) = 0$ .

# Chapter 5

## Design of Polynomial Fuzzy Observer-Controller

Apart from T-S fuzzy observer, the polynomial fuzzy observer has also been developed for PFMB control system, which generalizes the T-S one. In this chapter, the polynomial fuzzy observer-controller with unmeasurable premise variables is designed. Two methods are applied to derive convex stability conditions: refined completing square approach and matrix decoupling technique. Additionally, the designed polynomial fuzzy observer-controller is extended for systems where only sampled-output measurements are available. The membership functions of the designed polynomial observer-controller are optimized by the improved gradient descent method for better performance.

### 5.1 Design of Polynomial Fuzzy Observer-Controller Using Matrix Decoupling Technique

The polynomial fuzzy observer-controller can be employed for PFMB control systems when full states are not available for performing feedback control. It motivates the author to investigate the system stability of PFMB observer-control systems. We consider the polynomial fuzzy controller and polynomial fuzzy observer whose premise membership functions depend on estimated premise variables. Matrix decoupling technique [54] is employed to achieve convex SOS-based stability conditions. Compared with [60], we obtain the polynomial observer gains and controller gains in one step rather than two steps. The premise variables are unmeasurable which are more general than measurable premise variables, and the output matrices are allowed to be polynomial matrices instead of constant matrices.

This section is organized as follows. In Subsection 5.1.1, the new formulation of polynomial fuzzy model, polynomial fuzzy observer and polynomial fuzzy controller are described. In Subsection 5.1.2, stability analysis is conducted for PFMB observer-control system. In Subsection 5.1.3, simulation examples are provided to

demonstrate the feasibility and validity of stability conditions. In Subsection 5.1.4, a conclusion is drawn.

### 5.1.1 Preliminary

Due to the consideration of unmeasurable system states, the monomial form  $\hat{\mathbf{x}}(\mathbf{x}(t))$  in (2.5) is difficult to be taken into account. Therefore, the new formulation of polynomial fuzzy model, polynomial fuzzy observer and polynomial fuzzy controller are described first.

#### 5.1.1.1 Polynomial Fuzzy Model

The  $i^{th}$  rule of the polynomial fuzzy model for the nonlinear system is presented as follows [3]:

$$\begin{aligned} \text{Rule } i : & \text{ IF } f_1(\mathbf{x}(t)) \text{ is } M_1^i \text{ AND } \cdots \text{ AND } f_\Psi(\mathbf{x}(t)) \text{ is } M_\Psi^i, \\ & \text{ THEN } \dot{\mathbf{x}}(t) = \mathbf{A}_i(\mathbf{x}(t))\mathbf{x}(t) + \mathbf{B}_i(\mathbf{x}(t))\mathbf{u}(t), \\ & \mathbf{y}(t) = \mathbf{C}_i(\mathbf{x}(t))\mathbf{x}(t), \end{aligned}$$

where  $\mathbf{x}(t) = [x_1(t), x_2(t), \dots, x_n(t)]^T$  is the state vector, and  $n$  is the dimension of the nonlinear system;  $f_\eta(\mathbf{x}(t))$  is the premise variable corresponding to its fuzzy term  $M_\eta^i$  in rule  $i$ ,  $\eta = 1, 2, \dots, \Psi$ , and  $\Psi$  is a positive integer;  $\mathbf{A}_i(\mathbf{x}(t)) \in \mathbb{R}^{n \times n}$  and  $\mathbf{B}_i(\mathbf{x}(t)) \in \mathbb{R}^{n \times m}$  are the known polynomial system and input matrices, respectively;  $\mathbf{u}(t) \in \mathbb{R}^m$  is the control input vector;  $\mathbf{y}(t) \in \mathbb{R}^l$  is the output vector;  $\mathbf{C}_i(\mathbf{x}(t)) \in \mathbb{R}^{l \times n}$  is the polynomial output matrix. The dynamics of the nonlinear system is given by

$$\begin{aligned} \dot{\mathbf{x}}(t) &= \sum_{i=1}^p w_i(\mathbf{x}(t)) \left( \mathbf{A}_i(\mathbf{x}(t))\mathbf{x}(t) + \mathbf{B}_i(\mathbf{x}(t))\mathbf{u}(t) \right), \\ \mathbf{y}(t) &= \sum_{i=1}^p w_i(\mathbf{x}(t)) \mathbf{C}_i(\mathbf{x}(t))\mathbf{x}(t), \end{aligned} \quad (5.1)$$

where  $p$  is the number of rules in the polynomial fuzzy model;  $w_i(\mathbf{x}(t))$  is the normalized grade of membership,  $w_i(\mathbf{x}(t)) = \frac{\prod_{\eta=1}^{\Psi} \mu_{M_\eta^i}(f_\eta(\mathbf{x}(t)))}{\sum_{k=1}^p \prod_{\eta=1}^{\Psi} \mu_{M_\eta^k}(f_\eta(\mathbf{x}(t)))}$ ,  $w_i(\mathbf{x}(t)) \geq 0$ ,  $i = 1, 2, \dots, p$ , and  $\sum_{i=1}^p w_i(\mathbf{x}(t)) = 1$ ;  $\mu_{M_\eta^i}(f_\eta(\mathbf{x}(t)))$ ,  $\eta = 1, 2, \dots, \Psi$ , are grades of membership corresponding to the fuzzy term  $M_\eta^i$ .

#### 5.1.1.2 Polynomial Fuzzy Observer

For brevity, time  $t$  is dropped from now. Considering premise variable  $f_\eta(\mathbf{x})$  depending on unmeasurable states  $\mathbf{x}$ , we apply the following polynomial fuzzy observer to estimate the states in (5.1). The  $i^{th}$  rule of the polynomial fuzzy observer is described

as follows:

$$\begin{aligned} \text{Rule } i : & \text{ IF } f_1(\check{\mathbf{x}}) \text{ is } M_1^i \text{ AND } \cdots \text{ AND } f_\Psi(\check{\mathbf{x}}) \text{ is } M_\Psi^i, \\ & \text{ THEN } \dot{\check{\mathbf{x}}} = \mathbf{A}_i(\check{\mathbf{x}})\check{\mathbf{x}} + \mathbf{B}_i(\check{\mathbf{x}})\mathbf{u} + \mathbf{L}_i(\check{\mathbf{x}})(\mathbf{y} - \check{\mathbf{y}}), \\ & \check{\mathbf{y}} = \mathbf{C}_i(\check{\mathbf{x}})\check{\mathbf{x}}, \end{aligned}$$

where  $\check{\mathbf{x}} \in \mathfrak{R}^n$  is the estimated state  $\mathbf{x}$ ;  $\check{\mathbf{y}} \in \mathfrak{R}^l$  is the estimated output  $\mathbf{y}$ ;  $\mathbf{L}_i(\check{\mathbf{x}}) \in \mathfrak{R}^{n \times l}$  is the polynomial observer gain. The polynomial fuzzy observer is given by

$$\begin{aligned} \dot{\check{\mathbf{x}}} &= \sum_{i=1}^p w_i(\check{\mathbf{x}}) \left( \mathbf{A}_i(\check{\mathbf{x}})\check{\mathbf{x}} + \mathbf{B}_i(\check{\mathbf{x}})\mathbf{u} + \mathbf{L}_i(\check{\mathbf{x}})(\mathbf{y} - \check{\mathbf{y}}) \right), \\ \check{\mathbf{y}} &= \sum_{i=1}^p w_i(\check{\mathbf{x}}) \mathbf{C}_i(\check{\mathbf{x}})\check{\mathbf{x}}. \end{aligned} \quad (5.2)$$

It can be seen from (5.2) that the membership functions of polynomial fuzzy observer depend on estimated system states  $\check{\mathbf{x}}$  rather than original system states  $\mathbf{x}$ .

#### 5.1.1.3 Polynomial Fuzzy Controller

With PDC design approach [1, 3], the  $i^{th}$  rule of the polynomial fuzzy controller is described as follows:

$$\begin{aligned} \text{Rule } i : & \text{ IF } f_1(\check{\mathbf{x}}) \text{ is } M_1^i \text{ AND } \cdots \text{ AND } f_\Psi(\check{\mathbf{x}}) \text{ is } M_\Psi^i, \\ & \text{ THEN } \mathbf{u} = \mathbf{G}_i(\check{\mathbf{x}})\check{\mathbf{x}}, \end{aligned}$$

where  $\mathbf{G}_i(\check{\mathbf{x}}) \in \mathfrak{R}^{m \times N}$  is the polynomial controller gain. The polynomial fuzzy controller is given by

$$\mathbf{u} = \sum_{i=1}^p w_i(\check{\mathbf{x}}) \mathbf{G}_i(\check{\mathbf{x}})\check{\mathbf{x}}. \quad (5.3)$$

Note that in (5.3) both the premise variable and the controller gain depend on estimated states  $\check{\mathbf{x}}$ .

### 5.1.2 Stability Analysis

In this section, the stability analysis is carried out for PFMB observer-control systems. The formulation of closed-loop PFMB observer-control systems are provided first. Then based on Lyapunov stability theory, stability conditions are obtained in terms of SOS. Matrix decoupling technique is employed to obtain convex SOS-based stability conditions.

The estimation error is defined as  $\mathbf{e} = \mathbf{x} - \check{\mathbf{x}}$ , and then we have the closed-loop system (shown in Fig. 4.1) consisting of the polynomial fuzzy model (5.1), the

polynomial fuzzy controller (5.3) and the polynomial fuzzy observer (5.2) as follows:

$$\begin{aligned} \dot{\mathbf{x}} = & \sum_{i=1}^p \sum_{j=1}^p w_i(\mathbf{x}) w_j(\check{\mathbf{x}}) \left( (\mathbf{A}_i(\mathbf{x}) + \mathbf{B}_i(\mathbf{x}) \mathbf{G}_j(\check{\mathbf{x}})) \check{\mathbf{x}} \right. \\ & \left. + \mathbf{A}_i(\mathbf{x}) \mathbf{e} \right), \end{aligned} \quad (5.4)$$

$$\begin{aligned} \dot{\check{\mathbf{x}}} = & \sum_{i=1}^p \sum_{j=1}^p \sum_{k=1}^p w_i(\mathbf{x}) w_j(\check{\mathbf{x}}) w_k(\check{\mathbf{x}}) \left( (\mathbf{A}_j(\check{\mathbf{x}}) + \mathbf{B}_j(\check{\mathbf{x}}) \mathbf{G}_k(\check{\mathbf{x}}) \right. \\ & \left. + \mathbf{L}_j(\check{\mathbf{x}}) (\mathbf{C}_i(\mathbf{x}) - \mathbf{C}_k(\check{\mathbf{x}}))) \check{\mathbf{x}} + \mathbf{L}_j(\check{\mathbf{x}}) \mathbf{C}_i(\mathbf{x}) \mathbf{e} \right), \end{aligned} \quad (5.5)$$

$$\begin{aligned} \dot{\mathbf{e}} = & \sum_{i=1}^p \sum_{j=1}^p \sum_{k=1}^p w_i(\mathbf{x}) w_j(\check{\mathbf{x}}) w_k(\check{\mathbf{x}}) \left( (\mathbf{A}_i(\mathbf{x}) - \mathbf{A}_j(\check{\mathbf{x}}) \right. \\ & \left. + (\mathbf{B}_i(\mathbf{x}) - \mathbf{B}_j(\check{\mathbf{x}})) \mathbf{G}_k(\check{\mathbf{x}}) - \mathbf{L}_j(\check{\mathbf{x}}) (\mathbf{C}_i(\mathbf{x}) - \mathbf{C}_k(\check{\mathbf{x}}))) \check{\mathbf{x}} \right. \\ & \left. + (\mathbf{A}_i(\mathbf{x}) - \mathbf{L}_j(\check{\mathbf{x}}) \mathbf{C}_i(\mathbf{x})) \mathbf{e} \right). \end{aligned} \quad (5.6)$$

The control objective is to make the augmented observer-control system ((5.5) and (5.6)) asymptotically stable, i.e.,  $\check{\mathbf{x}} \rightarrow 0$  and  $\mathbf{e} \rightarrow 0$  as time  $t \rightarrow \infty$ , by determining the polynomial controller gain  $\mathbf{G}_k(\check{\mathbf{x}})$  and polynomial observer gain  $\mathbf{L}_j(\check{\mathbf{x}})$ .

**Theorem 5** *The augmented PFMB observer-control system (formed by (5.5) and (5.6)) is guaranteed to be asymptotically stable if there exist matrices  $\mathbf{X} \in \Re^{n \times n}$ ,  $\mathbf{Y} \in \Re^{n \times n}$ ,  $\mathbf{N}_k(\check{\mathbf{x}}) \in \Re^{m \times n}$ ,  $\mathbf{M}_j(\check{\mathbf{x}}) \in \Re^{n \times l}$ ,  $k = 1, 2, \dots, p$ ,  $j = 1, 2, \dots, p$ , and predefined scalars  $\alpha_1 > 0$ ,  $\alpha_2 > 0$ ,  $\beta > 0$  such that the following SOS-based conditions are satisfied:*

$$\nu^T (\mathbf{X} - \varepsilon_1 \mathbf{I}) \nu \text{ is SOS}; \quad (5.7)$$

$$\nu^T (\mathbf{Y} - \varepsilon_2 \mathbf{I}) \nu \text{ is SOS}; \quad (5.8)$$

$$\begin{aligned} & -\nu^T (\Phi_{ijk}(\mathbf{x}, \check{\mathbf{x}}) + \Phi_{ikj}(\mathbf{x}, \check{\mathbf{x}}) + \varepsilon_3(\mathbf{x}, \check{\mathbf{x}}) \mathbf{I}) \nu \text{ is SOS} \\ & \forall i, j \leq k; \end{aligned} \quad (5.9)$$

$$\begin{aligned} & -\nu^T (\Theta_{ijk}(\mathbf{x}, \check{\mathbf{x}}) + \Theta_{ikj}(\mathbf{x}, \check{\mathbf{x}}) + \varepsilon_4(\mathbf{x}, \check{\mathbf{x}}) \mathbf{I}) \nu \text{ is SOS} \\ & \forall i, j \leq k; \end{aligned} \quad (5.10)$$

where

$$\Phi_{ijk}(\mathbf{x}, \check{\mathbf{x}}) = \begin{bmatrix} \tilde{\Gamma}_{ijk}(\mathbf{x}, \check{\mathbf{x}}) & \Phi^{(12)} & \Phi^{(13)} \\ * & -\frac{1}{\alpha_1} \mathbf{Y} & \mathbf{0} \\ * & * & -\frac{1}{\beta} \mathbf{I} \end{bmatrix}, \quad (5.11)$$

$$\Theta_{ijk}(\mathbf{x}, \check{\mathbf{x}}) = \begin{bmatrix} \tilde{\Lambda}_{ij}(\mathbf{x}, \check{\mathbf{x}}) & \Theta^{(12)} & \tilde{\Theta}_{ijk}^{(13)}(\mathbf{x}, \check{\mathbf{x}}) \\ * & -\frac{1}{\alpha_2} \mathbf{I} & \mathbf{0} \\ * & * & -\beta \mathbf{I} \end{bmatrix}, \quad (5.12)$$

$$\tilde{\Gamma}_{ijk}(\mathbf{x}, \check{\mathbf{x}}) = \begin{bmatrix} \hat{\Xi}_{jk}^{(11)}(\check{\mathbf{x}}) + \hat{\Xi}_{jk}^{(11)}(\check{\mathbf{x}})^T & \hat{\Xi}_{ijk}^{(21)}(\mathbf{x}, \check{\mathbf{x}})^T \\ * & -\alpha_2 \mathbf{I} \end{bmatrix}, \quad (5.13)$$

$$\tilde{\Lambda}_{ij}(\mathbf{x}, \check{\mathbf{x}}) = \begin{bmatrix} -\alpha_1 \mathbf{Y} & \tilde{\Xi}_{ij}^{(12)}(\mathbf{x}, \check{\mathbf{x}}) \\ * & \tilde{\Xi}_{ij}^{(22)}(\mathbf{x}, \check{\mathbf{x}}) + \tilde{\Xi}_{ij}^{(22)}(\mathbf{x}, \check{\mathbf{x}})^T \end{bmatrix}, \quad (5.14)$$

$$\Phi^{(12)} = [\mathbf{I} \quad \mathbf{0}]^T, \quad (5.15)$$

$$\Phi^{(13)} = [\mathbf{X} \quad \mathbf{0}]^T, \quad (5.16)$$

$$\Theta^{(12)} = [\mathbf{0} \quad \mathbf{Y}]^T, \quad (5.17)$$

$$\tilde{\Theta}_{ijk}^{(13)}(\mathbf{x}, \check{\mathbf{x}}) = [\tilde{\mathbf{H}}_{ijk}(\mathbf{x}, \check{\mathbf{x}})^T \quad -\tilde{\mathbf{H}}_{ijk}(\mathbf{x}, \check{\mathbf{x}})^T]^T, \quad (5.18)$$

$$\hat{\Xi}_{jk}^{(11)}(\check{\mathbf{x}}) = \mathbf{A}_j(\check{\mathbf{x}})\mathbf{X} + \mathbf{B}_j(\check{\mathbf{x}})\mathbf{N}_k(\check{\mathbf{x}}), \quad (5.19)$$

$$\begin{aligned} \hat{\Xi}_{ijk}^{(21)}(\mathbf{x}, \check{\mathbf{x}}) &= (\mathbf{A}_i(\mathbf{x}) - \mathbf{A}_j(\check{\mathbf{x}}))\mathbf{X} \\ &\quad + (\mathbf{B}_i(\mathbf{x}) - \mathbf{B}_j(\check{\mathbf{x}}))\mathbf{N}_k(\check{\mathbf{x}}), \end{aligned} \quad (5.20)$$

$$\tilde{\Xi}_{ij}^{(12)}(\mathbf{x}, \check{\mathbf{x}}) = \mathbf{M}_j(\check{\mathbf{x}})\mathbf{C}_i(\mathbf{x}), \quad (5.21)$$

$$\tilde{\Xi}_{ij}^{(22)}(\mathbf{x}, \check{\mathbf{x}}) = \mathbf{Y}\mathbf{A}_i(\mathbf{x}) - \mathbf{M}_j(\check{\mathbf{x}})\mathbf{C}_i(\mathbf{x}), \quad (5.22)$$

$$\tilde{\mathbf{H}}_{ijk}(\mathbf{x}, \check{\mathbf{x}}) = \mathbf{M}_j(\check{\mathbf{x}})(\mathbf{C}_i(\mathbf{x}) - \mathbf{C}_k(\check{\mathbf{x}})); \quad (5.23)$$

$\nu$  is an arbitrary vector independent of  $\mathbf{x}$  with appropriate dimensions;  $\varepsilon_1 > 0, \varepsilon_2 > 0, \varepsilon_3(\mathbf{x}, \check{\mathbf{x}}) > 0$  and  $\varepsilon_4(\mathbf{x}, \check{\mathbf{x}}) > 0$  are predefined scalar polynomials; and the polynomial controller and observer gains are given by  $\mathbf{G}_k(\check{\mathbf{x}}) = \mathbf{N}_k(\check{\mathbf{x}})\mathbf{X}^{-1}$  and  $\mathbf{L}_j(\check{\mathbf{x}}) = \mathbf{Y}^{-1}\mathbf{M}_j(\check{\mathbf{x}})$ , respectively.

**Proof** Defining the augmented vector  $\mathbf{z} = [\check{\mathbf{x}}^T \quad \mathbf{e}^T]^T$  and the summation term  $\sum_{i,j,k=1}^p \tilde{w}_{ijk} = \sum_{i=1}^p \sum_{j=1}^p \sum_{k=1}^p w_i(\mathbf{x})w_j(\check{\mathbf{x}})w_k(\check{\mathbf{x}})$ , the augmented PFMB observer-control system is written as

$$\dot{\mathbf{z}} = \sum_{i,j,k=1}^p \tilde{w}_{ijk} \Xi_{ijk}(\mathbf{x}, \check{\mathbf{x}})\mathbf{z}, \quad (5.24)$$

where

$$\Xi_{ijk}(\mathbf{x}, \check{\mathbf{x}}) = \begin{bmatrix} \Xi_{jk}^{(11)}(\check{\mathbf{x}}) + \mathbf{H}_{ijk}(\mathbf{x}, \check{\mathbf{x}}) & \Xi_{ij}^{(12)}(\mathbf{x}, \check{\mathbf{x}}) \\ \Xi_{ijk}^{(21)}(\mathbf{x}, \check{\mathbf{x}}) - \mathbf{H}_{ijk}(\mathbf{x}, \check{\mathbf{x}}) & \Xi_{ij}^{(22)}(\mathbf{x}, \check{\mathbf{x}}) \end{bmatrix}, \quad (5.25)$$

$$\Xi_{jk}^{(11)}(\check{\mathbf{x}}) = \mathbf{A}_j(\check{\mathbf{x}}) + \mathbf{B}_j(\check{\mathbf{x}})\mathbf{G}_k(\check{\mathbf{x}}), \quad (5.26)$$

$$\Xi_{ijk}^{(21)}(\mathbf{x}, \check{\mathbf{x}}) = \mathbf{A}_i(\mathbf{x}) - \mathbf{A}_j(\check{\mathbf{x}}) + (\mathbf{B}_i(\mathbf{x}) - \mathbf{B}_j(\check{\mathbf{x}}))\mathbf{G}_k(\check{\mathbf{x}}), \quad (5.27)$$

$$\Xi_{ij}^{(12)}(\mathbf{x}, \check{\mathbf{x}}) = \mathbf{L}_j(\check{\mathbf{x}})\mathbf{C}_i(\mathbf{x}), \quad (5.28)$$

$$\Xi_{ij}^{(22)}(\mathbf{x}, \check{\mathbf{x}}) = \mathbf{A}_i(\mathbf{x}) - \mathbf{L}_j(\check{\mathbf{x}})\mathbf{C}_i(\mathbf{x}), \quad (5.29)$$

$$\mathbf{H}_{ijk}(\mathbf{x}, \check{\mathbf{x}}) = \mathbf{L}_j(\check{\mathbf{x}})(\mathbf{C}_i(\mathbf{x}) - \mathbf{C}_k(\check{\mathbf{x}})). \quad (5.30)$$

The procedure of the proof is shown in Fig. 5.1. As can be seen, the matrix decoupling technique will separate the conditions into two parts and convex conditions will be obtained for both parts.

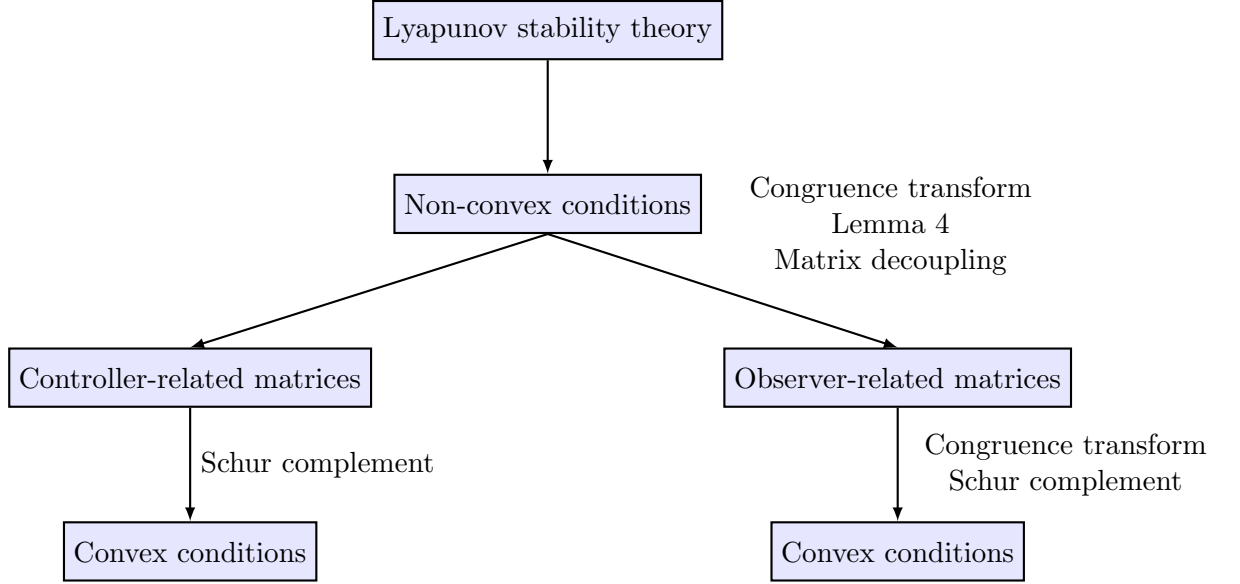


Figure 5.1: Procedure of the proof for Theorem 5.

The following Lyapunov function candidate is employed to investigate the stability of the augmented PFMB observer-control system (5.24):

$$V(\mathbf{z}) = \mathbf{z}^T \mathbf{P} \mathbf{z}, \quad (5.31)$$

where  $\mathbf{P} = \begin{bmatrix} \mathbf{X}^{-1} & \mathbf{0} \\ \mathbf{0} & \mathbf{Y} \end{bmatrix}$ ,  $\mathbf{X} > 0$ ,  $\mathbf{Y} > 0$ , and thus  $\mathbf{P} > 0$ . The time derivative of Lyapunov function is

$$\dot{V}(\mathbf{z}) = \sum_{i,j,k=1}^p \tilde{w}_{ijk} \mathbf{z}^T (\mathbf{P} \Xi_{ijk}(\mathbf{x}, \check{\mathbf{x}}) + \Xi_{ijk}(\mathbf{x}, \check{\mathbf{x}})^T \mathbf{P}) \mathbf{z}. \quad (5.32)$$

Therefore,  $\dot{V}(\mathbf{z}) < 0$  holds if

$$\sum_{i,j,k=1}^p \tilde{w}_{ijk} (\mathbf{P} \Xi_{ijk}(\mathbf{x}, \check{\mathbf{x}}) + \Xi_{ijk}(\mathbf{x}, \check{\mathbf{x}})^T \mathbf{P}) < 0. \quad (5.33)$$

**Remark 20** *The augmented PFMB observer-control system (5.24) is guaranteed to be asymptotically stable if  $V(\mathbf{z}) > 0$  by satisfying  $\mathbf{P} > 0$  and  $\dot{V}(\mathbf{z}) < 0$  by satisfying (5.33) excluding  $\mathbf{x} = \mathbf{0}$ . It should be noted that the condition (5.33) is not convex. If the condition (5.33) is applied, the polynomial fuzzy controller gain  $\mathbf{G}_k(\check{\mathbf{x}})$  and polynomial fuzzy observer gain  $\mathbf{L}_j(\check{\mathbf{x}})$  are needed to be pre-determined.*

In the following, we apply congruence transformation and matrix decoupling technique to obtain convex SOS stability conditions such that the polynomial fuzzy controller gain  $\mathbf{G}_k(\check{\mathbf{x}})$  and polynomial fuzzy observer gain  $\mathbf{L}_j(\check{\mathbf{x}})$  can be obtained using convex programming techniques.

Performing congruence transformation to (5.33) by pre-multiplying and post-multiplying  $\mathbf{P}^{-1} = \begin{bmatrix} \mathbf{X} & \mathbf{0} \\ \mathbf{0} & \mathbf{Y}^{-1} \end{bmatrix}$  to both sides and denoting  $\mathbf{N}_k(\check{\mathbf{x}}) = \mathbf{G}_k(\check{\mathbf{x}})\mathbf{X}$ , we have

$$\sum_{i,j,k=1}^p \tilde{w}_{ijk}(\hat{\Xi}_{ijk}(\mathbf{x}, \check{\mathbf{x}}) + \hat{\Xi}_{ijk}(\mathbf{x}, \check{\mathbf{x}})^T) < 0, \quad (5.34)$$

where

$$\hat{\Xi}_{ijk}(\mathbf{x}, \check{\mathbf{x}}) = \begin{bmatrix} \hat{\Xi}_{jk}^{(11)}(\check{\mathbf{x}}) + \mathbf{H}_{ijk}(\mathbf{x}, \check{\mathbf{x}})\mathbf{X} & \hat{\Xi}_{ij}^{(12)}(\mathbf{x}, \check{\mathbf{x}}) \\ \hat{\Xi}_{ijk}^{(21)}(\mathbf{x}, \check{\mathbf{x}}) - \mathbf{H}_{ijk}(\mathbf{x}, \check{\mathbf{x}})\mathbf{X} & \hat{\Xi}_{ij}^{(22)}(\mathbf{x}, \check{\mathbf{x}}) \end{bmatrix}, \quad (5.35)$$

$$\hat{\Xi}_{ij}^{(12)}(\mathbf{x}, \check{\mathbf{x}}) = \mathbf{L}_j(\check{\mathbf{x}})\mathbf{C}_i(\mathbf{x})\mathbf{Y}^{-1}, \quad (5.36)$$

$$\hat{\Xi}_{ij}^{(22)}(\mathbf{x}, \check{\mathbf{x}}) = \mathbf{A}_i(\mathbf{x})\mathbf{Y}^{-1} - \mathbf{L}_j(\check{\mathbf{x}})\mathbf{C}_i(\mathbf{x})\mathbf{Y}^{-1}, \quad (5.37)$$

$\hat{\Xi}_{jk}^{(11)}(\check{\mathbf{x}})$  and  $\hat{\Xi}_{ijk}^{(21)}(\mathbf{x}, \check{\mathbf{x}})$  are defined in (5.19) and (5.20), respectively.

Applying Lemma 4, we have

$$\begin{aligned} & \sum_{i,j,k=1}^p \tilde{w}_{ijk}(\hat{\Xi}_{ijk}(\mathbf{x}, \check{\mathbf{x}}) + \hat{\Xi}_{ijk}(\mathbf{x}, \check{\mathbf{x}})^T) \\ & \leq \sum_{i,j,k=1}^p \tilde{w}_{ijk} \left( \Upsilon_{ijk}(\mathbf{x}, \check{\mathbf{x}}) + \beta \Phi^{(13)}(\Phi^{(13)})^T \right) \\ & \quad + \frac{1}{\beta} \left( \sum_{i,j,k=1}^p \tilde{w}_{ijk} \Theta_{ijk}^{(13)}(\mathbf{x}, \check{\mathbf{x}}) \right) \left( \sum_{i,j,k=1}^p \tilde{w}_{ijk} \Theta_{ijk}^{(13)}(\mathbf{x}, \check{\mathbf{x}}) \right)^T, \end{aligned} \quad (5.38)$$

where

$$\begin{aligned} \Upsilon_{ijk}(\mathbf{x}, \check{\mathbf{x}}) = & \begin{bmatrix} \hat{\Xi}_{jk}^{(11)}(\check{\mathbf{x}}) + \hat{\Xi}_{jk}^{(11)}(\check{\mathbf{x}})^T & \hat{\Xi}_{ij}^{(12)}(\mathbf{x}, \check{\mathbf{x}}) + \hat{\Xi}_{ijk}^{(21)}(\mathbf{x}, \check{\mathbf{x}})^T \\ * & \hat{\Xi}_{ij}^{(22)}(\mathbf{x}, \check{\mathbf{x}}) + \hat{\Xi}_{ij}^{(22)}(\mathbf{x}, \check{\mathbf{x}})^T \end{bmatrix}, \end{aligned} \quad (5.39)$$

$$\Theta_{ijk}^{(13)}(\mathbf{x}, \check{\mathbf{x}}) = [\mathbf{H}_{ijk}(\mathbf{x}, \check{\mathbf{x}})^T \quad -\mathbf{H}_{ijk}(\mathbf{x}, \check{\mathbf{x}})^T]^T, \quad (5.40)$$

$\Phi^{(13)}$  is defined in (5.16).

Using matrix decoupling technique [54] to further separate decision variables in order to obtain convex SOS stability conditions, we rewrite  $\Upsilon_{ijk}(\mathbf{x}, \check{\mathbf{x}})$  as follows:

$$\Upsilon_{ijk}(\mathbf{x}, \check{\mathbf{x}}) = \Gamma_{ijk}(\mathbf{x}, \check{\mathbf{x}}) + \Lambda_{ij}(\mathbf{x}, \check{\mathbf{x}}), \quad (5.41)$$

where

$$\Gamma_{ijk}(\mathbf{x}, \check{\mathbf{x}}) =$$



$$\begin{bmatrix} \hat{\Xi}_{jk}^{(11)}(\check{\mathbf{x}}) + \hat{\Xi}_{jk}^{(11)}(\check{\mathbf{x}})^T + \alpha_1 \mathbf{Y}^{-1} & \hat{\Xi}_{ijk}^{(21)}(\mathbf{x}, \check{\mathbf{x}})^T \\ * & -\alpha_2 \mathbf{I} \end{bmatrix}, \quad (5.42)$$

$$\Lambda_{ij}(\mathbf{x}, \check{\mathbf{x}}) = \begin{bmatrix} -\alpha_1 \mathbf{Y}^{-1} & \hat{\Xi}_{ij}^{(12)}(\mathbf{x}, \check{\mathbf{x}}) \\ * & \hat{\Xi}_{ij}^{(22)}(\mathbf{x}, \check{\mathbf{x}}) + \alpha_2 \mathbf{I} \end{bmatrix}. \quad (5.43)$$

**Remark 21** The decoupled matrix in (5.42) is related to the polynomial fuzzy controller gain  $\mathbf{G}_k(\check{\mathbf{x}})$  while the one in (5.43) is related to the polynomial fuzzy observer gain  $\mathbf{L}_j(\check{\mathbf{x}})$ . In this case, more arrangement can be imposed on (5.43) without affecting (5.42) which is already a convex problem. Other techniques such as completing square (Lemma 4 and Lemma 5) [53] and Finsler's lemma [55] can also be used to further separate decision variables instead of matrix decoupling technique [54]. However, they increase the dimension of matrices or increase the number of decision variables resulting in higher computational demand. In contrast, using matrix decoupling technique leads to smaller dimension of matrices or less number of decision variables at the expense of larger number of stability conditions.

Hence,  $\dot{V}(\mathbf{z}) < 0$  holds if

$$\sum_{i,j,k=1}^p \tilde{w}_{ijk} \left( \Gamma_{ijk}(\mathbf{x}, \check{\mathbf{x}}) + \beta \Phi^{(13)}(\Phi^{(13)})^T \right) < 0, \quad (5.44)$$

$$\begin{aligned} & \sum_{i,j,k=1}^p \tilde{w}_{ijk} \Lambda_{ij}(\mathbf{x}, \check{\mathbf{x}}) + \frac{1}{\beta} \left( \sum_{i,j,k=1}^p \tilde{w}_{ijk} \Theta_{ijk}^{(13)}(\mathbf{x}, \check{\mathbf{x}}) \right) \\ & \times \left( \sum_{i,j,k=1}^p \tilde{w}_{ijk} \Theta_{ijk}^{(13)}(\mathbf{x}, \check{\mathbf{x}}) \right)^T < 0. \end{aligned} \quad (5.45)$$

Performing congruence transformation to (5.45) by pre-multiplying and post-multiplying  $\text{diag}\{\mathbf{Y}, \mathbf{Y}\}$  to both sides, denoting  $\mathbf{M}_j(\check{\mathbf{x}}) = \mathbf{Y} \mathbf{L}_j(\check{\mathbf{x}})$ , and then applying Schur complement to both (5.44) and (5.45), we obtain

$$\sum_{i,j,k=1}^p \tilde{w}_{ijk} \Phi_{ijk}(\mathbf{x}, \check{\mathbf{x}}) < 0, \quad (5.46)$$

$$\sum_{i,j,k=1}^p \tilde{w}_{ijk} \Theta_{ijk}(\mathbf{x}, \check{\mathbf{x}}) < 0, \quad (5.47)$$

where  $\Phi_{ijk}(\mathbf{x}, \check{\mathbf{x}})$  and  $\Theta_{ijk}(\mathbf{x}, \check{\mathbf{x}})$  are defined in (5.11) and (5.12), respectively. By grouping terms with same membership functions,  $\dot{V}(\mathbf{z}) < 0$  can be achieved by satisfying conditions (5.9) and (5.10). The proof is completed.

### 5.1.3 Simulation Examples

In this section, two simulation examples are provided to validate the proposed stability conditions. In the first example, we consider the stabilization control problem

for an inverted pendulum using the proposed PFMB observer-controller. In the second example, a nonlinear mass-spring-damper system is also stabilized by the designed PFMB observer-controller.

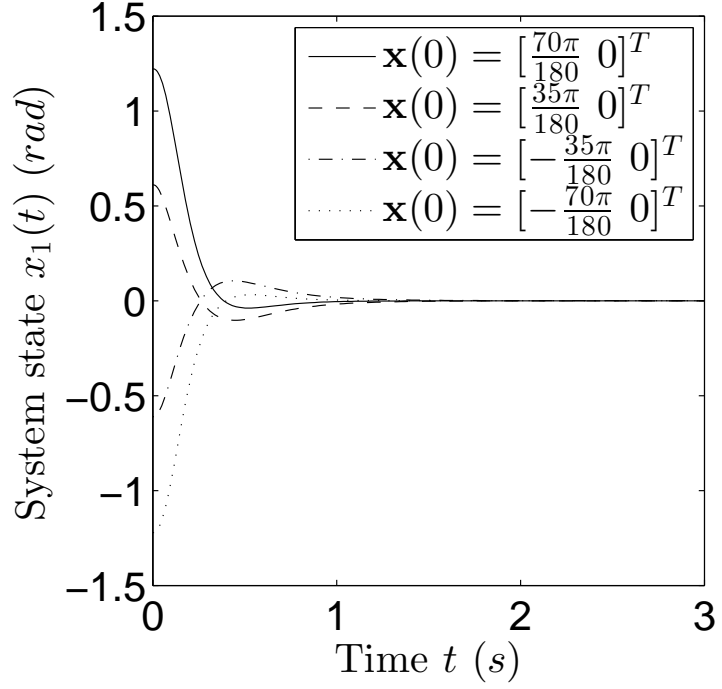
### 5.1.3.1 Inverted Pendulum

In this example, we consider the same inverted pendulum on a cart as in (4.71). Defining the region of interest as  $x_1 \in [-\frac{70\pi}{180}, \frac{70\pi}{180}]$ , the nonlinear term  $f_1(x_1) = \frac{\cos(x_1)}{4L/3 - am_p L \cos^2(x_1)}$  is represented by sector nonlinearity technique [9] as follows:  $f_1(x_1) = \mu_{M_1^1}(x_1)f_{1_{min}} + \mu_{M_1^2}(x_1)f_{1_{max}}$ , where  $\mu_{M_1^1}(x_1) = \frac{f_1(x_1) - f_{1_{max}}}{f_{1_{min}} - f_{1_{max}}}$ ,  $\mu_{M_1^2}(x_1) = 1 - \mu_{M_1^1}(x_1)$ ,  $f_{1_{min}} = 0.5222$ ,  $f_{1_{max}} = 1.7647$ . To reduce computational burden, other nonlinear terms  $\sin(x_1)$  and  $\tan(x_1)$  are approximated by polynomials:  $\sin(x_1) \approx s_1 x_1$  and  $\tan(x_1) \approx t_1 x_1$ , where  $s_1 = 0.8578$  and  $t_1 = 1.5534$ . As a result, the inverted pendulum is described by a 2-rule polynomial fuzzy model. The system and input matrices in each rule are given by  $\mathbf{A}_1(x_2) = \begin{bmatrix} 0 & 1 \\ a_1(x_2) & 0 \end{bmatrix}$ ,  $\mathbf{A}_2(x_2) = \begin{bmatrix} 0 & 1 \\ a_2(x_2) & 0 \end{bmatrix}$ ,  $\mathbf{B}_1 = [0 \quad -f_{1_{min}}a]^T$ , and  $\mathbf{B}_2 = [0 \quad -f_{1_{max}}a]^T$ , where  $a_1(x_2) = f_{1_{min}}(gt_1 - am_p L x_2^2 s_1)$ ,  $a_2(x_2) = f_{1_{max}}(gt_1 - am_p L x_2^2 s_1)$ . The measurement of output provided by sensors may be affected by some physical influence such as the angular velocity of the inverted pendulum. Therefore, similar to the example in [54], we suppose the output is a function of system states:  $y = x_1 + 0.01x_1x_2$ . Then the output matrices are  $\mathbf{C}_1(x_2) = \mathbf{C}_2(x_2) = [1 + 0.01x_2 \quad 0]$ . The membership functions are  $w_1(x_1) = \mu_{M_1^1}(x_1)$  and  $w_2(x_1) = \mu_{M_1^2}(x_1)$ . It is assumed that both system states  $x_1$  and  $x_2$  are unmeasurable.

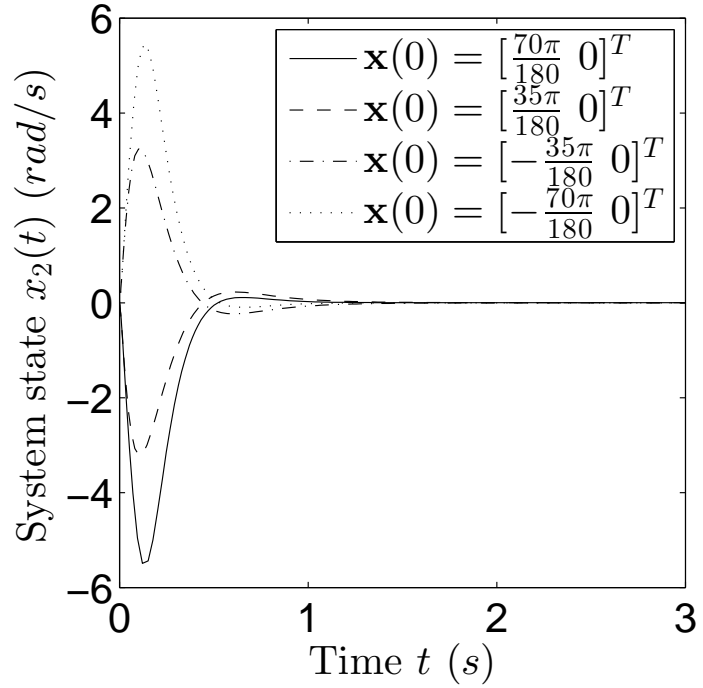
It can be seen that the premise variable  $f_1(x_1)$  and the output matrix  $\mathbf{C}_i(x_2)$  all depend on unmeasurable system states  $x_1$  or  $x_2$ , and thus Theorem 5 is employed to obtain a PFMB observer-controller to stabilize the inverted pendulum. We choose  $\alpha_1 = 1 \times 10^3$ ,  $\alpha_2 = 1 \times 10^6$ ,  $\beta = 1 \times 10^{-2}$ ,  $\mathbf{N}_k(\check{x}_2)$  of degree 0 and 2,  $\mathbf{M}_j(\check{x}_2)$  of degree 0 and 1,  $\varepsilon_1 = \varepsilon_2 = 1 \times 10^{-3}$  and  $\varepsilon_3 = \varepsilon_4 = 1 \times 10^{-7}$ . The polynomial controller gains are obtained as  $\mathbf{G}_1(\check{x}_2) = [-1.1623 \times 10^{-2}\check{x}_2^2 + 1.5144 \times 10^3 \quad 2.5661 \times 10^{-2}\check{x}_2^2 + 1.6857 \times 10^2]$  and  $\mathbf{G}_2(\check{x}_2) = [-1.2124 \times 10^{-1}\check{x}_2^2 + 7.7898 \times 10^2 \quad 2.7568 \times 10^{-2}\check{x}_2^2 + 1.0284 \times 10^2]$ , and the polynomial observer gains are obtained as  $\mathbf{L}_1(\check{x}_2) = [-6.0760 \times 10^{-2}\check{x}_2 + 1.1223 \times 10^2 \quad -3.5682 \times 10^{-2}\check{x}_2 + 1.2580 \times 10^2]^T$  and  $\mathbf{L}_2(\check{x}_2) = [-6.0760 \times 10^{-2}\check{x}_2 + 1.1223 \times 10^2 \quad -3.5682 \times 10^{-2}\check{x}_2 + 1.2580 \times 10^2]^T$ .

We apply the above polynomial controller gains and polynomial observer gains to the original dynamic system of the inverted pendulum (4.71). Considering 4 different initial conditions, the inverted pendulum is successfully stabilized where the time response of system states are shown in Fig. 5.2. To demonstrate the estimated system states offered by the polynomial fuzzy observer, we choose one of the above initial conditions  $\mathbf{x}(0) = [\frac{70\pi}{180} \quad 0]^T$  and  $\check{\mathbf{x}}(0) = [\frac{35\pi}{180} \quad 0]^T$  for demonstration purposes and the estimated system states are shown in Fig. 5.3. The corresponding control

input is shown in Fig. 5.4. It can be seen that the proposed polynomial fuzzy observer is an effective tool for nonlinear systems to observe unmeasurable states.

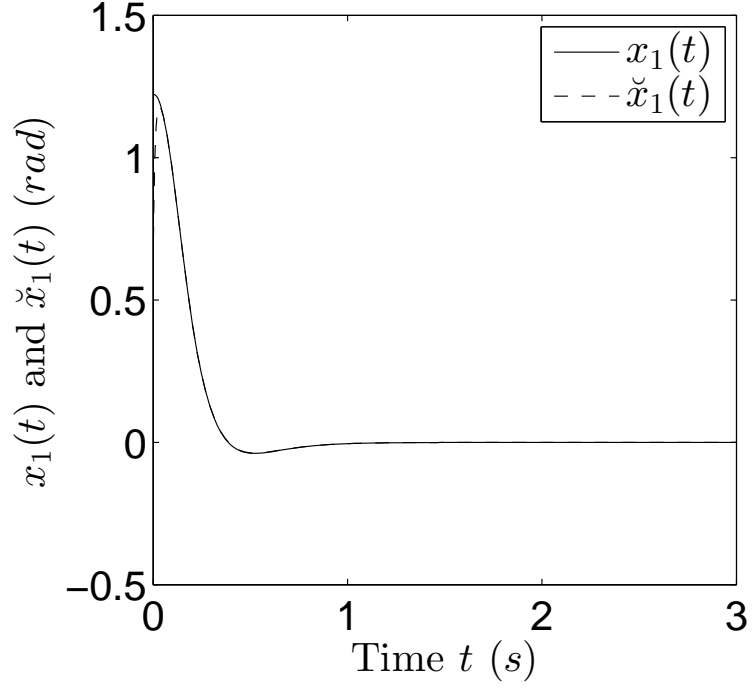


(a) Time response of  $x_1(t)$ .

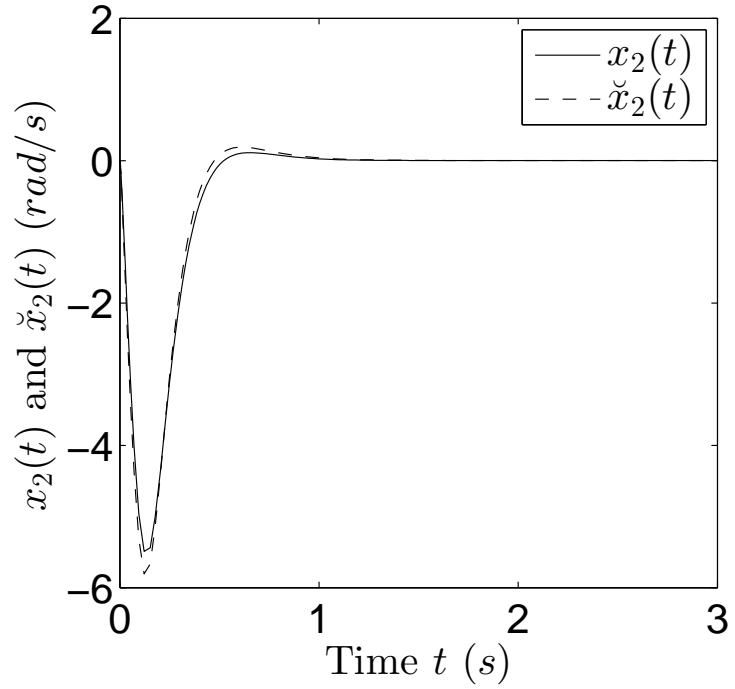


(b) Time response of  $x_2(t)$ .

Figure 5.2: Time response of system states of the inverted pendulum with 4 different initial conditions.



(a) Time response of  $x_1(t)$  and  $\check{x}_1(t)$ .



(b) Time response of  $x_2(t)$  and  $\check{x}_2(t)$ .

Figure 5.3: Time response of system states and estimated states for  $\mathbf{x}(0) = [\frac{70\pi}{180} \ 0]^T$ .

### 5.1.3.2 Nonlinear Mass-Spring-Damper System

We follow the same control strategy in previous example to stabilize a nonlinear mass-spring-damper system as shown in Fig. 5.5 whose dynamics is given by [88]

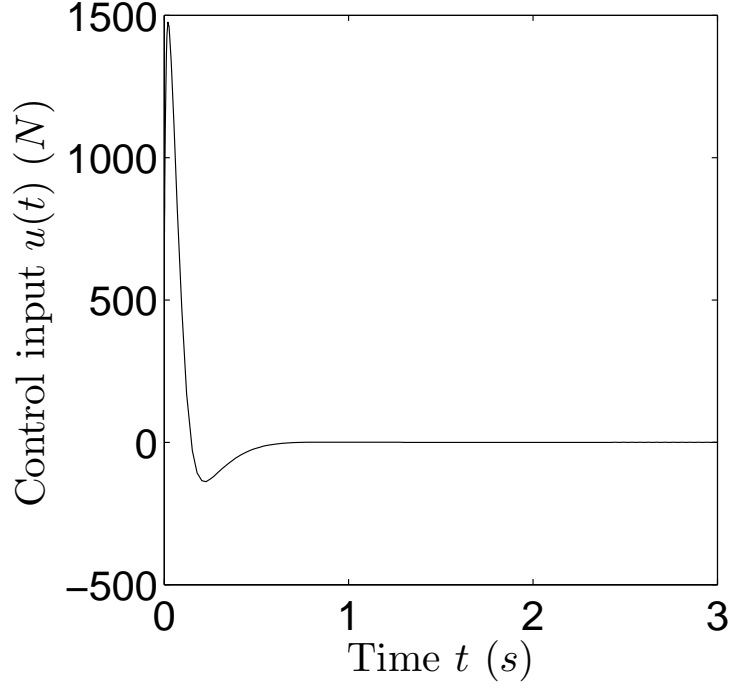


Figure 5.4: Time response of control input  $u(t)$  for  $\mathbf{x}(0) = [\frac{70\pi}{180} \ 0]^T$ .

and stated as follows:

$$M\ddot{x}(t) + g(x(t), \dot{x}(t)) + f(x(t)) = \phi(\dot{x}(t))u(t), \quad (5.48)$$

where  $M$  is the mass;  $g(x(t), \dot{x}(t)) = D(c_1x(t) + c_2\dot{x}(t)^3 + c_3(t)\dot{x}(t))$ ,  $f(x(t)) = K(c_4x(t) + c_5x(t)^3 + c_6x(t))$  and  $\phi(\dot{x}(t)) = 1.4387 + c_7\dot{x}(t)^2 + c_8 \cos(5\dot{x}(t))$  are the damper nonlinearity, the spring nonlinearity and the input nonlinearity, respectively;  $M = D = K = 1$ ,  $c_1 = 0$ ,  $c_2 = 1$ ,  $c_3 = -0.3$ ,  $c_4 = 0.01$ ,  $c_5 = 0.1$ ,  $c_6 = 0.3$ ,  $c_7 = -0.03$ ,  $c_8 = 0.2$ ; and  $u(t)$  is the force.

Time  $t$  is dropped from now for simplicity. Denoting  $x_1$  and  $x_2$  as  $x$  and  $\dot{x}$ , respectively, and  $\mathbf{x} = [x_1 \ x_2]^T$ , we obtain the following state space form:

$$\begin{aligned} \dot{x}_1 &= x_2, \\ \dot{x}_2 &= \frac{1}{M}(-g(x_1, x_2) - f(x_1) + \phi(x_2)u). \end{aligned} \quad (5.49)$$

The nonlinear term  $f_1(x_2) = \cos(5x_2)$  is represented by sector nonlinearity technique [9] as follows:  $f_1(x_2) = \mu_{M_1^1}(x_2)f_{1_{min}} + \mu_{M_1^2}(x_2)f_{1_{max}}$ , where  $\mu_{M_1^1}(x_2) = \frac{f_1(x_2) - f_{1_{max}}}{f_{1_{min}} - f_{1_{max}}}$ ,  $\mu_{M_1^2}(x_2) = 1 - \mu_{M_1^1}(x_2)$ ,  $f_{1_{min}} = -1$ ,  $f_{1_{max}} = 1$ . As a result, the nonlinear mass-spring-damper system is described by a 2-rule polynomial fuzzy model. The system and input matrices in each rule are given by  $\mathbf{A}_1(\mathbf{x}) = \mathbf{A}_2(\mathbf{x}) = \begin{bmatrix} 0 & 1 \\ a_1(x_1) & a_2(x_2) \end{bmatrix}$ ,  $\mathbf{B}_1(x_2) = [0 \ b_1(x_2)]^T$ , and  $\mathbf{B}_2(x_2) = [0 \ b_2(x_2)]^T$ , where  $a_1(x_1) = -\frac{1}{M}(Dc_3 + K(c_4 + c_6) + Kc_5x_1^2)$ ,  $a_2(x_2) = -\frac{1}{M}(Dc_2 + Dc_2x_2^2)$ ,  $b_1(x_2) = \frac{1}{M}(1.4387 + c_7x_2^2 + c_8f_{1_{min}})$ ,

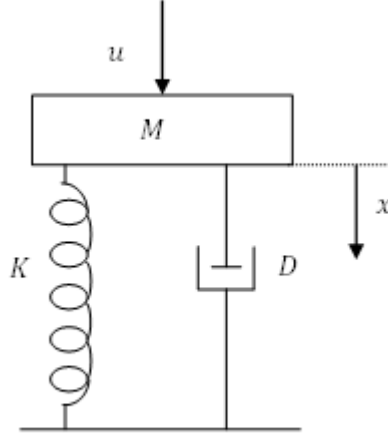
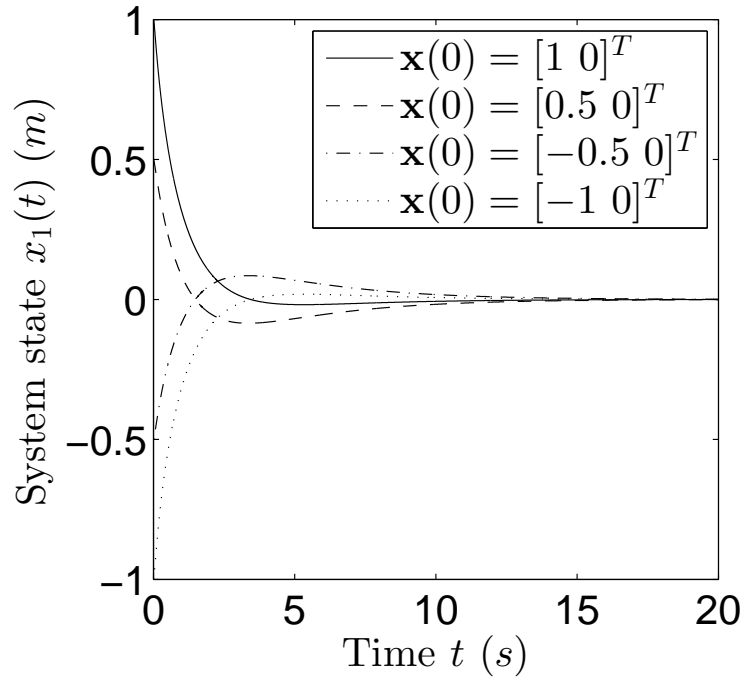


Figure 5.5: The nonlinear mass-spring-damper system.

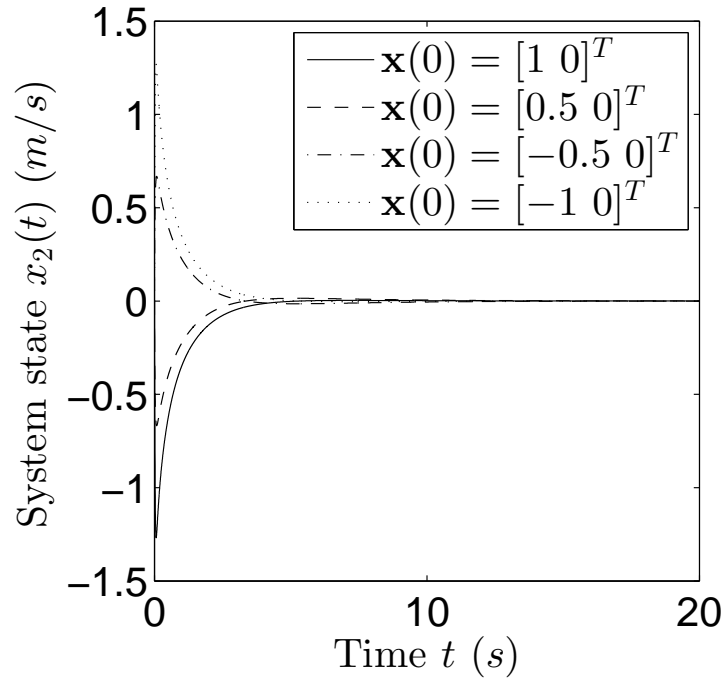
$b_2(x_2) = \frac{1}{M}(1.4387 + c_7 x_2^2 + c_8 f_{1_{max}})$ . In addition, the output matrices are  $\mathbf{C}_1 = \mathbf{C}_2 = [1 \ 0]$ . The membership functions are  $w_1(x_2) = \mu_{M_1^1}(x_2)$  and  $w_2(x_2) = \mu_{M_1^2}(x_2)$ .

It can be seen that the premise variable  $f_1(x_2)$  depends on unmeasurable system state  $x_2$ , and thus Theorem 5 is employed to design a PFMB observer-controller to stabilize the nonlinear mass-spring-damper system. We choose  $\mathbf{N}_k(\check{x}_1)$  of degree 0 and 2,  $\mathbf{M}_j(\check{x}_1)$  of degree 0 and 2, and keep other settings the same as Example 5.1.3.1. The polynomial controller gains are obtained as  $\mathbf{G}_1(\check{x}_1) = [-1.4754 \times 10^{-1} \check{x}_1^2 - 1.0447 \times 10^{-1} - 4.8074 \times 10^{-2} \check{x}_1^2 - 3.3439 \times 10^{-1}]$  and  $\mathbf{G}_2(\check{x}_1) = [-6.4731 \times 10^{-2} \check{x}_1^2 - 9.8315 \times 10^{-1} - 3.9791 \times 10^{-2} \check{x}_1^2 - 3.3442 \times 10^{-1}]$ , and the polynomial observer gains are obtained as  $\mathbf{L}_1(\check{x}_2) = [4.1689 \times 10^{-3} \check{x}_1^2 + 9.2052 \times 10^2 \quad 4.1692 \times 10^{-3} \check{x}_1^2 + 1.0648 \times 10^3]^T$  and  $\mathbf{L}_2(\check{x}_2) = [4.1689 \times 10^{-3} \check{x}_1^2 + 9.2052 \times 10^2 \quad 4.1692 \times 10^{-3} \check{x}_1^2 + 1.0648 \times 10^3]^T$ .

Considering 4 different initial conditions, the time response of system states are shown in Fig. 5.6 which shows that the nonlinear mass-spring-damper system can be stabilized by the designed polynomial fuzzy observer-controller. Choosing initiation conditions  $\mathbf{x}(0) = [1 \ 0]^T$  and  $\check{\mathbf{x}}(0) = [0 \ 0]^T$  as an example, the estimated system states are shown in Fig. 5.7. Consequently, it is feasible to apply the proposed PFMB observer-control strategy for stabilization of nonlinear systems. Note that in Fig. 5.7(a), the estimated state follows the original state quickly and it can only be seen in the zoom-in figure.

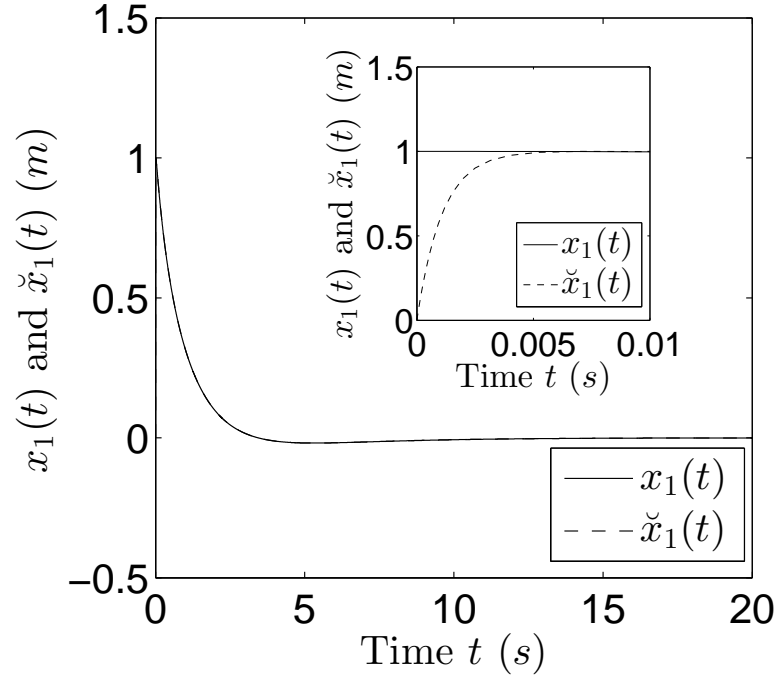


(a) Time response of  $x_1(t)$ .

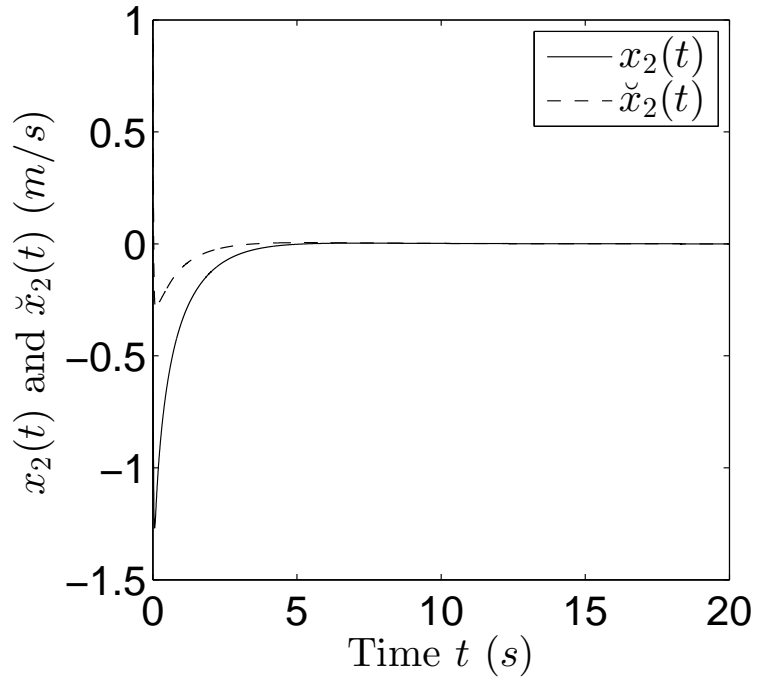


(b) Time response of  $x_2(t)$ .

Figure 5.6: Time response of system states of the mass-spring-damper system with 4 different initial conditions.



(a) Time response of  $x_1(t)$  and  $\hat{x}_1(t)$ .



(b) Time response of  $x_2(t)$  and  $\hat{x}_2(t)$ .

Figure 5.7: Time response of system states and estimated states for  $\mathbf{x}(0) = [1 \ 0]^T$ .

#### 5.1.4 Conclusion

In this section, the stability of PFMB observer-control system has been investigated. The polynomial controller gains and polynomial observer gains are allowed to be a function of estimated states. Moreover, the premise variables are allowed to be



unmeasurable which complicates the stability analysis but enhances the applicability of the proposed PFMB observer-control scheme. Matrix decoupling technique has been employed in the stability analysis to obtain convex SOS stability conditions. Simulation examples have been presented to verify the stability analysis results and demonstrate the effectiveness of the proposed PFMB observer-control scheme.

## 5.2 Design of Polynomial Fuzzy Observer-Controller Using Completing Square Approach

### 5.2.1 Introduction

In this section, we design PFMB observer-controller using completing square approach instead of matrix decoupling technique. Compared with [60], we obtain the polynomial observer gains and controller gains in one step rather than two steps. The premise variables are unmeasurable which are more general than measurable premise variables, and the output matrices are allowed to be polynomial matrices instead of constant matrices. To achieve the one-step design, the completing square approach refining the one in [53] is employed to derive the convex stability conditions in terms of SOS. Compared with [53], the number of manually designed parameters is reduced from 4 to 3, and the polynomial fuzzy model considered in this section is more general than the T-S fuzzy model. Compared with matrix decoupling technique, the completing square approach leads to smaller number of stability conditions at the expense of larger dimension of matrices.

This section is organized as follows. The formulation of non-PDC polynomial fuzzy observer and polynomial fuzzy controller is presented in Subsection 5.2.2. Stability analysis of the PFMB observer-control system is conducted in Subsection 5.2.3. Finally, a conclusion is drawn in Subsection 5.2.4. Note that simulation examples will be presented together with an optimization method in Subsection 5.4.3.

### 5.2.2 Preliminary

The PDC approach is not applied in this section for observer-controller design since the membership functions will be optimized in the following sections. Therefore, we provide the non-PDC form of the polynomial fuzzy observer and the polynomial fuzzy controller here. Note that PDC approach can also be applied and we will compare this optimization method with PDC approach in the simulation examples.

### 5.2.2.1 Polynomial Fuzzy Observer

For brevity, time  $t$  is dropped from now. Define  $\check{\mathbf{x}} \in \mathbb{R}^n$  as the estimated system state vector and  $\check{\mathbf{y}} \in \mathbb{R}^l$  as the estimated system output vector. The following polynomial fuzzy observer is applied to estimate the states  $\mathbf{x}$  in (5.1):

$$\begin{aligned}\dot{\check{\mathbf{x}}} &= \sum_{i=1}^p m_i(\check{\mathbf{x}}) \left( \mathbf{A}_i(\check{\mathbf{x}})\check{\mathbf{x}} + \mathbf{B}_i(\check{\mathbf{x}})\mathbf{u} + \mathbf{L}_i(\check{\mathbf{x}})(\mathbf{y} - \check{\mathbf{y}}) \right), \\ \check{\mathbf{y}} &= \sum_{i=1}^p m_i(\check{\mathbf{x}}) \mathbf{C}_i(\check{\mathbf{x}})\check{\mathbf{x}},\end{aligned}\tag{5.50}$$

where  $\mathbf{L}_i(\check{\mathbf{x}}) \in \mathbb{R}^{n \times l}$  is the polynomial observer gain;  $m_i(\check{\mathbf{x}})$  is the membership function to be chosen and optimized, which satisfies  $\sum_{i=1}^p m_i(\check{\mathbf{x}}) = 1$ .

**Remark 22** *Since we consider unmeasurable premise variables  $f_\eta(\mathbf{x})$  for the polynomial fuzzy model, the membership functions of the polynomial fuzzy observer  $m_i(\check{\mathbf{x}})$  should be allowed to depend on estimated system states  $\check{\mathbf{x}}$  rather than the original system states  $\mathbf{x}$ . Furthermore, the system output matrix  $\mathbf{C}_i(\mathbf{x})$  is allowed to be a function of system states  $\mathbf{x}$  instead of constant matrix  $\mathbf{C}_i$ . The above settings include those in [60] as particular cases.*

### 5.2.2.2 Polynomial Fuzzy Controller

With the obtained estimated system states  $\check{\mathbf{x}}$  from (5.50), The polynomial fuzzy controller is described as follows:

$$\mathbf{u} = \sum_{i=1}^p m_i(\check{\mathbf{x}}) \mathbf{G}_i(\check{\mathbf{x}})\check{\mathbf{x}},\tag{5.51}$$

where  $\mathbf{G}_i(\check{\mathbf{x}}) \in \mathbb{R}^{m \times n}$  is the polynomial controller gain.

**Remark 23** *The PDC approach with  $m_i(\check{\mathbf{x}}) = w_i(\check{\mathbf{x}}), i = 1, 2, \dots, p$  is not necessarily applied in this section. Instead, the membership function of the polynomial fuzzy observer-controller  $m_i(\check{\mathbf{x}})$  will be optimized in the following sections such that the performance of the closed-loop system is better than when using PDC approach. Furthermore, the shapes of the membership function  $m_i(\check{\mathbf{x}})$  can be chosen freely by users for different purposes. For example, the shapes can be chosen to be simpler than those of  $w_i(\mathbf{x})$  to reduce the complexity of the observer-controller, or chosen to include the PDC approach as a special case for the comparison of performance during the optimization.*

## 5.2.3 Stability Analysis

In this section, we conduct the stability analysis for PFMB observer-control systems. In the following, the dynamics of the closed-loop system is given first. Then, the

stability conditions are derived based on the Lyapunov stability theory. The control synthesis is achieved by solving the stability conditions.

The estimation error is defined as  $\mathbf{e} = \mathbf{x} - \check{\mathbf{x}}$ , and then we have the closed-loop system (shown in Fig. 4.1) consisting of the polynomial fuzzy model (5.1), the polynomial fuzzy controller (5.51) and the polynomial fuzzy observer (5.50) as follows:

$$\dot{\mathbf{x}} = \sum_{i=1}^p \sum_{j=1}^p w_i(\mathbf{x}) m_j(\check{\mathbf{x}}) \left( (\mathbf{A}_i(\mathbf{x}) + \mathbf{B}_i(\mathbf{x}) \mathbf{G}_j(\check{\mathbf{x}})) \mathbf{x} - \mathbf{B}_i(\mathbf{x}) \mathbf{G}_j(\check{\mathbf{x}}) \mathbf{e} \right), \quad (5.52)$$

$$\begin{aligned} \dot{\check{\mathbf{x}}} = & \sum_{i=1}^p \sum_{j=1}^p \sum_{k=1}^p w_i(\mathbf{x}) m_j(\check{\mathbf{x}}) m_k(\check{\mathbf{x}}) \left( (\mathbf{A}_j(\check{\mathbf{x}}) + \mathbf{B}_j(\check{\mathbf{x}}) \mathbf{G}_k(\check{\mathbf{x}}) \right. \\ & + \mathbf{L}_j(\check{\mathbf{x}}) (\mathbf{C}_i(\mathbf{x}) - \mathbf{C}_k(\check{\mathbf{x}}))) \mathbf{x} + (-\mathbf{A}_j(\check{\mathbf{x}}) - \mathbf{B}_j(\check{\mathbf{x}}) \mathbf{G}_k(\check{\mathbf{x}}) \\ & \left. + \mathbf{L}_j(\check{\mathbf{x}}) \mathbf{C}_k(\check{\mathbf{x}})) \mathbf{e} \right), \end{aligned} \quad (5.53)$$

$$\begin{aligned} \dot{\mathbf{e}} = & \sum_{i=1}^p \sum_{j=1}^p \sum_{k=1}^p w_i(\mathbf{x}) m_j(\check{\mathbf{x}}) m_k(\check{\mathbf{x}}) \left( (\mathbf{A}_i(\mathbf{x}) - \mathbf{A}_j(\check{\mathbf{x}}) \right. \\ & + (\mathbf{B}_i(\mathbf{x}) - \mathbf{B}_j(\check{\mathbf{x}})) \mathbf{G}_k(\check{\mathbf{x}}) - \mathbf{L}_j(\check{\mathbf{x}}) (\mathbf{C}_i(\mathbf{x}) - \mathbf{C}_k(\check{\mathbf{x}}))) \mathbf{x} \\ & \left. + (\mathbf{A}_j(\check{\mathbf{x}}) - (\mathbf{B}_i(\mathbf{x}) - \mathbf{B}_j(\check{\mathbf{x}})) \mathbf{G}_k(\check{\mathbf{x}}) - \mathbf{L}_j(\check{\mathbf{x}}) \mathbf{C}_k(\mathbf{x})) \mathbf{e} \right). \end{aligned} \quad (5.54)$$

The control objective is to make the augmented PFMB observer-control system (formed by (5.52) and (5.54)) asymptotically stable, i.e.,  $\mathbf{x} \rightarrow 0$  and  $\mathbf{e} \rightarrow 0$  as time  $t \rightarrow \infty$ , by determining the polynomial controller gain  $\mathbf{G}_k(\check{\mathbf{x}})$  and polynomial observer gain  $\mathbf{L}_j(\check{\mathbf{x}})$ .

**Theorem 6** *The augmented PFMB observer-control system (formed by (5.52) and (5.54)) is guaranteed to be asymptotically stable if there exist matrices  $\mathbf{X} \in \Re^{n \times n}$ ,  $\mathbf{Y} \in \Re^{n \times n}$ ,  $\mathbf{N}_k(\check{\mathbf{x}}) \in \Re^{m \times n}$ ,  $\mathbf{M}_j(\check{\mathbf{x}}) \in \Re^{n \times l}$ ,  $k, j \in \{1, 2, \dots, p\}$  and predefined scalars  $\gamma_1 > 0, \gamma_2 > 0, \gamma_3$  such that the following SOS-based conditions are satisfied:*

$$\nu_1^T (\mathbf{X} - \varepsilon_1 \mathbf{I}) \nu_1 \text{ is SOS}; \quad (5.55)$$

$$\nu_2^T (\mathbf{Y} - \varepsilon_2 \mathbf{I}) \nu_2 \text{ is SOS}; \quad (5.56)$$

$$\begin{aligned} & -\nu_3^T (\Phi_{ijk}(\mathbf{x}, \check{\mathbf{x}}) + \Phi_{ikj}(\mathbf{x}, \check{\mathbf{x}}) + \varepsilon_3(\mathbf{x}, \check{\mathbf{x}}) \mathbf{I}) \nu_3 \text{ is SOS} \\ & \forall i, j \leq k; \end{aligned} \quad (5.57)$$

where

$$\begin{aligned} \Phi_{ijk}(\mathbf{x}, \check{\mathbf{x}}) = & \begin{bmatrix} \Theta_{ijk}(\mathbf{x}, \check{\mathbf{x}}) & \tilde{\Phi}^{(12)} & \tilde{\Phi}_j^{(13)}(\check{\mathbf{x}}) \\ * & -\frac{1}{\gamma_1} \mathbf{I} & \mathbf{0} \\ * & * & -\frac{1}{\gamma_2} \mathbf{I} \end{bmatrix}, \\ \Theta_{ijk}(\mathbf{x}, \check{\mathbf{x}}) = & \end{aligned} \quad (5.58)$$

$$\begin{bmatrix} \Gamma_{ijk}(\mathbf{x}, \check{\mathbf{x}}) & \tilde{\Theta}_{ijk}^{(12)}(\mathbf{x}, \check{\mathbf{x}}) & \tilde{\Theta}_{ik}^{(13)}(\mathbf{x}, \check{\mathbf{x}}) & \Theta^{(14)} \\ * & -\gamma_1 \mathbf{I} & \mathbf{0} & \mathbf{0} \\ * & * & -\gamma_2 \mathbf{I} & \mathbf{0} \\ * & * & * & \Theta_{jk}^{(44)}(\check{\mathbf{x}}) \end{bmatrix}, \quad (5.59)$$

$$\Gamma_{ijk}(\mathbf{x}, \check{\mathbf{x}}) = \begin{bmatrix} \tilde{\Xi}_{ik}^{(11)}(\mathbf{x}, \check{\mathbf{x}}) + \tilde{\Xi}_{ik}^{(11)}(\mathbf{x}, \check{\mathbf{x}})^T & \tilde{\Xi}_{ik}^{(12)}(\mathbf{x}, \check{\mathbf{x}}) \\ * & -2\gamma_3 \mathbf{X} \end{bmatrix}, \quad (5.60)$$

$$\tilde{\Phi}^{(12)} = [\mathbf{0}_{n \times (3n+l)} \quad \mathbf{Y}]^T, \quad (5.61)$$

$$\tilde{\Phi}_j^{(13)}(\check{\mathbf{x}}) = [\mathbf{0}_{l \times (3n+l)} \quad \mathbf{M}_j(\check{\mathbf{x}})^T]^T, \quad (5.62)$$

$$\tilde{\Theta}_{ijk}^{(12)}(\mathbf{x}, \check{\mathbf{x}}) = [\tilde{\mathbf{H}}_{ijk}(\mathbf{x}, \check{\mathbf{x}}) \quad \tilde{\mathbf{K}}_{ijk}(\mathbf{x}, \check{\mathbf{x}})]^T, \quad (5.63)$$

$$\tilde{\Theta}_{ik}^{(13)}(\mathbf{x}, \check{\mathbf{x}}) = [(\mathbf{C}_i(\mathbf{x}) - \mathbf{C}_k(\check{\mathbf{x}}))\mathbf{X} \quad \mathbf{0}_{l \times n}]^T, \quad (5.64)$$

$$\Theta^{(14)} = [\mathbf{0}_{n \times n} \quad \gamma_3 \mathbf{I}]^T, \quad (5.65)$$

$$\Theta_{jk}^{(44)}(\check{\mathbf{x}}) = \hat{\Xi}_{jk}^{(22)}(\check{\mathbf{x}}) + \hat{\Xi}_{jk}^{(22)}(\check{\mathbf{x}})^T, \quad (5.66)$$

$$\tilde{\Xi}_{ik}^{(11)}(\mathbf{x}, \check{\mathbf{x}}) = \mathbf{A}_i(\mathbf{x})\mathbf{X} + \mathbf{B}_i(\mathbf{x})\mathbf{N}_k(\check{\mathbf{x}}), \quad (5.67)$$

$$\tilde{\Xi}_{ik}^{(12)}(\mathbf{x}, \check{\mathbf{x}}) = -\mathbf{B}_i(\mathbf{x})\mathbf{N}_k(\check{\mathbf{x}}), \quad (5.68)$$

$$\hat{\Xi}_{jk}^{(22)}(\check{\mathbf{x}}) = \mathbf{Y}\mathbf{A}_j(\check{\mathbf{x}}) - \mathbf{M}_j(\check{\mathbf{x}})\mathbf{C}_k(\check{\mathbf{x}}), \quad (5.69)$$

$$\tilde{\mathbf{H}}_{ijk}(\mathbf{x}, \check{\mathbf{x}}) = (\mathbf{A}_i(\mathbf{x}) - \mathbf{A}_j(\check{\mathbf{x}}))\mathbf{X} + (\mathbf{B}_i(\mathbf{x}) - \mathbf{B}_j(\check{\mathbf{x}}))\mathbf{N}_k(\check{\mathbf{x}}), \quad (5.70)$$

$$\tilde{\mathbf{K}}_{ijk}(\mathbf{x}, \check{\mathbf{x}}) = -(\mathbf{B}_i(\mathbf{x}) - \mathbf{B}_j(\check{\mathbf{x}}))\mathbf{N}_k(\check{\mathbf{x}}); \quad (5.71)$$

$\nu_1, \nu_2, \nu_3$  are arbitrary vectors independent of  $\mathbf{x}$  and  $\check{\mathbf{x}}$  with appropriate dimensions;  $\varepsilon_1 > 0, \varepsilon_2 > 0$  and  $\varepsilon_3(\mathbf{x}, \check{\mathbf{x}}) > 0$  are predefined scalar polynomials; and the polynomial controller and observer gains are given by  $\mathbf{G}_k(\check{\mathbf{x}}) = \mathbf{N}_k(\check{\mathbf{x}})\mathbf{X}^{-1}$  and  $\mathbf{L}_j(\check{\mathbf{x}}) = \mathbf{Y}^{-1}\mathbf{M}_j(\check{\mathbf{x}})$ , respectively. The number of decision variables is  $n^2 + n + pn_t(mn + nl)$  where  $n_t$  is the number of terms in each entry of the polynomial matrices  $\mathbf{N}_k(\check{\mathbf{x}})$  and  $\mathbf{M}_j(\check{\mathbf{x}})$ . The number of SOS conditions is  $\frac{1}{2}(p^3 + p^2) + 2$ .

**Proof** Defining the augmented vector  $\mathbf{z} = [\mathbf{x}^T \quad \mathbf{e}^T]^T$  and the summation term  $\sum_{i,j,k=1}^p \tilde{w}_{ijk} \equiv \sum_{i=1}^p \sum_{j=1}^p \sum_{k=1}^p w_i(\mathbf{x})m_j(\check{\mathbf{x}})m_k(\check{\mathbf{x}})$ , the augmented PFMB observer-control system is written as

$$\dot{\mathbf{z}} = \sum_{i,j,k=1}^p \tilde{w}_{ijk} \Xi_{ijk}(\mathbf{x}, \check{\mathbf{x}})\mathbf{z}, \quad (5.72)$$

where

$$\Xi_{ijk}(\mathbf{x}, \check{\mathbf{x}}) = \begin{bmatrix} \Xi_{ik}^{(11)}(\mathbf{x}, \check{\mathbf{x}}) & \Xi_{ik}^{(12)}(\mathbf{x}, \check{\mathbf{x}}) \\ \Xi_{ijk}^{(21)}(\mathbf{x}, \check{\mathbf{x}}) + \mathbf{H}_{ijk}(\mathbf{x}, \check{\mathbf{x}}) & \Xi_{jk}^{(22)}(\check{\mathbf{x}}) + \mathbf{K}_{ijk}(\mathbf{x}, \check{\mathbf{x}}) \end{bmatrix}, \quad (5.73)$$

$$\Xi_{ik}^{(11)}(\mathbf{x}, \check{\mathbf{x}}) = \mathbf{A}_i(\mathbf{x}) + \mathbf{B}_i(\mathbf{x})\mathbf{G}_k(\check{\mathbf{x}}), \quad (5.74)$$

$$\Xi_{ijk}^{(21)}(\mathbf{x}, \check{\mathbf{x}}) = -\mathbf{L}_j(\check{\mathbf{x}})(\mathbf{C}_i(\mathbf{x}) - \mathbf{C}_k(\check{\mathbf{x}})), \quad (5.75)$$

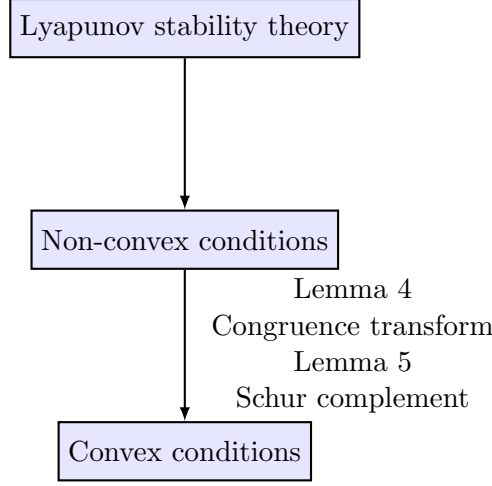


Figure 5.8: Procedure of the proof for Theorem 6.

$$\Xi_{ik}^{(12)}(\mathbf{x}, \check{\mathbf{x}}) = -\mathbf{B}_i(\mathbf{x})\mathbf{G}_k(\check{\mathbf{x}}), \quad (5.76)$$

$$\Xi_{jk}^{(22)}(\check{\mathbf{x}}) = \mathbf{A}_j(\check{\mathbf{x}}) - \mathbf{L}_j(\check{\mathbf{x}})\mathbf{C}_k(\check{\mathbf{x}}), \quad (5.77)$$

$$\mathbf{H}_{ijk}(\mathbf{x}, \check{\mathbf{x}}) = \mathbf{A}_i(\mathbf{x}) - \mathbf{A}_j(\check{\mathbf{x}}) + (\mathbf{B}_i(\mathbf{x}) - \mathbf{B}_j(\check{\mathbf{x}}))\mathbf{G}_k(\check{\mathbf{x}}), \quad (5.78)$$

$$\mathbf{K}_{ijk}(\mathbf{x}, \check{\mathbf{x}}) = -(\mathbf{B}_i(\mathbf{x}) - \mathbf{B}_j(\check{\mathbf{x}}))\mathbf{G}_k(\check{\mathbf{x}}). \quad (5.79)$$

The procedure of the proof is shown in Fig. 5.8. As can be seen, the completing square approach (Lemmas 4 and 5) will be applied to obtain convex conditions.

The following Lyapunov function candidate is employed to investigate the stability of the augmented PFMB observer-control system (5.72):

$$V(\mathbf{z}) = \mathbf{z}^T \mathbf{P} \mathbf{z}, \quad (5.80)$$

where  $\mathbf{P} = \begin{bmatrix} \mathbf{X}^{-1} & \mathbf{0} \\ \mathbf{0} & \mathbf{Y} \end{bmatrix}$ ,  $\mathbf{X} > 0$ ,  $\mathbf{Y} > 0$ , and thus  $\mathbf{P} > 0$ .

The time derivative of  $V(\mathbf{z})$  is

$$\dot{V}(\mathbf{z}) = \sum_{i,j,k=1}^p \tilde{w}_{ijk} \mathbf{z}^T (\mathbf{P} \Xi_{ijk}(\mathbf{x}, \check{\mathbf{x}}) + \Xi_{ijk}(\mathbf{x}, \check{\mathbf{x}})^T \mathbf{P}) \mathbf{z}. \quad (5.81)$$

Therefore,  $\dot{V}(\mathbf{z}) < 0$  holds if (the conservativeness is introduced)

$$\sum_{i,j,k=1}^p \tilde{w}_{ijk} (\mathbf{P} \Xi_{ijk}(\mathbf{x}, \check{\mathbf{x}}) + \Xi_{ijk}(\mathbf{x}, \check{\mathbf{x}})^T \mathbf{P}) < 0. \quad (5.82)$$

The augmented PFMB observer-control system (5.72) is guaranteed to be asymptotically stable if  $V(\mathbf{z}) > 0$  by satisfying  $\mathbf{P} > 0$  and  $\dot{V}(\mathbf{z}) < 0$  by satisfying (5.82) excluding  $\mathbf{x} = \mathbf{0}$ . However, the condition (5.82) is not convex, which cannot be solved by convex programming technique. In what follows, we apply the refined

completing square approach (Lemmas 4 and 5) and congruence transformation to derive (conservatively) convex SOS conditions such that the polynomial controller gain  $\mathbf{G}_k(\check{\mathbf{x}})$  and the polynomial observer gain  $\mathbf{L}_j(\check{\mathbf{x}})$  can be obtained in one step.

Denoting  $\mathbf{M}_j(\check{\mathbf{x}}) = \mathbf{Y}\mathbf{L}_j(\check{\mathbf{x}})$ , (5.82) becomes

$$\sum_{i,j,k=1}^p \tilde{w}_{ijk}(\hat{\Xi}_{ijk}(\mathbf{x}, \check{\mathbf{x}}) + \hat{\Xi}_{ijk}(\mathbf{x}, \check{\mathbf{x}})^T) < 0, \quad (5.83)$$

where

$$\hat{\Xi}_{ijk}(\mathbf{x}, \check{\mathbf{x}}) = \begin{bmatrix} \mathbf{X}^{-1}\Xi_{ik}^{(11)}(\mathbf{x}, \check{\mathbf{x}}) & \mathbf{X}^{-1}\Xi_{ik}^{(12)}(\mathbf{x}, \check{\mathbf{x}}) \\ \hat{\Xi}_{ijk}^{(21)}(\mathbf{x}, \check{\mathbf{x}}) + \mathbf{Y}\mathbf{H}_{ijk}(\mathbf{x}, \check{\mathbf{x}}) & \hat{\Xi}_{jk}^{(22)}(\check{\mathbf{x}}) + \mathbf{Y}\mathbf{K}_{ijk}(\mathbf{x}, \check{\mathbf{x}}) \end{bmatrix}, \quad (5.84)$$

$$\hat{\Xi}_{ijk}^{(21)}(\mathbf{x}, \check{\mathbf{x}}) = -\mathbf{M}_j(\check{\mathbf{x}})(\mathbf{C}_i(\mathbf{x}) - \mathbf{C}_k(\check{\mathbf{x}})), \quad (5.85)$$

and  $\hat{\Xi}_{jk}^{(22)}(\check{\mathbf{x}})$  is defined in (5.69).

Applying Lemma 4, we have

$$\begin{aligned} & \sum_{i,j,k=1}^p \tilde{w}_{ijk}(\hat{\Xi}_{ijk}(\mathbf{x}, \check{\mathbf{x}}) + \hat{\Xi}_{ijk}(\mathbf{x}, \check{\mathbf{x}})^T) \\ &= \sum_{i,j,k=1}^p \tilde{w}_{ijk} \left( \Upsilon_{ijk}(\mathbf{x}, \check{\mathbf{x}}) + \Theta_{ijk}^{(12)}(\mathbf{x}, \check{\mathbf{x}}) \Phi^{(12)T} \right. \\ & \quad + \Phi^{(12)} \Theta_{ijk}^{(12)}(\mathbf{x}, \check{\mathbf{x}})^T + \Theta_{ik}^{(13)}(\mathbf{x}, \check{\mathbf{x}}) \Phi_j^{(13)}(\check{\mathbf{x}})^T \\ & \quad \left. + \Phi_j^{(13)}(\check{\mathbf{x}}) \Theta_{ik}^{(13)}(\mathbf{x}, \check{\mathbf{x}})^T \right) \\ &\leq \sum_{i,j,k=1}^p \tilde{w}_{ijk} \Upsilon_{ijk}(\mathbf{x}, \check{\mathbf{x}}) + \gamma_1 \Phi^{(12)} \Phi^{(12)T} \\ & \quad + \frac{1}{\gamma_1} \left( \sum_{i,j,k=1}^p \tilde{w}_{ijk} \Theta_{ijk}^{(12)}(\mathbf{x}, \check{\mathbf{x}}) \right) \left( \sum_{i,j,k=1}^p \tilde{w}_{ijk} \Theta_{ijk}^{(12)}(\mathbf{x}, \check{\mathbf{x}}) \right)^T \\ & \quad + \gamma_2 \left( \sum_{i,j,k=1}^p \tilde{w}_{ijk} \Phi_j^{(13)}(\check{\mathbf{x}}) \right) \left( \sum_{i,j,k=1}^p \tilde{w}_{ijk} \Phi_j^{(13)}(\check{\mathbf{x}}) \right)^T \\ & \quad + \frac{1}{\gamma_2} \left( \sum_{i,j,k=1}^p \tilde{w}_{ijk} \Theta_{ik}^{(13)}(\mathbf{x}, \check{\mathbf{x}}) \right) \left( \sum_{i,j,k=1}^p \tilde{w}_{ijk} \Theta_{ik}^{(13)}(\mathbf{x}, \check{\mathbf{x}}) \right)^T \\ &= \sum_{i,j,k=1}^p \tilde{w}_{ijk} \hat{\Upsilon}_{ijk}(\mathbf{x}, \check{\mathbf{x}}) + \\ & \quad + \frac{1}{\gamma_1} \left( \sum_{i,j,k=1}^p \tilde{w}_{ijk} \Theta_{ijk}^{(12)}(\mathbf{x}, \check{\mathbf{x}}) \right) \left( \sum_{i,j,k=1}^p \tilde{w}_{ijk} \Theta_{ijk}^{(12)}(\mathbf{x}, \check{\mathbf{x}}) \right)^T \\ & \quad + \frac{1}{\gamma_2} \left( \sum_{i,j,k=1}^p \tilde{w}_{ijk} \Theta_{ik}^{(13)}(\mathbf{x}, \check{\mathbf{x}}) \right) \left( \sum_{i,j,k=1}^p \tilde{w}_{ijk} \Theta_{ik}^{(13)}(\mathbf{x}, \check{\mathbf{x}}) \right)^T, \quad (5.86) \end{aligned}$$

where

$$\Upsilon_{ijk}(\mathbf{x}, \check{\mathbf{x}}) = \begin{bmatrix} \Upsilon_{ik}^{(11)}(\mathbf{x}, \check{\mathbf{x}}) & \mathbf{X}^{-1}\Xi_{ik}^{(12)}(\mathbf{x}, \check{\mathbf{x}}) \\ * & \hat{\Xi}_{jk}^{(22)}(\check{\mathbf{x}}) + \hat{\Xi}_{jk}^{(22)}(\check{\mathbf{x}})^T \end{bmatrix}, \quad (5.87)$$

$$\Upsilon_{ik}^{(11)}(\mathbf{x}, \check{\mathbf{x}}) = \mathbf{X}^{-1}\Xi_{ik}^{(11)}(\mathbf{x}, \check{\mathbf{x}}) + (\mathbf{X}^{-1}\Xi_{ik}^{(11)}(\mathbf{x}, \check{\mathbf{x}}))^T, \quad (5.88)$$

$$\Phi^{(12)} = [\mathbf{0}_{n \times n} \quad \mathbf{Y}]^T, \quad (5.89)$$

$$\Phi_j^{(13)}(\check{\mathbf{x}}) = [\mathbf{0}_{l \times n} \quad \mathbf{M}_j(\check{\mathbf{x}})^T]^T, \quad (5.90)$$

$$\Theta_{ijk}^{(12)}(\mathbf{x}, \check{\mathbf{x}}) = [\mathbf{H}_{ijk}(\mathbf{x}, \check{\mathbf{x}}) \quad \mathbf{K}_{ijk}(\mathbf{x}, \check{\mathbf{x}})]^T, \quad (5.91)$$

$$\Theta_{ik}^{(13)}(\mathbf{x}, \check{\mathbf{x}}) = [\mathbf{C}_i(\mathbf{x}) - \mathbf{C}_k(\check{\mathbf{x}}) \quad \mathbf{0}_{l \times n}]^T, \quad (5.92)$$

$$\hat{\Upsilon}_{ijk}(\mathbf{x}, \check{\mathbf{x}}) = \begin{bmatrix} \Upsilon_{ik}^{(11)}(\mathbf{x}, \check{\mathbf{x}}) & \mathbf{X}^{-1}\Xi_{ik}^{(12)}(\mathbf{x}, \check{\mathbf{x}}) \\ * & \hat{\Upsilon}_{jk}^{(22)}(\check{\mathbf{x}}) \end{bmatrix}, \quad (5.93)$$

$$\begin{aligned} \hat{\Upsilon}_{jk}^{(22)}(\check{\mathbf{x}}) &= \hat{\Xi}_{jk}^{(22)}(\check{\mathbf{x}}) + \hat{\Xi}_{jk}^{(22)}(\check{\mathbf{x}})^T + \gamma_1 \mathbf{Y} \mathbf{Y} \\ &+ \gamma_2 \left( \sum_{i,j,k=1}^p \tilde{w}_{ijk} \mathbf{M}_j(\check{\mathbf{x}}) \right) \left( \sum_{i,j,k=1}^p \tilde{w}_{ijk} \mathbf{M}_j(\check{\mathbf{x}}) \right)^T, \end{aligned} \quad (5.94)$$

and  $\gamma_1$  and  $\gamma_2$  are positive scalars.

There are two purposes of applying Lemma 4. One is separating matrix  $\mathbf{Y}$  from other unknown matrices. Another is leaving some convex (or convex after Schur complement) terms into  $\hat{\Upsilon}_{jk}^{(22)}(\check{\mathbf{x}})$  in (5.94). Subsequently, the purpose of applying Lemma 5 is exactly to preserve the convex terms in  $\hat{\Upsilon}_{jk}^{(22)}(\check{\mathbf{x}})$  from being affected by the following congruence transformation. When separating matrix  $\mathbf{Y}$ , other unknown matrices can all be grouped into  $\Theta_{ijk}^{(12)}(\mathbf{x}, \check{\mathbf{x}})$  in (5.91) such that only one design parameter is required, which is the reason that the number of design parameters is less than that in [53]. Note that the conservativeness is introduced by Lemmas 4 and 5.

Performing congruence transformation to both sides of (5.86) by pre-multiplying and post-multiplying  $\text{diag}\{\mathbf{X}, \mathbf{X}\}$  and denoting  $\mathbf{N}_k(\check{\mathbf{x}}) = \mathbf{G}_k(\check{\mathbf{x}})\mathbf{X}$ , then  $\dot{V}(\mathbf{z}) < 0$  holds if

$$\begin{aligned} & \sum_{i,j,k=1}^p \tilde{w}_{ijk} \tilde{\Upsilon}_{ijk}(\mathbf{x}, \check{\mathbf{x}}) \\ & + \frac{1}{\gamma_1} \left( \sum_{i,j,k=1}^p \tilde{w}_{ijk} \tilde{\Theta}_{ijk}^{(12)}(\mathbf{x}, \check{\mathbf{x}}) \right) \left( \sum_{i,j,k=1}^p \tilde{w}_{ijk} \tilde{\Theta}_{ijk}^{(12)}(\mathbf{x}, \check{\mathbf{x}}) \right)^T \\ & + \frac{1}{\gamma_2} \left( \sum_{i,j,k=1}^p \tilde{w}_{ijk} \tilde{\Theta}_{ik}^{(13)}(\mathbf{x}, \check{\mathbf{x}}) \right) \left( \sum_{i,j,k=1}^p \tilde{w}_{ijk} \tilde{\Theta}_{ik}^{(13)}(\mathbf{x}, \check{\mathbf{x}}) \right)^T \\ & < 0, \end{aligned} \quad (5.95)$$

where

$$\tilde{\mathbf{\Upsilon}}_{ijk}(\mathbf{x}, \check{\mathbf{x}}) = \begin{bmatrix} \tilde{\mathbf{\Xi}}_{ik}^{(11)}(\mathbf{x}, \check{\mathbf{x}}) + \tilde{\mathbf{\Xi}}_{ik}^{(11)}(\mathbf{x}, \check{\mathbf{x}})^T & \tilde{\mathbf{\Xi}}_{ik}^{(12)}(\mathbf{x}, \check{\mathbf{x}}) \\ * & \mathbf{X} \hat{\mathbf{\Upsilon}}_{jk}^{(22)}(\check{\mathbf{x}}) \mathbf{X} \end{bmatrix}, \quad (5.96)$$

and  $\tilde{\mathbf{\Theta}}_{ijk}^{(12)}(\mathbf{x}, \check{\mathbf{x}})$ ,  $\tilde{\mathbf{\Theta}}_{ik}^{(13)}(\mathbf{x}, \check{\mathbf{x}})$ ,  $\tilde{\mathbf{\Xi}}_{ik}^{(11)}(\mathbf{x}, \check{\mathbf{x}})$  and  $\tilde{\mathbf{\Xi}}_{ik}^{(12)}(\mathbf{x}, \check{\mathbf{x}})$ , are defined in (5.63), (5.64), (5.67) and (5.68), respectively.

By grouping terms with same membership functions,  $\dot{V}(\mathbf{z}) < 0$  holds if

$$\begin{aligned} & \sum_{i,j,k=1}^p \tilde{w}_{ijk} \left( \tilde{\mathbf{\Upsilon}}_{ijk}(\mathbf{x}, \check{\mathbf{x}}) + \tilde{\mathbf{\Upsilon}}_{ikj}(\mathbf{x}, \check{\mathbf{x}}) \right) \\ & + \frac{2}{\gamma_1} \left( \sum_{i,j,k=1}^p \tilde{w}_{ijk} \tilde{\mathbf{\Theta}}_{ijk}^{(12)}(\mathbf{x}, \check{\mathbf{x}}) \right) \left( \sum_{i,j,k=1}^p \tilde{w}_{ijk} \tilde{\mathbf{\Theta}}_{ijk}^{(12)}(\mathbf{x}, \check{\mathbf{x}}) \right)^T \\ & + \frac{2}{\gamma_2} \left( \sum_{i,j,k=1}^p \tilde{w}_{ijk} \tilde{\mathbf{\Theta}}_{ik}^{(13)}(\mathbf{x}, \check{\mathbf{x}}) \right) \left( \sum_{i,j,k=1}^p \tilde{w}_{ijk} \tilde{\mathbf{\Theta}}_{ik}^{(13)}(\mathbf{x}, \check{\mathbf{x}}) \right)^T \\ & < 0. \end{aligned} \quad (5.97)$$

Applying Lemma 5 to the term  $\mathbf{X}(\hat{\mathbf{\Upsilon}}_{jk}^{(22)}(\check{\mathbf{x}}) + \hat{\mathbf{\Upsilon}}_{kj}^{(22)}(\check{\mathbf{x}}))\mathbf{X}$  (the conservativeness is introduced), we have

$$\begin{aligned} & \mathbf{X}(\hat{\mathbf{\Upsilon}}_{jk}^{(22)}(\check{\mathbf{x}}) + \hat{\mathbf{\Upsilon}}_{kj}^{(22)}(\check{\mathbf{x}}))\mathbf{X} \\ & = 2\mathbf{X} \frac{\hat{\mathbf{\Upsilon}}_{jk}^{(22)}(\check{\mathbf{x}}) + \hat{\mathbf{\Upsilon}}_{kj}^{(22)}(\check{\mathbf{x}})}{2} \mathbf{X} \\ & \leq 2 \left( -\gamma_3^2 \left( \frac{\hat{\mathbf{\Upsilon}}_{jk}^{(22)}(\check{\mathbf{x}}) + \hat{\mathbf{\Upsilon}}_{kj}^{(22)}(\check{\mathbf{x}})}{2} \right)^{-1} - 2\gamma_3 \mathbf{X} \right), \end{aligned} \quad (5.98)$$

where  $\gamma_3$  is an arbitrary scalar.

Then  $\dot{V}(\mathbf{z}) < 0$  holds if

$$\begin{aligned} & \sum_{i,j,k=1}^p \tilde{w}_{ijk} \left( \mathbf{\Gamma}_{ijk}(\mathbf{x}, \check{\mathbf{x}}) + \mathbf{\Gamma}_{ikj}(\mathbf{x}, \check{\mathbf{x}}) \right) \\ & - 2\mathbf{\Theta}^{(14)} \left( \frac{\hat{\mathbf{\Upsilon}}_{jk}^{(22)}(\check{\mathbf{x}}) + \hat{\mathbf{\Upsilon}}_{kj}^{(22)}(\check{\mathbf{x}})}{2} \right)^{-1} \mathbf{\Theta}^{(14)T} \\ & + \frac{2}{\gamma_1} \left( \sum_{i,j,k=1}^p \tilde{w}_{ijk} \tilde{\mathbf{\Theta}}_{ijk}^{(12)}(\mathbf{x}, \check{\mathbf{x}}) \right) \left( \sum_{i,j,k=1}^p \tilde{w}_{ijk} \tilde{\mathbf{\Theta}}_{ijk}^{(12)}(\mathbf{x}, \check{\mathbf{x}}) \right)^T \\ & + \frac{2}{\gamma_2} \left( \sum_{i,j,k=1}^p \tilde{w}_{ijk} \tilde{\mathbf{\Theta}}_{ik}^{(13)}(\mathbf{x}, \check{\mathbf{x}}) \right) \left( \sum_{i,j,k=1}^p \tilde{w}_{ijk} \tilde{\mathbf{\Theta}}_{ik}^{(13)}(\mathbf{x}, \check{\mathbf{x}}) \right)^T \\ & < 0, \end{aligned} \quad (5.99)$$

where  $\mathbf{\Gamma}_{ijk}(\mathbf{x}, \check{\mathbf{x}})$  and  $\mathbf{\Theta}^{(14)}$  are defined in (5.60) and (5.65).



By Schur complement, we have

$$\sum_{i,j,k=1}^p \tilde{w}_{ijk} (\Phi_{ijk}(\mathbf{x}, \check{\mathbf{x}}) + \Phi_{ikj}(\mathbf{x}, \check{\mathbf{x}})) < 0, \quad (5.100)$$

where  $\Phi_{ijk}(\mathbf{x}, \check{\mathbf{x}})$  is defined in (5.58).

Therefore,  $\dot{V}(\mathbf{z}) < 0$  if condition (5.97) holds which can be achieved by satisfying condition (5.57). Note that the conservativeness is introduced [3, 12] by using SOS conditions. The proof is completed.

#### 5.2.4 Conclusion

In this section, the polynomial fuzzy observer with unmeasurable premise variable has been designed based on the polynomial fuzzy model using refined completing square approach. To draw a distinction from existing papers [53, 60], more general settings (polynomial fuzzy model, unmeasurable premise variables), less design steps and parameters have been attained in this section. Note that simulation examples will be presented together with an optimization method in Subsection 5.4.3. In the future, the problems of applying polynomial Lyapunov function in the fuzzy observer-control system are left to be solved.

### 5.3 Combination with Sampled-Output Measurement

#### 5.3.1 Introduction

Although sampled-data polynomial fuzzy observer-controller are relatively less investigated, it is vital to the nonlinear control systems when full states are not available for performing feedback control. In this section, we consider the polynomial fuzzy observer using sampled-output measurements for state estimation. Input-delay approach [63] is employed to investigate the system stability. Compared with [70–72] with T-S fuzzy observer using sampled-output measurements, the proposed polynomial fuzzy observer has more of the general form.

This section is organized as follows. In Subsection 5.3.2, stability analysis is conducted for PFMB observer-control system under sampled-output measurements. In Subsection 5.3.3, simulation examples are provided to demonstrate the feasibility and validity of stability conditions. In Subsection 5.3.4, a conclusion is drawn.

#### 5.3.2 Stability Analysis

In Subsection 5.1.2, matrix decoupling technique is employed to obtain convex SOS-based stability conditions. In this section, using similar techniques, we extend the

stability analysis to PFMB observer-control systems with sampled-output measurement.

Considering premise variable  $f_\eta(\mathbf{x})$  depending on unmeasurable system states  $\mathbf{x}$  and output matrix  $\mathbf{C}_i$  not depending on system states  $\mathbf{x}$ , we denote sampled output  $\mathbf{y}$  as  $\mathbf{y}_s$ , where  $\mathbf{y}_s = \mathbf{y}(t_{\tilde{s}})$ ,  $t_{\tilde{s}}, \tilde{s} = 1, 2, \dots, \infty$ , is the sampling time and  $t_{\tilde{s}+1} - t_{\tilde{s}} \leq h$ . The input-delay approach [63] is employed to represent the sampling behavior. Denoting  $\tau(t) = t - t_{\tilde{s}} < h$  for  $t_{\tilde{s}} \leq t < t_{\tilde{s}+1}$ , the sampled output vector can be written as  $\mathbf{y}_s = \mathbf{y}(t - \tau(t))$ . Similarly, the sampled system state vector can be written as  $\mathbf{x}_s = \mathbf{x}(t - \tau(t))$ .

**Remark 24** *In case using sampled-output measurements, the output matrix  $\mathbf{C}_i$  does not depend on system states  $\mathbf{x}$ . If  $\mathbf{C}_i(\mathbf{x})$  is considered to be a polynomial matrix of  $\mathbf{x}$ ,  $\mathbf{C}_i(\mathbf{x}_s)$  and  $\mathbf{C}_i(\check{\mathbf{x}}_s)$  will exist in the stability analysis which is more difficult to be handled. Therefore, constant output matrix  $\mathbf{C}_i$  is considered in this section to ease the design and analysis.*

We apply the following polynomial fuzzy observer to estimate the system states in (5.1):

$$\begin{aligned}\dot{\check{\mathbf{x}}} &= \sum_{j=1}^p w_j(\check{\mathbf{x}}) \left( \mathbf{A}_j(\check{\mathbf{x}})\check{\mathbf{x}} + \mathbf{B}_j(\check{\mathbf{x}})\mathbf{u} + \mathbf{L}_j(\check{\mathbf{x}})(\mathbf{y}_s - \check{\mathbf{y}}_s) \right), \\ \mathbf{y}_s &= \sum_{i=1}^p w_i(\mathbf{x}_s) \mathbf{C}_i \mathbf{x}_s, \\ \check{\mathbf{y}}_s &= \sum_{l=1}^p w_l(\check{\mathbf{x}}_s) \mathbf{C}_l \check{\mathbf{x}}_s,\end{aligned}\tag{5.101}$$

where  $\check{\mathbf{x}}_s \in \mathbb{R}^n$  and  $\check{\mathbf{y}}_s \in \mathbb{R}^l$  are the estimated sampled system states and output, respectively.

With the PDC design approach [1, 3], the polynomial fuzzy controller is given in (5.3). Recalling that the estimation error is defined as  $\mathbf{e} = \mathbf{x} - \check{\mathbf{x}}$ , we define the sampled estimation error as  $\mathbf{e}_s = \mathbf{x}_s - \check{\mathbf{x}}_s$ , and then we have the closed-loop system (shown in Fig. 5.9) consisting of the polynomial fuzzy model (5.1), the polynomial fuzzy controller (5.3) and the polynomial fuzzy observer (5.101) as follows:

$$\begin{aligned}\dot{\mathbf{x}} &= \sum_{i=1}^p \sum_{j=1}^p w_i(\mathbf{x}) w_j(\check{\mathbf{x}}) \left( (\mathbf{A}_i(\mathbf{x}) + \mathbf{B}_i(\mathbf{x}) \mathbf{G}_j(\check{\mathbf{x}})) \check{\mathbf{x}} \right. \\ &\quad \left. + \mathbf{A}_i(\mathbf{x}) \mathbf{e} \right),\end{aligned}\tag{5.102}$$

$$\begin{aligned}\dot{\check{\mathbf{x}}} &= \sum_{i=1}^p \sum_{j=1}^p \sum_{k=1}^p \sum_{l=1}^p w_i(\mathbf{x}_s) w_j(\check{\mathbf{x}}) w_k(\check{\mathbf{x}}) w_l(\check{\mathbf{x}}_s) \left( (\mathbf{A}_j(\check{\mathbf{x}}) \right. \\ &\quad \left. + \mathbf{B}_j(\check{\mathbf{x}}) \mathbf{G}_k(\check{\mathbf{x}})) \check{\mathbf{x}} + \mathbf{L}_j(\check{\mathbf{x}}) (\mathbf{C}_i - \mathbf{C}_l) \check{\mathbf{x}}_s \right. \\ &\quad \left. + \mathbf{L}_j(\check{\mathbf{x}}) \mathbf{C}_i \mathbf{e}_s \right),\end{aligned}\tag{5.103}$$

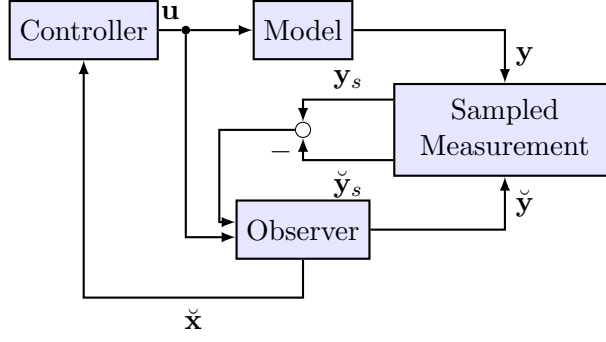


Figure 5.9: A block diagram of PFMB observer-control systems with sampled-output measurement.

$$\begin{aligned} \dot{\mathbf{e}} = & \sum_{i=1}^p \sum_{j=1}^p \sum_{k=1}^p \sum_{l=1}^p \sum_{m=1}^p w_i(\mathbf{x}_s) w_j(\check{\mathbf{x}}) w_k(\check{\mathbf{x}}) w_l(\check{\mathbf{x}}_s) w_m(\mathbf{x}) \\ & \left( (\mathbf{A}_m(\mathbf{x}) - \mathbf{A}_j(\check{\mathbf{x}}) + (\mathbf{B}_m(\mathbf{x}) - \mathbf{B}_j(\check{\mathbf{x}})) \mathbf{G}_k(\check{\mathbf{x}})) \check{\mathbf{x}} \right. \\ & \left. + \mathbf{A}_m(\mathbf{x}) \mathbf{e} - \mathbf{L}_j(\check{\mathbf{x}}) (\mathbf{C}_i - \mathbf{C}_l) \check{\mathbf{x}}_s - \mathbf{L}_j(\check{\mathbf{x}}) \mathbf{C}_i \mathbf{e}_s \right). \end{aligned} \quad (5.104)$$

The control objective is to make the augmented observer-control system ((5.103) and (5.104)) asymptotically stable, i.e.,  $\check{\mathbf{x}} \rightarrow 0$  and  $\mathbf{e} \rightarrow 0$  as time  $t \rightarrow \infty$ , by determining the polynomial controller gain  $\mathbf{G}_k(\check{\mathbf{x}})$  and polynomial observer gain  $\mathbf{L}_j(\check{\mathbf{x}})$ .

**Theorem 7** *The augmented PFMB observer-control system (formed by (5.103) and (5.104)) is guaranteed to be asymptotically stable if there exist matrices  $\mathbf{X} \in \Re^{n \times n}$ ,  $\mathbf{Y} \in \Re^{n \times n}$ ,  $\tilde{\mathbf{Q}} \in \Re^{2n \times 2n}$ ,  $\mathbf{N}_k(\check{\mathbf{x}}) \in \Re^{m \times n}$ ,  $\mathbf{M}_j(\check{\mathbf{x}}) \in \Re^{n \times l}$ ,  $k = 1, 2, \dots, p$ ,  $j = 1, 2, \dots, p$ , and predefined scalars  $\alpha_1 > 0$ ,  $\alpha_2 > 0$ ,  $\alpha_3 > 0$ ,  $\alpha_4 > 0$ ,  $\beta > 0$  and  $\gamma$  such that the following SOS-based conditions are satisfied:*

$$\nu^T (\mathbf{X} - \varepsilon_1 \mathbf{I}) \nu \text{ is SOS}; \quad (5.105)$$

$$\nu^T (\mathbf{Y} - \varepsilon_2 \mathbf{I}) \nu \text{ is SOS}; \quad (5.106)$$

$$\nu^T (\tilde{\mathbf{Q}} - \varepsilon_3 \mathbf{I}) \nu \text{ is SOS}; \quad (5.107)$$

$$\begin{aligned} & - \nu^T (\Phi_{jkm}(\mathbf{x}, \check{\mathbf{x}}) + \Phi_{kjm}(\mathbf{x}, \check{\mathbf{x}}) + \varepsilon_4(\mathbf{x}, \check{\mathbf{x}}) \mathbf{I}) \nu \text{ is SOS} \\ & \forall m, j \leq k; \end{aligned} \quad (5.108)$$

$$- \nu^T (\Theta_{ijlm}(\mathbf{x}, \check{\mathbf{x}}) + \varepsilon_5(\mathbf{x}, \check{\mathbf{x}}) \mathbf{I}) \nu \text{ is SOS } \forall i, j, l, m; \quad (5.109)$$

where

$$\begin{aligned} \Phi_{jkm}(\mathbf{x}, \check{\mathbf{x}}) = & \begin{bmatrix} \tilde{\Gamma}_{jkm}(\mathbf{x}, \check{\mathbf{x}}) & \tilde{\Phi}^{(12)} & \Phi^{(13)} \\ * & -\frac{1}{\beta} \mathbf{I} & \mathbf{0} \\ * & * & -\frac{1}{\alpha_2} \mathbf{Y} \end{bmatrix}, \\ \Theta_{ijlm}(\mathbf{x}, \check{\mathbf{x}}) = & \end{aligned} \quad (5.110)$$

$$\begin{bmatrix} \tilde{\Lambda}_{ijm}(\mathbf{x}, \check{\mathbf{x}}) & \Theta^{(12)} & \Theta^{(13)} & \Theta^{(14)} & \tilde{\Theta}_{ijl}^{(15)}(\check{\mathbf{x}}) \\ * & -\frac{1}{\alpha_1}\mathbf{I} & \mathbf{0} & \mathbf{0} & \mathbf{0} \\ * & * & -\frac{1}{\alpha_4}\mathbf{I} & \mathbf{0} & \mathbf{0} \\ * & * & * & -\frac{1}{\alpha_3}\mathbf{I} & \mathbf{0} \\ * & * & * & * & -\beta\mathbf{I} \end{bmatrix}, \quad (5.111)$$

$$\tilde{\Gamma}_{jkm}(\mathbf{x}, \check{\mathbf{x}}) = \begin{bmatrix} \Gamma_{jkm}^{(11)}(\mathbf{x}, \check{\mathbf{x}}) & \mathbf{0} & \Gamma_{jkm}^{(14)}(\mathbf{x}, \check{\mathbf{x}}) \\ * & -\alpha_4\mathbf{I} & \mathbf{0} \\ * & * & \tilde{\Gamma}^{(44)} \end{bmatrix}, \quad (5.112)$$

$$\tilde{\Phi}^{(12)} = [\mathbf{0}_{N \times 2N} \quad \mathbf{X} \quad \mathbf{0}_{N \times 2N}]^T, \quad (5.113)$$

$$\Phi^{(13)} = [\mathbf{0}_{N \times 3N} \quad \mathbf{I} \quad \mathbf{0}_{N \times N}]^T, \quad (5.114)$$

$$\begin{aligned} \tilde{\Lambda}_{ijm}(\mathbf{x}, \check{\mathbf{x}}) = & \\ & \begin{bmatrix} \tilde{\Lambda}_m^{(11)}(\mathbf{x}) - \tilde{\mathbf{Q}} & \tilde{\Lambda}_{ij}^{(12)}(\check{\mathbf{x}}) + \tilde{\mathbf{Q}} & \mathbf{0} & \tilde{\Lambda}_m^{(14)}(\mathbf{x}) \\ * & -2\tilde{\mathbf{Q}} & \tilde{\mathbf{Q}} & \tilde{\Lambda}_{ij}^{(24)}(\check{\mathbf{x}}) \\ * & * & -\tilde{\mathbf{Q}} & \mathbf{0} \\ * & * & * & \gamma^2\tilde{\mathbf{Q}} + \tilde{\Lambda}^{(44)} \end{bmatrix}, \end{aligned} \quad (5.115)$$

$$\Theta^{(12)} = [\mathbf{0}_{N \times N} \quad \mathbf{Y} \quad \mathbf{0}_{N \times 6N}]^T, \quad (5.116)$$

$$\Theta^{(13)} = [\mathbf{0}_{N \times 2N} \quad \mathbf{Y} \quad \mathbf{0}_{N \times 5N}]^T, \quad (5.117)$$

$$\Theta^{(14)} = [\mathbf{0}_{N \times 7N} \quad \mathbf{Y}]^T, \quad (5.118)$$

$$\begin{aligned} \tilde{\Theta}_{ijl}^{(15)}(\check{\mathbf{x}}) = & [\tilde{\mathbf{H}}_{ijl}(\check{\mathbf{x}})^T \quad -\tilde{\mathbf{H}}_{ijl}(\check{\mathbf{x}})^T \quad \mathbf{0}_{N \times 4N} \\ & h\tilde{\mathbf{H}}_{ijl}(\check{\mathbf{x}})^T \quad -h\tilde{\mathbf{H}}_{ijl}(\check{\mathbf{x}})^T]^T, \end{aligned} \quad (5.119)$$

$$\Gamma_{jkm}^{(11)}(\mathbf{x}, \check{\mathbf{x}}) = \begin{bmatrix} \hat{\Xi}_{jk}^{(11)}(\check{\mathbf{x}}) + \hat{\Xi}_{jk}^{(11)}(\check{\mathbf{x}})^T & \hat{\Xi}_{jkm}^{(21)}(\mathbf{x}, \check{\mathbf{x}})^T \\ * & -\alpha_1\mathbf{I} \end{bmatrix}, \quad (5.120)$$

$$\Gamma_{jkm}^{(14)}(\mathbf{x}, \check{\mathbf{x}}) = \begin{bmatrix} h\hat{\Xi}_{jk}^{(11)}(\check{\mathbf{x}})^T & h\hat{\Xi}_{jkm}^{(21)}(\mathbf{x}, \check{\mathbf{x}})^T \\ \mathbf{0} & \mathbf{0} \end{bmatrix}, \quad (5.121)$$

$$\tilde{\Gamma}^{(44)} = \begin{bmatrix} -2\gamma\mathbf{X} & \mathbf{0} \\ \mathbf{0} & -\alpha_3\mathbf{I} \end{bmatrix}, \quad (5.122)$$

$$\tilde{\Lambda}_m^{(11)}(\mathbf{x}) = \begin{bmatrix} \mathbf{0} & \mathbf{0} \\ \mathbf{0} & \tilde{\Xi}_m^{(22)}(\mathbf{x}) + \tilde{\Xi}_m^{(22)}(\mathbf{x})^T \end{bmatrix}, \quad (5.123)$$

$$\tilde{\Lambda}_{ij}^{(12)}(\check{\mathbf{x}}) = \begin{bmatrix} \mathbf{0} & \tilde{\mathbf{K}}_{ij}(\check{\mathbf{x}}) \\ \mathbf{0} & -\tilde{\mathbf{K}}_{ij}(\check{\mathbf{x}}) \end{bmatrix}, \quad (5.124)$$

$$\tilde{\Lambda}_m^{(14)}(\mathbf{x}) = \begin{bmatrix} \mathbf{0} & \mathbf{0} \\ \mathbf{0} & h\tilde{\Xi}_m^{(22)}(\mathbf{x})^T \end{bmatrix}, \quad (5.125)$$

$$\tilde{\Lambda}_{ij}^{(24)}(\check{\mathbf{x}}) = \begin{bmatrix} \mathbf{0} & \mathbf{0} \\ h\tilde{\mathbf{K}}_{ij}(\check{\mathbf{x}})^T & -h\tilde{\mathbf{K}}_{ij}(\check{\mathbf{x}})^T \end{bmatrix}, \quad (5.126)$$

$$\tilde{\Lambda}^{(44)} = \begin{bmatrix} -\alpha_2\mathbf{Y} & \mathbf{0} \\ \mathbf{0} & -2\gamma\mathbf{Y} \end{bmatrix}, \quad (5.127)$$

$$\hat{\Xi}_{jk}^{(11)}(\check{\mathbf{x}}) = \mathbf{A}_j(\check{\mathbf{x}})\mathbf{X} + \mathbf{B}_j(\check{\mathbf{x}})\mathbf{N}_k(\check{\mathbf{x}}), \quad (5.128)$$

$$\begin{aligned}\hat{\Xi}_{jkm}^{(21)}(\mathbf{x}, \check{\mathbf{x}}) &= (\mathbf{A}_m(\mathbf{x}) - \mathbf{A}_j(\check{\mathbf{x}}))\mathbf{X} \\ &\quad + (\mathbf{B}_m(\mathbf{x}) - \mathbf{B}_j(\check{\mathbf{x}}))\mathbf{N}_k(\check{\mathbf{x}}),\end{aligned}\quad (5.129)$$

$$\tilde{\Xi}_m^{(22)}(\mathbf{x}) = \mathbf{Y}\mathbf{A}_m(\mathbf{x}), \quad (5.130)$$

$$\tilde{\mathbf{K}}_{ij}(\check{\mathbf{x}}) = \mathbf{M}_j(\check{\mathbf{x}})\mathbf{C}_i, \quad (5.131)$$

$$\tilde{\mathbf{H}}_{ijl}(\check{\mathbf{x}}) = \mathbf{M}_j(\check{\mathbf{x}})(\mathbf{C}_i - \mathbf{C}_l); \quad (5.132)$$

$\nu$  is an arbitrary vector independent of  $\mathbf{x}$  with appropriate dimensions;  $\varepsilon_1 > 0, \varepsilon_2 > 0, \varepsilon_3 > 0, \varepsilon_4(\mathbf{x}, \check{\mathbf{x}}) > 0$  and  $\varepsilon_5(\mathbf{x}, \check{\mathbf{x}}) > 0$  are predefined scalar polynomials; and the polynomial controller and polynomial observer gains are given by  $\mathbf{G}_k(\check{\mathbf{x}}) = \mathbf{N}_k(\check{\mathbf{x}})\mathbf{X}^{-1}$  and  $\mathbf{L}_j(\check{\mathbf{x}}) = \mathbf{Y}^{-1}\mathbf{M}_j(\check{\mathbf{x}})$ , respectively.

**Proof** Defining the augmented vectors  $\mathbf{z} = [\check{\mathbf{x}}^T \quad \mathbf{e}^T]^T, \mathbf{z}_s = [\check{\mathbf{x}}_s^T \quad \mathbf{e}_s^T]^T$ , and the summation term  $\sum_{i,j,k,l,m=1}^p \tilde{w}_{ijklm} = \sum_{i=1}^p \sum_{j=1}^p \sum_{k=1}^p \sum_{l=1}^p \sum_{m=1}^p w_i(\mathbf{x}_s)w_j(\check{\mathbf{x}})w_k(\check{\mathbf{x}})w_l(\check{\mathbf{x}}_s)w_m(\mathbf{x})$ , the augmented system becomes

$$\dot{\mathbf{z}} = \sum_{i,j,k,l,m=1}^p \tilde{w}_{ijklm} (\hat{\mathbf{A}}_{jkm}(\mathbf{x}, \check{\mathbf{x}})\mathbf{z} + \hat{\mathbf{B}}_{ijl}(\check{\mathbf{x}})\mathbf{z}_s), \quad (5.133)$$

where

$$\hat{\mathbf{A}}_{jkm}(\mathbf{x}, \check{\mathbf{x}}) = \begin{bmatrix} \Xi_{jk}^{(11)}(\check{\mathbf{x}}) & \mathbf{0} \\ \Xi_{jkm}^{(21)}(\mathbf{x}, \check{\mathbf{x}}) & \Xi_m^{(22)}(\mathbf{x}) \end{bmatrix}, \quad (5.134)$$

$$\hat{\mathbf{B}}_{ijl}(\check{\mathbf{x}}) = \begin{bmatrix} \mathbf{H}_{ijl}(\check{\mathbf{x}}) & \mathbf{K}_{ij}(\check{\mathbf{x}}) \\ -\mathbf{H}_{ijl}(\check{\mathbf{x}}) & -\mathbf{K}_{ij}(\check{\mathbf{x}}) \end{bmatrix}, \quad (5.135)$$

$$\Xi_{jk}^{(11)}(\check{\mathbf{x}}) = \mathbf{A}_j(\check{\mathbf{x}}) + \mathbf{B}_j(\check{\mathbf{x}})\mathbf{G}_k(\check{\mathbf{x}}), \quad (5.136)$$

$$\Xi_{jkm}^{(21)}(\mathbf{x}, \check{\mathbf{x}}) = \mathbf{A}_m(\mathbf{x}) - \mathbf{A}_j(\check{\mathbf{x}}) + (\mathbf{B}_m(\mathbf{x}) - \mathbf{B}_j(\check{\mathbf{x}}))\mathbf{G}_k(\check{\mathbf{x}}), \quad (5.137)$$

$$\Xi_m^{(22)}(\mathbf{x}) = \mathbf{A}_m(\mathbf{x}), \quad (5.138)$$

$$\mathbf{K}_{ij}(\check{\mathbf{x}}) = \mathbf{L}_j(\check{\mathbf{x}})\mathbf{C}_i, \quad (5.139)$$

$$\mathbf{H}_{ijl}(\check{\mathbf{x}}) = \mathbf{L}_j(\check{\mathbf{x}})(\mathbf{C}_i - \mathbf{C}_l). \quad (5.140)$$

The procedure of the proof is shown in Fig. 5.10. As can be seen, the matrix decoupling technique will separate the conditions into two parts and convex conditions will be obtained for both parts.

The following Lyapunov function candidate is employed to investigate the stability of the augmented PFMB observer-control system with sampled-output measurements (5.133):

$$V(\mathbf{z}) = \mathbf{z}^T \mathbf{P} \mathbf{z} + h \int_{-h}^0 \int_{t+\sigma}^t \dot{\mathbf{z}}(\varphi)^T \mathbf{Q} \dot{\mathbf{z}}(\varphi) d\varphi d\sigma, \quad (5.141)$$

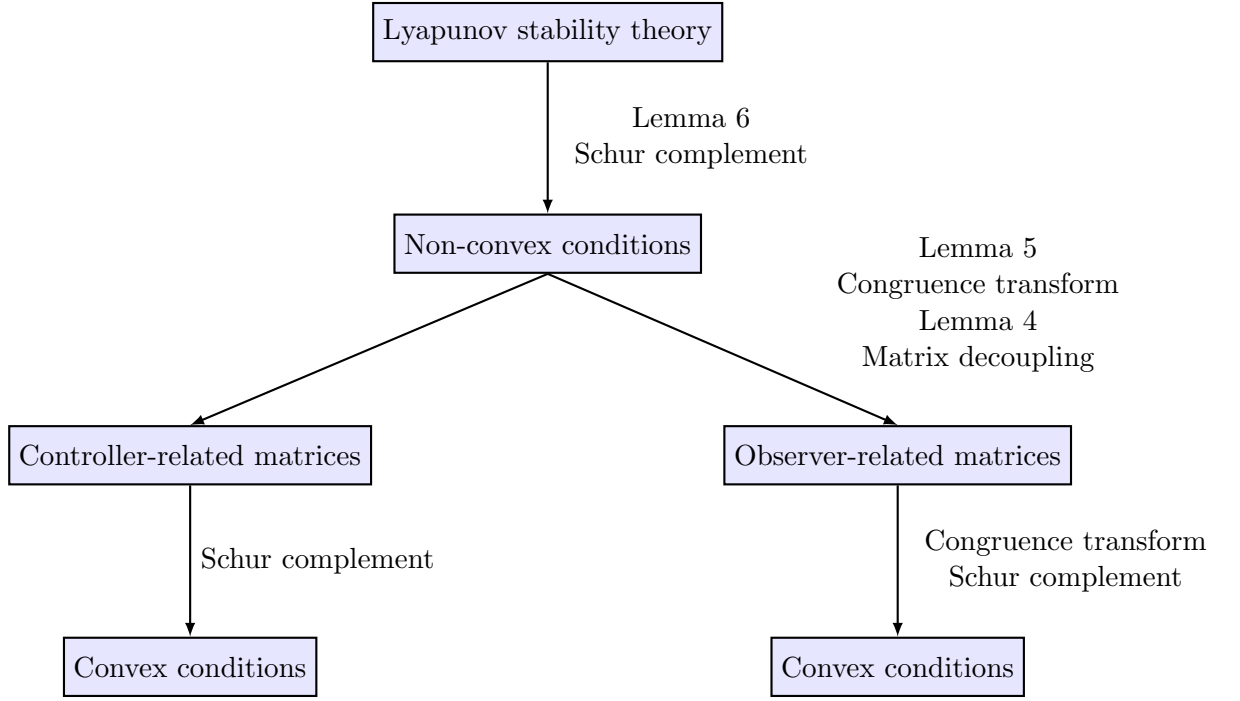


Figure 5.10: Procedure of the proof for Theorem 7.

where  $\mathbf{Q} > 0$ ,  $\mathbf{P} = \begin{bmatrix} \mathbf{X}^{-1} & \mathbf{0} \\ \mathbf{0} & \mathbf{Y} \end{bmatrix}$ ,  $\mathbf{X} > 0$ ,  $\mathbf{Y} > 0$ , and thus  $\mathbf{P} > 0$ . The time derivative of  $V(\mathbf{z})$  is obtained as follows:

$$\dot{V}(\mathbf{z}) = \dot{\mathbf{z}}^T \mathbf{P} \mathbf{z} + \mathbf{z}^T \mathbf{P} \dot{\mathbf{z}} + h^2 \dot{\mathbf{z}}^T \mathbf{Q} \dot{\mathbf{z}} - h \int_{t-h}^t \dot{\mathbf{z}}(\varphi)^T \mathbf{Q} \dot{\mathbf{z}}(\varphi) d\varphi. \quad (5.142)$$

Denoting augmented vectors  $\mathbf{z}_h = [\check{\mathbf{x}}(t-h)^T \quad \mathbf{e}(t-h)^T]^T$ ,  $\mathbf{Z} = [\mathbf{z}^T \quad \mathbf{z}_s^T \quad \mathbf{z}_h^T]^T$ , and using Lemma 6, we obtain

$$\begin{aligned} & -h \int_{t-h}^t \dot{\mathbf{z}}(\varphi)^T \mathbf{Q} \dot{\mathbf{z}}(\varphi) d\varphi \\ & \leq -(\mathbf{z} - \mathbf{z}_s)^T \mathbf{Q} (\mathbf{z} - \mathbf{z}_s) - (\mathbf{z}_s - \mathbf{z}_h)^T \mathbf{Q} (\mathbf{z}_s - \mathbf{z}_h). \end{aligned} \quad (5.143)$$

Then  $\dot{V}(\mathbf{z})$  becomes

$$\begin{aligned} \dot{V}(\mathbf{z}) & \leq \mathbf{Z}^T \left( \sum_{i,j,k,l,m=1}^p \tilde{w}_{ijklm} \Upsilon_{ijklm}^{(11)}(\mathbf{x}, \check{\mathbf{x}}) \right. \\ & \quad + \left( \sum_{i,j,k,l,m=1}^p \tilde{w}_{ijklm} \Upsilon_{ijklm}^{(12)}(\mathbf{x}, \check{\mathbf{x}}) \right) \mathbf{P}^{-1} \mathbf{Q} \mathbf{P}^{-1} \\ & \quad \times \left. \left( \sum_{i,j,k,l,m=1}^p \tilde{w}_{ijklm} \Upsilon_{ijklm}^{(12)}(\mathbf{x}, \check{\mathbf{x}}) \right)^T \right) \mathbf{Z}, \end{aligned} \quad (5.144)$$

where

$$\Upsilon_{ijklm}^{(11)}(\mathbf{x}, \check{\mathbf{x}}) = \begin{bmatrix} \Omega(\mathbf{x}, \check{\mathbf{x}}) & \mathbf{P}\hat{\mathbf{B}}_{ijl}(\mathbf{x}, \check{\mathbf{x}}) + \mathbf{Q} & \mathbf{0} \\ * & -2\mathbf{Q} & \mathbf{Q} \\ * & * & -\mathbf{Q} \end{bmatrix}, \quad (5.145)$$

$$\Omega(\mathbf{x}, \check{\mathbf{x}}) = \mathbf{P}\hat{\mathbf{A}}_{jkm}(\mathbf{x}, \check{\mathbf{x}}) + \hat{\mathbf{A}}_{jkm}(\mathbf{x}, \check{\mathbf{x}})^T \mathbf{P} - \mathbf{Q}, \quad (5.146)$$

$$\Upsilon_{ijklm}^{(12)}(\mathbf{x}, \check{\mathbf{x}}) = [h\mathbf{P}\hat{\mathbf{A}}_{jkm}(\mathbf{x}, \check{\mathbf{x}}) \quad h\mathbf{P}\hat{\mathbf{B}}_{ijl}(\mathbf{x}, \check{\mathbf{x}}) \quad \mathbf{0}]^T. \quad (5.147)$$

Using Schur complement,  $\dot{V}(\mathbf{z}) < 0$  holds if

$$\sum_{i,j,k,l,m=1}^p \tilde{w}_{ijklm} \Upsilon_{ijklm}(\mathbf{x}, \check{\mathbf{x}}) < 0, \quad (5.148)$$

where

$$\Upsilon_{ijklm}(\mathbf{x}, \check{\mathbf{x}}) = \begin{bmatrix} \Upsilon_{ijklm}^{(11)}(\mathbf{x}, \check{\mathbf{x}}) & \Upsilon_{ijklm}^{(12)}(\mathbf{x}, \check{\mathbf{x}}) \\ * & -\mathbf{P}\mathbf{Q}^{-1}\mathbf{P} \end{bmatrix}. \quad (5.149)$$

Applying Lemma 5 to the term  $-\mathbf{P}\mathbf{Q}^{-1}\mathbf{P}$  and then performing congruence transformation to (5.148) by pre-multiplying and post-multiplying  $\text{diag}\{\mathbf{P}^{-1}, \mathbf{P}^{-1}, \mathbf{P}^{-1}, \mathbf{P}^{-1}\}$ , we have

$$\sum_{i,j,k,l,m=1}^p \tilde{w}_{ijklm} \hat{\Upsilon}_{ijklm}(\mathbf{x}, \check{\mathbf{x}}) < 0, \quad (5.150)$$

where

$$\hat{\Upsilon}_{ijklm}(\mathbf{x}, \check{\mathbf{x}}) = \begin{bmatrix} \hat{\Upsilon}_{jkm}^{(11)}(\mathbf{x}, \check{\mathbf{x}}) - \hat{\mathbf{Q}} & \hat{\Upsilon}_{ijl}^{(12)}(\check{\mathbf{x}}) + \hat{\mathbf{Q}} & \mathbf{0} & \hat{\Upsilon}_{jkm}^{(14)}(\mathbf{x}, \check{\mathbf{x}}) \\ * & -2\hat{\mathbf{Q}} & \hat{\mathbf{Q}} & \hat{\Upsilon}_{ijl}^{(24)}(\check{\mathbf{x}}) \\ * & * & -\tilde{\mathbf{Q}} & \mathbf{0} \\ * & * & * & \gamma^2 \hat{\mathbf{Q}} + \hat{\Upsilon}^{(44)} \end{bmatrix}, \quad (5.151)$$

$$\hat{\Upsilon}_{jkm}^{(11)}(\mathbf{x}, \check{\mathbf{x}}) = \begin{bmatrix} \hat{\Xi}_{jk}^{(11)}(\check{\mathbf{x}}) + \hat{\Xi}_{jk}^{(11)}(\check{\mathbf{x}})^T & \hat{\Xi}_{jkm}^{(21)}(\mathbf{x}, \check{\mathbf{x}})^T \\ * & \hat{\Xi}_m^{(22)}(\mathbf{x}) + \hat{\Xi}_m^{(22)}(\mathbf{x})^T \end{bmatrix}, \quad (5.152)$$

$$\hat{\Upsilon}_{ijl}^{(12)}(\check{\mathbf{x}}) = \begin{bmatrix} \mathbf{H}_{ijl}(\check{\mathbf{x}})\mathbf{X} & \hat{\mathbf{K}}_{ij}(\check{\mathbf{x}}) \\ -\mathbf{H}_{ijl}(\check{\mathbf{x}})\mathbf{X} & -\hat{\mathbf{K}}_{ij}(\check{\mathbf{x}}) \end{bmatrix}, \quad (5.153)$$

$$\hat{\Upsilon}_{jkm}^{(14)}(\mathbf{x}, \check{\mathbf{x}}) = \begin{bmatrix} h\hat{\Xi}_{jk}^{(11)}(\check{\mathbf{x}})^T & h\hat{\Xi}_{jkm}^{(21)}(\mathbf{x}, \check{\mathbf{x}})^T \\ \mathbf{0} & h\hat{\Xi}_m^{(22)}(\mathbf{x})^T \end{bmatrix}, \quad (5.154)$$

$$\hat{\Upsilon}_{ijl}^{(24)}(\check{\mathbf{x}}) = \begin{bmatrix} h\mathbf{X}\mathbf{H}_{ijl}(\check{\mathbf{x}})^T & -h\mathbf{X}\mathbf{H}_{ijl}(\check{\mathbf{x}})^T \\ h\hat{\mathbf{K}}_{ij}(\check{\mathbf{x}})^T & -h\hat{\mathbf{K}}_{ij}(\check{\mathbf{x}})^T \end{bmatrix}, \quad (5.155)$$

$$\hat{\mathbf{Y}}^{(44)} = \begin{bmatrix} -2\gamma\mathbf{X} & \mathbf{0} \\ \mathbf{0} & -2\gamma\mathbf{Y}^{-1} \end{bmatrix}, \quad (5.156)$$

$$\hat{\Xi}_m^{(22)}(\mathbf{x}) = \mathbf{A}_m(\mathbf{x})\mathbf{Y}^{-1}, \quad (5.157)$$

$$\hat{\mathbf{K}}_{ij}(\check{\mathbf{x}}) = \mathbf{L}_j(\check{\mathbf{x}})\mathbf{C}_i\mathbf{Y}^{-1}, \quad (5.158)$$

$$\hat{\mathbf{Q}} = \mathbf{P}^{-1}\mathbf{Q}\mathbf{P}^{-1}, \quad (5.159)$$

$\hat{\Xi}_{jk}^{(11)}(\check{\mathbf{x}})$  and  $\hat{\Xi}_{jkm}^{(21)}(\mathbf{x}, \check{\mathbf{x}})$  are defined in (5.128) and (5.129), respectively.

Similar to the development in Subsection 5.1.2, applying Lemma 4 and matrix decoupling technique [54] to further separate decision variables, we get

$$\begin{aligned} & \sum_{i,j,k,l,m=1}^p \tilde{w}_{ijklm} \hat{\mathbf{Y}}_{ijklm}(\mathbf{x}, \check{\mathbf{x}}) \\ & \leq \sum_{i,j,k,l,m=1}^p \tilde{w}_{ijklm} \left( \mathbf{\Gamma}_{jkm}(\mathbf{x}, \check{\mathbf{x}}) + \mathbf{\Lambda}_{ijm}(\mathbf{x}, \check{\mathbf{x}}) \right. \\ & \quad \left. + \beta \mathbf{\Phi}^{(12)}(\mathbf{\Phi}^{(12)})^T \right) + \frac{1}{\beta} \left( \sum_{i,j,k,l,m=1}^p \tilde{w}_{ijklm} \mathbf{\Theta}_{ijl}^{(15)}(\check{\mathbf{x}}) \right) \\ & \quad \times \left( \sum_{i,j,k,l,m=1}^p \tilde{w}_{ijklm} \mathbf{\Theta}_{ijl}^{(15)}(\check{\mathbf{x}}) \right)^T, \end{aligned} \quad (5.160)$$

where

$$\mathbf{\Phi}^{(12)} = [\mathbf{0}_{N \times 2N} \quad \mathbf{X} \quad \mathbf{0}_{N \times 5N}]^T, \quad (5.161)$$

$$\begin{aligned} \mathbf{\Theta}_{ijl}^{(15)}(\check{\mathbf{x}}) = & [\mathbf{H}_{ijl}(\check{\mathbf{x}})^T \quad -\mathbf{H}_{ijl}(\check{\mathbf{x}})^T \quad \mathbf{0}_{N \times 4N} \\ & h\mathbf{H}_{ijl}(\check{\mathbf{x}})^T \quad -h\mathbf{H}_{ijl}(\check{\mathbf{x}})^T]^T, \end{aligned} \quad (5.162)$$

$$\mathbf{\Gamma}_{jkm}(\mathbf{x}, \check{\mathbf{x}}) = \begin{bmatrix} \mathbf{\Gamma}_{jkm}^{(11)}(\mathbf{x}, \check{\mathbf{x}}) & \mathbf{0} & \mathbf{0} & \mathbf{\Gamma}_{jkm}^{(14)}(\mathbf{x}, \check{\mathbf{x}}) \\ * & \mathbf{\Gamma}^{(22)} & \mathbf{0} & \mathbf{0} \\ * & * & \mathbf{0} & \mathbf{0} \\ * & * & * & \mathbf{\Gamma}^{(44)} \end{bmatrix}, \quad (5.163)$$

$$\mathbf{\Gamma}^{(22)} = \begin{bmatrix} -\alpha_4\mathbf{I} & \mathbf{0} \\ \mathbf{0} & \mathbf{0} \end{bmatrix}, \quad (5.164)$$

$$\mathbf{\Gamma}^{(44)} = \begin{bmatrix} -2\gamma\mathbf{X} + \alpha_2\mathbf{Y}^{-1} & \mathbf{0} \\ \mathbf{0} & -\alpha_3\mathbf{I} \end{bmatrix}, \quad (5.165)$$

$$\begin{aligned} \mathbf{\Lambda}_{ijm}(\mathbf{x}, \check{\mathbf{x}}) = & \begin{bmatrix} \mathbf{\Lambda}_m^{(11)}(\mathbf{x}) - \hat{\mathbf{Q}} & \mathbf{\Lambda}_{ij}^{(12)}(\check{\mathbf{x}}) + \hat{\mathbf{Q}} & \mathbf{0} & \mathbf{\Lambda}_m^{(14)}(\mathbf{x}) \\ * & \mathbf{\Lambda}^{(22)} - 2\hat{\mathbf{Q}} & \hat{\mathbf{Q}} & \mathbf{\Lambda}_{ij}^{(24)}(\check{\mathbf{x}}) \\ * & * & -\hat{\mathbf{Q}} & \mathbf{0} \\ * & * & * & \gamma^2\hat{\mathbf{Q}} + \mathbf{\Lambda}^{(44)} \end{bmatrix}, \end{aligned} \quad (5.166)$$



$$\mathbf{\Lambda}_m^{(11)}(\mathbf{x}) = \begin{bmatrix} \mathbf{0} & \mathbf{0} \\ \mathbf{0} & \hat{\Xi}_m^{(22)}(\mathbf{x}) + \hat{\Xi}_m^{(22)}(\mathbf{x})^T + \alpha_1 \mathbf{I} \end{bmatrix}, \quad (5.167)$$

$$\mathbf{\Lambda}_{ij}^{(12)}(\check{\mathbf{x}}) = \begin{bmatrix} \mathbf{0} & \hat{\mathbf{K}}_{ij}(\check{\mathbf{x}}) \\ \mathbf{0} & -\hat{\mathbf{K}}_{ij}(\check{\mathbf{x}}) \end{bmatrix}, \quad (5.168)$$

$$\mathbf{\Lambda}_m^{(14)}(\mathbf{x}) = \begin{bmatrix} \mathbf{0} & \mathbf{0} \\ \mathbf{0} & h\hat{\Xi}_m^{(22)}(\mathbf{x})^T \end{bmatrix}, \quad (5.169)$$

$$\mathbf{\Lambda}^{(22)} = \begin{bmatrix} \alpha_4 \mathbf{I} & \mathbf{0} \\ \mathbf{0} & \mathbf{0} \end{bmatrix}, \quad (5.170)$$

$$\mathbf{\Lambda}_{ij}^{(24)}(\check{\mathbf{x}}) = \begin{bmatrix} \mathbf{0} & \mathbf{0} \\ h\hat{\mathbf{K}}_{ij}(\check{\mathbf{x}})^T & -h\hat{\mathbf{K}}_{ij}(\check{\mathbf{x}})^T \end{bmatrix}, \quad (5.171)$$

$$\mathbf{\Lambda}^{(44)} = \begin{bmatrix} -\alpha_2 \mathbf{Y}^{-1} & \mathbf{0} \\ \mathbf{0} & -2\gamma \mathbf{Y}^{-1} + \alpha_3 \mathbf{I} \end{bmatrix}, \quad (5.172)$$

$\mathbf{\Gamma}_{jkm}^{(11)}(\mathbf{x}, \check{\mathbf{x}})$ ,  $\mathbf{\Gamma}_{jkm}^{(14)}(\mathbf{x}, \check{\mathbf{x}})$  are defined in (5.120) and (5.121), respectively.

Denoting the summation terms  $\sum_{j,k,m=1}^p \tilde{w}_{jkm} = \sum_{j=1}^p \sum_{k=1}^p \sum_{m=1}^p w_j(\check{\mathbf{x}})w_k(\check{\mathbf{x}})w_m(\mathbf{x})$  and  $\sum_{i,j,l,m=1}^p \tilde{w}_{ijlm} = \sum_{i=1}^p \sum_{j=1}^p \sum_{l=1}^p \sum_{m=1}^p w_i(\mathbf{x}_s)w_j(\check{\mathbf{x}})w_l(\check{\mathbf{x}}_s)w_m(\mathbf{x})$ , then  $\dot{V}(\mathbf{z}) < 0$  holds if

$$\sum_{j,k,m=1}^p \tilde{w}_{jkm} \left( \mathbf{\Gamma}_{jkm}(\mathbf{x}, \check{\mathbf{x}}) + \beta \mathbf{\Phi}^{(12)}(\mathbf{\Phi}^{(12)})^T \right) < 0, \quad (5.173)$$

$$\begin{aligned} & \sum_{i,j,l,m=1}^p \tilde{w}_{ijlm} \mathbf{\Lambda}_{ijlm}(\mathbf{x}, \check{\mathbf{x}}) + \frac{1}{\beta} \left( \sum_{i,j,l,m=1}^p \tilde{w}_{ijlm} \mathbf{\Theta}_{ijl}^{(15)}(\check{\mathbf{x}}) \right) \\ & \times \left( \sum_{i,j,l,m=1}^p \tilde{w}_{ijlm} \mathbf{\Theta}_{ijl}^{(15)}(\check{\mathbf{x}}) \right)^T < 0. \end{aligned} \quad (5.174)$$

Performing congruence transformation to (5.174) by pre-multiplying and post-multiplying  $\text{diag}\{\mathbf{Y}, \mathbf{Y}, \mathbf{Y}, \mathbf{Y}, \mathbf{Y}, \mathbf{Y}, \mathbf{Y}, \mathbf{Y}\}$  to both sides and applying Schur complement to both (5.173) and (5.174), we obtain

$$\sum_{j,k,m=1}^p \tilde{w}_{jkm} \mathbf{\Phi}_{jkm}(\mathbf{x}, \check{\mathbf{x}}) < 0, \quad (5.175)$$

$$\sum_{i,j,l,m=1}^p \tilde{w}_{ijlm} \mathbf{\Theta}_{ijlm}(\mathbf{x}, \check{\mathbf{x}}) < 0, \quad (5.176)$$

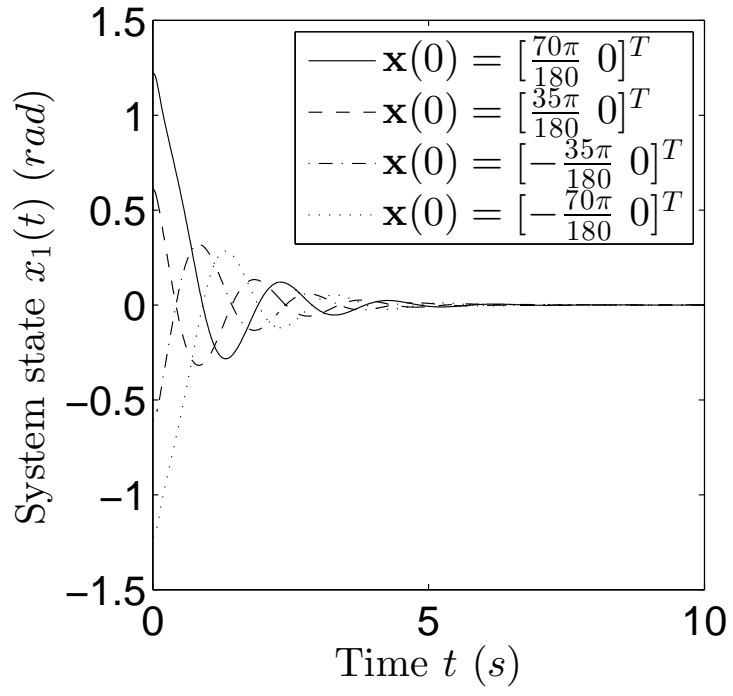
where  $\tilde{\mathbf{Q}} = \begin{bmatrix} \mathbf{Y} & \mathbf{0} \\ \mathbf{0} & \mathbf{Y} \end{bmatrix} \hat{\mathbf{Q}} \begin{bmatrix} \mathbf{Y} & \mathbf{0} \\ \mathbf{0} & \mathbf{Y} \end{bmatrix}$ ,  $\mathbf{\Phi}_{jkm}(\mathbf{x}, \check{\mathbf{x}})$  and  $\mathbf{\Theta}_{ijlm}(\mathbf{x}, \check{\mathbf{x}})$  are defined in (5.110) and (5.111), respectively. By grouping terms with same membership functions,  $\dot{V}(\mathbf{z}) < 0$  if conditions (5.108) and (5.109) hold. The proof is completed.

### 5.3.3 Simulation Examples

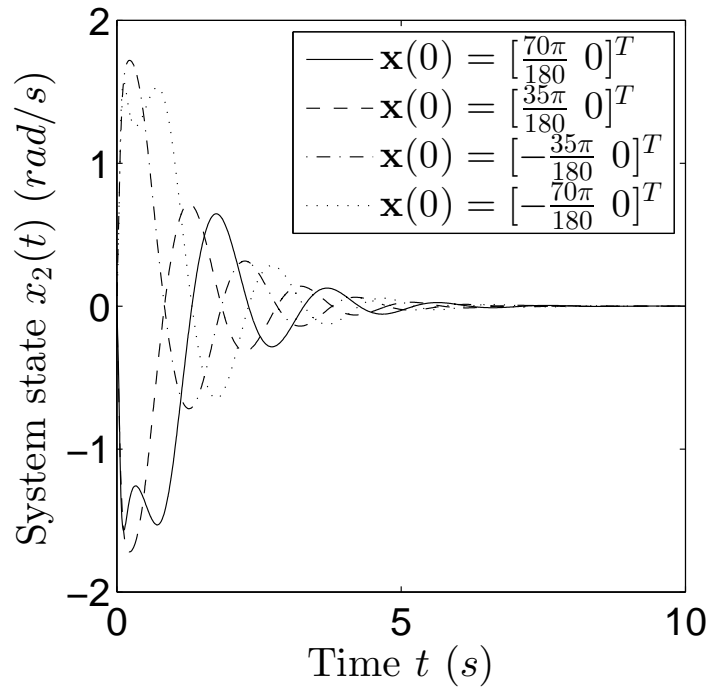
In this example, we consider the same inverted pendulum on a cart as in (4.71). In addition, sampled-output measurements are employed for the design of PFMB observer-controller where the sampling interval is chosen to be  $h = 0.05$  seconds. The output is assumed to be a function of system states:  $y = -0.161f_1(x_1) + 1.1841$ . Consequently, the output matrices are  $\mathbf{C}_1 = [1.1 \ 0]$  and  $\mathbf{C}_2 = [0.9 \ 0]$ . Other settings such as the fuzzy modeling are the same as Example 5.1.3.1.

Theorem 7 is employed for the design of PFMB observer-controller. We choose  $\alpha_1 = 1 \times 10^6, \alpha_2 = 1 \times 10^5, \alpha_3 = 1 \times 10^3, \alpha_4 = 1 \times 10^3, \beta = 1 \times 10^{-2}, \gamma = 1 \times 10^{-1}$ ,  $\mathbf{N}_k(\check{x}_2)$  of degree 0 and 2,  $\mathbf{M}_j(\check{x}_2)$  of degree 0 and 2,  $\varepsilon_1 = \varepsilon_2 = \varepsilon_3 = 1 \times 10^{-3}$ , and  $\varepsilon_4 = \varepsilon_5 = 1 \times 10^{-7}$ . The polynomial controller gains are obtained as  $\mathbf{G}_1(\check{x}_2) = [-2.1745 \times 10^{-1}\check{x}_2^2 + 1.1463 \times 10^3 \quad 3.8649 \times 10^{-2}\check{x}_2^2 + 4.6925 \times 10^2]$  and  $\mathbf{G}_2(\check{x}_2) = [-2.6277 \times 10^{-1}\check{x}_2^2 + 5.6804 \times 10^2 \quad 7.7914 \times 10^{-2}\check{x}_2^2 + 1.9794 \times 10^2]$ , and the polynomial observer gains are obtained as  $\mathbf{L}_1(\check{x}_2) = [8.3334 \times 10^{-13}\check{x}_2^2 + 1.5901 \times 10 \quad 1.8529 \times 10^{-11}\check{x}_2^2 + 2.3319 \times 10]^T$  and  $\mathbf{L}_2(\check{x}_2) = [6.6685 \times 10^{-12}\check{x}_2^2 + 1.5901 \times 10 \quad 3.0865 \times 10^{-11}\check{x}_2^2 + 2.3319 \times 10]^T$ .

The above polynomial controller gains and polynomial observer gains are applied to the original dynamic system of the inverted pendulum (4.71). Considering 4 different initial conditions, the time response of system states are shown in Fig. 5.11 which shows that the inverted pendulum can be successfully stabilized. Choosing initiation conditions  $\mathbf{x}(0) = [\frac{70\pi}{180} \ 0]^T$  and  $\check{\mathbf{x}}(0) = [\frac{35\pi}{180} \ 0]^T$  for demonstration, the estimated system states are shown in Fig. 5.12. The corresponding sampled output and control input are shown in Fig. 5.13. As is exhibited in Fig. 5.13(a), the measured output is kept to be constant during the sampling interval. Although the sampling activity increases the difficulty of controlling the inverted pendulum, the proposed polynomial fuzzy observer-controller can successfully stabilize the inverted pendulum using the sampled-output measurements.

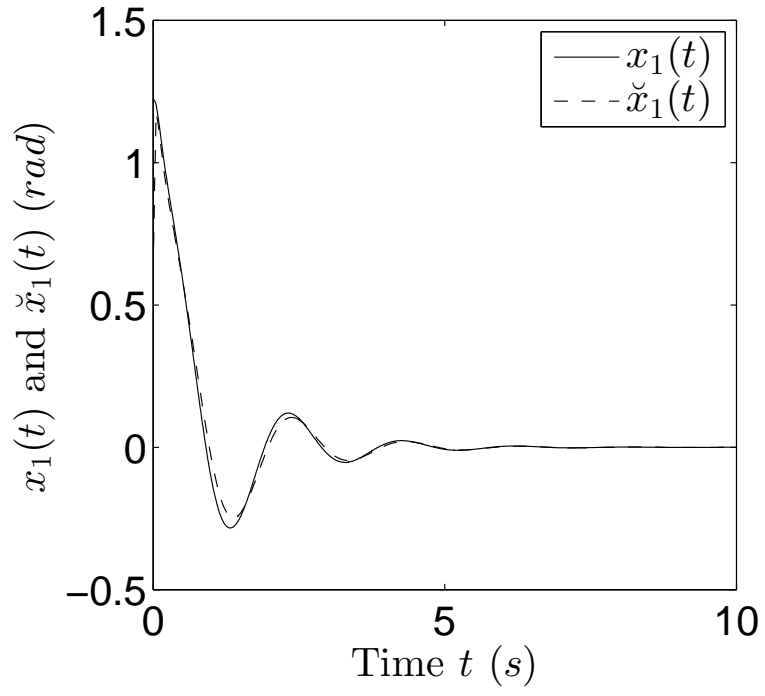


(a) Time response of  $x_1(t)$ .

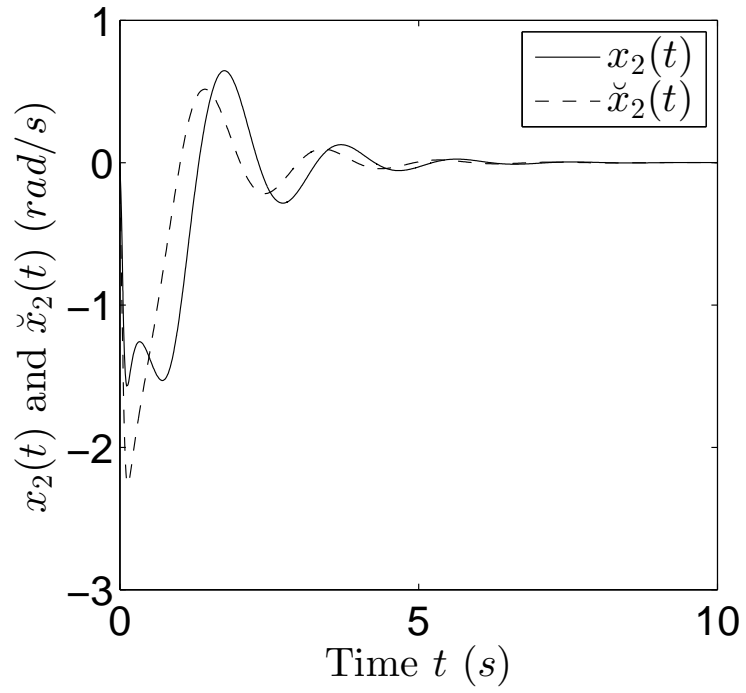


(b) Time response of  $x_2(t)$ .

Figure 5.11: Time response of system states of the inverted pendulum with 4 different initial conditions.

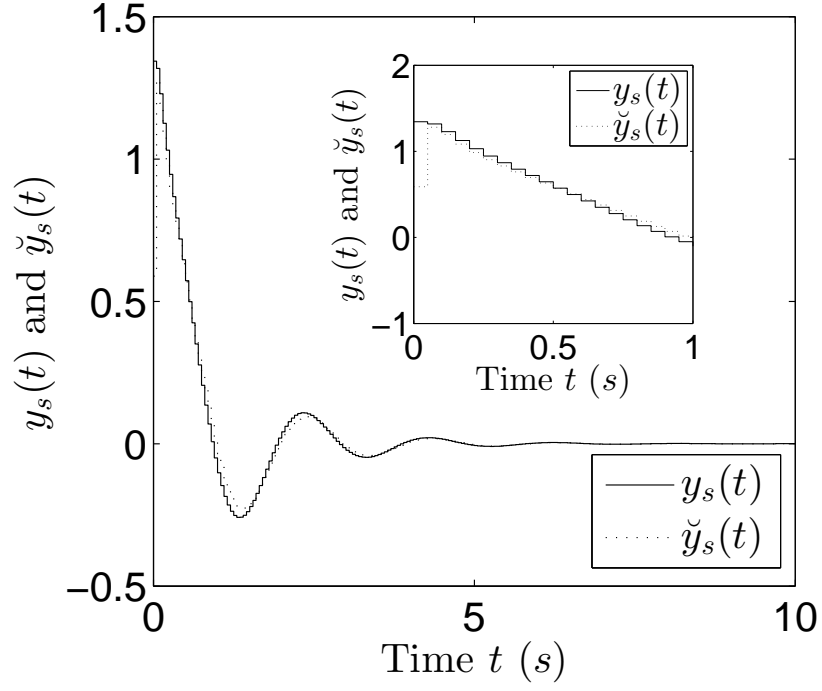


(a) Time response of  $x_1(t)$  and  $\check{x}_1(t)$ .

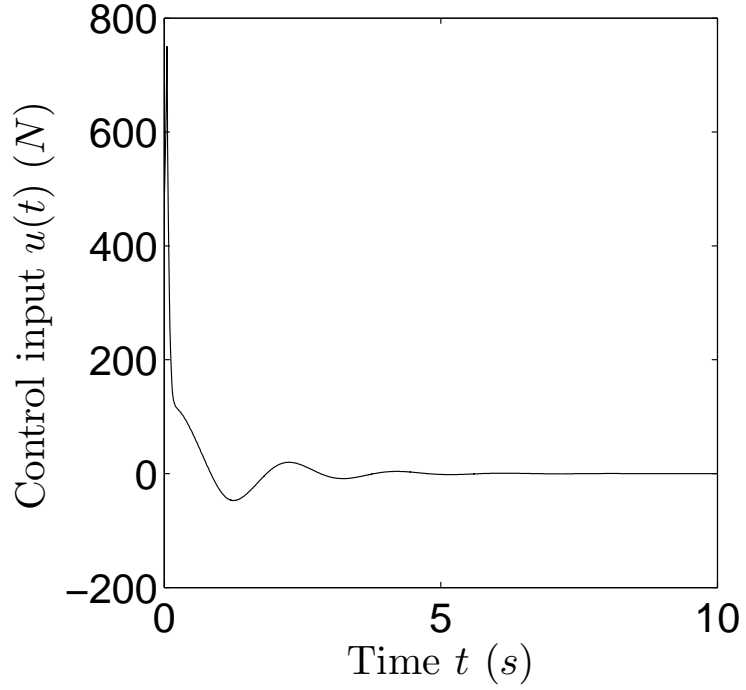


(b) Time response of  $x_2(t)$  and  $\check{x}_2(t)$ .

Figure 5.12: Time response of system states and estimated states for  $\mathbf{x}(0) = \begin{bmatrix} \frac{70\pi}{180} & 0 \end{bmatrix}^T$ .



(a) Time response of  $y_s(t)$  and  $\check{y}_s(t)$ .



(b) Time response of  $u(t)$ .

Figure 5.13: Time response of sampled output, estimated sampled output and control input for  $\mathbf{x}(0) = [\frac{70\pi}{180} \ 0]^T$ .

To compare the proposed control strategy with some relevant published papers, the polynomial fuzzy model used to represent the inverted pendulum is more general than T-S fuzzy model considered in [70–72]. The unmeasurable premise variables appeared in these examples provide more freedom for designing polynomial fuzzy

model than measurable premise variables in [60]. Furthermore, one step design of the observer-controller is achieved instead of two steps [60] or iterative procedure [66]. The controller is allowed to be polynomial and the output matrix  $\mathbf{C}$  is allowed to be different in each fuzzy rule, both of which are more general than what proposed in [69]. Additionally, the maximum sampling interval 0.018 seconds achieved in [66] for the inverted pendulum is exceeded to 0.05 seconds in this section benefited from the continuous-time polynomial fuzzy observer. Note that 0.05 seconds may not be the maximum sampling interval for this method since the interval can become larger achieved by adjusting the predefined parameters or the degree of polynomial matrices in the theorem.

### 5.3.4 Conclusion

In this section, the stability of PFMB observer-control system with sampled-output measurements has been investigated. Matrix decoupling technique has been employed in the stability analysis to obtain convex SOS stability conditions. Simulation examples have been presented to verify the stability analysis results and demonstrate the effectiveness of the proposed PFMB observer-control scheme.

## 5.4 Optimization of Membership Functions

### 5.4.1 Introduction

In this section, we aim to improve the performance of the PFMB observer-control system by optimizing the membership functions of the polynomial fuzzy observer-controller. The optimal membership functions in this section are understood in the following way: given a cost function, a set of linear (or polynomial) observer-controllers, and the form of membership function with some parameters to be optimized, the optimal membership functions are the ones that combine the linear observer-controllers to form a fuzzy observer-controller which provides the lowest cost subject to the system stability. The gradient descent approach improving the one in [76] is exploited to achieve the optimization, which provides better performance than PDC approach. Compared with [76], the observer-based system is considered in this section and the cost function is generalized by taking into account the control input. More precise gradients are obtained by considering the summation-one property of the membership functions.

This section is organized as follows. The optimization of membership functions of the polynomial observer-controller is carried out in Subsection 5.4.2. Simulation examples demonstrate the proposed design and optimization method in Subsection 5.4.3. Finally, a conclusion is drawn in Subsection 5.4.4.

### 5.4.2 Algorithm Design

After designing the polynomial observer-controller gains from Subsection 5.2.3, the subsequent objective is to optimize the membership functions of the polynomial fuzzy observer-controller  $m_i(\check{\mathbf{x}})$  in (5.50) and (5.51).

It is assumed that  $0 \leq m_i(\check{\mathbf{x}}, \alpha_i) \leq 1$  is designed as any differentiable functions with respect to both  $\check{\mathbf{x}}$  and  $\alpha_i$ , where  $\alpha_i = [\alpha_{i1} \ \alpha_{i2} \ \cdots \ \alpha_{iq_i}]^T, i = 1, 2, \dots, p-1$  ( $p$  is the number of fuzzy rules), are parameters to be optimized (*e.g.* Gaussian membership functions with mean and standard deviation to be determined). Then all parameters to be optimized are denoted as  $\alpha = [\alpha_1^T \ \alpha_2^T \ \cdots \ \alpha_{p-1}^T]^T$ . It is noted that the last membership function is defined as  $m_p(\check{\mathbf{x}}, \alpha_1, \dots, \alpha_{p-1}) = 1 - \sum_{i=1}^{p-1} m_i(\check{\mathbf{x}}, \alpha_i)$  such that the condition  $\sum_{i=1}^p m_i(\check{\mathbf{x}}, \alpha_i) = 1$  is satisfied. For brevity, we denote  $\alpha_p = f(\alpha_1, \dots, \alpha_{p-1})$  and  $m_p(\check{\mathbf{x}}, \alpha_1, \dots, \alpha_{p-1}) = m_p(\check{\mathbf{x}}, \alpha_p)$ .

The cost function to be minimized in this section is defined in the following general form:

$$J(\alpha) = \int_0^{T_t} \varphi(\mathbf{x}(t), \check{\mathbf{x}}(t), \alpha) dt + \psi(\mathbf{x}(T_t), \check{\mathbf{x}}(T_t), \alpha), \quad (5.177)$$

where  $T_t$  is the total time;  $\varphi$  and  $\psi$  are any differentiable functions with respect to  $\mathbf{x}$ ,  $\check{\mathbf{x}}$  and  $\alpha$ .

**Remark 25** In (5.177), the term  $\int_0^{T_t} \varphi(\mathbf{x}(t), \check{\mathbf{x}}(t), \alpha) dt$  reflects the performance throughout time 0 to  $T_t$  and the term  $\psi(\mathbf{x}(T_t), \check{\mathbf{x}}(T_t), \alpha)$  addresses the final state of the system at time  $T_t$ . Since we consider the equilibrium point to be  $\mathbf{x} = \mathbf{0}$ , these two terms are normally chosen to be non-negative such that the minimum is  $J(\alpha) = 0$  when  $\mathbf{x} = \mathbf{0}$ . Both of these two terms are functions of  $\mathbf{x}, \check{\mathbf{x}}$  and  $\alpha$  such that the estimated states  $\check{\mathbf{x}}$  and the control input  $\mathbf{u}(\check{\mathbf{x}}, \alpha)$  are allowed to exist in the cost function, which are more general than [76–78].

The constraint of the optimization is the dynamics of the closed-loop system (5.52) and (5.53) which is rearranged as follows:

$$\begin{aligned} \begin{bmatrix} \dot{\mathbf{x}} \\ \dot{\check{\mathbf{x}}} \end{bmatrix} &= \sum_{i=1}^p \sum_{j=1}^p m_i(\check{\mathbf{x}}, \alpha_i) m_j(\check{\mathbf{x}}, \alpha_j) \mathbf{g}_{ij}(\mathbf{x}, \check{\mathbf{x}}), \\ \mathbf{x}(0) &= \mathbf{x}_0, \quad \check{\mathbf{x}}(0) = \check{\mathbf{x}}_0, \end{aligned} \quad (5.178)$$

where  $\mathbf{g}_{ij}(\mathbf{x}, \check{\mathbf{x}}) = \sum_{k=1}^p w_k(\mathbf{x}) \begin{bmatrix} \mathbf{g}_{ijk}^{(11)}(\mathbf{x}, \check{\mathbf{x}}) \\ \mathbf{g}_{ijk}^{(21)}(\mathbf{x}, \check{\mathbf{x}}) \end{bmatrix}$ ,  $\mathbf{g}_{ijk}^{(11)}(\mathbf{x}, \check{\mathbf{x}}) = \mathbf{A}_k(\mathbf{x})\mathbf{x} + \mathbf{B}_k(\mathbf{x})\mathbf{G}_i(\check{\mathbf{x}})\check{\mathbf{x}}$ ,  $\mathbf{g}_{ijk}^{(21)}(\mathbf{x}, \check{\mathbf{x}}) = (\mathbf{A}_j(\check{\mathbf{x}}) + \mathbf{B}_j(\check{\mathbf{x}})\mathbf{G}_i(\check{\mathbf{x}}))\check{\mathbf{x}} + \mathbf{L}_j(\check{\mathbf{x}})(\mathbf{C}_k(\mathbf{x})\mathbf{x} - \mathbf{C}_i(\check{\mathbf{x}})\check{\mathbf{x}})$ ; polynomial observer-controller gains  $\mathbf{G}_i(\check{\mathbf{x}})$  and  $\mathbf{L}_j(\check{\mathbf{x}})$  are obtained from Section 5.2.3. It is also assumed that the initial condition  $\mathbf{x}_0$  is known such that the optimization can be carried out offline.

**Remark 26** Under the condition  $\sum_{i=1}^p m_i(\check{\mathbf{x}}, \alpha_i) = 1$ , the calculated dynamics of the PFMB system (5.178) is equivalent to the dynamics of the original nonlinear system. In [76], however, the calculated dynamics is different from the dynamics of the original nonlinear system without considering the summation-one condition. Since the gradients will be calculated based on the obtained dynamics, the gradients calculated in this section will be more precise than those in [76].

The task is to optimize  $\alpha$  according to the given performance index (5.177) under the constraint (5.178). In what follows, we propose sufficient conditions for the stationary points of the cost function, and then apply the gradient descent method to find the parameters achieving the local minimum.

Applying the Lagrange multiplier  $\lambda(t) \in \mathbb{R}^{1 \times 2n}$  to combine the constraint (5.178) (rearranged as a zero term) into the cost function (5.177):

$$\begin{aligned} & \tilde{J}(\alpha, \lambda) \\ &= \int_0^{T_t} \left( \varphi(\mathbf{x}, \check{\mathbf{x}}, \alpha) + \lambda \left( \sum_{i=1}^p \sum_{j=1}^p m_i(\check{\mathbf{x}}, \alpha_i) m_j(\check{\mathbf{x}}, \alpha_j) \mathbf{g}_{ij}(\mathbf{x}, \check{\mathbf{x}}) \right. \right. \\ & \quad \left. \left. - [\dot{\mathbf{x}}^T \quad \dot{\check{\mathbf{x}}}^T]^T \right) \right) dt + \psi(\mathbf{x}(T_t), \check{\mathbf{x}}(T_t), \alpha). \end{aligned} \quad (5.179)$$

Note that the constraint (5.178) is placed in the integration from time 0 to  $T_t$  such that  $\lambda$  can be determined to eliminate some unknown variables in the following.

**Theorem 8** A stationary point of the cost function (5.179) is obtained when the parameters  $\alpha = [\alpha_1^T \quad \alpha_2^T \quad \cdots \quad \alpha_{p-1}^T]^T$  (where  $\alpha_i = [\alpha_{i1} \quad \alpha_{i2} \quad \cdots \quad \alpha_{iq_i}]^T, i = 1, 2, \dots, p-1$ ) are chosen such that

$$\begin{aligned} & \frac{\partial \tilde{J}(\alpha, \lambda)}{\partial \alpha_{kl}} \\ &= \int_0^{T_t} \left( \lambda \sum_{i=1}^p m_i(\check{\mathbf{x}}, \alpha_i) \left( \frac{\partial m_k(\check{\mathbf{x}}, \alpha_k)}{\partial \alpha_{kl}} (\mathbf{g}_{ik}(\mathbf{x}, \check{\mathbf{x}}) + \mathbf{g}_{ki}(\mathbf{x}, \check{\mathbf{x}})) \right. \right. \\ & \quad \left. \left. + \frac{\partial m_p(\check{\mathbf{x}}, \alpha_p)}{\partial \alpha_{kl}} (\mathbf{g}_{ip}(\mathbf{x}, \check{\mathbf{x}}) + \mathbf{g}_{pi}(\mathbf{x}, \check{\mathbf{x}})) \right) \right. \\ & \quad \left. + \frac{\partial \varphi(\mathbf{x}, \check{\mathbf{x}}, \alpha)}{\partial \alpha_{kl}} \right) dt + \frac{\partial \psi(\mathbf{x}(T_t), \check{\mathbf{x}}(T_t), \alpha)}{\partial \alpha_{kl}} \\ &= 0, \quad \forall k = 1, 2, \dots, p-1, l = 1, 2, \dots, q_k, \end{aligned} \quad (5.180)$$

where  $\mathbf{x}$  and  $\check{\mathbf{x}}$  are given by the constraint (5.178) and the Lagrange multiplier  $\lambda(t)$  is chosen such that

$$\begin{aligned} \dot{\lambda} = & - \left[ \frac{\partial \varphi(\mathbf{x}, \check{\mathbf{x}}, \alpha)}{\partial \mathbf{x}} \quad \frac{\partial \varphi(\mathbf{x}, \check{\mathbf{x}}, \alpha)}{\partial \check{\mathbf{x}}} \right] \\ & - \lambda \sum_{i=1}^p \sum_{j=1}^p \left( m_i(\check{\mathbf{x}}, \alpha_i) m_j(\check{\mathbf{x}}, \alpha_j) \left[ \frac{\partial \mathbf{g}_{ij}(\mathbf{x}, \check{\mathbf{x}})}{\partial \mathbf{x}} \quad \frac{\partial \mathbf{g}_{ij}(\mathbf{x}, \check{\mathbf{x}})}{\partial \check{\mathbf{x}}} \right] \right) \end{aligned}$$



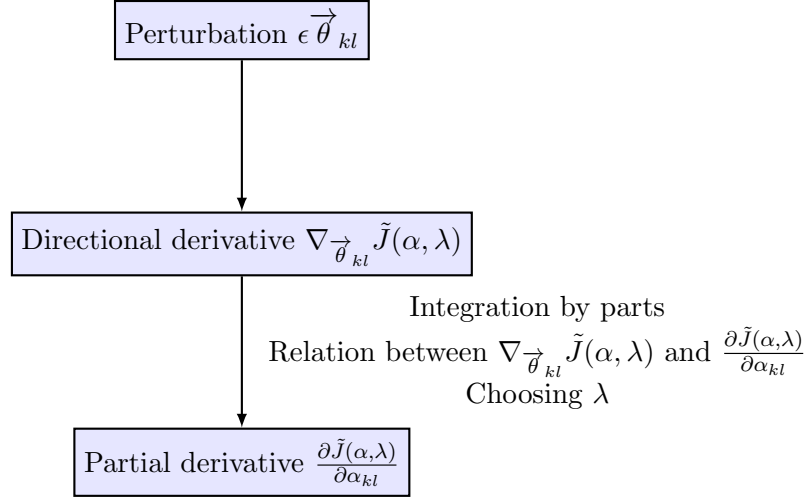


Figure 5.14: Procedure of proof for Theorem 8.

$$\begin{aligned}
& + \mathbf{g}_{ij}(\mathbf{x}, \check{\mathbf{x}})[\mathbf{0}_{1 \times n} \quad \frac{\partial m_i(\check{\mathbf{x}}, \alpha_i)}{\partial \check{\mathbf{x}}} m_j(\check{\mathbf{x}}, \alpha_j) \\
& + \frac{\partial m_j(\check{\mathbf{x}}, \alpha_j)}{\partial \check{\mathbf{x}}} m_i(\check{\mathbf{x}}, \alpha_i)]), \\
\lambda(T_t) = & \left[ \frac{\psi(\mathbf{x}(T_t), \check{\mathbf{x}}(T_t), \alpha)}{\partial \mathbf{x}} \quad \frac{\psi(\mathbf{x}(T_t), \check{\mathbf{x}}(T_t), \alpha)}{\partial \check{\mathbf{x}}} \right]. \tag{5.181}
\end{aligned}$$

**Proof** The structure of the following analysis is shown in Fig. 5.14 first. The variational method [76] is employed to obtain  $\frac{\partial \tilde{J}(\alpha, \lambda)}{\partial \alpha_{kl}}$  in (5.180), since it is difficult to calculate the partial derivative directly. In other words, the perturbation and directional derivative will be obtained first instead of the partial derivative.

Denoting the perturbed parameters as  $\alpha_\epsilon = \alpha + \epsilon \vec{\theta}_{kl} = [\alpha_1^T, \dots, \alpha_{k\epsilon}^T, \dots, \alpha_{p-1}^T]^T$ , where  $\epsilon \ll 1$  and  $\vec{\theta}_{kl} = [0, \dots, 0, \theta_{kl}, 0, \dots, 0]^T, k = 1, 2, \dots, p-1, l = 1, 2, \dots, q_k$ , the resulting variation in the dynamics of the system becomes  $\mathbf{x}_\epsilon = \mathbf{x} + \epsilon \eta_1(t)$  and  $\check{\mathbf{x}}_\epsilon = \check{\mathbf{x}} + \epsilon \eta_2(t)$ . Note that in parameters  $\alpha_\epsilon$ , only the  $l^{th}$  entry of  $\alpha_{k\epsilon}$  is perturbed. Also,  $\eta_1(0) = \eta_2(0) = \mathbf{0}$  since the initial conditions  $\mathbf{x}_\epsilon(0) = \mathbf{x}(0) = \mathbf{x}_0, \check{\mathbf{x}}_\epsilon(0) = \check{\mathbf{x}}(0) = \check{\mathbf{x}}_0$  are unchanged. For brevity, we denote  $\alpha_{p\epsilon} = f(\alpha_1, \dots, \alpha_{k\epsilon}, \dots, \alpha_{p-1})$ . Therefore, the perturbed cost function is

$$\begin{aligned}
& \tilde{J}_\epsilon(\alpha_\epsilon, \lambda) \\
= & \int_0^{T_t} \left( \varphi(\mathbf{x}_\epsilon, \check{\mathbf{x}}_\epsilon, \alpha_\epsilon) + \lambda \left( m_1(\check{\mathbf{x}}_\epsilon, \alpha_1) m_1(\check{\mathbf{x}}_\epsilon, \alpha_1) \mathbf{g}_{11}(\mathbf{x}_\epsilon, \check{\mathbf{x}}_\epsilon) \right. \right. \\
& + \dots + m_1(\check{\mathbf{x}}_\epsilon, \alpha_1) m_k(\check{\mathbf{x}}_\epsilon, \alpha_{k\epsilon}) \mathbf{g}_{1k}(\mathbf{x}_\epsilon, \check{\mathbf{x}}_\epsilon) \\
& + \dots + m_p(\check{\mathbf{x}}_\epsilon, \alpha_{p\epsilon}) m_p(\check{\mathbf{x}}_\epsilon, \alpha_{p\epsilon}) \mathbf{g}_{pp}(\mathbf{x}_\epsilon, \check{\mathbf{x}}_\epsilon) \\
& \left. \left. - [\dot{\mathbf{x}}_\epsilon^T \quad \dot{\check{\mathbf{x}}}_\epsilon^T]^T \right) \right) dt + \psi(\mathbf{x}_\epsilon(T_t), \check{\mathbf{x}}_\epsilon(T_t), \alpha_\epsilon). \tag{5.182}
\end{aligned}$$

Taking the directional derivative of  $\tilde{J}(\alpha, \lambda)$  along the direction  $\vec{\theta}_{kl}$ , we have

$$\begin{aligned}
& \nabla_{\vec{\theta}_{kl}} \tilde{J}(\alpha, \lambda) \\
&= \lim_{\epsilon \rightarrow 0} \frac{\tilde{J}_\epsilon(\alpha_\epsilon, \lambda) - \tilde{J}(\alpha, \lambda)}{\epsilon} \\
&= \lim_{\epsilon \rightarrow 0} \frac{\tilde{J}_\epsilon(\epsilon) - \tilde{J}_\epsilon(0)}{\epsilon - 0} \\
&= \left. \frac{d\tilde{J}_\epsilon(\epsilon)}{d\epsilon} \right|_{\epsilon=0} \\
&= \int_0^{T_t} \left( \frac{\varphi(\mathbf{x}, \check{\mathbf{x}}, \alpha)}{\partial \mathbf{x}} \eta_1 + \frac{\varphi(\mathbf{x}, \check{\mathbf{x}}, \alpha)}{\partial \check{\mathbf{x}}} \eta_2 + \frac{\varphi(\mathbf{x}, \check{\mathbf{x}}, \alpha)}{\partial \alpha_{kl}} \theta_{kl} \right. \\
&\quad + \lambda \sum_{i=1}^p \sum_{j=1}^p (m_i(\check{\mathbf{x}}, \alpha_i) m_j(\check{\mathbf{x}}, \alpha_j) \left( \frac{\mathbf{g}_{ij}(\mathbf{x}, \check{\mathbf{x}})}{\partial \mathbf{x}} \eta_1 \right. \\
&\quad + \frac{\mathbf{g}_{ij}(\mathbf{x}, \check{\mathbf{x}})}{\partial \check{\mathbf{x}}} \eta_2) + \mathbf{g}_{ij}(\mathbf{x}, \check{\mathbf{x}}) \left( \frac{\partial m_i(\check{\mathbf{x}}, \alpha_i)}{\partial \check{\mathbf{x}}} m_j(\check{\mathbf{x}}, \alpha_j) \right. \\
&\quad + \left. \frac{\partial m_j(\check{\mathbf{x}}, \alpha_j)}{\partial \check{\mathbf{x}}} m_i(\check{\mathbf{x}}, \alpha_i) \right) \eta_2) \\
&\quad + \lambda \sum_{i=1}^p m_i(\check{\mathbf{x}}, \alpha_i) \left( \frac{\partial m_k(\check{\mathbf{x}}, \alpha_k)}{\partial \alpha_{kl}} (\mathbf{g}_{ik}(\mathbf{x}, \check{\mathbf{x}}) + \mathbf{g}_{ki}(\mathbf{x}, \check{\mathbf{x}})) \right. \\
&\quad + \left. \frac{\partial m_p(\check{\mathbf{x}}, \alpha_p)}{\partial \alpha_{kl}} (\mathbf{g}_{ip}(\mathbf{x}, \check{\mathbf{x}}) + \mathbf{g}_{pi}(\mathbf{x}, \check{\mathbf{x}})) \right) \theta_{kl} \\
&\quad - \lambda [\dot{\eta}_1^T \quad \dot{\eta}_2^T]^T dt + \frac{\psi(\mathbf{x}(T_t), \check{\mathbf{x}}(T_t), \alpha)}{\partial \mathbf{x}} \eta_1(T_t) \\
&\quad + \frac{\psi(\mathbf{x}(T_t), \check{\mathbf{x}}(T_t), \alpha)}{\partial \check{\mathbf{x}}} \eta_2(T_t) + \frac{\psi(\mathbf{x}(T_t), \check{\mathbf{x}}(T_t), \alpha)}{\partial \alpha_{kl}} \theta_{kl}. \tag{5.183}
\end{aligned}$$

In (5.183), to deal with  $\int_0^{T_t} -\lambda [\dot{\eta}_1^T \quad \dot{\eta}_2^T]^T dt$ , we exploit integration by parts. Defining  $\eta = [\eta_1^T \quad \eta_2^T]^T$  and recalling that  $\eta_1(0) = \eta_2(0) = \mathbf{0}$ , we have

$$\begin{aligned}
\int_0^{T_t} -\lambda [\dot{\eta}_1^T \quad \dot{\eta}_2^T]^T dt &= -(\lambda \eta) \Big|_0^{T_t} + \int_0^{T_t} \dot{\lambda} \eta dt \\
&= -\lambda(T_t) \eta(T_t) + \int_0^{T_t} \dot{\lambda} \eta dt. \tag{5.184}
\end{aligned}$$

Substituting (5.184) into (5.183) and grouping terms, we have

$$\begin{aligned}
& \nabla_{\vec{\theta}_{kl}} \tilde{J}(\alpha, \lambda) \\
&= \int_0^{T_t} \left( \left[ \frac{\varphi(\mathbf{x}, \check{\mathbf{x}}, \alpha)}{\partial \mathbf{x}} \quad \frac{\varphi(\mathbf{x}, \check{\mathbf{x}}, \alpha)}{\partial \check{\mathbf{x}}} \right] \right. \\
&\quad + \lambda \sum_{i=1}^p \sum_{j=1}^p (m_i(\check{\mathbf{x}}, \alpha_i) m_j(\check{\mathbf{x}}, \alpha_j) \left[ \frac{\mathbf{g}_{ij}(\mathbf{x}, \check{\mathbf{x}})}{\partial \mathbf{x}} \quad \frac{\mathbf{g}_{ij}(\mathbf{x}, \check{\mathbf{x}})}{\partial \check{\mathbf{x}}} \right] \\
&\quad + \mathbf{g}_{ij}(\mathbf{x}, \check{\mathbf{x}}) [\mathbf{0}_{1 \times n} \quad \frac{\partial m_i(\check{\mathbf{x}}, \alpha_i)}{\partial \check{\mathbf{x}}} m_j(\check{\mathbf{x}}, \alpha_j) + \frac{\partial m_j(\check{\mathbf{x}}, \alpha_j)}{\partial \check{\mathbf{x}}} m_i(\check{\mathbf{x}}, \alpha_i)] \theta_{kl} \\
&\quad \left. + \frac{\psi(\mathbf{x}(T_t), \check{\mathbf{x}}(T_t), \alpha)}{\partial \mathbf{x}} \eta_1(T_t) + \frac{\psi(\mathbf{x}(T_t), \check{\mathbf{x}}(T_t), \alpha)}{\partial \check{\mathbf{x}}} \eta_2(T_t) + \frac{\psi(\mathbf{x}(T_t), \check{\mathbf{x}}(T_t), \alpha)}{\partial \alpha_{kl}} \theta_{kl} \right) dt
\end{aligned}$$

$$\begin{aligned}
& \times m_i(\check{\mathbf{x}}, \alpha_i)] + \dot{\lambda}) \eta dt + \theta_{kl} \left( \int_0^{T_t} \left( \lambda \sum_{i=1}^p m_i(\check{\mathbf{x}}, \alpha_i) \right. \right. \\
& \times \left( \frac{\partial m_k(\check{\mathbf{x}}, \alpha_k)}{\partial \alpha_{kl}} (\mathbf{g}_{ik}(\mathbf{x}, \check{\mathbf{x}}) + \mathbf{g}_{ki}(\mathbf{x}, \check{\mathbf{x}})) + \frac{\partial m_p(\check{\mathbf{x}}, \alpha_p)}{\partial \alpha_{kl}} \right. \\
& \times (\mathbf{g}_{ip}(\mathbf{x}, \check{\mathbf{x}}) + \mathbf{g}_{pi}(\mathbf{x}, \check{\mathbf{x}})) + \left. \left. \frac{\varphi(\mathbf{x}, \check{\mathbf{x}}, \alpha)}{\partial \alpha_{kl}} \right) dt \right. \\
& + \left. \frac{\psi(\mathbf{x}(T_t), \check{\mathbf{x}}(T_t), \alpha)}{\partial \alpha_{kl}} \right) \\
& + \left( \left[ \frac{\psi(\mathbf{x}(T_t), \check{\mathbf{x}}(T_t), \alpha)}{\partial \mathbf{x}} \quad \frac{\psi(\mathbf{x}(T_t), \check{\mathbf{x}}(T_t), \alpha)}{\partial \check{\mathbf{x}}} \right] \right. \\
& \left. - \lambda(T_t) \right) \eta(T_t). \tag{5.185}
\end{aligned}$$

To find the relation between  $\nabla_{\vec{\theta}_{kl}} \tilde{J}(\alpha, \lambda)$  in (5.185) and  $\frac{\partial \tilde{J}(\alpha, \lambda)}{\partial \alpha_{kl}}$  in (5.180), we have

$$\begin{aligned}
\nabla_{\vec{\theta}_{kl}} \tilde{J}(\alpha, \lambda) &= \left. \frac{d\tilde{J}_\epsilon(\epsilon)}{d\epsilon} \right|_{\epsilon=0} \\
&= \left( \frac{\partial \tilde{J}_\epsilon(\alpha_\epsilon, \lambda)}{\partial \alpha_{kl}} \theta_{kl} \right) \Big|_{\epsilon=0} \\
&= \frac{\partial \tilde{J}(\alpha, \lambda)}{\partial \alpha_{kl}} \theta_{kl}. \tag{5.186}
\end{aligned}$$

By choosing  $\lambda$  as in (5.181) and substituting (5.186) into (5.185), we can eliminate the unknown variables  $\eta$  and  $\theta_{kl}$ , and obtain the expression for  $\frac{\partial \tilde{J}(\alpha, \lambda)}{\partial \alpha_{kl}}$  as in (5.180). The proof is completed.

The following gradient descent algorithm [76] is employed to optimize the parameters  $\alpha$  at each iteration  $i$ :

**Initialize** the counter  $i$ , the step size  $\beta^{(i)}$  and the parameters  $\alpha^{(i)}$

**while** *stopping criteria are not met* **do**

compute  $\mathbf{x}$  and  $\check{\mathbf{x}}$  forward from time 0 to  $T_t$  by (5.178);

compute  $\lambda$  backward from time  $T_t$  to 0 by (5.181);

compute the gradient  $\nabla \tilde{J}(\alpha^{(i)}) = \left[ \frac{\partial \tilde{J}(\alpha)}{\partial \alpha_{11}^{(i)}} \quad \frac{\partial \tilde{J}(\alpha)}{\partial \alpha_{12}^{(i)}} \quad \dots \quad \frac{\partial \tilde{J}(\alpha)}{\partial \alpha_{(p-1)q(p-1)}^{(i)}} \right]^T$  by (5.180);

update the parameters  $\alpha^{(i+1)} = \alpha^{(i)} - \beta^{(i)} \nabla \tilde{J}(\alpha^{(i)})$ ;

$i \leftarrow i + 1$

**end**

**Result:** optimal parameters  $\alpha$

The algorithm terminates when the stopping criteria are met, for instance, the change of the gradient  $|\nabla \tilde{J}(\alpha^{(i+1)}) - \nabla \tilde{J}(\alpha^{(i)})|$  is smaller than a limit or the maximum number of iterations is reached.

### 5.4.3 Simulation Examples

In this section, four examples are provided to show the procedure of applying the design and optimization methods to control nonlinear systems. A numerical model is handled first, followed by three physical models.

#### 5.4.3.1 Numerical Example

Consider the nonlinear system extended from [60]:

$$\begin{aligned}\dot{x}_1 &= \sin(x_1) + 5x_2 + (x_2^2 + 5)u, \\ \dot{x}_2 &= -x_1 - x_2^3, \\ y &= x_1 + 0.1x_1x_2^2.\end{aligned}$$

Defining the region of interest as  $x_1 \in (-\infty, \infty)$ , the nonlinear term  $f_1(x_1) = \frac{\sin(x_1)}{x_1}$  is represented by sector nonlinearity technique [9] as follows:  $f_1(x_1) = \mu_{M_1^1}(x_1)f_{1_{max}} + \mu_{M_1^2}(x_1)f_{1_{min}}$ , where  $\mu_{M_1^1}(x_1) = \frac{f_1(x_1) - f_{1_{min}}}{f_{1_{max}} - f_{1_{min}}}$ ,  $\mu_{M_1^2}(x_1) = 1 - \mu_{M_1^1}(x_1)$ ,  $f_{1_{min}} = -0.2172$ ,  $f_{1_{max}} = 1.0000$ . The system is exactly described by a 2-rule polynomial fuzzy model:

$$\begin{aligned}\dot{\mathbf{x}} &= \sum_{i=1}^2 w_i(x_1) (\mathbf{A}_i(x_2)\mathbf{x} + \mathbf{B}_i(x_2)u), \\ y &= \sum_{i=1}^2 w_i(x_1) \mathbf{C}_i(x_2)\mathbf{x},\end{aligned}$$

where  $\mathbf{x} = [x_1 \ x_2]^T$ ;  $\mathbf{A}_1(x_2) = \begin{bmatrix} f_{1_{max}} & 5 \\ -1 & -x_2^2 \end{bmatrix}$ ,  $\mathbf{A}_2(x_2) = \begin{bmatrix} f_{1_{min}} & 5 \\ -1 & -x_2^2 \end{bmatrix}$ ,  $\mathbf{B}_1(x_2) = \mathbf{B}_2(x_2) = [x_2^2 + 5 \ 0]^T$ , and  $\mathbf{C}_1(x_2) = \mathbf{C}_2(x_2) = [1 + 0.1x_2^2 \ 0]$ ; the membership functions are  $w_i(x_1) = \mu_{M_1^i}(x_1)$ ,  $i = 1, 2$ . It is assumed that both system states  $x_1$  and  $x_2$  are unmeasurable. Note that with the enhanced modeling capability of the polynomial fuzzy model, the polynomial term  $x_2^2$  does not need to be modeled by the sector nonlinearity technique. Otherwise, 2 more rules are required and the only local stability in  $x_2$  can be guaranteed.

Theorem 6 is employed to design the PFMB observer-controller to stabilize the system. We choose  $\gamma_1 = 1 \times 10^{-3}$ ,  $\gamma_2 = 1 \times 10^{-4}$ ,  $\gamma_3 = 1$ ,  $\mathbf{N}_k(\check{x}_2)$  of degree 0 and 2 in  $\check{x}_2$ ,  $\mathbf{M}_j(\check{x}_2)$  of degree 0 and 2 in  $\check{x}_2$ , and  $\varepsilon_1 = \varepsilon_2 = \varepsilon_3 = 1 \times 10^{-4}$ . The polynomial controller gains are obtained as  $\mathbf{G}_1(\check{x}_2) = [-1.7202 \times 10^{-1} \check{x}_2^2 - 3.5836 \times 10^{-1} \quad -6.0958 \times 10^{-2} \check{x}_2^2 - 3.0850 \times 10^{-1}]$  and  $\mathbf{G}_2(\check{x}_2) = [-1.8171 \times 10^{-1} \check{x}_2^2 - 4.1202 \times 10^{-1} \quad -7.9720 \times 10^{-2} \check{x}_2^2 - 2.6510 \times 10^{-1}]$ , and the polynomial observer gains are obtained as  $\mathbf{L}_1(\check{x}_2) = [3.8483\check{x}_2 + 6.7683 \quad 1.2525\check{x}_2 + 2.9268]^T$  and  $\mathbf{L}_2(\check{x}_2) = [3.8713\check{x}_2 + 5.6684 \quad 1.2599\check{x}_2 + 2.8682]^T$ .

**Remark 27** When users cannot manually determine the predefined parameters in Theorem 6 to find solutions, some algorithms such as genetic algorithm can be em-

ployed to search for feasible parameters. Moreover, less conservative form of the completing square approach can be applied, which however requires more predefined parameters.

To optimize the membership functions  $m_i(\check{x}_1)$  of the polynomial fuzzy observer-controller, the Gaussian membership function is applied:  $m_1(\check{x}_1, \alpha_1) = e^{-\frac{(\check{x}_1 - \alpha_{11})^2}{2\alpha_{12}^2}}$  and  $m_2(\check{x}_1, \alpha_1) = 1 - m_1(\check{x}_1, \alpha_1)$ , where  $\alpha = [\alpha_1^T]^T = [\alpha_{11} \ \alpha_{12}]^T$  are the parameters to be optimized. We consider  $\varphi(\mathbf{x}, \check{\mathbf{x}}, \alpha) = \mathbf{x}^T \mathbf{Q} \mathbf{x} + u(\check{\mathbf{x}}, \alpha)^T R u(\check{\mathbf{x}}, \alpha)$ ,  $\psi(\mathbf{x}(T_t), \check{\mathbf{x}}(T_t), \alpha) = \mathbf{x}(T_t)^T \mathbf{S} \mathbf{x}(T_t)$  in the cost function (5.177), where  $\mathbf{Q} = \begin{bmatrix} 1 & 0 \\ 0 & 1 \end{bmatrix}$ ,  $R = 1$ ,  $\mathbf{S} = \begin{bmatrix} 100 & 0 \\ 0 & 100 \end{bmatrix}$ . The total time is  $T_t = 10$  seconds, and the initial conditions are  $\mathbf{x}_0 = [5 \ 0]^T$ ,  $\check{\mathbf{x}}_0 = [0 \ 0]^T$ . The stopping criterion is that the change of the gradient  $|\nabla \tilde{J}(\alpha^{(i+1)}) - \nabla \tilde{J}(\alpha^{(i)})|$  is less than 0.01. Choosing the step size  $\beta^{(i)} = 5$  (moderate step size should be chosen to avoid divergence and slow convergence speed) for all iterations  $i$  and initializing the parameters  $\alpha^{(0)} = [0 \ 1]^T$ , we obtain the optimized results  $\alpha_{11} = 2.3137$ ,  $\alpha_{12} = 1.1873$  and corresponding cost  $J(\alpha) = 6.7519$ . Comparing with the cost  $J = 7.1428$  obtained by PDC approach ( $m_i(\check{x}_1) = w_i(\check{x}_1)$ ,  $i = 1, 2$ ), the optimized membership functions provide better performance.

To verify the optimized membership functions and cost, the gradient  $\nabla J(\alpha)$  is shown in Fig. 5.15 generated by sampling parameters  $\alpha$ . It can be seen that the lower costs occur when  $\alpha_{11}$  is around 2.5 and  $\alpha_{12}$  is around  $\pm 1.5$ , which coincides with the optimized parameters.

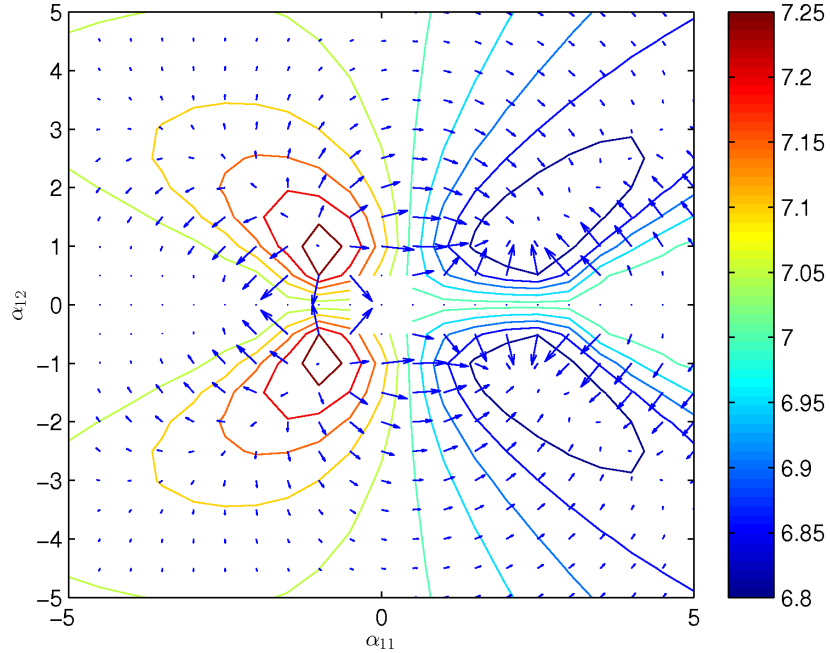
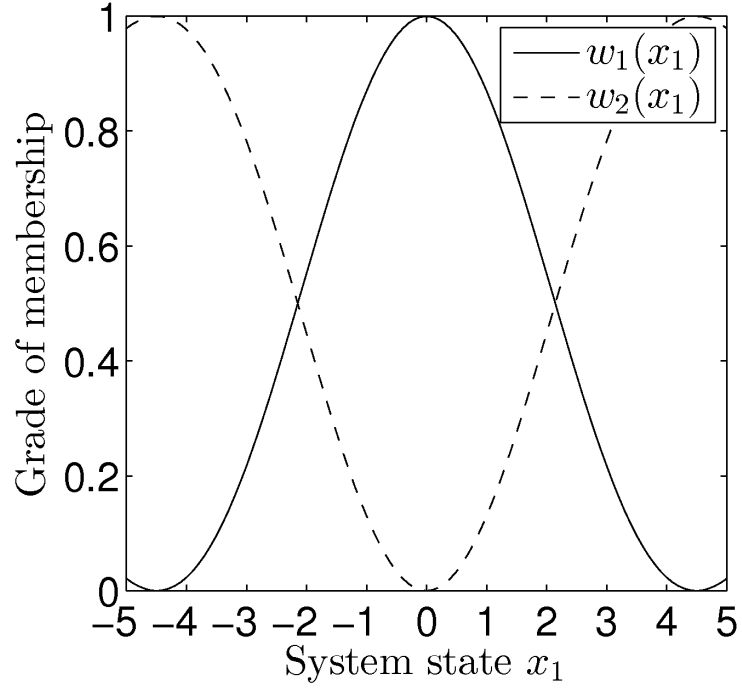
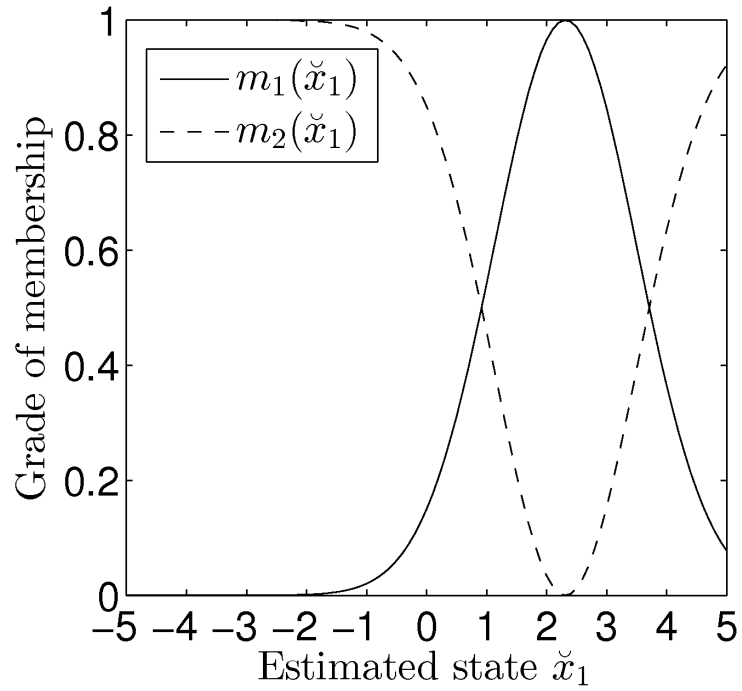


Figure 5.15: The descent of the gradient  $\nabla J(\alpha)$ , where the arrow indicates the direction of the gradient descent and the contour indicates the value of the cost  $J(\alpha)$ .

The original membership function  $w_i(x_1)$  for the polynomial fuzzy model and the optimized membership function  $m_i(\check{x}_1)$  for the polynomial fuzzy observer-controller are shown in Fig. 5.16(a) and Fig. 5.16(b), respectively. As shown in the figures, the optimized membership functions are different from the original membership function of the polynomial fuzzy model, which results in different performance compared with the PDC approach. It is noted that the stability is still guaranteed since the previously employed positive and summation-one properties of membership functions remain unchanged.



(a)  $w_i(x_1)$  for the polynomial fuzzy model.



(b) Optimized  $m_i(\check{x}_1)$  for the polynomial fuzzy observer-controller.

Figure 5.16: Membership functions.

Applying the designed polynomial observer-controller gains and the optimized membership functions to control the nonlinear system, the responses of system states, estimated states and their counterparts by PDC approach are shown in Fig. 5.17 and Fig. 5.18. The control input is shown in Fig. 5.19. The optimized membership functions perform better than the PDC approach with less overshoot and

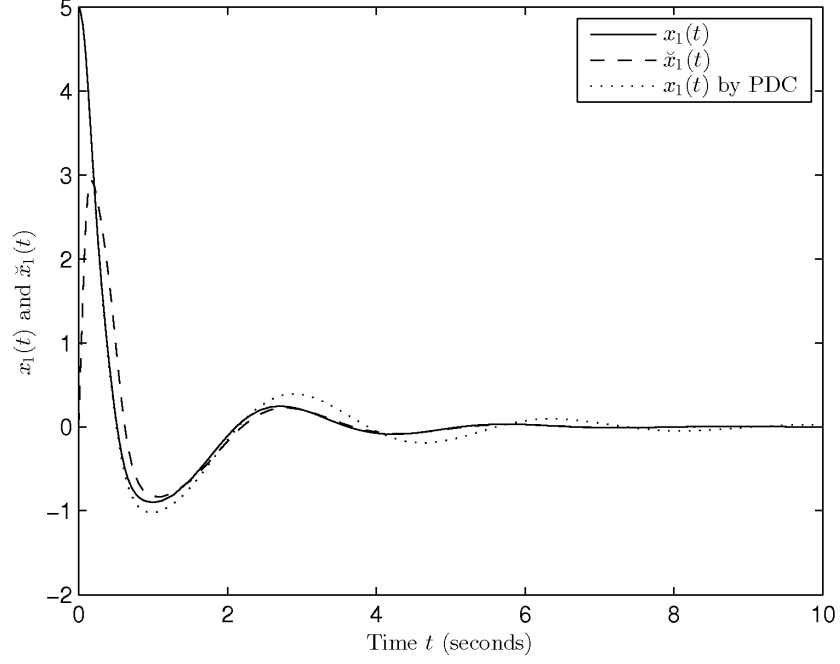


Figure 5.17: Time response of system state  $x_1$ , its estimation  $\check{x}_1$  and its counterpart by PDC approach.

settling time.

#### 5.4.3.2 Nonlinear Mass-Spring-Damper System

Following the same procedure in Example 5.4.3.1, we try to stabilize a nonlinear mass-spring-damper system as in (5.48). Denoting  $x_1$  and  $x_2$  as  $x$  and  $\dot{x}$ , respectively, we obtain the following state space form:

$$\begin{aligned}\dot{x}_1 &= x_2, \\ \dot{x}_2 &= \frac{1}{M}(-g(x_1, x_2) - f(x_1) + \phi(x_2)u), \\ y &= x_1.\end{aligned}$$

The nonlinear term  $f_1(x_2) = \cos(5x_2)$  is represented by sector nonlinearity technique [9] as follows:  $f_1(x_2) = \mu_{M_1^1}(x_2)f_{1_{min}} + \mu_{M_1^2}(x_2)f_{1_{max}}$ , where  $\mu_{M_1^1}(x_2) = \frac{f_1(x_2) - f_{1_{max}}}{f_{1_{min}} - f_{1_{max}}}$ ,  $\mu_{M_1^2}(x_2) = 1 - \mu_{M_1^1}(x_2)$ ,  $f_{1_{min}} = -1$ ,  $f_{1_{max}} = 1$ . Therefore, the nonlinear mass-spring-damper system is precisely described by a 2-rule polynomial fuzzy model:

$$\begin{aligned}\dot{\mathbf{x}} &= \sum_{i=1}^2 w_i(x_2) \left( \mathbf{A}_i(\mathbf{x})\mathbf{x} + \mathbf{B}_i(x_2)u \right), \\ y &= \sum_{i=1}^2 w_i(x_2) \mathbf{C}_i \mathbf{x},\end{aligned}$$



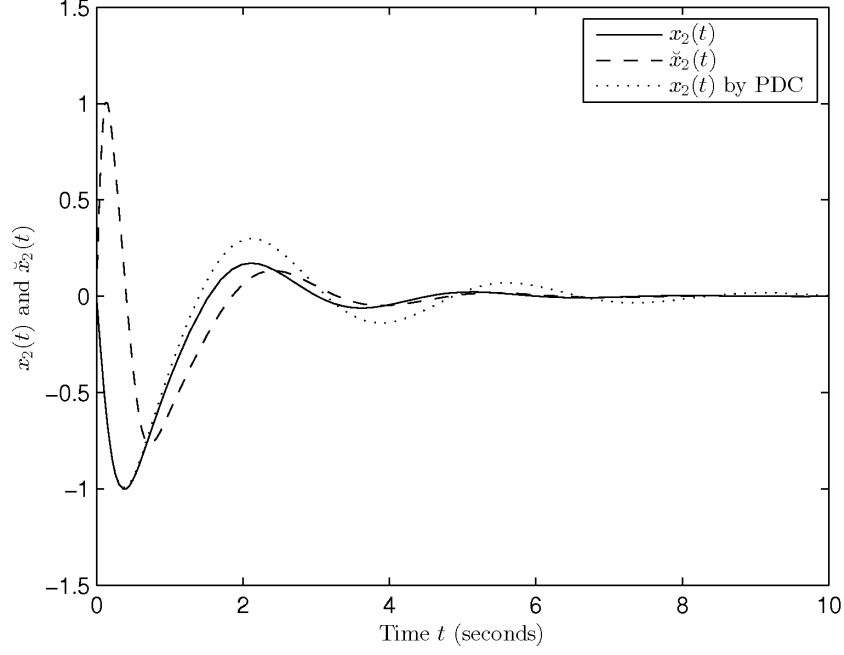


Figure 5.18: Time response of system state  $x_2$ , its estimation  $\check{x}_2$  and its counterpart by PDC approach.

where  $\mathbf{x} = [x_1 \ x_2]^T$ ;  $\mathbf{A}_1(\mathbf{x}) = \mathbf{A}_2(\mathbf{x}) = \begin{bmatrix} 0 & 1 \\ a_1(x_1) & a_2(x_2) \end{bmatrix}$ ,  $a_1(x_1) = -\frac{1}{M}(Dc_1 + K(c_4 + c_6) + Kc_5x_1^2)$ ,  $a_2(x_2) = -\frac{1}{M}(Dc_3 + Dc_2x_2^2)$ ;  $\mathbf{B}_1(x_2) = [0 \ b_1(x_2)]^T$ ,  $\mathbf{B}_2(x_2) = [0 \ b_2(x_2)]^T$ ,  $b_1(x_2) = \frac{1}{M}(1.4387 + c_7x_2^2 + c_8f_{1_{min}})$ ,  $b_2(x_2) = \frac{1}{M}(1.4387 + c_7x_2^2 + c_8f_{1_{max}})$ ;  $\mathbf{C}_1 = \mathbf{C}_2 = [1 \ 0]$ ; the membership functions are  $w_i(x_2) = \mu_{M_1^i}(x_2)$ ,  $i = 1, 2$ . Again, the polynomial fuzzy model demonstrates its superiority by keeping polynomial terms  $x_1^2$  and  $x_2^2$ . Otherwise,  $2^3 = 8$  rules in total are required to precisely model the nonlinear mass-spring-damper system with only local stability in both  $x_1$  and  $x_2$ .

It is implied that the premise variable  $f_1(x_2)$  depends on unmeasurable system state  $x_2$ , and thus Theorem 6 is employed to design the PFMB observer-controller with unmeasurable premise variables. We choose  $\gamma_1 = 1 \times 10^6$ ,  $\gamma_2 = 1 \times 10^{-3}$ ,  $\gamma_3 = 1 \times 10^{-2}$ ,  $\mathbf{N}_k(\check{x}_1)$  of degree 0 and 2 in  $\check{x}_1$ ,  $\mathbf{M}_j(\check{x}_1)$  of degree 0 and 2 in  $\check{x}_1$ ,  $\varepsilon_1 = \varepsilon_2 = 1 \times 10^{-4}$ , and  $\varepsilon_3 = 1 \times 10^{-6}$ . The polynomial controller gains are obtained as  $\mathbf{G}_1(\check{x}_1) = [-4.3492 \times 10^{-1}\check{x}_1^2 - 8.3374 \times 10^{-2} \quad -2.7182\check{x}_1^2 - 1.0842]$  and  $\mathbf{G}_2(\check{x}_1) = [-4.2491 \times 10^{-1}\check{x}_1^2 - 2.8176 \times 10^{-1} \quad -2.7888\check{x}_1^2 - 1.4408]$ , and the polynomial observer gains are obtained as  $\mathbf{L}_1(\check{x}_2) = [7.4229 \times 10^{-3}\check{x}_1^2 + 2.1987 \times 10^2 \quad 4.9731 \times 10^{-2}\check{x}_1^2 + 6.0260 \times 10^2]^T$  and  $\mathbf{L}_2(\check{x}_2) = [7.4219 \times 10^{-3}\check{x}_1^2 + 2.1987 \times 10^2 \quad 4.9577 \times 10^{-2}\check{x}_1^2 + 6.0218 \times 10^2]^T$ .

**Remark 28** The existing polynomial fuzzy observer [60] fails to deal with Examples 5.4.3.1 and 5.4.3.2 since it requires the premise variable to be measurable. To further compare with the two-step procedure in [60], we simplify the model in Example 5.4.3.2 by assuming the premise variable is measurable. However, by choosing the degree of

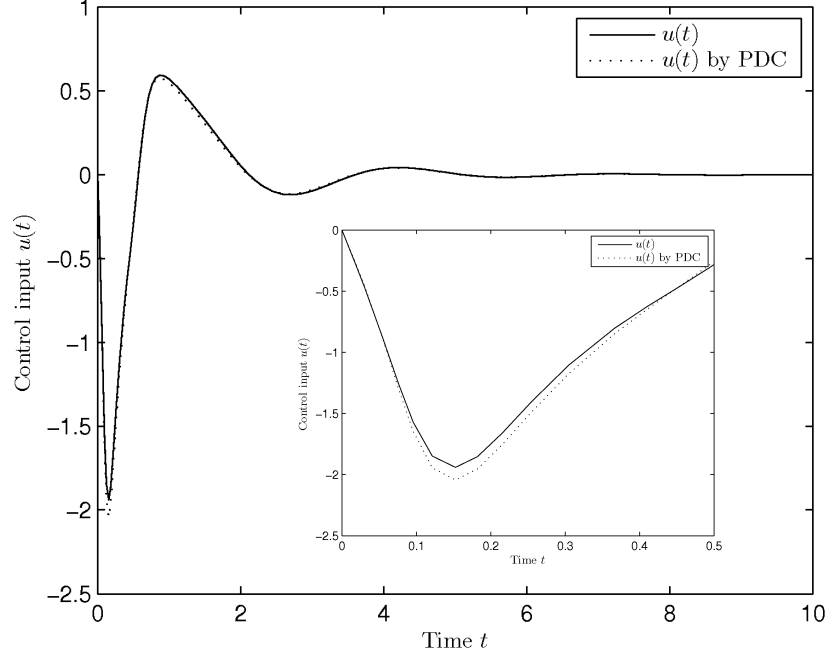


Figure 5.19: Time response of the control input  $u$  and its counterpart by PDC approach.

*polynomial matrix variables the same as those in this section, no feasible solution is found. Consequently, the proposed polynomial fuzzy observer with one-step design is less conservative than the two-step procedure in [60].*

To optimize the membership functions, in this example, we choose the sinusoidal membership function:  $m_1(\check{x}_2, \alpha_1) = \frac{1}{2}(\sin(\alpha_{11}\check{x}_2 + \alpha_{12}) + 1)$  and  $m_2(\check{x}_2, \alpha_1) = 1 - m_1(\check{x}_2, \alpha_1)$ , where  $\alpha = [\alpha_1^T]^T = [\alpha_{11} \ \alpha_{12}]^T$  are the parameters to be optimized. The cost function, total time and stopping criteria are the same as in Example 5.4.3.1. The initial conditions are  $\mathbf{x}_0 = [1 \ 0]^T$ ,  $\check{\mathbf{x}}_0 = [0 \ 0]^T$ . Choosing the step size  $\beta^{(i)} = 2$  for all iterations  $i$  and initializing the parameters  $\alpha^{(0)} = [0 \ 0]^T$ , we obtain the optimized results  $\alpha_{11} = 0.5347, \alpha_{12} = 0.5747$  and corresponding cost  $J(\alpha) = 6.4968$ , which is still better than the cost  $J = 6.6349$  obtained by PDC approach ( $m_i(\check{x}_2) = w_i(\check{x}_2), i = 1, 2$ ).

To show the mechanism of the optimization, the descent of the gradient  $\nabla J(\alpha)$  is shown in Fig. 5.20 and the original membership function  $w_i(x_2)$  and the optimized membership function  $m_i(\check{x}_2)$  are exhibited in Figs. 5.21(a) and 5.21(b), respectively. It can be summarized that the local minima appear periodically in terms of the phase  $\alpha_{12}$ , which is consistent of the property of the sinusoidal function. The PDC approach is included in the optimization by considering  $\alpha_{11} = 5, \alpha_{12} = -\frac{\pi}{2}$ . As can be seen, the cost value of this point in Fig. 5.20 is larger than the one found by the optimization.

**Remark 29** *When the optimization is non-convex, the local minima may be found*

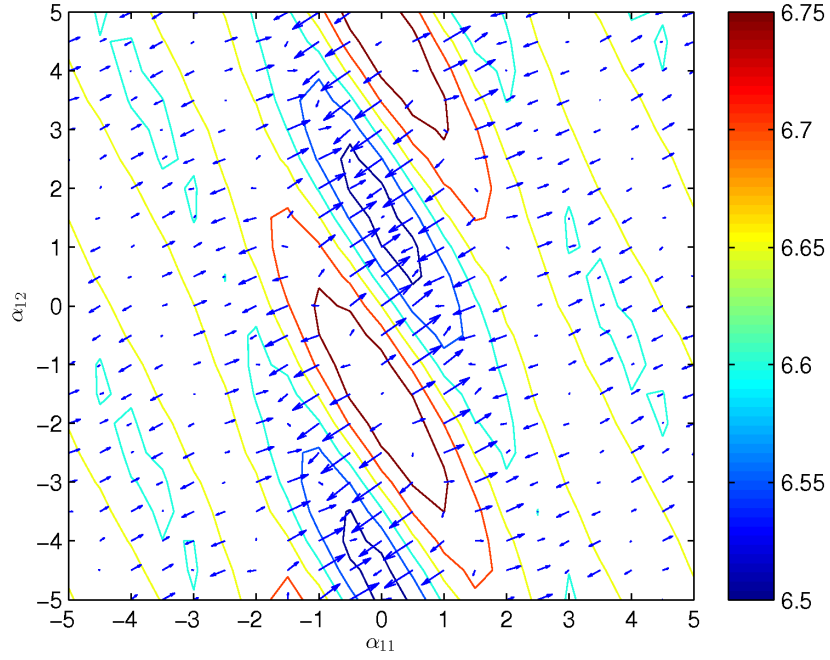
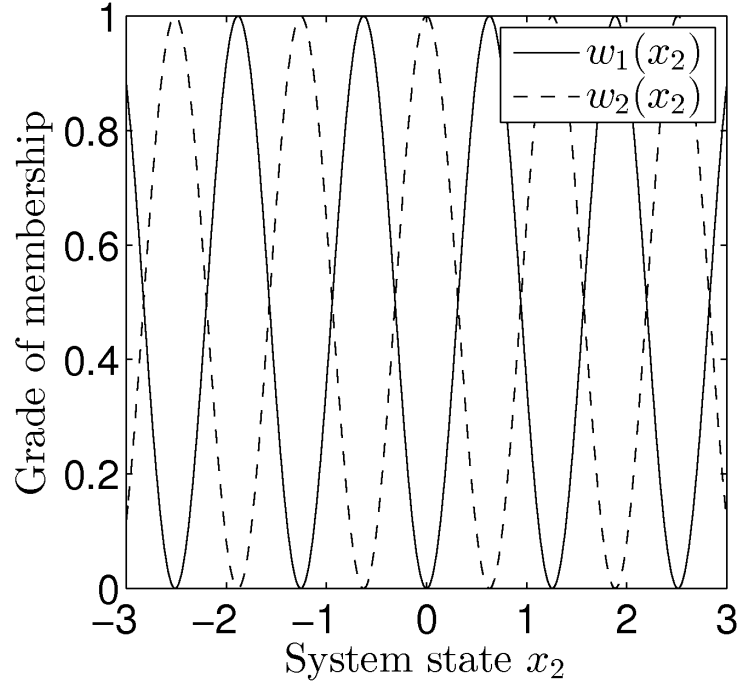
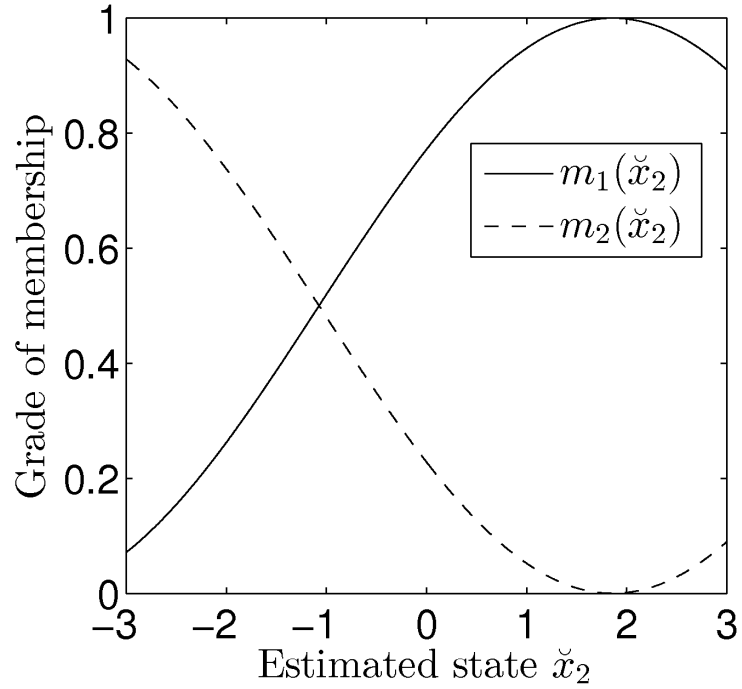


Figure 5.20: The descent of the gradient  $\nabla J(\alpha)$ , where the arrow indicates the direction of the gradient descent and the contour indicates the value of the cost  $J(\alpha)$ .

by the gradient descent approach instead of the global minima. Therefore, the resulting performance depends on the initial conditions of the optimization. However, a better performance than PDC approach can still be guaranteed by setting the initial condition of the optimization as the PDC approach, namely choosing the form of  $m_i(\check{\mathbf{x}}, \alpha_i)$  and  $\alpha^{(0)}$  such that  $m_i(\check{\mathbf{x}}, \alpha_i) = w_i(\check{\mathbf{x}})$ . In this way, the optimized performance is better than or at least equal to the PDC approach.



(a)  $w_i(x_2)$  for the polynomial fuzzy model.



(b) Optimized  $m_i(\check{x}_2)$  for the polynomial fuzzy observer-controller.

Figure 5.21: Membership functions.

Applying the designed polynomial observer-controller gains and the optimized membership functions to control the nonlinear mass-spring-damping system, the responses of system states, estimated states and their counterparts by PDC approach are shown in Figs. 5.22 and 5.23. The response of the control input is shown in Fig. 5.24. Although the optimized membership functions lead to slightly more overshoot

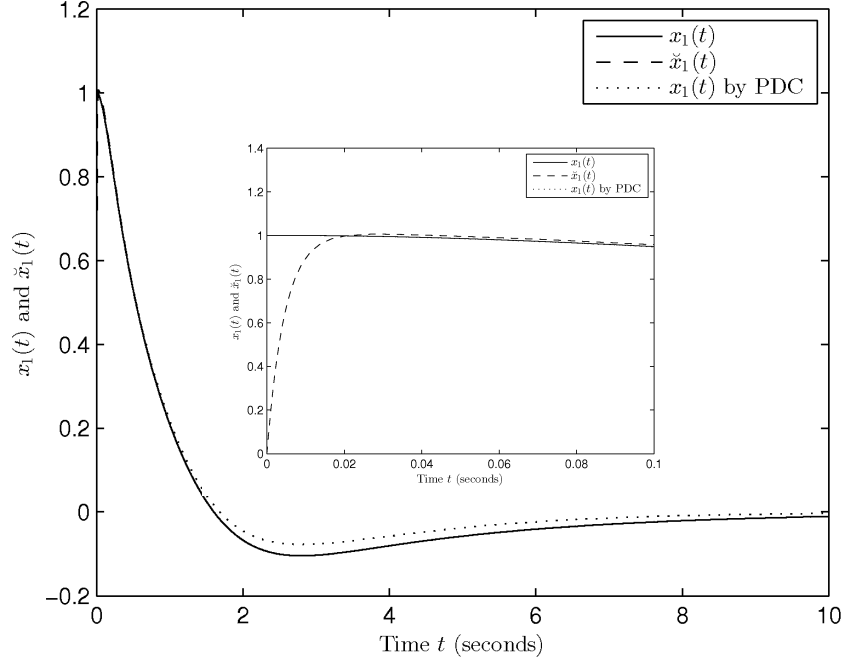


Figure 5.22: Time response of system state  $x_1$ , its estimation  $\hat{x}_1$  and its counterpart by PDC approach.

in  $x_1$ , they save much more control energy<sup>1</sup> in  $u$ . In other words, the optimization finds a better trade-off between the performance of the system states and the control energy, which results in a lower overall cost. In short, the proposed design and optimization of polynomial fuzzy observer-controller are feasible for controlling nonlinear systems. Note that in Fig. 5.22, the estimated state follows the original state quickly and it can only be seen in the zoom-in figure.

#### 5.4.3.3 Ball-and-Beam System

In this example, we further test the proposed approach on a system with higher dimension, namely the ball-and-beam system [88] as shown in Fig. 5.25 with the following state-space form:

$$\begin{aligned}\dot{x}_1 &= x_2, \\ \dot{x}_2 &= B(x_1 x_4^2 - g \sin(x_3)), \\ \dot{x}_3 &= x_4, \\ \dot{x}_4 &= u, \\ \mathbf{y} &= [x_1 \quad x_2 \quad x_4]^T.\end{aligned}$$

where  $x_1$  and  $x_2$  are the position and velocity of the ball, respectively;  $x_3$  and  $x_4$  are the angle and angular velocity of the beam, respectively;  $u$  is the control input;

<sup>1</sup>Defined as a quadratic term  $u(\check{\mathbf{x}}, \alpha)^T R u(\check{\mathbf{x}}, \alpha)$  in the cost function for this example.

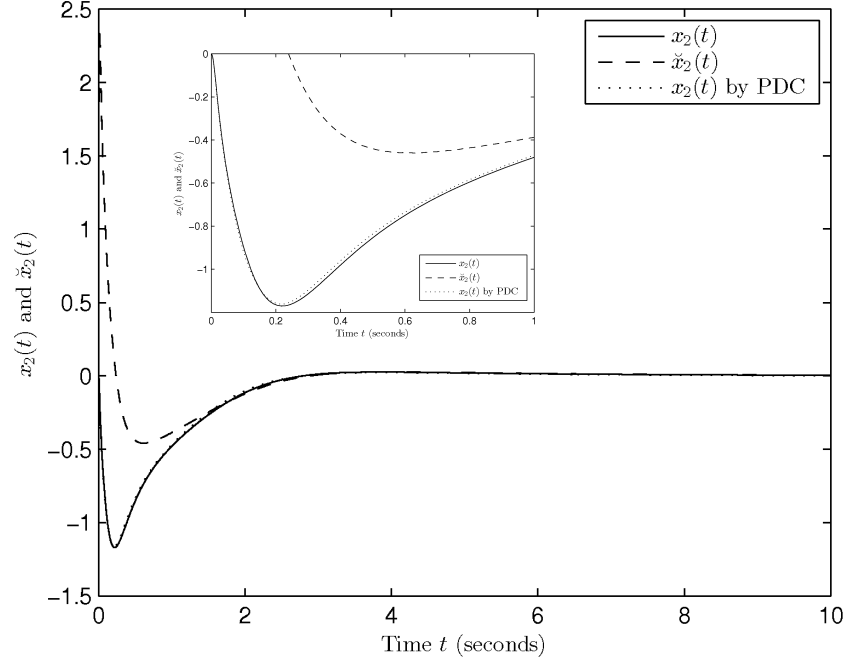


Figure 5.23: Time response of system state  $x_2$ , its estimation  $\check{x}_2$  and its counterpart by PDC approach.

$\mathbf{y}$  is the output vector;  $B = 0.6$ ;  $g = 10m/s^2$ .

Defining the region of interest as  $x_3 \in [-\frac{20\pi}{180}, \frac{20\pi}{180}]$ , the nonlinear term  $f_1(x_3) = \frac{\sin(x_3)}{x_3}$  is represented by sector nonlinearity technique [9] as follows:  $f_1(x_3) = \mu_{M_1^1}(x_3)f_{1_{min}} + \mu_{M_1^2}(x_3)f_{1_{max}}$ , where  $\mu_{M_1^1}(x_3) = \frac{f_{1_{max}} - f_1(x_3)}{f_{1_{max}} - f_{1_{min}}}$ ,  $\mu_{M_1^2}(x_3) = 1 - \mu_{M_1^1}(x_3)$ ,  $f_{1_{min}} = 0.9798$ ,  $f_{1_{max}} = 1.0000$ . The system is exactly described by a 2-rule polynomial fuzzy model:

$$\begin{aligned}\dot{\mathbf{x}} &= \sum_{i=1}^2 w_i(x_3) (\mathbf{A}_i(x_4)\mathbf{x} + \mathbf{B}_i u), \\ y &= \sum_{i=1}^2 w_i(x_3) \mathbf{C}_i \mathbf{x},\end{aligned}$$

where

$$\mathbf{x} = [x_1 \quad x_2 \quad x_3 \quad x_4]^T,$$

$$\mathbf{A}_1(x_4) = \begin{bmatrix} 0 & 1 & 0 & 0 \\ Bx_4^2 & 0 & -Bgf_{1_{min}} & 0 \\ 0 & 0 & 0 & 1 \\ 0 & 0 & 0 & 0 \end{bmatrix}, \mathbf{A}_2(x_4) = \begin{bmatrix} 0 & 1 & 0 & 0 \\ Bx_4^2 & 0 & -Bgf_{1_{max}} & 0 \\ 0 & 0 & 0 & 1 \\ 0 & 0 & 0 & 0 \end{bmatrix},$$

$$\mathbf{B}_1 = \mathbf{B}_2 = [0 \quad 0 \quad 0 \quad 1]^T, \mathbf{C}_1 = \mathbf{C}_2 = \begin{bmatrix} 1 & 0 & 0 & 0 \\ 0 & 1 & 0 & 0 \\ 0 & 0 & 0 & 1 \end{bmatrix};$$

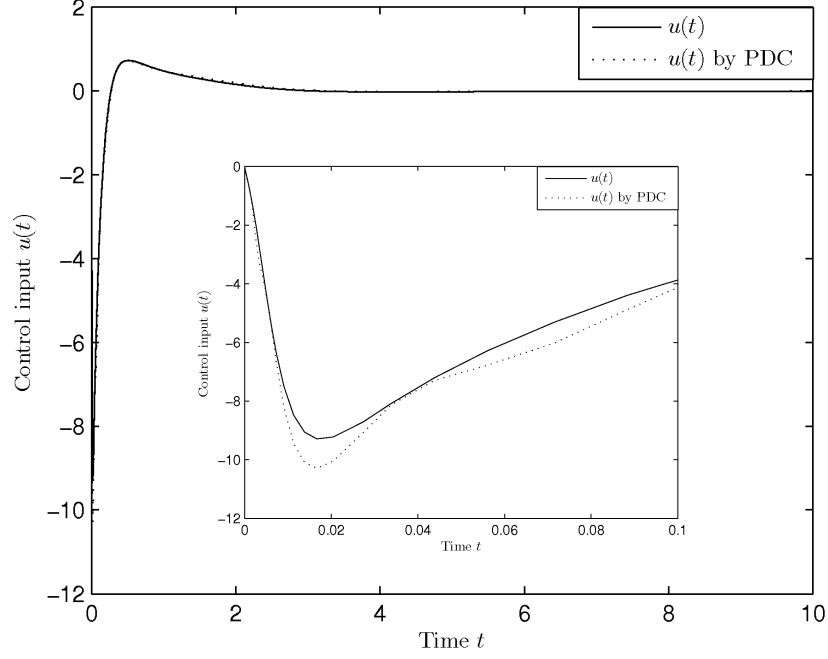


Figure 5.24: Time response of the control input  $u$  and its counterpart by PDC approach.

the membership functions are  $w_i(x_3) = \mu_{M_1^i}(x_3), i = 1, 2$ . Again, the polynomial fuzzy model demonstrates its superiority by keeping the polynomial term  $x_4^2$ . Otherwise,  $2^2 = 4$  rules are required by T-S fuzzy model in [88].

It is implied that the premise variable  $f_1(x_3)$  depends on unmeasurable system state  $x_3$ , and thus Theorem 6 is employed to design the PFMB observer-controller with unmeasurable premise variables. We choose  $\gamma_1 = 1 \times 10^{-6}, \gamma_2 = 1 \times 10^{-2}, \gamma_3 = 2$ ,  $\mathbf{N}_k(\check{x}_4)$  of degree 0 and 2 in  $\check{x}_4$ ,  $\mathbf{M}_j(\check{x}_4)$  of degree 0 and 2 in  $\check{x}_4$ ,  $\varepsilon_1 = \varepsilon_2 = 1 \times 10^{-4}$  and  $\varepsilon_3 = 1 \times 10^{-6}$ . Note that the predefined parameters  $\gamma_1, \gamma_2, \gamma_3$  are chosen by trial-and-error. Users can try different magnitudes until a feasible solution is found. The obtained polynomial observer-controller gains are:

$$\mathbf{G}_1(\check{x}_4) = [3.3079 \times 10^{-1} \check{x}_4^2 + 2.6902 \quad 7.6596 \times 10^{-2} \check{x}_4^2 + 2.5305 \\ - 2.1583 \times 10^{-1} \check{x}_4^2 - 1.0746 \times 10 \quad - 6.5337 \times 10^{-2} \check{x}_4^2 - 4.3596],$$

$$\mathbf{G}_2(\check{x}_4) = [3.3078 \times 10^{-1} \check{x}_4^2 + 2.7261 \quad 7.6595 \times 10^{-2} \check{x}_4^2 + 2.5393 \\ - 2.1583 \times 10^{-1} \check{x}_4^2 - 1.0765 \times 10 \quad - 6.5337 \times 10^{-2} \check{x}_4^2 - 4.3655],$$

$$\mathbf{L}_1(\check{x}_4) =$$

$$\begin{bmatrix} 2.16 \times 10^{-2} \check{x}_4^2 + 5.57 & 1.97 \times 10^{-1} \check{x}_4^2 + 5.18 \times 10 & -3.74 \times 10^{-4} \check{x}_4^2 - 2.11 \times 10^{-1} \\ 2.01 \times 10^{-1} \check{x}_4^2 + 5.07 \times 10 & 2.85 \check{x}_4^2 + 7.52 \times 10^2 & -4.99 \times 10^{-3} \check{x}_4^2 - 3.37 \\ -6.39 \times 10^{-3} \check{x}_4^2 - 1.55 & -1.14 \times 10^{-1} \check{x}_4^2 - 3.00 \times 10 & 8.18 \times 10^{-4} \check{x}_4^2 + 3.00 \times 10^{-1} \\ -2.95 \times 10^{-4} \check{x}_4^2 - 7.18 \times 10^{-2} & -5.16 \times 10^{-3} \check{x}_4^2 - 1.35 & 4.72 \times 10^{-5} \check{x}_4^2 + 1.62 \times 10^{-2} \end{bmatrix},$$

$$\mathbf{L}_2(\check{x}_4) =$$

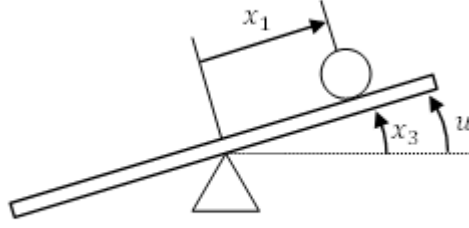


Figure 5.25: The ball-and-beam system .

$$\begin{bmatrix} 2.16 \times 10^{-2} \check{x}_4^2 + 5.57 & 1.97 \times 10^{-1} \check{x}_4^2 + 5.18 \times 10 & -3.74 \times 10^{-4} \check{x}_4^2 - 2.12 \times 10^{-1} \\ 2.01 \times 10^{-1} \check{x}_4^2 + 5.07 \times 10 & 2.85 \check{x}_4^2 + 7.52 \times 10^2 & -4.99 \times 10^{-3} \check{x}_4^2 - 3.39 \\ -6.39 \times 10^{-3} \check{x}_4^2 - 1.55 & -1.14 \times 10^{-1} \check{x}_4^2 - 3.00 \times 10 & 8.18 \times 10^{-4} \check{x}_4^2 + 3.01 \times 10^{-1} \\ -2.95 \times 10^{-4} \check{x}_4^2 - 7.18 \times 10^{-2} & -5.16 \times 10^{-3} \check{x}_4^2 - 1.35 & 4.72 \times 10^{-5} \check{x}_4^2 + 1.63 \times 10^{-2} \end{bmatrix}.$$

To optimize the membership functions  $m_i(\check{x}_3)$  of the polynomial fuzzy observer-controller, the Gaussian membership function is applied:  $m_1(\check{x}_3, \alpha_1) = e^{-\frac{(\check{x}_3 - \alpha_{11})^2}{2\alpha_{12}^2}}$  and  $m_2(\check{x}_3, \alpha_1) = 1 - m_1(\check{x}_3, \alpha_1)$ , where  $\alpha = [\alpha_1^T]^T = [\alpha_{11} \ \alpha_{12}]^T$  are the parameters to be optimized. The cost function, total time and stopping criteria are the same as in Example 5.4.3.1. The initial conditions are  $\mathbf{x}_0 = [0.25 \ 0 \ 0.1 \ 0]^T$ ,  $\check{\mathbf{x}}_0 = [0.25 \ 0 \ 0 \ 0]^T$ . Choosing the step size  $\beta^{(i)} = 1$  for all iterations  $i$  and initializing the parameters  $\alpha^{(0)} = [0.1 \ 0.1]^T$ , we obtain the optimized results  $\alpha_{11} = -0.0872$ ,  $\alpha_{12} = 0.3147$  and the corresponding cost  $J(\alpha) = 1.5068$ , which is still better than the cost  $J = 1.5266$  obtained by PDC approach ( $m_i(\check{x}_3) = w_i(\check{x}_3)$ ,  $i = 1, 2$ ).

Applying the designed polynomial observer-controller gains and the optimized membership functions to control the ball-and-beam system, the responses of system states and estimated states are shown in Figs. 5.26 and 5.27. Again, the example demonstrates the applicability of the proposed design and optimization strategy.

**Remark 30** *The numerical complexity of applying Theorems 6 and 8 are shown in Tables 5.1 and 5.2, respectively. For Theorem 6, the computational time increases as the number of polynomial terms, the polynomial degrees, the dimension of the system and the number of fuzzy rules increase. As is known, the computational demand is relatively higher for the SOS technique compared with the LMI technique. For Theorem 8, the computational time also increases when the system is more complicated. This limitation makes the proposed optimization method only applicable offline instead of online.*



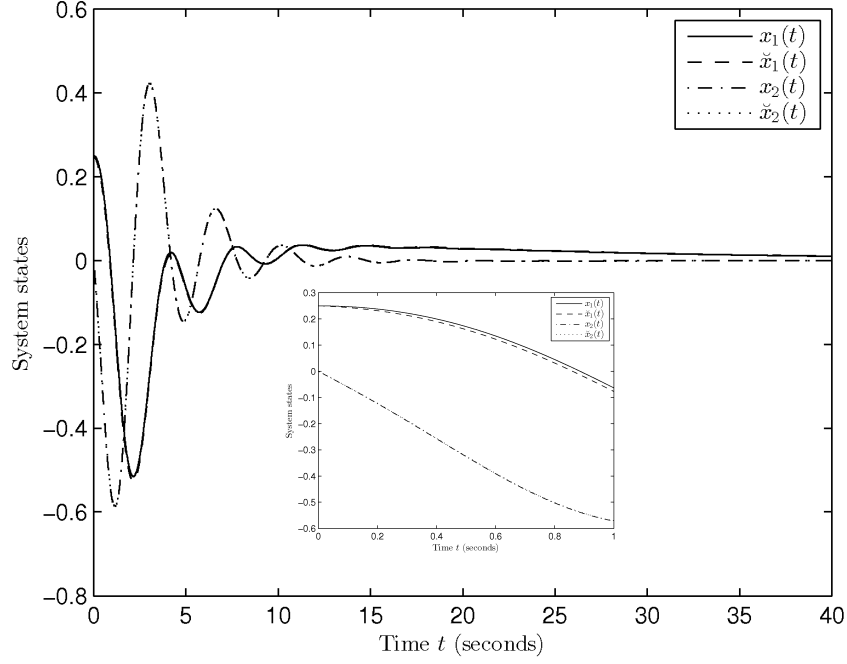


Figure 5.26: Time response of system state  $x_1$ , its estimation  $\hat{x}_1$  and its counterpart by PDC approach.

Table 5.1: Numerical complexity of Theorem 6.

	Polynomial terms in model	Decision variables	SOS conditions	Computational time (minutes)
Example 5.4.3.1	1	22	8	1.6
Example 5.4.3.2	2	22	8	66.0
Example 5.4.3.3	1	84	8	21.4

#### 5.4.3.4 Mobile Robot Navigation

In this example, we try to compare the proposed optimization scheme with the existing method in [76]. The following unicycle model (an idealized two-wheeled robot cart moving in a two-dimensional world) as shown in Fig. 5.28 is employed to study the mobile robot navigation problem [76]:

$$\begin{aligned}\dot{x}_1 &= v \cos(x_3), \\ \dot{x}_2 &= v \sin(x_3), \\ \dot{x}_3 &= u,\end{aligned}$$

where  $(x_1, x_2)$  is the Cartesian coordinate of the center of the unicycle;  $x_3 \in (-\pi, \pi]$  is its orientation with respect to the  $x_1$ -axis;  $v = 1$ ;  $u$  is the control input. Defining  $\mathbf{x} = [x_1 \ x_2 \ x_3]^T$  and  $\mathbf{z} = [x_1 \ x_2]^T$ , the control objective is to navigate the mobile

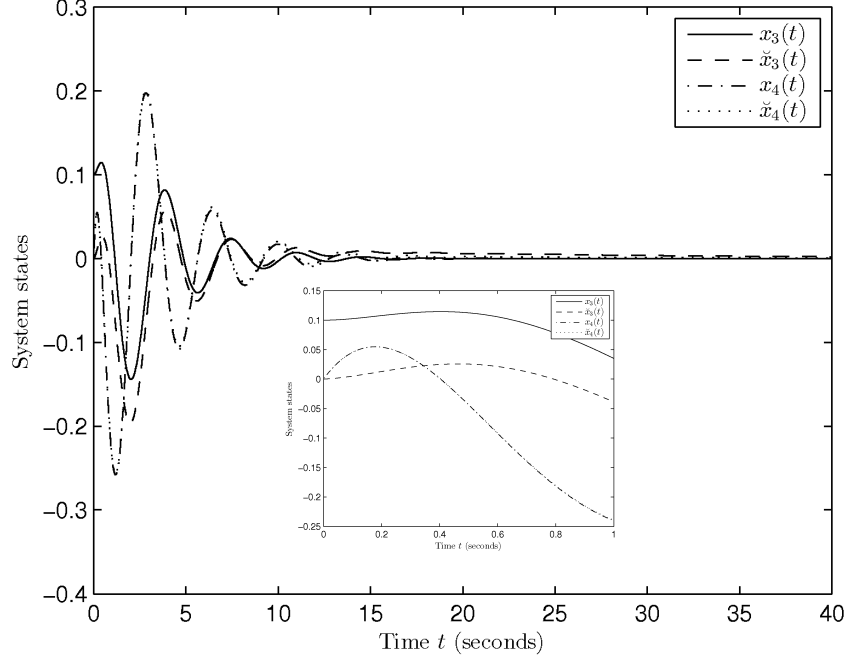


Figure 5.27: Time response of system state  $x_2$ , its estimation  $\check{x}_2$  and its counterpart by PDC approach.

Table 5.2: Numerical complexity of Theorem 8.

	Computational time (minutes/iteration)	Iterations
Example 5.4.3.1	4.5	6
Example 5.4.3.2	26.5	7
Example 5.4.3.3	92.1	4

robot from initial position  $\mathbf{x}_0 = [-1.5 \ 0 \ 0]^T$  to goal position  $\mathbf{z}_g = [x_{1g} \ x_{2g}]^T = [3 \ 0]^T$  and avoid the obstacle  $\mathbf{z}_a = [x_{1a} \ x_{2a}]^T = [0 \ 0]^T$ .

Since the method in [76] cannot deal with fuzzy observer, we only employ fuzzy controller and assume all states are measurable. The fuzzy controller is given by:

$$u = \sum_{i=1}^2 m_i(x_1, \alpha_1) u_i,$$

where  $m_1(x_1, \alpha_1) = 1 - e^{-\alpha_{11}(x_1 - x_{1a})^2}$  and  $m_2(x_1, \alpha_1) = 1 - m_1(x_1, \alpha_1)$  are the membership functions with parameter  $\alpha = [\alpha_1^T]^T = \alpha_{11}$  to be optimized;  $u_1 = C_g(\phi_g(\mathbf{z}) - x_3)$  and  $u_2 = C_a(\pi + \phi_a(\mathbf{z}) - x_3)$  are predefined control laws for behaviors “go-to-goal” and “avoid-obstacle”, respectively;  $C_g = 10, C_a = 1$ ;  $\phi_g(\mathbf{z}) = \arctan(x_{2g} - x_2, x_{1g} - x_1)$  and  $\phi_a(\mathbf{z}) = \arctan(x_{2a} - x_2, x_{1a} - x_1)$  can be understood as angles from the goal position and the obstacle respectively to the robot when the robot is oriented to  $x_1$ -axis.

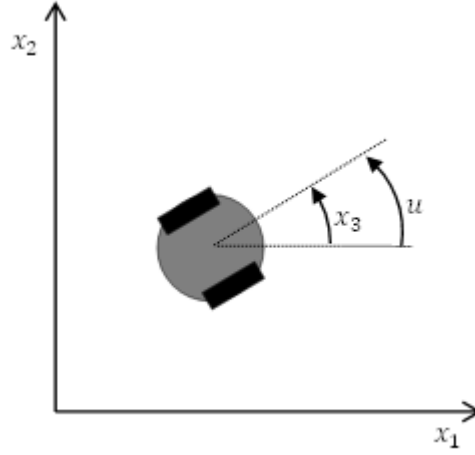


Figure 5.28: The unicycle model.

Table 5.3: Comparison of optimization algorithms.

	Cost	Number of parameters	Computational time (minutes/iteration)	Iterations
Theorem 8	0.5590	1	1.5	10
[76]	0.6013	2	3.4	5

We consider  $\varphi(\mathbf{x}, \check{\mathbf{x}}, \alpha) = ae^{-b\|\mathbf{z}-\mathbf{z}_a\|^2} + c\|\mathbf{z}-\mathbf{z}_g\|^2$ ,  $\psi(\mathbf{x}(T_t), \check{\mathbf{x}}(T_t), \alpha) = 0$  in the cost function (5.177), where  $a = 2, b = 10, c = 0.01$ . The first part  $ae^{-b\|\mathbf{z}-\mathbf{z}_a\|^2}$  is used to drive the mobile robot away from the obstacle, and the second part  $c\|\mathbf{z}-\mathbf{z}_g\|^2$  is used to drive the mobile robot to the goal position. The total time and stopping criteria are the same as in Example 5.4.3.1. Choosing the step size  $\beta^{(i)} = 1$  for all iterations  $i$  and initializing the parameters  $\alpha^{(0)} = 1$ , we obtain the optimized results  $\alpha_{11} = 0.7200$  and the trajectory of the mobile robot is shown in Fig. 5.29. Since the robot rotates and translates simultaneously, the robot does not move exactly towards the goal, which results in oscillation around the goal. The oscillation can be reduced by increasing the rotating coefficient  $C_g$  or decreasing the translating coefficient  $v$ .

**Remark 31** The comparison with [76] is summarized in Table 5.3. The settings of [76] are the same as those in Example 5.4.3.4 except  $m_2(x_1, \alpha_2) = e^{-\alpha_{21}(x_1-x_{1a})^2}$ ,  $u = \frac{\sum_{i=1}^2 m_i(x_1, \alpha_i)u_i}{\sum_{i=1}^2 m_i(x_1, \alpha_i)}$  and  $\alpha_{11}, \alpha_{21} \in [0.1, 10]$ . Using these settings, it can be seen that  $m_2(x_1, \alpha_2)$  is independent of  $m_1(x_1, \alpha_1)$  and thus  $\sum_{i=1}^2 m_i(x_1, \alpha_i) \neq 1$  during the calculation of the gradient. Although the normalization is imposed on the final control signal  $u = \frac{\sum_{i=1}^2 m_i(x_1, \alpha_i)u_i}{\sum_{i=1}^2 m_i(x_1, \alpha_i)}$ , this is not considered in the algorithm and the calculated gradient is imprecise. Therefore, compared with existing approach, Theorem 8 provides more accurate gradient and less number of parameters to be optimized, which leads to lower cost and less computational time.

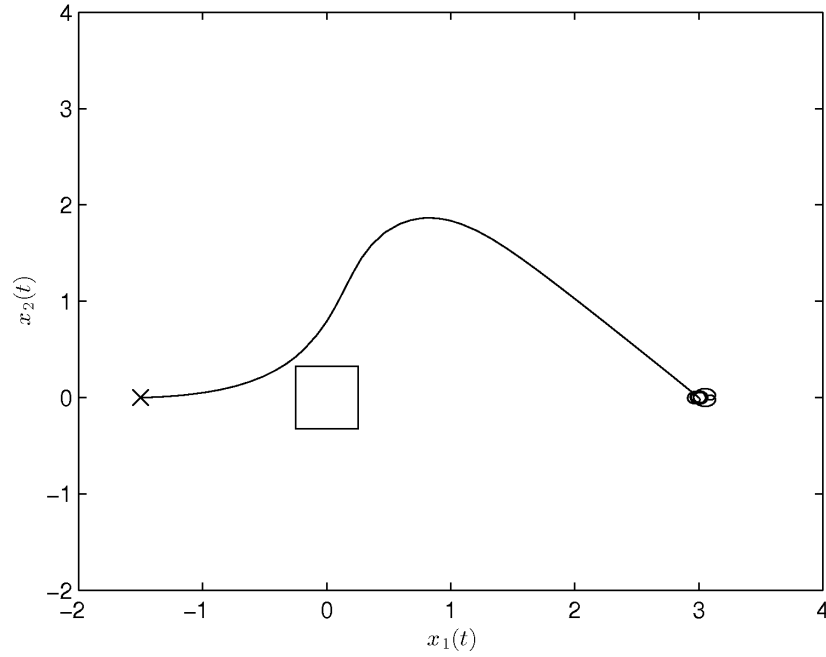


Figure 5.29: The trajectory of the mobile robot where “ $\times$ ” indicates the initial position and “ $\square$ ” indicates the obstacle position.

#### 5.4.4 Conclusion

In this section, the performance of FMB control strategy have been improved. The membership functions of the polynomial observer-controller have been optimized to minimize a general performance index. To draw a distinction from existing papers, more general settings (cost function) and more precise gradients have been attained in this section. Simulation examples have been provided to demonstrate the enhanced performance. In the future, shortening the optimization time to meet the requirement of online application can be further investigated.

# Chapter 6

## Conclusion and Future Work

### 6.1 Conclusion

In this thesis, the stability conditions of FMB control systems have been relaxed such that the applicability of FMB control scheme is improved. For T-S fuzzy model, the HODLF is employed to reduce the conservativeness of stability conditions. The HODLF generalizes the commonly used first order derivative. By exploiting the properties of membership functions and the dynamics of the FMB control system, convex and relaxed stability conditions can be derived. The comparison between the proposed HODLF and existing methods is summarized in Table 6.1. As shown in the table, the proposed HODLF exhibits lower conservativeness. Note that the two compared methods in [2] provide the same results in this thesis.

For polynomial fuzzy model, a general form of approximated membership functions is proposed, which is implemented by Taylor series expansion. TSMFs can be brought into stability conditions such that the relation between membership functions and system states is expressed. To further reduce the conservativeness, different types of information are taken into account: the boundary of membership functions, the property of membership functions and the boundary of operating domain. The comparison between the proposed TSMF and existing methods is summarized in Table 6.2. As shown in the table, the proposed TSMF exhibits lower conservativeness and more general form. Note that the analysis in [28] exploits some properties that cannot be implemented in this thesis and thus the proposed TSMF is not strictly relaxed than the method in [28].

Additionally, the applicability of FMB control scheme is also improved by considering fuzzy observer. Two types of T-S fuzzy observer have been designed for the case where system states are not measurable for state-feedback control. The first type is the relaxed T-S fuzzy observer. Premise membership functions depending on unmeasurable premise variables are considered to enhance the flexibility and applicability of the fuzzy observer-controller. Convex stability conditions are obtained through matrix decoupling technique. The proposed analysis is able to reduce the

Table 6.1: Comparison between the proposed HODLF and existing methods.

	Conservativeness	Boundary of membership functions
Proposed HODLF	Low	Required
Theorem 6 in [2] (fuzzy Lyapunov function)	High	Required
Theorem 7 in [2] (fuzzy Lyapunov function)	High	Not required

Table 6.2: Comparison between the proposed TSMF and existing methods.

	Conservativeness	Order of approximated membership functions
Proposed TSMF	Low	$\geq 1$
Piecewise linear membership functions [28]	Low	1
Remark 8 (no membership approximation)	High	N/A

number of predefined scalars by adequately choosing the augmented vector. The stability conditions are relaxed by membership-function-dependent approach which takes the information of membership functions into consideration in the stability analysis. The comparison between the proposed relaxed T-S fuzzy observer and existing methods is summarized in Table 6.3. As shown in the table, the proposed relaxed T-S fuzzy observer exhibits lower conservativeness and smaller number of predefined scalars. Note that the augmented vector is chosen differently from [54] and thus the proposed fuzzy observer is not strictly relaxed than the method in [54]. Also, the number of predefined scalars can be larger than 3 in [54] if other control problems are involved.

The second type is T-S fuzzy functional observer, which is designed to directly estimate the control input instead of the system states. A new form of fuzzy functional observer is proposed to facilitate the stability analysis such that the observer gains can be numerically obtained and the stability can be guaranteed simultaneously. The proposed form is also in favor of applying separation principle to separately design the fuzzy controller and the fuzzy functional observer. The comparison between the proposed relaxed T-S fuzzy functional observer and existing methods is summarized in Table 6.4. As shown in the table, the proposed T-S fuzzy functional observer exhibits lower order and guaranteed stability.

Apart from the T-S fuzzy observer, the polynomial fuzzy observer has also been designed to generalize the T-S fuzzy observer. Premise membership functions de-

Table 6.3: Comparison between the proposed relaxed T-S fuzzy observer and existing methods.

	Conservativeness	Number of predefined scalars
Proposed T-S fuzzy observer	Low	2
T-S fuzzy observer [54]	Low	3
Linear observer	High	N/A

Table 6.4: Comparison between the proposed T-S fuzzy functional observer and existing methods.

	Order of observer	How to obtain gains	Stability
Proposed T-S fuzzy functional observer	Low	Numerically	Guaranteed
T-S fuzzy functional observer [59]	Low	Analytically	To be checked
T-S fuzzy observer [11, 53–55]	High	Numerically	Guaranteed

pending on unmeasurable premise variables are also considered. The matrix decoupling technique and the refined completing square approach are employed to achieve convex stability conditions. The comparison between the proposed polynomial fuzzy observer and existing methods is summarized in Table 6.5. As shown in the table, the proposed polynomial fuzzy observer exhibits less design steps and more general form. In addition, the comparison between the two proposed polynomial fuzzy observers is summarized in Table 6.6. As shown in the table, both methods have their own advantages on the complexity of stability conditions.

We further extend the design and analysis to polynomial fuzzy observer-controller using sampled-data technique for nonlinear systems where only sampled-output measurements are available. The comparison between the proposed polynomial fuzzy observer under sampled-output measurement and existing methods is summarized in Table 6.7. As shown in the table, the proposed method exhibits more general form.

Moreover, the membership functions of the polynomial observer-controller are optimized by the improved gradient descent method, which outperforms the widely applied PDC approach according to a general performance index. The comparison between the proposed optimization algorithm and existing methods is summarized in Table 6.8. As shown in the table, the proposed method exhibits more general form and precise gradients.

Table 6.5: Comparison between the proposed polynomial fuzzy observer and existing methods.

	Design steps	Premise variables	Output matrices
Proposed polynomial fuzzy observer (by matrix decoupling)	One	Unmeasurable	Polynomial
Proposed polynomial fuzzy observer (by completing square)	One	Unmeasurable	Polynomial
Polynomial fuzzy observer [60]	Two	Measurable	T-S

Table 6.6: Comparison between the proposed polynomial fuzzy observer using matrix decoupling technique and completing square approach.

	Number of predefined scalars	Dimension of conditions	Number of conditions
Proposed observer (by matrix decoupling)	3	Small	Large
Proposed observer (by completing square)	3	Large	Small

Simulation examples have been provided to demonstrate the relaxation of the proposed stability conditions and the feasibility of designed fuzzy observer-controllers.

## 6.2 Future Work

The potential research directions are listed as follows:

- 1) Since the bounds of the derivative of membership functions are required for the proposed HODLF, more advanced techniques may be applied to meet or eliminate the boundary requirement of the derivative of membership functions. If there is no boundary requirement, the users will not need to check the derivative of membership functions which is more convenient to use. However, these advanced techniques may complicate the stability analysis, which need further investigation. Additionally, only up to second order derivatives are considered for HODLF, more terms with higher order derivatives can be employed. Moreover, the analysis for HODLF is still conservative which makes it not strictly relaxed than traditional Lyapunov functions. How to make it strictly relaxed than the traditional ones is an open problem for future work.
- 2) During the derivation using proposed TSMFs, the conservativeness is still introduced. Future work can be done to bring specific membership function  $v_{ri,l}(x_r)$  into stability conditions if  $v_{ri,l}(x_r)$  is chosen to be polynomials, which



Table 6.7: Comparison between the proposed polynomial fuzzy observer under sampled-output measurement and existing methods.

	Fuzzy model	Fuzzy controller	Output matrices	Output feedback
Proposed method	Polynomial	Polynomial	T-S	Observer
[69]	Polynomial	T-S	Constant	Static
[70–72]	T-S	T-S	T-S	Observer

Table 6.8: Comparison between the proposed optimization algorithm and existing methods.

	Fuzzy observer	Control input in cost function	Gradients
Proposed method	Polynomial	Yes	Precise
[76]	N/A	No	Not precise

has potential to further reduce the conservativeness. Except using Taylor series expansion to approximate the original membership functions, other approximation methods can also be applied such as some fitting algorithms. A comparison can be made for different approximation methods to show how the approximation errors influence the conservativeness. Apart from the theoretical points, the numerical errors and computational demands for applying this method need to be reduced. Perhaps computers with more powerful hardware should be employed.

- 3) The relaxation of T-S FMB observer-control systems is very preliminary since few work has been done for relaxation involving fuzzy observers. Other advanced methods of relaxation can be applied for systems involving fuzzy observer. The difficulty is that the premise variables in the membership functions are unmeasurable. In order to apply existing methods of relaxation for systems involving fuzzy observer, some modification should be made on existing methods to overcome the difficult of unmeasurable premise variables. Also, the same problems can be investigated for PFMB observer-control systems.
- 4) Only continuous-time system is investigated in this thesis. In discrete time, for example, the discrete-time T-S fuzzy functional observer can be investigated by extending existing discrete-time linear functional observer. The technique for discrete-time linear functional observer has already been developed, which is similar to continuous-time one. With existing technique, it will be straightforward to investigate discrete-time T-S fuzzy functional observer.
- 5) Only quadratic Lyapunov function is employed for the proposed polynomial

fuzzy observer. If polynomial Lyapunov function is employed, the conditions will be non-convex unless some strong assumptions are made on the input and output matrices of the fuzzy model. However, using polynomial Lyapunov function can relax the stability conditions since it is more general than quadratic Lyapunov function. The problems of applying polynomial Lyapunov function in the fuzzy observer-control system are left to be solved. Regarding to the non-convex conditions, there exist some algorithms for directly solving them. However, there is no guarantee that a feasible solution can be found even if there exists one. If a more effective algorithm with theoretical proof can be developed, the non-convex stability conditions can be directly used without any transformation or predefined parameters.

- 6) The proposed optimization of membership function for fuzzy observer-control systems can only be conducted offline due to the computational burden. How to shorten the time of optimization to meet the requirement of online application can be further investigated. The time of optimization comes from the iterative process of the gradient decent approach. If the optimal solution can be analytically calculated or the iterative process can be simplified, it will save much computational time.
- 7) The theoretical meaning of this work is to improve the applicability of FMB control approach. Only simulation examples have been provided to demonstrate the theoretical work. Therefore, it would be more persuasive if a real model can be employed for demonstration. To start with, some simple models such as the inverted pendulum, the ball-and-plate system and the memristor can be built. After a preliminary model has been built, some improvement can be made to reduce the errors between the real system and the simulated system. In this way, we can find out whether the proposed methods are effective to solve practical problems or whether they suffer from the practical environment such as modeling errors and uncertainties. Furthermore, since robotics and artificial intelligence are very popular in the modern world, the proposed methods can be applied to systems such as manipulators and mobile robots. The traditional methods for controlling manipulators highly rely on the real-time computation of Jacobian matrices. If FMB control approach can be applied, such real-time process may be eliminated to save time. Therefore, future collaboration with researchers from this field can be made in order to apply the proposed methods to state-of-the-art systems.

# Appendix A

## Proof of (4.58)

Consider the following two matrices:

$$\mathbf{P} = [\mathbf{G}_j^+ \quad \mathbf{I}_n],$$

$$\mathbf{Q} = \begin{bmatrix} \mathbf{I}_m & -\mathbf{G}_j \\ \mathbf{0} & \mathbf{I}_n \end{bmatrix},$$

where  $\mathbf{I}_n$  is  $n \times n$  identity matrix. Due to  $\mathbf{G}_j \in \Re^{m \times n}$  and  $\mathbf{G}_j^+ \in \Re^{n \times m}$ , we have  $\text{rank}(\mathbf{P}) = n$  and  $\text{rank}(\mathbf{Q}) = m + n$  where  $\mathbf{Q}$  is of full rank.

Therefore, we have

$$\text{rank}(\mathbf{PQ}) = \text{rank}(\mathbf{P}) = n,$$

where  $\mathbf{PQ} = [\mathbf{G}_j^+ \quad \mathbf{I}_n - \mathbf{G}_j^+ \mathbf{G}_j]$ . Due to  $[\mathbf{G}_j^+ \quad \mathbf{I}_n - \mathbf{G}_j^+ \mathbf{G}_j] \in \Re^{n \times (m+n)}$ ,  $[\mathbf{G}_j^+ \quad \mathbf{I}_n - \mathbf{G}_j^+ \mathbf{G}_j]$  is of full row rank.

According to the rank-nullity property [89], the rank of the left nullspace of  $[\mathbf{G}_j^+ \quad \mathbf{I}_n - \mathbf{G}_j^+ \mathbf{G}_j]$  is 0. Then we can get the equivalent relation:

$$\Phi_{ij}[\mathbf{G}_j^+ \quad \mathbf{I}_n - \mathbf{G}_j^+ \mathbf{G}_j] = \mathbf{0} \iff \Phi_{ij} = \mathbf{0}.$$

# Appendix B

## Boundary Information for Examples in Subsection 4.1.4

Table B.1: The upper bounds of membership functions for Example 4.1.4.1.

$\gamma_{111} = 9.9970 \times 10^{-1}$	$\gamma_{121} = 1.6970 \times 10^{-1}$	$\gamma_{131} = 9.6106 \times 10^{-2}$
$\gamma_{211} = 3.7987 \times 10^{-1}$	$\gamma_{221} = 6.4484 \times 10^{-2}$	$\gamma_{231} = 3.6519 \times 10^{-2}$
$\gamma_{311} = 9.9970 \times 10^{-1}$	$\gamma_{321} = 1.6970 \times 10^{-1}$	$\gamma_{331} = 9.6106 \times 10^{-2}$
$\gamma_{112} = 1.6970 \times 10^{-1}$	$\gamma_{122} = 1.4435 \times 10^{-1}$	$\gamma_{132} = 1.6970 \times 10^{-1}$
$\gamma_{212} = 6.4484 \times 10^{-2}$	$\gamma_{222} = 5.4850 \times 10^{-2}$	$\gamma_{232} = 6.4484 \times 10^{-2}$
$\gamma_{312} = 1.6970 \times 10^{-1}$	$\gamma_{322} = 1.4435 \times 10^{-1}$	$\gamma_{332} = 1.6970 \times 10^{-1}$
$\gamma_{113} = 9.6106 \times 10^{-2}$	$\gamma_{123} = 1.6970 \times 10^{-1}$	$\gamma_{133} = 9.9970 \times 10^{-1}$
$\gamma_{213} = 3.6519 \times 10^{-2}$	$\gamma_{223} = 6.4484 \times 10^{-2}$	$\gamma_{233} = 3.7987 \times 10^{-1}$
$\gamma_{313} = 9.6106 \times 10^{-2}$	$\gamma_{323} = 1.6970 \times 10^{-1}$	$\gamma_{333} = 9.9970 \times 10^{-1}$
$\gamma_{11} = 9.9980 \times 10^{-1}$	$\gamma_{12} = 3.7991 \times 10^{-1}$	$\gamma_{13} = 9.9980 \times 10^{-1}$
$\gamma_{21} = 3.7991 \times 10^{-1}$	$\gamma_{22} = 1.4436 \times 10^{-1}$	$\gamma_{23} = 3.7991 \times 10^{-1}$
$\gamma_{31} = 9.9980 \times 10^{-1}$	$\gamma_{32} = 3.7991 \times 10^{-1}$	$\gamma_{33} = 9.9980 \times 10^{-1}$

Table B.2: The upper bounds of membership functions for Example 4.1.4.2.

$\gamma_{112} = 3.1283 \times 10^{-2}$	$\gamma_{122} = 1.7340 \times 10^{-1}$
$\gamma_{212} = 1.4850 \times 10^{-1}$	$\gamma_{222} = 8.2310 \times 10^{-1}$
$\gamma_{11} = 3.8979 \times 10^{-2}$	$\gamma_{12} = 1.8503 \times 10^{-1}$
$\gamma_{21} = 1.8503 \times 10^{-1}$	$\gamma_{22} = 8.7828 \times 10^{-1}$

# Appendix C

## MATLAB Code Example

The MATLAB codes for simulation examples in Subsection 5.3.3 can be downloaded by the following link: [http://www.inf.kcl.ac.uk/staff/hklam/docs/MatlabCodes\(paper105\).zip](http://www.inf.kcl.ac.uk/staff/hklam/docs/MatlabCodes(paper105).zip). Readers may use the codes to easily implement the proposed polynomial fuzzy observer-controllers.

# References

- [1] H. O. Wang, K. Tanaka, and M. F. Griffin, “An approach to fuzzy control of nonlinear systems: stability and design issues,” *IEEE Trans. Fuzzy Syst.*, vol. 4, no. 1, pp. 14–23, Feb. 1996.
- [2] L. A. Mozelli, R. M. Palhares, and G. S. C. Avellar, “A systematic approach to improve multiple Lyapunov function stability and stabilization conditions for fuzzy systems,” *Inform. Sci.*, vol. 179, no. 8, pp. 1149–1162, Mar. 2009.
- [3] K. Tanaka, H. Yoshida, H. Ohtake, and H. O. Wang, “A sum of squares approach to modeling and control of nonlinear dynamical systems with polynomial fuzzy systems,” *IEEE Trans. Fuzzy Syst.*, vol. 17, no. 4, pp. 911–922, Aug. 2009.
- [4] K. Tanaka, H. Ohtake, and H. O. Wang, “Guaranteed cost control of polynomial fuzzy systems via a sum of squares approach,” *IEEE Trans. Syst., Man, Cybern. B, Cybern.*, vol. 39, no. 2, pp. 561–567, Apr. 2009.
- [5] T. Takagi and M. Sugeno, “Fuzzy identification of systems and its applications to modelling and control,” *IEEE Trans. Syst., Man, Cybern.*, vol. SMC-15, no. 1, pp. 116–132, Jan. 1985.
- [6] M. Sugeno and G. T. Kang, “Structure identification of fuzzy model,” *Fuzzy Sets Syst.*, vol. 28, no. 1, pp. 15–33, Oct. 1988.
- [7] T. M. Guerra, A. Sala, and K. Tanaka, “Fuzzy control turns 50: 10 years later,” *Fuzzy Sets Syst.*, vol. 281, pp. 168–182, 2015.
- [8] K. Tanaka and H. O. Wang, *Fuzzy Control Systems Design and Analysis: a Linear Matrix Inequality Approach*. New York: Wiley-Interscience, 2001.
- [9] A. Sala and C. Ariño, “Polynomial fuzzy models for nonlinear control: a Taylor-series approach,” *IEEE Trans. Fuzzy Syst.*, vol. 17, no. 6, pp. 284–295, Dec. 2009.
- [10] K. Chafaa, M. Ghanai, and L. Saidi, “General fuzzy models for dynamical systems,” in *2015 27th Int. Conf. Microelectronics (ICM)*, Dec. 2015, pp. 27–30.

- [11] K. Tanaka, T. Ikeda, and H. O. Wang, “Fuzzy regulators and fuzzy observers: relaxed stability conditions and LMI-based designs,” *IEEE Trans. Fuzzy Syst.*, vol. 6, no. 2, pp. 250–265, May 1998.
- [12] S. Prajna, A. Papachristodoulou, and P. A. Parrilo, “Nonlinear control synthesis by sum-of-squares optimization: a Lyapunov-based approach,” in *Proc. Asian Control Conf. (ASCC)*, vol. 1, Melbourne, Australia, Feb. 2004, pp. 157–165.
- [13] —, “Introducing SOSTOOLS: a general purpose sum of squares programming solver,” in *Proc. 41<sup>st</sup> IEEE Conf. Decision and Control*, vol. 1, Las Vegas, Nevada, USA, Dec. 2002, pp. 741–746.
- [14] J. F. Sturm, “Using SeDuMi 1.02, a Matlab toolbox for optimization over symmetric cones,” *Optimization Methods Software*, vol. 11, no. 1-4, pp. 625–653, 1999.
- [15] K. Tanaka, T. Komatsu, H. Ohtake, and H. O. Wang, “Micro helicopter control: LMI approach vs SOS approach,” in *IEEE Int. Conf. Fuzzy Syst., 2008. FUZZ-IEEE 2008. (IEEE World Congr. Computational Intell.)*, Jun. 2008, pp. 347–353.
- [16] J. L. Pitarch, “Contributions to fuzzy polynomial techniques for stability analysis and control,” *Ph.D. dissertation, Dept. de Ingeniera de Sistemas y Automatica (ISA), Univ. Politecnica de Valencia, Valencia, Spain*, 2013.
- [17] Y.-J. Chen, M. Tanaka, K. Tanaka, H. Ohtake, and H. O. Wang, “Brief paper - discrete polynomial fuzzy systems control,” *IET Control Theory Applicat.*, vol. 8, no. 4, pp. 288–296, Mar. 2014.
- [18] G. Feng, “A survey on analysis and design of model-based fuzzy control systems,” *IEEE Trans. Fuzzy Syst.*, vol. 14, no. 5, pp. 676–697, Oct. 2006.
- [19] A. Sala, “On the conservativeness of fuzzy and fuzzy-polynomial control of nonlinear systems,” *Annu. Rev. Control*, vol. 33, no. 1, pp. 48–58, 2009.
- [20] S. Boyd, L. E. Ghaoui, E. Feron, and V. Balakrishnan, *Linear Matrix Inequalities in System and Control Theory*. Society for Industrial and Applied Mathematics (SIAM), 1994.
- [21] X. Liu and Q. Zhang, “Approaches to quadratic stability conditions and  $H_\infty$  control designs for Takagi-Sugeno fuzzy systems,” *IEEE Trans. Fuzzy Syst.*, vol. 11, no. 6, pp. 830–839, Dec. 2003.
- [22] C. H. Fang, Y. S. Liu, S. W. Kau, L. Hong, and C. H. Lee, “A new LMI-based approach to relaxed quadratic stabilization of Takagi-Sugeno fuzzy control systems,” *IEEE Trans. Fuzzy Syst.*, vol. 14, no. 3, pp. 386–397, Jun. 2006.

- [23] A. Sala and C. Ariño, “Asymptotically necessary and sufficient conditions for stability and performance in fuzzy control: applications of Polya’s theorem,” *Fuzzy Sets Syst.*, vol. 158, no. 24, pp. 2671–2686, Jul. 2007.
- [24] J. C. Lo and J. R. Wan, “Studies on linear matrix inequality relaxations for fuzzy control systems via homogeneous polynomials,” *IET Control Theory Applicat.*, vol. 4, no. 11, pp. 2293–2302, Nov. 2010.
- [25] H. K. Lam and L. D. Seneviratne, “Stability analysis of polynomial fuzzy-model-based control systems under perfect/imperfect premise matching,” *IET Control Theory Applicat.*, vol. 5, no. 15, pp. 1689–1697, Oct. 2011.
- [26] H. K. Lam and S.-H. Tsai, “Stability analysis of polynomial-fuzzy-model-based control systems with mismatched premise membership functions,” *IEEE Trans. Fuzzy Syst.*, vol. 22, no. 1, pp. 223–229, Feb. 2014.
- [27] M. Narimani and H. K. Lam, “SOS-based stability analysis of polynomial fuzzy-model-based control systems via polynomial membership functions,” *IEEE Trans. Fuzzy Syst.*, vol. 18, no. 5, pp. 862–871, Oct. 2010.
- [28] H. K. Lam, “Polynomial fuzzy-model-based control systems: stability analysis via piecewise-linear membership functions,” *IEEE Trans. Fuzzy Syst.*, vol. 19, no. 3, pp. 588–593, Jun. 2011.
- [29] M. Bernal, T. M. Guerra, and A. Kruszewski, “A membership-function-dependent approach for stability analysis and controller synthesis of Takagi-Sugeno models,” *Fuzzy Sets Syst.*, vol. 160, no. 19, pp. 2776–2795, 2009.
- [30] H. K. Lam and M. Narimani, “Quadratic stability analysis of fuzzy-model-based control systems using staircase membership functions,” *IEEE Trans. Fuzzy Syst.*, vol. 18, no. 1, pp. 125–137, Feb. 2010.
- [31] H. K. Lam, “LMI-based stability analysis for fuzzy-model-based control systems using artificial T-S fuzzy model,” *IEEE Trans. Fuzzy Syst.*, vol. 19, no. 3, pp. 505–513, Jun. 2011.
- [32] H. K. Lam and J. Lauber, “Membership-function-dependent stability analysis of fuzzy-model-based control systems using fuzzy Lyapunov functions,” *Inform. Sci.*, vol. 232, pp. 253–266, May 2013.
- [33] G. Feng, C. L. Chen, D. Sun, and Y. Zhu, “ $H_\infty$  controller synthesis of fuzzy dynamic systems based on piecewise Lyapunov functions and bilinear matrix inequalities,” *IEEE Trans. Fuzzy Syst.*, vol. 13, no. 1, pp. 94–103, Feb. 2005.



- [34] J. Qiu, H. Tian, Q. Lu, and H. Gao, “Nonsynchronized robust filtering design for continuous-time T-S fuzzy affine dynamic systems based on piecewise Lyapunov functions,” *IEEE Trans. Cybern.*, vol. 43, no. 6, pp. 1755–1766, Dec. 2013.
- [35] H. K. Lam, M. Narimani, H. Li, and H. Liu, “Stability analysis of polynomial-fuzzy-model-based control systems using switching polynomial Lyapunov function,” *IEEE Trans. Fuzzy Syst.*, vol. 21, no. 5, pp. 800–813, Oct. 2013.
- [36] M. Bernal and T. Guerra, “Generalized nonquadratic stability of continuous-time Takagi-Sugeno models,” *IEEE Trans. Fuzzy Syst.*, vol. 18, no. 4, pp. 815–822, Aug. 2010.
- [37] J.-T. Pan, T. M. Guerra, S.-M. Fei, and A. Jaadari, “Nonquadratic stabilization of continuous T-S fuzzy models: LMI solution for a local approach,” *IEEE Trans. Fuzzy Syst.*, vol. 20, no. 3, pp. 594–602, Jun. 2012.
- [38] A. Butz, “Higher order derivatives of Liapunov functions,” *IEEE Trans. Automat. Control*, vol. 14, no. 1, pp. 111–112, Feb. 1969.
- [39] A. A. Ahmadi and P. A. Parrilo, “On higher order derivatives of Lyapunov functions,” in *2011 American Control Conf. (ACC)*, Jun. 2011, pp. 1313–1314.
- [40] S. F. Derakhshan, A. Fatehi, and M. G. Sharabiany, “Non-monotonic fuzzy state feedback controller design for discrete time T-S fuzzy systems,” in *9th Int. Conf. Fuzzy Syst. Knowledge Discovery (FSKD)*, May 2012, pp. 102–107.
- [41] S. F. Derakhshan and A. Fatehi, “Non-monotonic Lyapunov functions for stability analysis and stabilization of discrete time Takagi-Sugeno fuzzy systems,” *Int. J. Innovative Computing, Inform. Control*, vol. 10, no. 4, pp. 1567–1586, Aug. 2014.
- [42] —, “Non-monotonic robust  $H_2$  fuzzy observer-based control for discrete time nonlinear systems with parametric uncertainties,” *Int. J. Syst. Sci.*, vol. 46, no. 12, pp. 2134–2149, 2015.
- [43] A. Kruszewski and T. M. Guerra, “New approaches for the stabilization of discrete Takagi-Sugeno fuzzy models,” in *44th IEEE Conf. Decision and Control and 2005 Eur. Control Conf. CDC-ECC '05*, Dec. 2005, pp. 3255–3260.
- [44] A. Kruszewski, R. Wang, and T. M. Guerra, “Nonquadratic stabilization conditions for a class of uncertain nonlinear discrete time TS fuzzy models: a new approach,” *IEEE Trans. Automat. Control*, vol. 53, no. 2, pp. 606–611, Mar. 2008.

- [45] T. M. Guerra, H. Kerkeni, J. Lauber, and L. Vermeiren, "An efficient Lyapunov function for discrete T-S models: observer design," *IEEE Trans. Fuzzy Syst.*, vol. 20, no. 1, pp. 187–192, Feb. 2012.
- [46] Z. Lendek, T. M. Guerra, and J. Lauber, "Controller design for TS models using delayed nonquadratic Lyapunov functions," *IEEE Trans. Cybern.*, vol. 45, no. 3, pp. 453–464, Mar. 2015.
- [47] H. K. Lam and J. C. Lo, "Output regulation of polynomial-fuzzy-model-based control systems," *IEEE Trans. Fuzzy Syst.*, vol. 2, no. 21, pp. 262–274, Apr. 2013.
- [48] H. K. Lam, F. H. F. Leung, and P. K. S. Tam, "Fuzzy control of a class of multivariable nonlinear systems subject to parameter uncertainties: model reference approach," *Int. J. Approximate Reasoning*, vol. 26, no. 2, pp. 129–144, 2001.
- [49] H. K. Lam and W. K. Ling, "Sampled-data fuzzy controller for continuous nonlinear systems," *IET Control Theory Applicat.*, vol. 2, no. 1, pp. 32–39, Jan. 2008.
- [50] H. K. Lam and L. D. Seneviratne, "Tracking control of sampled-data fuzzy-model-based control systems," *IET Control Theory Applicat.*, vol. 3, no. 1, pp. 56–67, Jan. 2009.
- [51] J. Yoneyama, M. Nishikawa, H. Katayama, and A. Ichikawa, "Design of output feedback controllers for Takagi-Sugeno fuzzy systems," *Fuzzy Sets Syst.*, vol. 121, no. 1, pp. 127–148, 2001.
- [52] S. K. Nguang and P. Shi, " $H_\infty$  fuzzy output feedback control design for nonlinear systems: an LMI approach," *IEEE Trans. Fuzzy Syst.*, vol. 11, no. 3, pp. 331–340, Jun. 2003.
- [53] T. M. Guerra, A. Kruszewski, L. Vermeiren, and H. Tirmant, "Conditions of output stabilization for nonlinear models in the Takagi-Sugeno's form," *Fuzzy Sets Syst.*, vol. 157, no. 9, pp. 1248–1259, 2006.
- [54] C. S. Tseng and B. S. Chen, "Robust fuzzy observer-based fuzzy control design for nonlinear discrete-time systems with persistent bounded disturbances," *IEEE Trans. Fuzzy Syst.*, vol. 17, no. 3, pp. 711–723, Jun. 2009.
- [55] M. H. Asemani and V. J. Majd, "A robust observer-based controller design for uncertain T-S fuzzy systems with unknown premise variables via LMI," *Fuzzy Sets Syst.*, vol. 212, no. 0, pp. 21–40, 2013.

- [56] X. H. Chang and G. H. Yang, "A descriptor representation approach to observer-based control synthesis for discrete-time fuzzy systems," *Fuzzy Sets Syst.*, vol. 185, no. 1, pp. 38–51, 2011.
- [57] X. J. Ma and Z. Q. Sun, "Analysis and design of fuzzy reduced-dimensional observer and fuzzy functional observer," *Fuzzy Sets Syst.*, vol. 120, no. 1, pp. 35–63, 2001.
- [58] M. Darouach, "Existence and design of functional observers for linear systems," *IEEE Trans. Automat. Control*, vol. 45, no. 5, pp. 940–943, May 2000.
- [59] M. S. Fadali, "Fuzzy functional observers for dynamic TSK systems," in *The 14th IEEE Int. Conf. Fuzzy Syst.*, May 2005, pp. 389–394.
- [60] K. Tanaka, H. Ohtake, T. Seo, M. Tanaka, and H. O. Wang, "Polynomial fuzzy observer designs: a sum-of-squares approach," *IEEE Trans. Syst., Man, Cybern. B, Cybern.*, vol. 42, no. 5, pp. 1330–1342, Oct. 2012.
- [61] S. Lall and G. Dullerud, "An LMI solution to the robust synthesis problem for multi-rate sampled-data systems," *Automatica*, vol. 37, no. 12, pp. 1909–1922, 2001.
- [62] L. S. Hu, J. Lam, Y. Y. Cao, and H. H. Shao, "A linear matrix inequality (LMI) approach to robust  $H_2$  sampled-data control for linear uncertain systems," *IEEE Trans. Syst., Man, Cybern. B, Cybern.*, vol. 33, no. 1, pp. 149–155, Feb. 2003.
- [63] E. Fridman, A. Seuret, and J. P. Richard, "Robust sampled-data stabilization of linear systems: an input delay approach," *Automatica*, vol. 40, no. 8, pp. 1441–1446, 2004.
- [64] D. W. Kim and H. J. Lee, "Sampled-data observer-based output-feedback fuzzy stabilization of nonlinear systems: exact discrete-time design approach," *Fuzzy Sets Syst.*, vol. 201, no. 0, pp. 20–39, 2012.
- [65] H. K. Lam and F. H. F. Leung, "Sampled-data fuzzy controller for time-delay nonlinear system: LMI-based and fuzzy-model-based approaches," *IEEE Trans. Syst., Man, Cybern. B, Cybern.*, vol. 37, no. 3, pp. 617–629, Jun. 2007.
- [66] H. Gao and T. Chen, "Stabilization of nonlinear systems under variable sampling: a fuzzy control approach," *IEEE Trans. Fuzzy Syst.*, vol. 15, no. 5, pp. 972–983, Oct. 2007.
- [67] H. K. Lam, "Sampled-data fuzzy-model-based control systems: stability analysis with consideration of analogue-to-digital converter and digital-to-analogue

- converter,” *IET Control Theory Applicat.*, vol. 4, no. 7, pp. 1131–1144, Jul. 2010.
- [68] X. L. Zhu, B. Chen, D. Yue, and Y. Wang, “An improved input delay approach to stabilization of fuzzy systems under variable sampling,” *IEEE Trans. Fuzzy Syst.*, vol. 20, no. 2, pp. 330–341, Apr. 2012.
- [69] H. K. Lam, “Stabilization of nonlinear systems using sampled-data output-feedback fuzzy controller based on polynomial-fuzzy-model-based control approach,” *IEEE Trans. Syst., Man, Cybern. B, Cybern.*, vol. 42, no. 1, pp. 258–267, Feb. 2012.
- [70] S. K. Nguang and P. Shi, “Fuzzy  $H_\infty$  output feedback control of nonlinear systems under sampled measurements,” *Automatica*, vol. 39, no. 12, pp. 2169–2174, 2003.
- [71] H. Zhang, H. Yan, Q. Chen, and T. Liu, “Quantised  $H_\infty$  control for sampled fuzzy systems,” *IET Control Theory Applicat.*, vol. 6, no. 17, pp. 2686–2695, Nov. 2012.
- [72] C. P. G. Flores, B. C. Toledo, J. P. G. Sandoval, S. D. Gennaro, and V. G. Alvarez, “A reset observer with discrete/continuous measurements for a class of fuzzy nonlinear systems,” *J. Franklin Inst.*, vol. 350, no. 8, pp. 1974–1991, 2013.
- [73] H. Li, X. Sun, H. R. Karimi, and B. Niu, “Dynamic output-feedback passivity control for fuzzy systems under variable sampling,” *Math. Problems Eng.*, vol. 2013, 2013.
- [74] H. Li, X. Jing, H. K. Lam, and P. Shi, “Fuzzy sampled-data control for uncertain vehicle suspension systems,” *IEEE Trans. Cybern.*, vol. PP, no. 99, pp. 1–1, Sept. 2013.
- [75] R. Babuska and M. Oosterom, “Design of optimal membership functions for fuzzy gain-scheduled control,” in *FUZZ '03. 12th IEEE Int. Conf. Fuzzy Syst., 2003*, vol. 1, May 2003, pp. 476–481.
- [76] T. R. Mehta and M. Egerstedt, “Optimal membership functions for multi-modal control,” in *2006 American Control Conf.*, Jun. 2006, pp. 2658–2663.
- [77] —, “Multi-modal control using adaptive motion description languages,” *Automatica*, vol. 44, no. 7, pp. 1912–1917, 2008.
- [78] —, “An optimal control approach to mode generation in hybrid systems,” *Nonlinear Analysis: Theory, Methods & Applications*, vol. 65, no. 5, pp. 963–983, 2006.

- [79] H. K. Khalil and J. W. Grizzle, *Nonlinear systems*. Prentice Hall New Jersey, 1996, vol. 3.
- [80] L. Xie and C. E. De Souza, “Robust  $H_\infty$  control for linear systems with norm-bounded time-varying uncertainty,” *IEEE Trans. Autom. Control*, vol. 37, no. 8, pp. 1188–1191, Aug. 1992.
- [81] K. Gu, “An integral inequality in the stability problem of time-delay systems,” in *2000 Proc. 39th IEEE Conf. Decision and Control*, vol. 3, 2000, pp. 2805–2810.
- [82] C. Ariño and A. Sala, “Extensions to “stability analysis of fuzzy control systems subject to uncertain grades of membership”,” *IEEE Trans. Syst., Man, Cybern. B, Cybern.*, vol. 38, no. 2, pp. 558–563, Apr. 2008.
- [83] G. B. Arfken and H. J. Weber, *Mathematical Methods for Physicists*. Elsevier, 2005.
- [84] C. C. Duong, K. Guelton, and N. Manamanni, “A SOS based alternative to LMI approaches for non-quadratic stabilization of continuous-time Takagi-Sugeno fuzzy systems,” in *2013 IEEE Int. Conf. Fuzzy Syst. (FUZZ)*, July 2013, pp. 1–7.
- [85] J. Yoneyama, M. Nishikawa, H. Katayama, and A. Ichikawa, “Output stabilization of Takagi-Sugeno fuzzy systems,” *Fuzzy Sets Syst.*, vol. 111, no. 2, pp. 253–266, 2000.
- [86] T. L. Fernando, H. M. Trinh, and L. Jennings, “Functional observability and the design of minimum order linear functional observers,” *IEEE Trans. Automat. Control*, vol. 55, no. 5, pp. 1268–1273, May 2010.
- [87] C. R. Rao and S. K. Mitra, *Generalized Inverse of Matrices and Its Applications*. Wiley New York, 1971.
- [88] H. K. Lam, F. H. F. Leung, and P. K. S. Tam, “Stable and robust fuzzy control for uncertain nonlinear systems,” *IEEE Trans. Syst., Man, Cybern. A, Syst., Humans*, vol. 30, no. 6, pp. 825–840, Nov. 2000.
- [89] G. Strang, *Linear Algebra and Its Applications*. Brooks Cole, 2005.